Bose-Fermi Mixtures: A Mean-Field Study

Marin Bukov

Master Thesis
Physics Department
LMU Munich

First Advisor: Prof. Dr. Lode Pollet
Second Advisor: Prof. Dr. Immanuel Bloch

June 7th, 2013

Declaration of Authorship

I declare that this thesis was composed by myself and that the work contained therein is my own, except where explicitly stated otherwise in the text.

Marin Bukov
June 7th, 2013

Acknowledgements

First and foremost, I would like to thank my advisor Lode Pollet for the numerous discussions without which finishing this thesis would have been impossible. He always found time to help with both conceptual issues as well technical details, which stimulated me in studying the problem rigorously, and at the same time intuitively. It was a great fun to frequently discuss the physics of bosons and fermions with him during my stay in his group.

During the entire period of writing the thesis, my office colleagues Stephan Langer, Peter Kroiß, Thomas Bilitewski and Jens Grimm provided a very relaxing and particularly friendly working atmosphere. It was a fantastic experience to discuss various physics problems with them, and they helped me a great deal when I struggled with the implementation of the numerical solution of the equations found in this thesis.

Many thanks go also to Thomas Barthel who was ready to provide help any time especially when Lode was absent, as well as to Jad Halimeh who is constantly refreshing the atmosphere in the group.

I very much appreciate the help of Immanuel Bloch, Ulrich Schneider and Simon Fölling who put a huge effort to make the most counter-intuitive and confusing quantum phenomena understandable. I owe most of my physical intuition about cold atom systems to them. Special thanks go to Marcos Atala who in particular showed me how to make fancy cartoons and pictures to visualize abstract ideas.

I must properly stress the contribution of Michael Kay with the help of whom I managed to prove the small linear algebra theorem of Appendix A. This nontrivial result was the fundamental cornerstone for the development of a big part of the thesis. I would also like to use this opportunity to thank Michael Haack for the several discussions we had on non-relativistic supersymmetry.

A \Biggg{Thank You} goes to Alessandro Michelangeli for his constant guiding and support during my studies at the LMU.

Also, I am particularly grateful to the TMP coordinator Robert Helling for the enormous support in conceptual, bureaucratic and organisational issues. I'd like to thank all my friends without whom I wouldn't have had such a nice experience in the course of preparing and writing this thesis.

Last but not least, I'd like to appreciate the help of Jan von Delft, Oleg Yevtushenko and Fabian Heidrich-Meisner during my entire master studies at the LMU Munich.

Abstract

We study the low-energy properties of the spinful Bose-Fermi Hubbard model on a simple cubic lattice for attractive fermion-fermion and repulsive boson-boson interactions at half-filling for the fermions and unit-filling for the bosons. Recent DMFT results predict a variety of phases, including superfluids, charge density waves, mixed states and supersolids. We develop a self-consistent mean-field scheme which allows for all orders to appear and determine the ground state of the system by comparing the corresponding energies. In the double superfluid phase, we consider possibilities for exotic extended s-, p- and d-wave boson-assisted superfluidity.

This thesis is organized as follows:

- In Chapter 1 we give a short motivation and briefly summarize recent experimental and theoretical studies of the model.
- Chapter 2 discusses the Bose-Hubbard model. After reviewing the celebrated ground state phase diagram within mean-field, we study the behaviour of the bosonic system in the presence of a staggered potential.
- In Chapter 3 we revisit the Fermi-Hubbard model. We discuss the relation between a charge density wave and a superfluid state both from a group theoretical point of view taking into account the symmetries of the system, and within mean-field. Further, we generalize the discussion to the case of the Fermi-Hubbard model in a staggered potential.
- Chapter 4 deals with the Bose-Fermi mixture within mean-field theory. We develop a decoupling scheme taking into account the back action of one species on the other, and study the resulting phase diagram by solving the self-consistency equations. We compare our result to recent DMFT simulations.
- In Chapter 5, we address the possibility of realizing unconventional pairing mechanisms due to boson-mediated attraction between the fermions in the deep superfluid limit.
- In Chapter 6, we briefly study the supersymmetric Bose-Fermi mixture above the quantum degenerate regime. We derive an effective field theory for the system and show that SUSY is restrictive enough to induce tremendous simplifications in the model.

Contents

1 Introduction **1**
- 1.1 Motivation . . . 1
- 1.2 A Brief Survey of Recent Experiments . . . 2
- 1.3 Theoretical Proposals . . . 3

2 Lattice Bosons in a Staggered Potential **7**
- 2.1 The Bose-Hubbard Model . . . 7
  - 2.1.1 From a Mott Insulator to a Superfluid: A Quantum Phase Transition 8
  - 2.1.2 MI - SF Transition: The Cumulant Expansion . . . 11
  - 2.1.3 The Superfluid Phase: Bogoliubov Approximation . . . 13
- 2.2 The Bose-Hubbard Model with a Staggered Potential . . . 16
  - 2.2.1 Free Bosons in a Staggered Field . . . 16
  - 2.2.2 The Mott Insulator-Superfluid Transition in the Presence of a Staggered Field . . . 21
  - 2.2.3 Induced Supersolidity and the Generalized Bogoliubov Approximation 25
- 2.3 Conclusion . . . 34

3 The Fermi-Hubbard Model **37**
- 3.1 BCS Theory of Superconductivity . . . 38
- 3.2 Charge Density Waves . . . 41
- 3.3 Symmetries of the Fermi Hubbard Model . . . 44
  - 3.3.1 Lieb-Mattis and Particle-Hole Symmetries . . . 44
  - 3.3.2 The Full SO(4) Symmetry Group . . . 46
- 3.4 Phase Diagram of the FHM and the BCS-BEC Crossover . . . 48
- 3.5 Double MF-Description of the FHM at Half-Filling . . . 50
- 3.6 FHM away from Half-Filling . . . 54
  - 3.6.1 FHM in a Staggered Potential . . . 57
  - 3.6.2 Nearest-Neighbour Interactions and the Extended FHM . . . 58
- 3.7 Conclusions . . . 60

4 Bose-Fermi Mixtures **63**
- 4.1 Properties of the Model . . . 64
- 4.2 Analysis of the DMFT Phase Diagram at Half-Filling . . . 65
- 4.3 Mean-Field Theory of the Bose-Fermi Mixture . . . 68
- 4.4 Mean-Field Phase Diagram of the BFM . . . 72
- 4.5 Outlook . . . 75

5 Unconventional Superfluidity in Bose-Fermi Mixtures **77**
5.1 Introduction . . . 77
5.2 Unconventional Pairing . . . 79
5.3 Singlet Pairing . . . 80
5.4 Triplet Pairing . . . 83
5.5 Approximate Results for the Critical Temperature . . . 83
5.5.1 Calculation of φ_1 and $\tilde{\varphi}_p$ . . . 84
5.6 Approximate Results . . . 87
5.7 Analysis of the Results . . . 90
5.8 Conclusions . . . 91

6 Supersymmetric Bose-Fermi Mixtures **93**
6.1 Introduction . . . 93
6.2 The Spinful Bose-Fermi Mixture . . . 94
6.3 Supersymmetric extension of the Galilean Group . . . 95
6.3.1 The İnönü-Wigner Contraction . . . 95
6.3.2 The Non-relativistic SUSY Algebra . . . 97
6.4 Superfield Description . . . 98
6.5 Propagator and Diagrammatics . . . 99
6.6 SUSY Breaking . . . 103
6.7 Conclusion . . . 104

A Generalized Bogoliubov Transformations **105**
A.1 Motivation . . . 105
A.2 Fermionic Bogoliubov Transformations . . . 107
A.3 Bosonic Bogoliubov Transformations . . . 109

B Effective Action for Mixtures of (hardcore) Bosons **115**

C SUSY Calculations **121**
C.1 Derivation of the Hamiltonian . . . 121
C.2 Evaluation of the Hartree Diagram . . . 122

Chapter 1

Introduction

1.1 Motivation

Typical models of condensed matter systems describe interacting fermions in ion lattices. The physical picture behind them is given by electrons interacting via the electromagnetic Coulomb force in the presence of the much heavier ions. The latter are often assumed to be static due to the huge mass they have compared to the electrons and are thought of as a periodic background potential in which the electrons move. Most of the well-established theories of solid state physics consider the kinetic energy of the electrons to be much larger than their potential energy, so that part of them essentially becomes free to move about. Indeed, this description is very successful to explain the physics behind (semi-)conductors and insulators.

Unfortunately, it breaks down once the kinetic and potential energies become comparable to each other. This is the case of strongly-interacting electrons and the physics behind materials displaying such behaviour is significantly less understood. The main reason for this is that one needs models to describe very complicated many-body systems which are simple enough and mathematically tractable. On top of this, experiments usually deal with samples of materials which contain impurities and this severely aggregates the verification of theoretical descriptions.

As a bridge in between comes cold atom physics with its remarkable controllability over model parameters and impurity doping. Using red-detuned laser beams one is able to cool down fermionic and bosonic alkali atoms beyond the limit of quantum degeneracy. Moreover, it is also possible to create artificial optical lattices which mimic their ion counterparts and allow one to study purely quantum many-body effects in the laboratory. In some cases, it is possible to experimentally realize exact condensed matter models of strongly correlated systems and study their behaviour. This gives an unprecedented opportunity to compare theoretical and experimental studies, which lies at the heart of physics.

In this thesis, we provide a mean-field study of the ground state properties of the 3D Bose-Fermi Hubbard model, also known as the Bose-Fermi mixture (BFM). It describes strongly correlated bosons and fermions in an optical (ion) lattice. Studying the interaction between bosons and fermions is required for many purposes. Mainly, one is interested in the modification of pronounced features of one species, such as superconductivity and superfluidity, by the other. For instance, a central idea in the theory of superconductivity is the phonon-mediated attraction between the fermions. Therefore, the studies of boson-assisted superfluidity at-

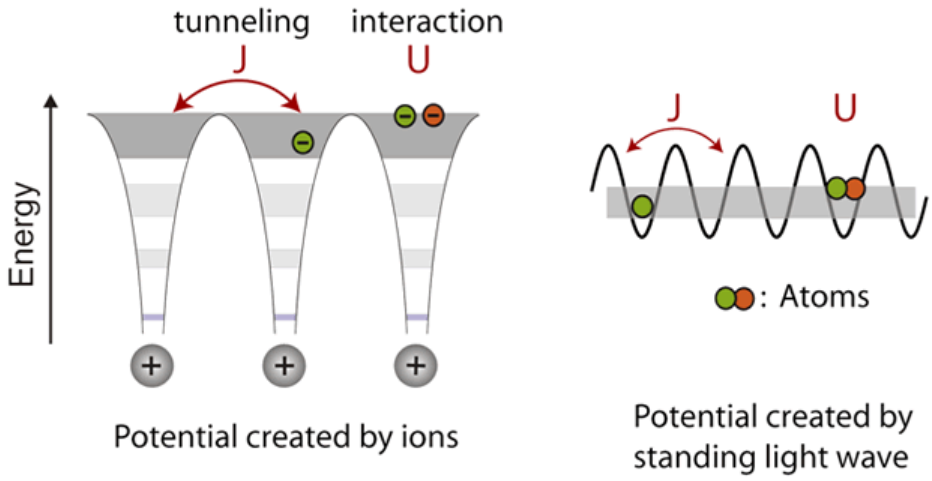

Figure 1.1: Analogy between ion (crystal) lattices in solid materials and artificial optical lattices (image by the Quantum Optics Group of LMU, [41])

tract a lot of attention as a prospective quantum simulator of superconductivity. Another possibility that opens up with the investigation of the BFM is revealing the physics of Fermi polarons [59] which can be thought of as fermions dressed in a bosonic field, or even more exotic examples, such as quarks exchanging gluons via the Strong Force. Bose-Fermi mixtures can further be used to experimentally test unconventional pairing mechanisms, important for p- and d-wave superconductivity. It has also been proposed to look for special collective excitation modes as remainders of a broken supersymmetry in this non-relativistic setup.

In the following, we are interested in the phase diagram of the spinful Bose-Fermi Hubbard model. Recent single-site dynamical mean-field theory (DMFT) results [2] suggest a variety of phases that might occur at low temperatures, including superfluid phases, charge density waves, and even exotic supersolids. The theoretical description of these mixed phases poses a significant challenge due to the complexity of the physical system. It is, therefore, worthwhile to seek effective and simple minimal descriptions that model the essentials of the relevant physics in each phase correctly.

1.2 A Brief Survey of Recent Experiments

After the series of successful experiments on the Bose-Hubbard model in 2002 [22], the ground state properties and the phase diagram have been experimentally measured in excellent agreement with theoretical predictions and numerical simulations. These experiments pioneered the study of condensed matter systems using cold atoms. Several years later, fermionic superfluids have been realized in the laboratory with ^{6}Li atoms, using Feshbach resonances to tune the strength of the interaction to the attractive side. This also allowed to experimentally examine the physics of the BEC-BCS crossover [62]. Since the usual cooling protocol includes evaporative cooling which relies entirely on interaction-induced thermalization, it is much harder to cool down a fermionic system, as the s-wave channel is effectively being closed at low-temperatures by the Pauli Principle. Therefore, sympathetic cooling [19], which makes

use of bosons interacting with the fermions is employed.

Spin-polarized Bose-Fermi mixtures have been realized experimentally using cold bosonic ^{87}Rb and fermionic ^{40}K atoms in 3D optical lattices. The first experiments of the mixture in the presence of a fixed attractive background scattering length found a decrease in the bosonic visibility, which points towards a shift in the Mott insulator to superfluid transition. Although different proposals such as self-trapping [42, 35, 51, 59], adiabatic heating [23, 11, 45], or corrections due to higher bands [51, 37] have been made, none of them has been clearly identified.

Another experiment on the spin-polarized BFM found an asymmetry between the strong repulsive and attractive interspecies interactions, analyzing the ^{87}Rb momentum distribution function [6]. The shift of the transition line on the attractive side has been confirmed and attributed to self-trapping. Multiband spectroscopy has been employed to measure the band structure with high accuracy [24]. This experiment reported a reduction of the fermion tunneling energy, depending on the relative atom numbers. The effect has been interpreted as an interaction-induced increase of the lattice depth due to self-trapping.

A comprehensive description of the relevant experimental methods and results can also be found in [58].

1.3 Theoretical Proposals

Theoretical investigations of Bose-Fermi mixtures have been initiated in the late 90's after the celebrated realization of Bose-Einstein condensation in 1995 [32, 44], which triggered theoretical research in the field. First, bosonic mixtures were intensively investigated but soon the theoretical community turned to the exciting possibilities for realization of exotic phases of matter given by the BFM.

The spinful Bose-Fermi Hubbard Hamiltonian is given by

$$\begin{aligned} H = &- t_b \sum_{\langle ij \rangle} (b_i^\dagger b_j + h.c.) - \mu_b \sum_i n_i + \frac{U_{bb}}{2} \sum_i n_i(n_i - 1) \\ &- t_f \sum_{\langle ij \rangle, \sigma} (c_{i\sigma}^\dagger c_{j\sigma} + h.c.) - \mu_f \sum_i m_i + U_{ff} \sum_i m_{i\uparrow} m_{i\downarrow} \\ &+ U_{bf} \sum_i n_i m_i. \end{aligned} \tag{1.1}$$

Here, the b's and the c's represent bosonic and fermionic operators, respectively. The corresponding particle number operators are given by n_i and $m_i = m_{i\uparrow} + m_{i\downarrow}$. The bosons (fermions) are allowed to hop to nearest-neighbouring sites of the lattice, denoted by $\langle ij \rangle$, thereby gaining energy t_b (t_f). Finally, the chemical potentials of the species μ_b (μ_f) determine the lattice filling. A schematic and intuitive picture of the system is given in 1.2.

Initially, the attention of many authors was targeted towards the boson-induced pairing of the fermions. Indeed, it has been shown [54] that to first order the fermionic interaction is renormalized as

$$U_{ind}(k, \omega) = U_{bf}^2 \chi(k, \omega), \tag{1.2}$$

where $\chi(k, \omega)$ is the bosonic response function. Deep into the superfluid regime the Bogoliubov

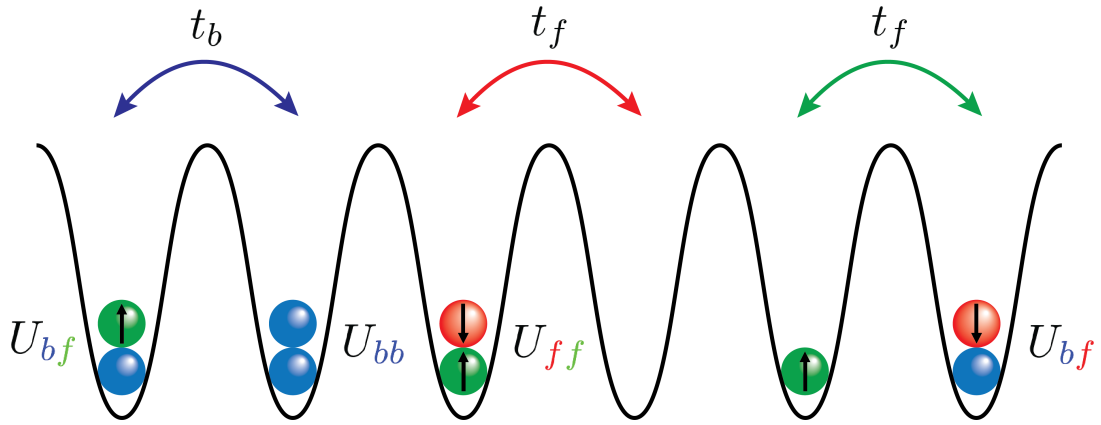

Figure 1.2: The spinful Bose-Fermi Hubbard model: bosons (blue) and fermions of spin up (green) and spin down (red) are subject to on-site interactions U_{bb} and U_{ff}, while the boson-fermion on-site interaction strength is set by U_{bf}. Bosons and fermions of either spin gain energy by hopping to nearest neighbouring sites with amplitudes t_b and t_f, respectively.

approximation can be employed, and it takes the form

$$U_{ind}(k,\omega) = \frac{U_{bf}^2 2n\left(zt_b + \varepsilon_k^{(b)}\right)}{\omega^2 - \left(zt_b + \varepsilon_k^{(b)}\right)\left(\left(zt_b + \varepsilon_k^{(b)}\right) + 2nU_{bb}\right)}, \tag{1.3}$$

where n is the average boson occupation, z is the coordination number and $\varepsilon_k^{(b)}$ is the bosonic dispersion relation.

An effective interaction potential can be obtained using the T-matrix formalism, and the corresponding s-wave scattering length has been calculated with the help of field-theoretical methods [7]. The frequency dependence of the induced interaction is responsible for retardation effects. However, when the bosonic sound velocity is (much) smaller than the Fermi velocity, the ω-dependence can be safely neglected, and the resulting interaction is always attractive. Therefore, a weak repulsive fermionic interaction can be overcome in favour of an attractive effective one, leading to a Cooper instability in the s-wave channel [53]. For attractive fermionic interactions, the BCS transition temperature is proposed to have increased due to the induced interaction, [25].

Properties of the dilute Bose-Fermi mixture have been investigated perturbatively, including the ground state energy, the bosonic momentum distribution function, and the superfluid/normal fractions. It was proposed that varying the mass ratios and the scattering lengths, it is possible to suppress the bosonic momentum distribution function at small momenta, while the bosonic superfluid density was found smaller than the total condensate fraction [52].

Concerning the ground state phase diagram, an exotic supersolid phase has been proposed for a BFM on a square lattice [9], characterized by simultaneous superfluid and crystalline orders. However, this phase relies heavily on the existence of the van Hove singularity in the 2D density of states, and is therefore suppressed exponentially in 3D.

The above papers all deal with the spin-polarized Bose-Fermi mixture. The superconducting transition temperature has been investigated in the strong coupling limit for the

spinful mixture in three dimensions in free space [56], where an analytical solution for the pairing transition temperature has been derived in the limit where retardation effects can be neglected. The critical s-wave pairing temperature was found to be several per cents of the Fermi energy.

One of the goals of this thesis is to develop a mean-field theory of the spinful Bose-Fermi mixture on a cubic lattice and determine the mean-field phase diagram from a numerical solution of the corresponding self-consistency equations.

Chapter 2

Lattice Bosons in a Staggered Potential

The Bose-Hubbard model and, in particular, its extensions including long-range interactions have been the focus of intense research in the last two decades. With the development of cold-atom experiments, it might soon be possible to observe supersolid and charge density wave phases characterized by an inhomogeneous density profile. Proposals for a mechanism for supersolidity in bosonic systems in the literature can be found from the early 70's up to present date [40, 33, 29]. Such phases are of interest to this work, since recent DMFT results [2] suggest that the BFM exhibits a supersolid phase for a certain range of the model parameters.

In this chapter, we review the Bose-Hubbard model and its properties. First, the phase boundary for the superfluid (SF) and Mott insulator (MI) transition is derived within the mean-field approximation, and extended to the presence of an alternating potential. We investigate the exactly solvable model of free bosons in a staggered potential, and demonstrate that condensation occurs not only for the $\vec{k} = 0$ mode, but also at $\vec{k} = \vec{\pi} = (\pi, \pi, \pi)$. This result is anticipated since both modes are equivalent in the reduced Brillouin zone, corresponding to a double unit cell which takes into account the reduced translational symmetry of the problem. We calculate the modifications to the MI-SF phase boundary. Further, the effect of the staggered potential in the SF phase is analyzed within a natural generalization of the Bogoliubov approximation, taking into account weak interactions between the bosons (compared to the hopping parameter).

2.1 The Bose-Hubbard Model

The Bose-Hubbard model was initially suggested to describe strongly correlated bosons in crystal lattices. Due to the fact that most particles found in solid state materials have fermionic nature, the experimental verification of theoretical predictions for bosonic systems has been achieved only recently [22].

The Hamiltonian is given by

$$H = -t_b \sum_{\langle ij \rangle} \left(b_i^\dagger b_j + h.c. \right) - \mu \sum_i n_i + \frac{U_{bb}}{2} \sum_i n_i \left(n_i - 1 \right). \tag{2.1}$$

The operators b_i and $b_i^\dagger$ obey bosonic commutation relations. As usual, $\langle ij \rangle$ denotes nearest neighbour pairs on the lattice. The hopping strength t_b is the energy gained by a boson when it 'hops' between nearest-neighbour sites due to quantum mechanical tunneling. The parameter μ is the chemical potential that fixes the filling (total number of particles per lattice site), and U_{bb} is the strength of the on-site interaction between the bosons, i.e. the energy one has to pay in order to accommodate two bosons on the same site. In the following, we are interested in unit filling (i.e. one boson per site on average), and μ will be chosen accordingly.

To gain physical insight into the behaviour of this system, consider first the case of no interactions: $U_{bb} = 0$. In this limit, the particles are free to move along the lattice without any restriction. Due to quantum statistics, the bosons will undergo Bose-Einstein condensation, occupying the lowest energy mode $k = 0$, as the dispersion relation for free particles in a simple cubic lattice reads $\varepsilon_k = -2t_b(\cos k_x + \cos k_y + \cos k_z)$. Each particle will maximally delocalize over the entire lattice (keeping the average density per site equal to unity). The phase-coherent system can then be described by a single wave function, corresponding to the ground state $|GS\rangle = \frac{1}{\sqrt{N!}} \left(b_{k=0}^\dagger\right)^N |0\rangle$, where $|0\rangle$ is the state with no particles. Since it is defined in momentum space, this state does not represent a state of a well-defined particle number (Fock state). Weak interactions will not destroy phase coherence, and the ground state in the limit $U_{bb}/t_b \to 0$ will be referred to as a superfluid (SF), according to the Landau criterion [18]

In the opposite limit (also known as the 'atomic limit'), we have $U_{bb}/t_b \to \infty$ and the dominant energy scale is given by the interaction energy. Therefore, the hopping events are kept to the minimum, and the kinetic energy can be safely neglected. To minimize the interaction energy, the bosons will tend to distribute themselves equally on every lattice site on average. In the case of unit filling, this means that we have only one particle per site. Moreover, the particles are localized quantum mechanically. The ground state is approximately (since $t_b \neq 0$) given by $|GS\rangle \approx \prod_i b_i^\dagger |0\rangle$,[1] which is a state of well-define particle number (corresponding to QM localization). This state is known as a Mott insulator (MI).

In between the limits discussed above, the model cannot be solved exactly, and so the ground state is not known. However, due to the bosonic nature of the particles, one might expect that at a certain critical value of U_{bb}/t_b the system undergoes a phase transition between the SF and the MI state. Since the model is exclusively dealt with at zero temperature, the phase transition will be purely due to the quantum uncertainty in localizing and dephasing the particles, and is therefore dubbed a quantum phase transition.

2.1.1 From a Mott Insulator to a Superfluid: A Quantum Phase Transition

The simplest way to find the approximate boundary between the SF and the MI phases is to use mean-field (MF) theory. The usefulness of this method relies on the weakness of quantum fluctuations around a stable minimum of the classical action, and is highly dependent on dimensionality. In 1d systems quantum fluctuations destroy the order, and MF fails at any finite temperature. The situation is somewhat better in 2d, but the true power of MF can be appreciated in dimensions $d \geq 3$.[2] The reason for this lies deeply in the theory of the Renormalization Group and Critical Phenomena [31], and is beyond the scope of this review.

In the case of the BH model, in order to get a description for the MI phase, we treat the

[1] this is true up to $O(t_b/U_{bb})$, as will be discussed in 2.2.2

[2] MF even becomes exact beyond $d = 4$

hopping parameter t_b as a small quantity. We seek a description in which the Hamiltonian is diagonal in the Fock (or particle number) basis, since we expect to find localized bosons. The key concept of MF theory is to keep the fluctuations small. We can make use of this to decouple the hopping term as follows:

$$\left(b_i^\dagger - \langle b_i^\dagger \rangle\right)\left(b_j - \langle b_j \rangle\right) \overset{!}{\approx} 0. \tag{2.2}$$

Rearranging, we have $b_i^\dagger b_j \approx b_i^\dagger \langle b_j \rangle + \langle b_i^\dagger \rangle b_j - \langle b_i^\dagger \rangle \langle b_j \rangle$.[3] Let us denote the SF density by n_0, and if we define the SF order parameter by $\sqrt{n}_0 = \psi = \langle b_i^\dagger \rangle = \langle b_i \rangle$, the kinetic energy becomes

$$H_{\text{kin}} = z t_b N_s \psi^2 - z t_b \sum_i \left(b_i^\dagger + b_i\right) \psi. \tag{2.3}$$

Here $z = 2d$ is the coordination number for the simple cubic lattice, and N_s is the total number of sites. The MF decoupling turned a second order off-diagonal (w.r.t. the Fock basis) term in the Hamiltonian into a first order diagonal one, which can be safely treated perturbatively, whenever the SF order parameter ψ is small. Since in the MI phase we expect that $\psi = 0$, if we assume that ψ is continuous (corresponding to a second-order phase transition), this method will provide us with the phase boundary, i.e. the curve where ψ starts to emerge. To this end, we write down the new Hamiltonian of the system as

$$\begin{aligned} \bar{H}_{\text{MF}} &= \sum_i h_i, \\ h_i &= \frac{1}{2}\bar{U} n_i (n_i - 1) - \bar{\mu} n_i - \psi \left(b_i^\dagger + b_i\right) + \psi^2, \end{aligned} \tag{2.4}$$

where we conveniently rescaled the system parameters, the bar denoting $\bar{\cdot} = \cdot / z t_b$. It is noteworthy that h is now a local Hamiltonian. This fact simplifies the perturbative treatment using Fock states significantly, and allows us to drop the summation over i. We can now separate $h_i = H_0 + \psi V$, and do perturbation theory in ψ. Here $H_0 = \frac{1}{2}\bar{U} n_i (n_i - 1) - \bar{\mu} n_i + \psi^2$, and $V = -\left(b_i^\dagger + b_i\right)$. Due to the orthogonality of the Fock states with different number of particles, we see immediately that the first order correction to the GS energy vanishes. Therefore, we have

$$\begin{aligned} E_n^{(2)} &= \psi^2 \sum_{m \neq n} \frac{|\langle n|V|m\rangle|^2}{E_m^{(0)} - E_n^{(0)}} \\ &= \psi^2 \left(\frac{n+1}{\bar{\mu} - \bar{U} n} - \frac{n}{\bar{\mu} - \bar{U}(n-1)} \right) \end{aligned} \tag{2.5}$$

for the second order correction to the ground state energy per site with n particles. Hence, perturbation theory generates a series expansion of the GS energy in terms of the SF order parameter, as follows

$$E_{\text{GS}} = a_0 + a_2 \psi^2 + a_4 \psi^4 + \dots \tag{2.6}$$

[3] Notice that we neglect the overall phase of the order parameter and assume that it is given by a real number.

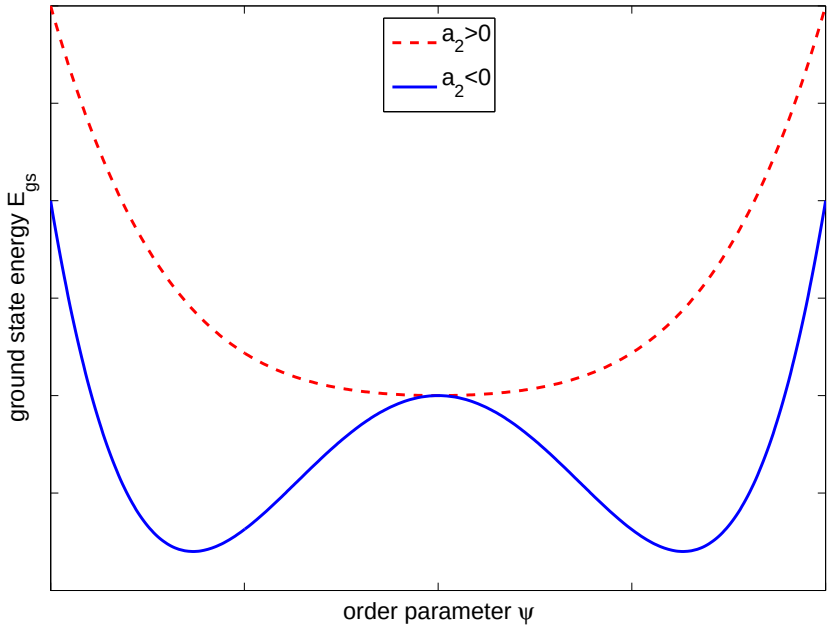

Figure 2.1: (color online): Schematic plot of the ground state energy as a function of the order parameter ψ: the Mexican hat potential. For $a > 0$ (symmetry not broken), the only minimum occurs at $\psi_0 = 0$, while for $a < 0$ we find non-trivial minima at $\pm\psi_0 \neq 0$.

Minimization of this expression w.r.t. ψ then fixes the SF order parameter and therefore the SF density n_0. The condition for the phase boundary is given by the equation $a_2 \stackrel{!}{=} 0$, since for $a_2 > 0$, one always has $\psi = 0$, while for $a_2 < 0$ we find two solutions $\psi_{1,2} \neq 0$. In the latter case, the system spontaneously chooses one of these 'vacua', and this phenomenon, usually referred to as 'Spontaneous Symmetry Breaking', lies at the heart of the Anderson-Higgs mechanism (see Fig. 2.1). In order for the theory to describe a stable minimum of the classical action, we require that the coefficient $a_4 > 0$.[4]

After making the procedure clear, the phase boundary is calculated to be

$$\bar{\mu}_{\pm} = \frac{1}{2}(\bar{U}_{bb}(2n-1)-1) \pm \sqrt{\bar{U}_{bb}^2 - 2\bar{U}_{bb}(2n+1)+1}, \tag{2.7}$$

which is plotted in Fig. 2.2. The different signs give the lower and upper boundary of the MI plateau for a given filling n. One observes the presence of the Mott plateaus. They are regions of constant particle number, and hence the whole phase is incompressible. The critical point $\bar{U}_c$ for a given filling n is given by the tip of the corresponding Mott lobe, and can be found by equating $\mu_- = \mu_+$. The expression reads $\bar{U}_c = 2n + 1 + \sqrt{(2n+1)^2 - 1}$. In our case of unit filling $n = 1$, we find $\left(\frac{U_{bb}}{t_b}\right)_c = 5.83z$.

[4]This is indeed the case, [50].

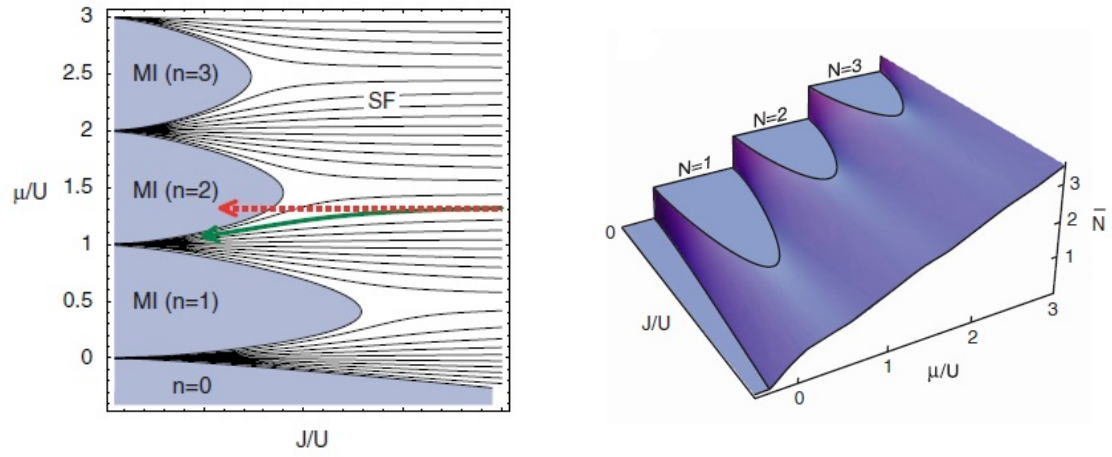

(a) (b)

Figure 2.2: (color online): Phase diagram of the Bose-Hubbard model: (a) Decreasing the value of t_b/U_{bb} (here J/U) at fixed μ, one enters a Mott lobe if the average density has been set precisely to an integer (red dashed line), while any deviation inevitably remains in the SF phase (solid green line). (b) Phase portrait of the Bose-Hubbard model. The MI phase is characterized by a constant average particle number leading to vanishing compressibility (figures adopted from [21]).

2.1.2 MI - SF Transition: The Cumulant Expansion

As we have seen, the MF description is useful to provide the leading order terms of the phase boundary. To improve the method, one needs to find a way to implement the effect of small fluctuations. In general, this is a hard task, which can be accomplished using quantum field theoretical methods. In fact, a further generalization including finite-T effects is possible [8, 13], so that the on-site interaction term is an arbitrary local function of the number operator $f_i(\hat{n}_i)$. It may even take different values at different lattice sites i. This can prove to be very useful to analyze the physics in the presence of an alternating or a trapping potential at extremely small but finite temperatures, the latter being the case in cold-atoms experiments. The only important condition is the locality of the interaction term (i.e. no nearest neighbour interactions or similar are allowed).

Since we want to apply this technique in a subsequent section, we revisit the main steps behind what shall be referred to as the *Cumulant Expansion Method* for deriving an Effective Action from BH-type Hamiltonians, [8]. For a trivial generalization of the method to several species, the reader is encouraged to consult Appendix B.

The starting point is the Hamiltonian

$$\begin{aligned} H &= H_0 + H_1 \\ H_0 &= \sum_i f_i(\hat{n}_i) \\ H_1 &= -\sum_{ij} t_{ij} b_i^\dagger b_j . \end{aligned} \tag{2.8}$$

Here f_i is an arbitrary site-dependent function, which includes the chemical potential, and the interaction term. Hence, H_0 models on-site interactions between the bosons, whose eigenenergies are readily calculated in the Fock basis to give $E = \sum_i f_i(n_i)$. The part H_1 is a generalized kinetic term, and will be treated perturbatively. The hopping constant t_b from the previous section is promoted to a hopping matrix t_{ij}, which is symmetric and has no diagonal elements (as these can always be absorbed into f_i).

Let us briefly outline the most important steps of this method:

1. Write down the generating functional, introducing current operators which break any global symmetries explicitly, and make it possible to look for the symmetry-broken phases.

2. Using imaginary-time formalism to incorporate finite-T effects, write down the total partition function via the evolution operator in a perturbative series expansion.

3. Note that since H_0 is not quadratic, one cannot apply Wick's theorem. However, as it is local, one employs the *Linked Cluster Theorem*, [13], to derive an on-site cumulant expansion for the free energy; the second cumulant being the Green's function of the free system.

4. Introduce the complex order parameter field ψ as the functional derivative of the free energy (calculated to the desired order in the hopping matrix t_{ij}) w.r.t. the corresponding current operator.

5. The Legendre transform of the free energy w.r.t. the order parameter ψ is the effective potential Γ for the order parameter to fourth order in ψ. Putting the coefficient in front of the term $|\psi|^2$ to zero yields the phase boundary.

Assuming a real, time and position-independent order parameter leads to the familiar expression for the effective potential which we identify with the ground state energy from the previous section:

$$\Gamma = N_s \frac{|\psi|^2}{a_2^{(0)}(0)} - |\psi|^2\gamma + O(\psi^4), \tag{2.9}$$

with $\gamma = \sum_{ij} t_{ij} = N_s z t_b$, and $a_2^{(0)}(j, \omega_m = 0)$ - the Matsubara transform of the Green's function to zeroth order in the hopping: $G_j^{(0)}(\tau) = \langle T_\tau b_j(0) b_j^\dagger(\tau)\rangle_{\mathcal{Z}_0}$, with $\mathcal{Z}_0 = \sum_{n=0}^{\infty} e^{-\beta f_i(n)}$ the partition function corresponding to H_0. Due to translational invariance, the Green's function is independent of the site index j, and hence $a_2^{(0)}(j, \omega_m = 0) = a_2^{(0)}(0)$.

To calculate an expression for the phase boundary, we thus need the zeroth order propagator $G_i^{(0)}(\omega_m)$, given by

$$a_2^{(0)}(i, \omega_m) = \frac{1}{\mathcal{Z}_0} \sum_{n=0}^{\infty} e^{-\beta f_i(n)} \left[\frac{n+1}{f_i(n+1) - f_i(n) - i\omega_m} - \frac{n}{f_i(n) - f_i(n-1) - i\omega_m} \right]. \tag{2.10}$$

At zero temperature, this expression reduces to

$$a_2^{(0)}(i, \omega) = \frac{n+1}{f_i(n+1) - f_i(n) - \omega} - \frac{n}{f_i(n) - f_i(n-1) - \omega}. \tag{2.11}$$

For $\omega = 0$ this turns out to be the same expression as in Eq. (2.5) when multiplied by ψ^2 in the formula for the effective action Eq. (2.9) above. The subsequent steps are the same as in Chapter 2.1.1, so there is no need to re-do the analysis. Let us emphasize that this method shall prove much easier to apply in the up-coming discussion when we introduce a staggered potential.

One could, in principle, continue the analysis and calculate other physical quantities of interest. However, we shall interrupt the discussion of the Mott phase at this point, and continue to the Bogoliubov description of the superfliud phase. We shall revisit the MI phase later on, but in the presence of a staggered potential.

2.1.3 The Superfluid Phase: Bogoliubov Approximation

After having analyzed the Bose-Hubbard model in the vicinity of the SF-MI phase transition, we turn our attention to the deep superfluid regime, where the order parameter ψ no longer can be assumed to be small. Therefore, the previous description in terms of perturbative series breaks down. In fact, in the case of weak interactions we expect that the superfluid density $n_0 \sim 1$, so that the system essentially resembles free bosons. In this case, the effect of interactions would be do deplete the condensate (usually referred to as 'quantum depletion'[5]). The physical picture behind this comes from scattering of a condensate off a non-condensate atom, in a way that the momentum of the non-condensate atom, which has initially been greater than zero (by definition of the condensate), is transferred to the condensate atom, thereby kicking it out of the condensate. As a result of momentum conservation, the non-condensate boson then condenses. Since this processes occur exclusively due to interactions, on average they maintain a constant fraction of the bosons out of the condensate (to be referred to as the 'excited fraction'). Therefore, even at zero temperature, the weakly interacting Bose gas never has all its constituents superfluid.

To model such a superfluid behaviour, it is natural to use a description in Fourier space, so that the kinetic energy operator is diagonal. Again, we are faced with the same problem as in the previous section, however, this time it is the interaction energy that is not diagonal. The BH Hamiltonian in momentum space reads

$$H = \sum_k (\varepsilon_k - \mu) b_k^\dagger b_k + \frac{U_{bb}}{2N_s} \sum_{k_1,k_2,k_3,k_4} b_{k_1}^\dagger b_{k_2}^\dagger b_{k_3} b_{k_4} \delta_{k_1+k_2,k_3+k_4}, \tag{2.12}$$

where the δ-function reflects momentum conservation. Keeping in mind that we want to describe the system in the limit, where the condensate fraction constitutes almost all of the bosons ($n_0 \sim 1$), and recalling that the condensate mode is at $\vec{k} = 0$, we are faced with the following problem. The ground state expectation value of the operators $\langle b_{k=0} \rangle \approx \langle b_{k=0}^\dagger \rangle \approx \sqrt{N_0}$ is of order $\sqrt{N_0} \gg 1$, whereas $\langle b_{k\neq 0} \rangle \approx \langle b_{k\neq 0}^\dagger \rangle \approx 1$ are all of order unity. This suggests the following approximation, known as the 'Bogoliubov approximation':

$$b_0 \longrightarrow b_0 + \sqrt{N_0}, \tag{2.13}$$

where for the new operators we have $\langle b_0 \rangle \approx \langle b_0^\dagger \rangle \approx 1$. The physical motivation for this is to

[5] A similar effect due to finite temperature is known as 'thermal depletion' and will not be taken under consideration in this chapter.

consider the condensate and the excited atoms separately.[6] Therefore, the new operators mix the excitations of the system above the SF ground state. Keeping only terms to quadratic order in the new operators, the Hamiltonian takes the form

$$\begin{aligned} H &\approx H_0 + \sqrt{N_0}(-zt_b + U_{bb}n_0 - \mu)\left(b_0^\dagger + b_0\right) \\ &\quad + \sum_k (\varepsilon_k - \mu + 2U_{bb}n_0) b_k^\dagger b_k + \frac{U_{bb}n_0}{2}\sum_k b_k^\dagger b_{-k}^\dagger + b_k b_{-k}, \\ H_0 &= (-zt_b - \mu)N_0 + \frac{U_{bb}n_0^2 N_s}{2}. \end{aligned} \tag{2.14}$$

For the approximation to describe the system around a stable equilibrium, we require that the linear terms in b_0 and $b_0^\dagger$ vanish, [50]. This condition provides the relation between the chemical potential and the condensate fraction as $\mu = -zt_b + U_{bb}n_0$. The constant H_0 shall soon become part of the ground state energy as a function of the condensate fraction, and represents just a constant energy shift. Thus, the goal is to diagonalize the Bogoliubov Hamiltonian

$$\begin{aligned} H_{\text{Bog}} &= \sum_k (\bar{\varepsilon}_k + U_{bb}n_0) b_k^\dagger b_k + \frac{U_{bb}n_0}{2}\sum_k b_k^\dagger b_{-k}^\dagger + b_k b_{-k} \\ &= \frac{1}{2}\sum_k \left(b_k^\dagger, b_{-k}\right) \begin{pmatrix} \bar{\varepsilon}_k + U_{bb}n_0 & U_{bb}n_0 \\ U_{bb}n_0 & \bar{\varepsilon}_k + U_{bb}n_0 \end{pmatrix} \begin{pmatrix} b_k \\ b_{-k}^\dagger \end{pmatrix} - \frac{1}{2}(\bar{\varepsilon}_k + U_{bb}n_0). \end{aligned} \tag{2.15}$$

Here we defined $\bar{\varepsilon}_k = \varepsilon_k + zt_b$. This can be easily done with the methods of Appendix A, using a pseudo-unitary[7] transformation M defined by $\vec{b}_k = M_k \vec{a}_k$ such that $M^\dagger H M$ is diagonal, where $(\vec{b}_k)^t = \left(b_k, b_{-k}^\dagger\right)$, and $(\vec{a}_k)^t = \left(a_k, a_{-k}^\dagger\right)$. The matrix M represents a hyperbolic rotation and is defined via

$$M = \begin{pmatrix} \sqrt{\frac{1}{2}\left(\frac{\bar{\varepsilon}_k + U_{bb}n_0}{E_k} + 1\right)} & \sqrt{\frac{1}{2}\left(\frac{\bar{\varepsilon}_k + U_{bb}n_0}{E_k} - 1\right)} \\ \sqrt{\frac{1}{2}\left(\frac{\bar{\varepsilon}_k + U_{bb}n_0}{E_k} - 1\right)} & \sqrt{\frac{1}{2}\left(\frac{\bar{\varepsilon}_k + U_{bb}n_0}{E_k} + 1\right)} \end{pmatrix}, \tag{2.16}$$

where $E_k = \sqrt{\bar{\varepsilon}_k^2 + 2U_{bb}n_0\bar{\varepsilon}_k}$ is the dispersion relation of the excitations (also known as the Bogoliubov spectrum). The diagonal Hamiltonian takes the form

$$\begin{aligned} H &= E_{\text{gs}} + \sum_k E_k a_k^\dagger a_k, \\ E_{\text{gs}} &= -\frac{U_{bb}n_0^2 N_s}{2} + \frac{1}{2}\sum_k E_k - (zt_b + U_{bb}n_0), \end{aligned} \tag{2.17}$$

[6] Some authors use the approximation in the from $b_0 \approx \sqrt{N_0}$, replacing the operator by its macroscopically occupied expectation value. We prefer the approximation (2.13), for it allows to fix the chemical potential by setting the linear terms in b_0 and $b_0^\dagger$ to zero. Also, notice that in the TD limit the two variations coincide, since the $k = 0$ mode does not contribute to the phase-space integrals, as it represents a set of measure zero.

[7] In doing the transformation, one must further require that the new operators also satisfy bosonic commutation relations, which results in the pseudo-unitarity of M: $M\Sigma M = \Sigma$, $\Sigma = \text{diag}(1, -1)$.

where we used that $\sum_k \varepsilon_k = 0$ by definition of the tight-binding dispersion. The operators a_k and $a_k^\dagger$ describe the excitations of the system, and the new ground state is defined by $a_k|GS\rangle = 0$ for all independent modes k.

The only quantity left to determine, in order to completely solve the approximated superfluid system, is the condensate fraction n_0. We can do this from the number equation by calculating the total particle density $n = N/N_s$ within a unit cell:

$$\begin{aligned} n &= \frac{1}{N_s}\langle GS|\hat{N}|GS\rangle = \frac{1}{N_s}\sum_k \langle b_k^\dagger b_k\rangle \longrightarrow \frac{N_0}{N_s} + \frac{1}{N_s}\sum_k \langle b_k^\dagger b_k\rangle \\ &= n_0 + \frac{1}{2N_s}\sum_k \langle \vec{b}_k^\dagger \mathbb{1} \vec{b}_k - 1\rangle = n_0 + \frac{1}{2N_s}\sum_k \langle \vec{a}_k^\dagger M_k^\dagger \mathbb{1} M_k \vec{a}_k - 1\rangle \\ &= n_0 + \frac{1}{2N_s}\sum_k \left(\left(\left(M^\dagger M \right)_k^{(22)} \right)^2 - 1 \right). \end{aligned} \tag{2.18}$$

Note that the matrix element $M_k^{(22)}$ also depends on the condensate fraction n_0. At unit filling $n = 1$, and (2.18) provides a self-consistency relation to find n_0. In the thermodynamic limit, we have

$$1 = n_0 + \frac{1}{2}\int_{\mathrm{BZ}} \frac{d^3k}{(2\pi)^3} \left(\frac{\bar{\varepsilon}_k + U_{bb} n_0}{E_k(n_0)} - 1 \right). \tag{2.19}$$

A numerical solution allows for a glimpse in the functional dependence of $n_0(t_b, U_{bb})$, as shown in Fig. 2.3 . As expected, interactions do deplete the condensate.

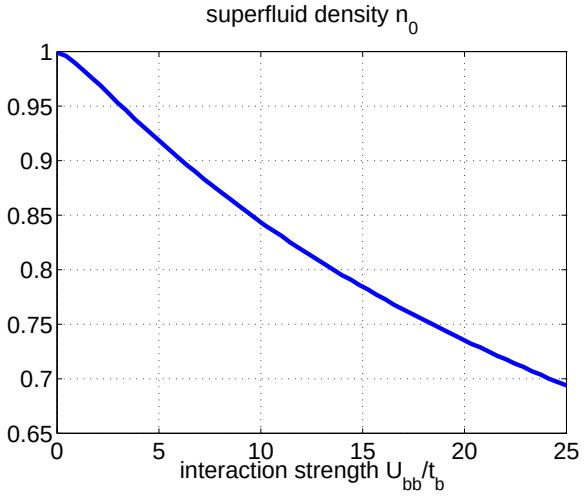

Figure 2.3: (color online): The SF fraction n_0 as a function of the interaction strength U_{bb}. A monotonic decrease in the condensate fraction n_0 is observed with increasing interaction strength.

Now that we have revised the most important features of the Bose-Hubbard model, we are ready to embark on a study of their generalization in the presence of a staggered potential.

2.2 The Bose-Hubbard Model with a Staggered Potential

In this section, we add a checker-board-type staggered potential to the Bose-Hubbard model. We investigate the system for an induced CDW and the effects it has on the condensate. Recently, Hen at. al [26] addressed a similar problem in the case of hardcore bosons. However, due to the hardcore constraint, they were only able to observe a CDW at half-filling.

The main question of interest is how an alternating potential modifies the familiar physics, derived in the previous sections. Since a staggered field will certainly reduce the particle density on half of the lattice sites, while increasing it on the remaining half it is natural to divide the entire lattice into two sublattices A and B, respectively. Hence, to be able to make use of translational invariance, we have to double the unit cell or, equivalently, reduce the Brillouin zone. As this procedure changes the band structure of the system, a possible scenario is that the condensate fraction is shared between several momentum modes. Indeed, as we will show shortly, this happens to be the case even for the free staggered Bose gas, where the alternating potential makes it possible to occupy the modes $\vec{k} = 0$ and $\vec{k} = \vec{\pi}$ simultaneously.

An interesting question in this context would be to quantify how much condensate is contained in each mode, and how this ratio changes with the strength of the staggered field. Intuitively, one would expect the $\vec{\pi}$ mode occupation to gradually increase when increasing the alternating potential. Since all particles are condensed in the non-interacting model, this results in a 'depletion' of the $\vec{k} = 0$ mode. In the case of an infinite potential strength, on the other hand, one expects all the particles to be forced to occupy one of the sublattices. We shall soon show that in this case the two modes accommodate half of the total condensate each.

After investigating the free case, we shall switch on weak interactions, and analyze the modification of the physics caused by them. To this end, we calculate the induced change in the MI-SF phase boundary. Further the Bogoliubov approximation is extended in a suitable way to generalize the case without a staggered field. The corresponding number equation is derived, and the shift of the particle density on each sublattice is determined.

2.2.1 Free Bosons in a Staggered Field

We start from the Hamiltonian for free bosons on a lattice at unit filling, and switch on an additional staggered field:

$$H = -t_b \sum_{\langle ij \rangle} \left(b_i^\dagger b_j + h.c. \right) - \mu \sum_i n_i + U_{bf} \sum_i \left[1 - \alpha \left(-1 \right)^i \right] n_i. \tag{2.20}$$

The alternating term has to be read as $(-1)^i = (-1)^{i_x + i_y + i_z}$ in $d = 3$. The staggering strength is measured by a parameter $\alpha \in [0, 1]$, while the total sign of the potential is kept positive, for reasons that will become clear in our subsequent discussion of the Bose-Fermi mixture. At this moment, the picture one has to keep in mind is that in the BF mixture, treating the density-density interspecies interaction within a self-consistent Hartree-Fock (or simply MF) approximation induces to first order a background potential for the bosons, given by the expectation value of the fermionic density. In the following, we solve this model exactly. This is possible, as it describes free bosons.

Again, to model a superfluid phase, it is advantageous to use a momentum-space description. The Hamiltonian (2.20) then takes the form

$$H = \sum_{k\in \mathrm{BZ}} \left(\varepsilon_k - \mu + U_{bf}\right) b_k^\dagger b_k - \alpha U_{bf} \sum_{k\in \mathrm{BZ}} b_{k+\pi}^\dagger b_k. \tag{2.21}$$

The kinetic energy is straightforward. The expression for the staggered term can be understood by writing $(-1)^i = e^{i\pi(i_x+i_y+i_z)}$. When performing the Fourier transform along each coordinate direction separately, each momentum direction acquires a shift of π. Summing over the lattice results in a δ-function of the momentum variables which, due to the shift reads $\delta_{k_1,k_2+\pi}$.[8]

To make progress, we need to reduce the Brillouin zone, defining new operators as follows

$$b_k = \begin{cases} \alpha_k & \text{for } \; k \in \mathrm{BZ}' \\ \beta_{k\pm\pi} & \text{for } \; k \notin \mathrm{BZ}' \end{cases} \tag{2.22}$$

The $\pm$-sign is used to flip one or several of the components of $\vec{\pi}$ simultaneously. The reduced Brillouin zone is defined as the part of the BZ in which the tight-binding dispersion becomes negative, formally given by $\mathrm{BZ}' = \{\vec{k} \in \mathrm{BZ} : \cos(k_x) + \cos(k_y) + \cos(k_z) \geq 0\}$. It is pictorially shown in 3D in Fig.2.4.

The Hamiltonian in the new operators reads

$$\begin{aligned} H &= \sum_{k\in \mathrm{BZ}'} \left(\varepsilon_k - \mu + U_{bf}\right) \alpha_k^\dagger \alpha_k + \left(-\varepsilon_k - \mu + U_{bf}\right) \beta_k^\dagger \beta_k - \alpha U_{bf} \sum_{k\in \mathrm{BZ}'} \left(\alpha_k^\dagger \beta_k + h.c.\right) \\ &= \sum_{k\in \mathrm{BZ}'} \left(\alpha_k^\dagger, \beta_k^\dagger\right) \begin{pmatrix} \varepsilon_k - \mu + U_{bf} & -\alpha U_{bf} \\ -\alpha U_{bf} & -\varepsilon_k - \mu + U_{bf} \end{pmatrix} \begin{pmatrix} \alpha_k \\ \beta_k \end{pmatrix}. \end{aligned} \tag{2.23}$$

Notice that in the reduced Brillouin zone BZ' the dispersion $\varepsilon_k \leq 0$ for all modes k. Diagonalizing the Hamiltonian is explained in detail in Appendix A. In this case, this should be done with a unitary(!) transformation $M^{\mathrm{free}} \in U(2)$, to preserve the bosonic commutator relations. Using the short-hand notation $(\vec{\alpha}_k)^t := (\alpha_k, \beta_k)$, we define a matrix M^{free} by $\vec{\alpha}_k = M^{\mathrm{free}} \vec{d}_k$, such that $\left(M^{\mathrm{free}}\right)^\dagger H M^{\mathrm{free}} = \mathit{diagonal}$, given by

$$M^{\mathrm{free}} = \begin{pmatrix} A^{\mathrm{free}} & B^{\mathrm{free}} \\ B^{\mathrm{free}} & -A^{\mathrm{free}} \end{pmatrix}, \tag{2.24}$$

with

$$A_k^{\mathrm{free}} = \sqrt{\frac{1}{2}\left(1 - \frac{\varepsilon_k}{\sqrt{\left(\alpha U_{bf}\right)^2 + \varepsilon_k^2}}\right)}, \quad B_k^{\mathrm{free}} = \sqrt{\frac{1}{2}\left(1 + \frac{\varepsilon_k}{\sqrt{\left(\alpha U_{bf}\right)^2 + \varepsilon_k^2}}\right)}. \tag{2.25}$$

The resulting Hamiltonian is diagonal in the operators $\vec{d}$, and reads

$$H = \left(U_{bf} - \mu\right) \frac{N_s}{2} + \sum_{k\in \mathrm{BZ}'} \epsilon_k \left(d_{1,k}^\dagger d_{1,k} - d_{2,k}^\dagger d_{2,k}\right), \tag{2.26}$$

with $\epsilon_k = -\sqrt{\left(\alpha U_{bf}\right)^2 + \varepsilon_k^2}$. The stability of the bosonic system requires the positivity of the Hamiltonian for all modes k,[9] which constrains the chemical potential to satisfy $\mu = U_{bf} - \sqrt{\left(\alpha U_{bf}\right)^2 + (z t_b)^2}$.

[8] we shall drop the vector arrows from the momenta from now on, here π has to be read as $\vec{\pi} = (\pi, \pi, \pi)$.

[9] for an explanation of this statement, please consult Appendix A

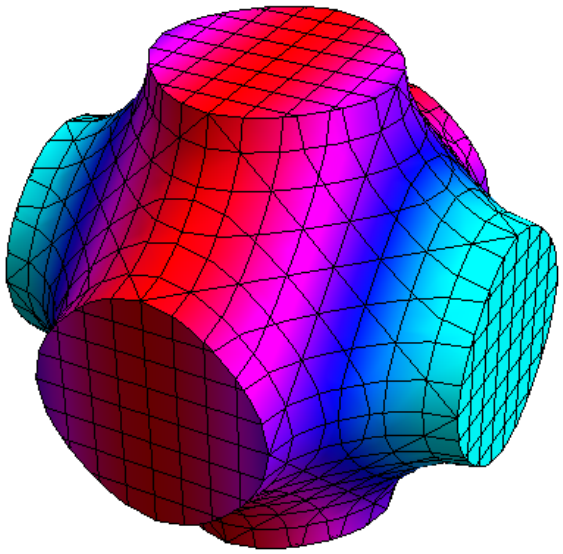

Figure 2.4: (color online): The reduced Brillouin zone of a simple cubic lattice has the shape of a pipe junction. It is the integration domain of merely all the integrals in this thesis, which are therefore calculated numerically (colours are used for aesthetic purposes only).

Having diagonalized the Hamiltonian, we can start discussing the physics of the system. First, observe that there is a lowest energy state in the spectrum - c.f. Fig. 2.5. Since we are dealing with free bosons, a BEC will form in the $\vec{k} = 0$ state in the band of the $d_{1,k}$ operators. Therefore, the ground state can be written as

$$|GS\rangle = \frac{1}{\sqrt{N!}} \left(d^{\dagger}_{1,k=0} \right)^{N} |0\rangle. \tag{2.27}$$

Notice that the energy of the condensate, $-\sqrt{(\alpha U_{bf})^2 + (zt_b)^2}$, is always higher than the corresponding value without the alternating potential, given by $-zt_b - \alpha U_{bf}$. This is expected, since the staggered potential induces a Charge Density Wave (CDW) which inevitably increases the kinetic energy of the system, compared to the flat density profile at $\alpha = 0$.

As a first check, let us calculate the expectation value of the particle number operator $\hat{N}$

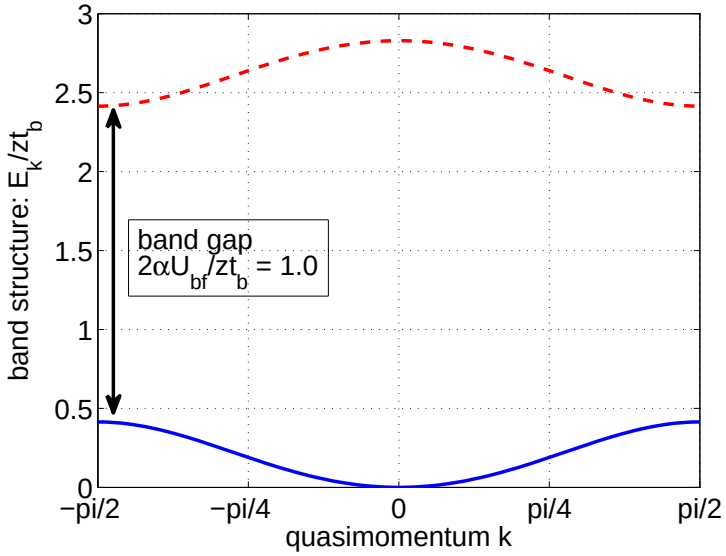

Figure 2.5: (color online): Band structure in the presence of the staggered field: an energy gap $2\alpha U_{bf}/zt_b$ opens at the edge of the reduced Brillouin zone.

in the ground state, which gives the total number of particles in the condensate:

$$\begin{aligned} N_0 &= \langle GS|\hat{N}|GS\rangle = \sum_{k\in \mathrm{BZ}} \langle GS|b_k^\dagger b_k|GS\rangle = \sum_{k\in \mathrm{BZ}'} \langle GS|\alpha_k^\dagger\alpha_k + \beta_k^\dagger\beta_k|GS\rangle \\ &= \sum_{k\in \mathrm{BZ}'} \langle GS|\vec{d}_k^\dagger \left(M^{\mathrm{free}}\right)^\dagger \mathbb{1} M^{\mathrm{free}} \vec{d}_k|GS\rangle = \sum_{k\in \mathrm{BZ}'} \langle GS|d_{1,k}^\dagger d_{1,k} + d_{2,k}^\dagger d_{2,k}|GS\rangle \\ &= \sum_{k\in \mathrm{BZ}'} \langle GS|d_{1,k}^\dagger d_{1,k}|GS\rangle = \sum_{k\in \mathrm{BZ}'} N\delta_{k,0} = N, \end{aligned} \tag{2.28}$$

where we used the unitarity of M^{free} in the first equality on the second line. As expected, all bosons are present in the ground state. The difference to the free case comes from the fact that the d_k operators are linear combinations of the operators b_k and $b_{k+\pi}$. Hence, a condensate at $\vec{k}=0$ in the band of the d_1 operators amounts to a linear superposition of states with condensates at $\vec{k}=0$ and $\vec{k}=\vec{\pi}$, respectively. This proves the macroscopic population of a second momentum mode, in contrast to the model without staggering.

A natural question to ask in this case is how much of the condensate can be found in the $\vec{k}=0$ and $\vec{k}=\vec{\pi}$ states. This can be calculated straightforwardly from

$$\begin{aligned} n_{k=0} &= \langle GS|\hat{n}_{k=0}|GS\rangle = \langle GS|\alpha_0^\dagger\alpha_0|GS\rangle = \langle GS|\vec{\alpha}_0^\dagger \begin{pmatrix} 1 & 0 \\ 0 & 0 \end{pmatrix} \vec{\alpha}_0|GS\rangle \\ &= \left\langle \left(A_0^{\mathrm{free}} d_{1,0}^\dagger + B_0^{\mathrm{free}} d_{2,0}^\dagger\right)\left(A_0^{\mathrm{free}} d_{1,0} + B_0^{\mathrm{free}} d_{2,0}\right)\right\rangle = \left(A_0^{\mathrm{free}}\right)^2 \langle d_{1,0}^\dagger d_{1,0}\rangle = \left(A_0^{\mathrm{free}}\right)^2 N, \\ n_{k=\pi} &= \langle GS|\hat{n}_{k=\pi}|GS\rangle = \langle GS|\beta_0^\dagger\beta_0|GS\rangle = \langle GS|\vec{\beta}_0^\dagger \begin{pmatrix} 0 & 0 \\ 0 & 1 \end{pmatrix} \vec{\beta}_0|GS\rangle \\ &= \left\langle \left(B_0^{\mathrm{free}} d_{1,0}^\dagger - A_0^{\mathrm{free}} d_{2,0}^\dagger\right)\left(B_0^{\mathrm{free}} d_{1,0} - A_0^{\mathrm{free}} d_{2,0}\right)\right\rangle = \left(B_0^{\mathrm{free}}\right)^2 \langle d_{1,0}^\dagger d_{1,0}\rangle = \left(B_0^{\mathrm{free}}\right)^2 N. \end{aligned} \tag{2.29}$$

From now, on we shall denote $A_0^{\text{free}} = A^{\text{free}}$ and $B_0^{\text{free}} = B^{\text{free}}$. As expected, we have $\left(A^{\text{free}}\right)^2 + \left(B^{\text{free}}\right)^2 = 1$, which agrees with our previous calculation of the total particle number in the ground state, and is equivalent to the unit filling condition. The parameters A^{free} and B^{free} represent the probability amplitude[10] of finding a boson in the $\vec{k} = 0$ and $\vec{k} = \vec{\pi}$ condensates, respectively. They depend on the two parameters of the model given by zt_b and αU_{bf} that define the two relevant energy scales in the problem. The fractions are plotted in Figs. 2.6 and 2.7.

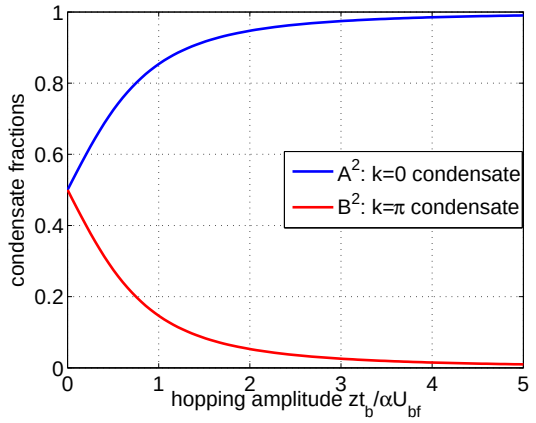

Figure 2.6: (color online): The condensate fractions at $\vec{k} = 0$ (blue line) and $\vec{k} = \vec{\pi}$ (red line) as a function of the hopping parameter $zt_b/\alpha U_{bf}$.

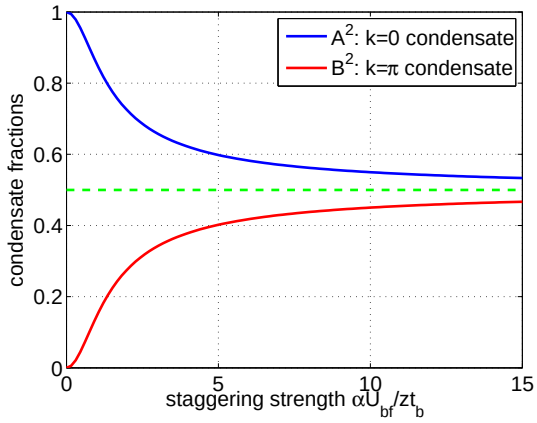

Figure 2.7: (color online): The condensate fractions at $\vec{k} = 0$ (blue line) and $\vec{k} = \vec{\pi}$ (red line) as a function of the staggering strength $\alpha U_{bf}/zt_b$.

Clearly, in the limit $\alpha \to 0$, we find $n_{k=0} \longrightarrow 1$ and $n_{k=\pi} \longrightarrow 0$, which reduces to the case of free bosons in a lattice. The opposite limit of infinite potential strength $\alpha U_{bf} \to \infty$ yields $n_{k=0} \searrow \frac{1}{2}$, and $n_{k=\pi} \nearrow \frac{1}{2}$, respectively. Therefore, for free bosons, the two condensates are never equally occupied, and $n_{k=0} > n_{k=\pi}$ is always satisfied.

The last issue that we address in our analysis of the free model is how the bosonic on-site density is modified due to the presence of the alternating potential. To this end, it is easiest to calculate the total density at the site $\vec{r}_i = 0$:

$$\begin{aligned} n_{\vec{r}_i=0} &= \langle GS|\hat{n}_{\vec{r}_i=0}|GS\rangle = \frac{1}{N_s}\sum_{k,k'\in \text{BZ}} \langle b_k^\dagger b_{k'}\rangle = \\ &= \frac{1}{N_s}\sum_{k,k'\in \text{BZ}'} \langle \vec{\alpha}_k^\dagger \begin{pmatrix} 1 & 1 \\ 1 & 1 \end{pmatrix} \vec{\alpha}_{k'}\rangle = \frac{1}{N_s}\sum_{k,k'\in \text{BZ}'} \langle \vec{d}_k^\dagger \left(M^{\text{free}}\right)^\dagger \begin{pmatrix} 1 & 1 \\ 1 & 1 \end{pmatrix} M^{\text{free}} \vec{d}_{k'}\rangle \\ &= \frac{N}{N_s}\left(1 + \frac{\alpha U_{bf}}{\sqrt{(\alpha U_{bf})^2 + (zt_b)^2}}\right). \end{aligned} \tag{2.30}$$

The condition for unit filling is given by $N = N_s$, which gets rid of the prefactor in (2.30). As we expected, the bosonic density at $\vec{r}_i = 0$ is enhanced, as the staggered potential lowers the energy of the levels at this site. Furthermore, by translational invariance,[11] this result holds

[10] we neglect the complex phase factor here
[11] with respect to the doubled unit cell

for all the sites on sublattice A. It will be useful to analyze the deviation of the density from the one at $\alpha = 0$:

$$\eta_0(U_{bf}, t_b) = \frac{\alpha U_{bf}}{\sqrt{(\alpha U_{bf})^2 + (zt_b)^2}}. \tag{2.31}$$

Clearly, we have $\eta_0 \in [0, 1]$ which must be the case at unit filling. If there is no alternating potential imposed, we recover the familiar unit filling result $\eta_0 = 0$. For infinite potential strength, on the other hand, we find $\eta_0 = 1$, and thus all the particles are in one of the sublattices, while the other sublattice is completely empty. It is also interesting to note that when the bosons are very fast, i.e. when $zt_b \gg \alpha U_{bf}$, the effect of the staggered field is diminished. The behaviour of $\eta_0(U_{bf}, t_b)$ is shown in Figs. 2.8 and 2.9.

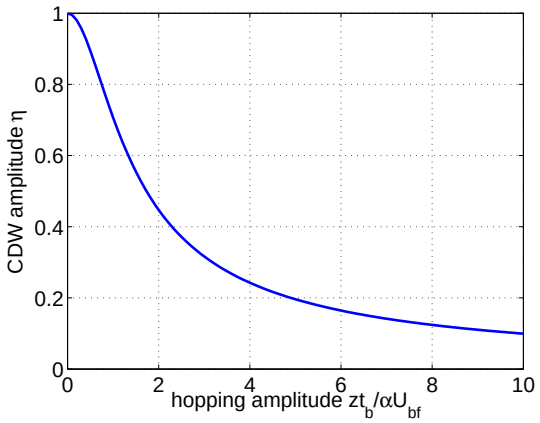

Figure 2.8: (color online): The CDW amplitude η_0 as a function of the hopping parameter $zt_b/\alpha Ubf$.

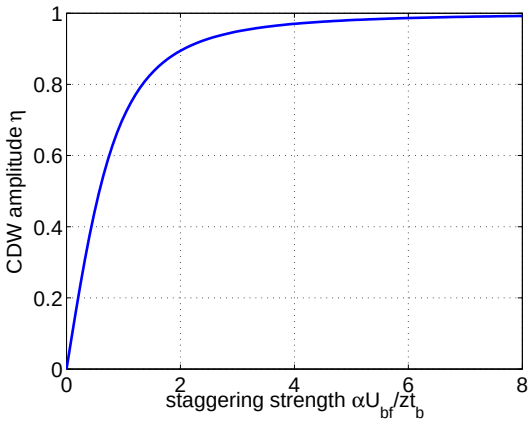

Figure 2.9: (color online): The CDW amplitude η_0 as a function of the hopping parameter $\alpha U_{bf}/zt_b$.

2.2.2 The Mott Insulator-Superfluid Transition in the Presence of a Staggered Field

In this section, we are interested in finding the phase boundary of the MI-SF transition in the presence of a staggered potential. Our results may be viewed as a generalization of the discussion in Section 2.1.1. Of particular interest is the functional behaviour of U_{bf} on the hopping parameter t_b at unit filling. Before we apply the Effective Action Approach to first order in the hopping element t_b, we gain more insight into the physical state deep into the MI phase with the alternating potential switched on.

Consider again the atomic limit $U_{bb}/t_b \gg 1$. As mentioned earlier, if there were no hopping at all, the ground state at unit filling would be given by the state $|\mathrm{IN}\rangle = \prod_i b_i^\dagger |0\rangle$. We shall refer to this state as the *ideal insulator* (IN) in the following. Turning on the nearest neighbour hopping produces corrections to this, which can be understood within first order perturbation theory. The ground state, on the other hand, acquires corrections of order t_b^2/U_{bb} due to a particle occasionally hopping on top one of its neighbours, and back. As this can be done by any particle with the same probability, quantum mechanics requires to sum the probability amplitudes for all possible ways this might happen. Hence, a better approximation to the

ground state is given by

$$|GS\rangle = |\mathrm{IN}\rangle + \frac{t_b}{U_{bb}} \sum_{\langle ij \rangle} b_i b_j^\dagger |\mathrm{IN}\rangle + O\left(\left(\frac{t_b}{U_{bb}}\right)^2\right) \tag{2.32}$$

This state is given in terms of pictures in Fig. 2.10

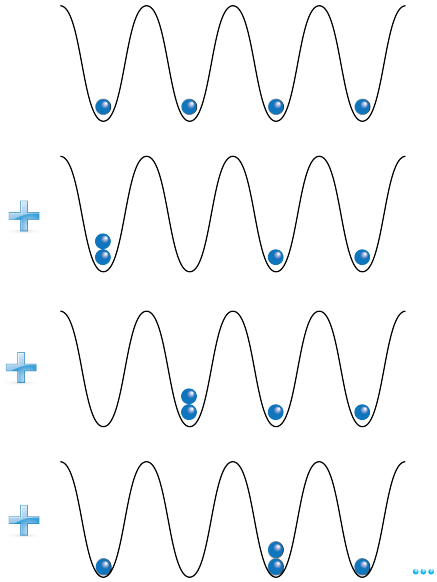

Figure 2.10: The Mott insulator state: the highest weight in the superposition has the ideal insulator (IN) state (on top). Below it, some of the first order corrections $\sim t_b/U_{bb}$ are shown.

Now, imagine we turn on the staggering αU_{bf}. Clearly, this shifts the energy levels up on every other site (which we shall refer to as sublattice B). Let us now split the first-order correction to this state in two sums over the two sublattices A and B:

$$\sum_{\langle ij \rangle} b_i b_j^\dagger |\mathrm{IN}\rangle = \sum_{j \in A} b_i b_j^\dagger |\mathrm{IN}\rangle + \sum_{j \in B} b_i b_j^\dagger |\mathrm{IN}\rangle \tag{2.33}$$

The states corresponding to the two sums on the r.h.s. are pictured in Fig. 2.11 for a $1d$ system. Due to the alternating potential, the two contributions from the first order correction in Eq. (2.33) will necessarily have different energy. According to our labelling, the states corresponding to the summation over the B sublattice will be energetically less favourable. An equivalent viewpoint would be to think of the chemical potential on the B sublattice to be shifted as $\mu_B \longrightarrow \mu - U_{bf}$. Therefore, if any alternating potential is switched on, no matter how weak, it would cause the dominant part of the corrections to the $|\mathrm{IN}\rangle$ to be such that the particles stack up on sublattice A. This process minimizes the total energy and leads naturally to a charge density wave (CDW) in the insulating phase.

Let us now abandon the atomic limit and approach the phase transition line. We want to apply the Cumulant Expansion method (cf. Appendix B) to the staggered system. To this end, the Green's function to zeroth order in the hopping amplitude t_b needs to be calculated. The crucial difference this time is that it will depend on the lattice site i, as the staggering

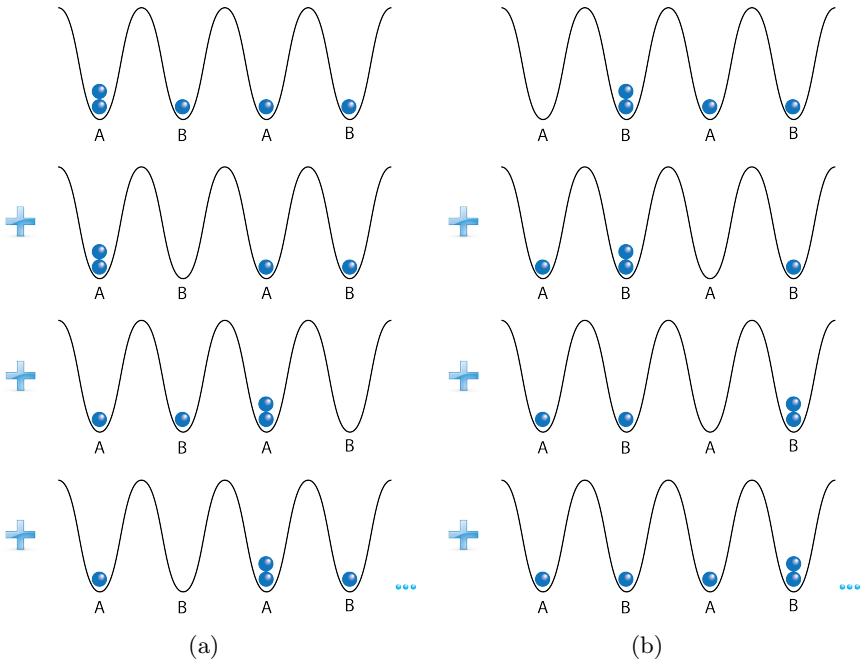

Figure 2.11: First order corrections to the ideal insulator in the presence of the staggered potential: sublattice A (a), sublattice B (b). The staggered potential makes it less favourable for a boson to hop to sublattice B. Therefore, the states from panel (a) are energetically preferred to these in (b).

order breaks translational symmetry.[12] On the other hand, part of the symmetry is still preserved, and so we only need to calculate $G^{(0)}_{A/B}$ on the two sublattices A and B.

We choose $\alpha = 1$ for simplicity, so that the external potential induces maximal staggering. For the generalized interaction term we have $f_i(n) = [U_{bf}(1+(-1)^i) - \mu]n + \frac{U_{bb}}{2}n(n-1)$. The Green's function at zero frequency, and $T = 0$ is then given by

$$\begin{aligned} G^{(0)}_A(0) &= \frac{n+1}{f_0(n+1) - f_0(n)} - \frac{n}{f_0(n) - f_0(n-1)} = \frac{\tilde{\mu} - \frac{U_{bb}}{2}}{(\tilde{\mu} + U_{bb}n)^2 - \left(\frac{U_{bb}}{2}\right)^2}, \\ G^{(0)}_B(0) &= \frac{n+1}{f_1(n+1) - f_1(n)} - \frac{n}{f_1(n) - f_1(n-1)} = \frac{-\mu - U_{bb}}{(-\mu + U_{bb}n)(-\mu - U_{bb} + U_{bb}n)}, \end{aligned} \tag{2.34}$$

with the shifted chemical potential $\tilde{\mu} = 2U_{bf} - \frac{U_{bb}}{2} - \mu$.

The effective potential takes the form

$$\Gamma[\psi] = \frac{N_s\psi^2}{2}\left(\frac{1}{G^{(0)}_A(0)} + \frac{1}{G^{(0)}_B(0)}\right) - \psi^2 z t_b N_s + O(\psi^4). \tag{2.35}$$

At this place we have done a further approximation: We assume that the effect of the staggered density on the order parameter is negligible in the immediate vicinity of the transition line as approached from within the SF phase. In principle, we would need to distinguish between the values the order parameter takes on the sublattices A and B, as is discussed in Appendix B. To argue that this does not play an important role, we start from the general case. There is indeed a coupling of the form $\psi^2_A\psi^2_B$, but it is of fourth order, and hence can be safely neglected for ψ near the phase boundary. In the remaining terms, we write $\psi_A = \psi + \eta$ and $\psi_B = \psi - \eta$, where η is small compared to ψ. The leading contribution from this transformation results in an additional term in the effective action which scales like $\left(\frac{1}{G_A} - \frac{1}{G_B}\right)2\eta\psi \sim U_{bf}\eta\psi$. Since $\eta \ll \psi$, this term will not influence the nature of the phase transition in the immediate vicinity of the critical line.

To find the phase boundary for a Landau second order transition, we need to set the coefficient in front of the quadratic term to zero. This yields

$$\begin{aligned} 2zt_b &\stackrel{!}{=} \frac{1}{G^{(0)}_A(0)} + \frac{1}{G^{(0)}_B(0)} \\ &= \frac{-2\mu^2 + 2\mu(2n-1)U_{bb} - (n-3)nU^2_{bb}}{\mu + U_{bb}} - \frac{n(n+1)U^2_{bb}}{\mu + U_{bb} - 2U_{bf}} + 2U_{bf}. \end{aligned} \tag{2.36}$$

For $U_{bf} = 0$, this reduces to the result of Section 2.1.2. The condition for unit filling is approximately satisfied with the choice of $\mu = \frac{U_{bb}}{2} + U_{bf}$, and $n = 1$. This yields

$$U_{bf} = \frac{U_{bb}}{2}\sqrt{\frac{6zt_b - U_{bb}}{\frac{2}{3}zt_b - U_{bb}}}. \tag{2.37}$$

The phase boundary is shown in Fig. 2.12. Notice the non-analytic behaviour of the curve at the intercepts with the two axes. For $t_b = 0$, the value $1/2$ is special, since increasing the ratio U_{bf}/U_{bb} beyond it makes it energetically favourable for the bosons to form a CDW

[12] The procedure is explained to somewhat greater detail in Appendix B

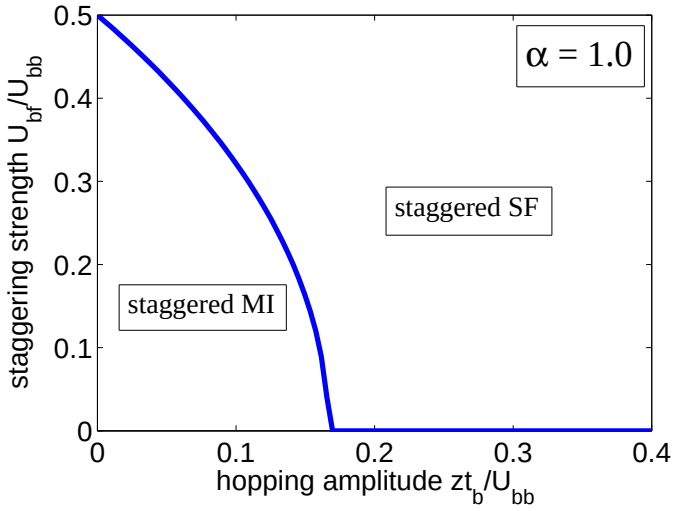

Figure 2.12: (color online): MI-SF phase boundary as a function of the hopping parameter

with a double occupancy on every other site. On the contrary, for $U_{bf}/U_{bb} < 1/2$, a uniform density minimizes the energy of the system. For $U_{bf} = 0$, we recover the MI to SF transition at $U_{bb}/t_b = 6z$, which is close to the previously calculated value of $U_{bb}/t_b = 5.83z$. The mismatch is due to the approximate value of the chemical potential used.

2.2.3 Induced Supersolidity and the Generalized Bogoliubov Approximation

Our next goal is to revisit and generalize the Bogoliubov approximation to the case of staggered potential. We are interested in analyzing the quantum depletion of the two condensates at $\vec{k} = 0$ and $\vec{k} = \vec{\pi}$ due to interactions. The latter also modify the amplitude of the induced charge density wave. Hence, we believe that (at least) to first order, the physical properties of a bosonic supersolid[13] is correctly described by the subsequent analysis.

The starting point is the Bose-Hubbard Hamiltonian in a staggered external field:

$$H = \sum_k (\varepsilon_k - \mu + U_{bf}) b_k^\dagger b_k - \alpha U_{bf} \sum_k b_{k+\pi}^\dagger b_k + \frac{U_{bb}}{2N_s} \sum_{k_1,k_2,k_3,k_4} b_{k_1}^\dagger b_{k_2}^\dagger b_{k_3} b_{k_4} \delta_{k_1+k_2,k_3+k_4}. \quad (2.38)$$

In the case of no staggered potential, the Bogoliubov prescription requires to separate the $\vec{k} = 0$ mode, since its occupation is macroscopic in the weakly-interacting regime. The motivation for this comes from the free model, which undergoes Bose-Einstein condensation populating the corresponding state macroscopically.

The results of Chapter 2.2.1 suggest that we should look for the condensate at $\vec{k} = \vec{\pi}$ as well. As will be shown below, the correct way of doing this is the following:

$$b_k \longrightarrow b_k + \begin{cases} A\sqrt{N_0}\delta_{k,0}, & k \in \mathrm{BZ}' \\ B\sqrt{N_0}\delta_{k\pm\pi,0}, & k \in \mathrm{BZ}\backslash\mathrm{BZ}'. \end{cases} \quad (2.39)$$

[13]Since the state considered in this section does not display a spontaneously broken charge symmetry, we shall avoid calling it a SS, and rather use the description 'staggered superfluid'.

To motivate this, recall that in the non-interacting case the condensate is in the $\vec{k} = 0$ mode of the $d_{1,k}$ operators. Denoting by N_0 the total condensate fraction, and applying the Bogoliubov prescription yields

$$d_{1,k} \longrightarrow d_{1,k} + \sqrt{N_0}\delta_{k,0}. \tag{2.40}$$

To understand what this means for the initial bosonic operators b_k, we need to invert the relation between the $\vec{d}_k$'s and the $\vec{\alpha}_k$'s:

$$\begin{aligned}
\vec{\alpha}_k = \left(M_k^{\text{free}}\right)^{-1}\vec{d}_k \longrightarrow \left(M_k^{\text{free}}\right)^{-1}\left(\vec{d}_k + \begin{pmatrix}\sqrt{N_0}\\ 0\end{pmatrix}\delta_{k,0}\right) &= \vec{\alpha}_k + \left(M_0^{\text{free}}\right)^{-1}\begin{pmatrix}\sqrt{N_0}\\ 0\end{pmatrix}\delta_{k,0} \\
\alpha_k \longrightarrow \alpha_k + \left(M_0^{\text{free}}\right)^{-1}_{11}\sqrt{N_0}\delta_{k,0} &= \alpha_k + A^{\text{free}}\sqrt{N_0}\delta_{k,0} \\
\beta_k \longrightarrow \beta_k + \left(M_0^{\text{free}}\right)^{-1}_{21}\sqrt{N_0}\delta_{k,0} &= \beta_k + B^{\text{free}}\sqrt{N_0}\delta_{k,0}.
\end{aligned} \tag{2.41}$$

Recalling again the relation between the operators α_k, β_k and b_k given in (2.22), we arrive at (2.39). As before, A denotes the probability amplitude of finding a bosons in the $\vec{k} = 0$ condensate, while B - the probability of finding it in the $\vec{k} = \vec{\pi}$ condensate. The superindex 'free' in these quantities refers to the free case, to distinguish them from the interacting one, as the interactions are expected to cause modifications. Again, they fulfil the relation $A^2+B^2 = 1$, as they measure fractions of the superfluid density. In the case of no interactions, we shall find $A = 1$ and $B = 0$, so that we recover the original Bogoliubov approximation.

Applying this procedure results in the following Hamiltonian:

- To 0^{th} order in the operators b_0 and b_π we have[14]

$$H_0 = N_0\left[-zt_b(A^2 - B^2) - \mu + U_{bf} - \alpha U_{bf}2AB\right] + N_s\frac{U_{bb}}{2}n_0^2(A^4+6A^2B^2+B^4). \tag{2.42}$$

- To 1^{st} order in the operators b_0 and b_π we find

$$\begin{aligned}
&\sqrt{N_0}\left[(-zt_b - \mu + U_{bf})A - \alpha U_{bf}B + n_0U_{bb}A(1 + 2B^2)\right](b_0^\dagger + b_0) \\
+&\sqrt{N_0}\left[(zt_b - \mu + U_{bf})B - \alpha U_{bf}A + n_0U_{bb}B(1 + 2A^2)\right](b_\pi^\dagger + b_\pi).
\end{aligned} \tag{2.43}$$

- We stop with the 2^{nd} order:

$$\sum_{k\in\text{BZ}}\xi_k b_k^\dagger b_k + h\sum_{k\in\text{BZ}}b_{k+\pi}^\dagger b_k + \frac{U}{2}\sum_{k\in\text{BZ}}\left(b_k^\dagger b_{-k}^\dagger + h.c.\right) + \frac{V}{2}\sum_{k\in\text{BZ}}\left(b_{k+\pi}^\dagger b_{-k}^\dagger + h.c.\right). \tag{2.44}$$

  where we used the abbreviations $U = U_{bb}n_0(A^2 + B^2) = U_{bb}n_0$, $V = U_{bb}n_02AB$, $\xi_k = \varepsilon_k + U_{bf} - \mu + 2U$, and $h = 2V - \alpha U_{bf}$.

For the approximate theory we require that the field fluctuations around the local extrema of the action are minimized, which is equivalent to setting the coefficients in front of the linear terms above to zero. Doing so, we obtain the following set of equations

$$\begin{aligned}
(-zt_b - \mu + U_{bf})A - \alpha U_{bf}B + n_0U_{bb}A(1 + 2B^2) &\stackrel{!}{=} 0, \\
(zt_b - \mu + U_{bf})B - \alpha U_{bf}A + n_0U_{bb}B(1 + 2A^2) &\stackrel{!}{=} 0,
\end{aligned} \tag{2.45}$$

[14] In the decoupling of the interaction term momentum conservation has to be taken into account.

with the nonlinear constraint $A^2 + B^2 = 1$.[15] We choose to view these coupled equations as equations for $\mu(n_0)$ and $A(n_0)$. The total average condensate fraction per site n_0 will then be determined self-consistently from the filling condition $n = 1$. by evaluating the total density n within the double unit cell (to take into account the staggering effects). Figs. 2.13 and 2.14 show the chemical potential μ as a function of U_{bb} and U_{bf}.

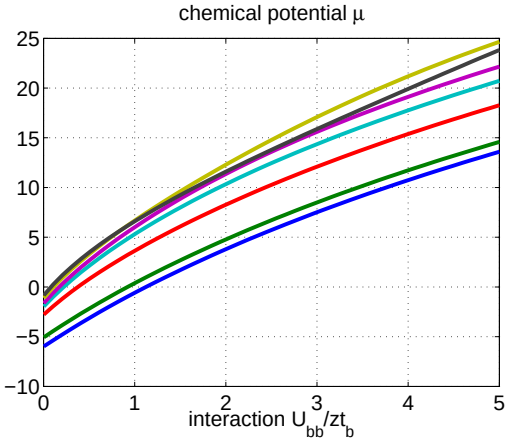

Figure 2.13: (color online): Chemical potential μ as a function of the interaction U_{bb}/zt_b for fixed values of $\alpha U_{bf} = 0$ (blue), 1 (green), 2 (red), 5 (cyan), 8 (purple), 10 (yellow) and 20 (black line).

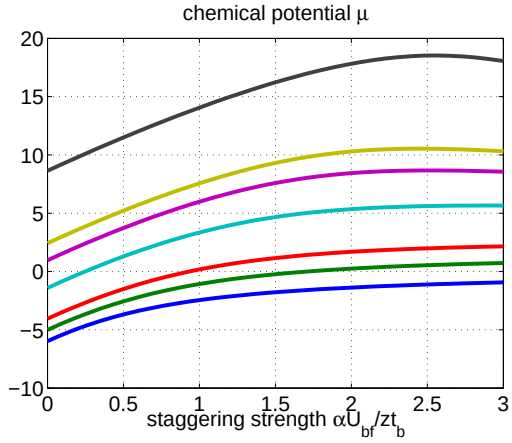

Figure 2.14: (color online): Chemical potential μ as a function of the interaction $\alpha U_{bf}/zt_b$ for fixed values of $U_{bb} = 0$ (blue), 1 (green), 5 (red), 8 (cyan), 10 (purple), 15 (yellow) and 20 (black line).

The exact modification of the two condensate fractions due to interactions is shown is Figs. 2.15 and 2.16 as a function of U_{bf} and U_{bb}. Notice that increasing the repulsive interactions effectively shifts part of the $\vec{k} = \vec{\pi}$ condensate back to the $\vec{k} = 0$ one. This acts as a counter mechanism to an increase of the potential strength, which favours the opposite effect, this increasing the ground state energy.

Before we continue, we do two quick checks: for $U_{bb} = 0$, we recover the well-known expressions $\mu = U_{bf} - \sqrt{(\alpha U_{bf})^2 + (zt_b)^2}$ and $A = A^{\text{free}}$, calculated in Section 2.2.1. On the other hand, setting $U_{bf} = 0$ results in $A = 1$ and $B = 0$. Hence, the second equation is trivially satisfied, while from the first one we find the chemical potential in the Bogoliubov approximation $\mu = -zt_b + n_0 U_{bb}$ from Section 2.1.3.

Solving Eqs. (2.45) in a closed form is possible in general, though the results are not particularly illuminating. The reason for this lies in the nonlinear constraint given above. It leads to a quadratic equation in the case of $U_{bb} = 0$ which is still nicely solvable. For finite U_{bb}, a higher-order non-linearity in the condensate amplitudes A and B is introduced, and solving the system amounts to finding the roots of a complicated polynomial. Therefore, we restrict our analysis to two perturbative regimes:

If we consider the limit of small staggering, we expect from the previous analysis that $A \approx 1$ and $B \approx 0$, i.e. very few of the condensed atoms will occupy the $\vec{k} = \vec{\pi}$-condensate. Then we can make the replacement $n_0 U_{bb} A(1 + 2B^2) \longrightarrow n_0 U_{bb} A$ and $n_0 U_{bb} B(1 + 2A^2) \longrightarrow 3 n_0 U_{bb} B$.

[15] This constraint can be conveniently incorporated by writing $A = \cos\theta$, but we shall not need this here. Nevertheless, the reader should keep in mind the A and B are not independent.

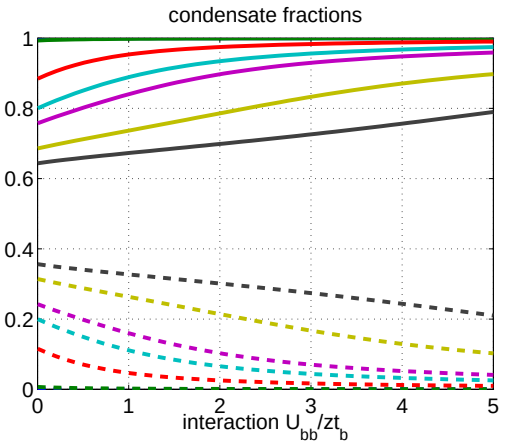

Figure 2.15: (color online): $\vec{k} = 0$ (solid) and $\vec{k} = \vec{\pi}$ (dashed) condensate fractions as a function of the interaction U_{bb}/zt_b for fixed values of $\alpha U_{bf} = 0$ (blue), 1 (green), 2 (red), 5 (cyan), 8 (purple), 10 (yellow) and 20 (black line).

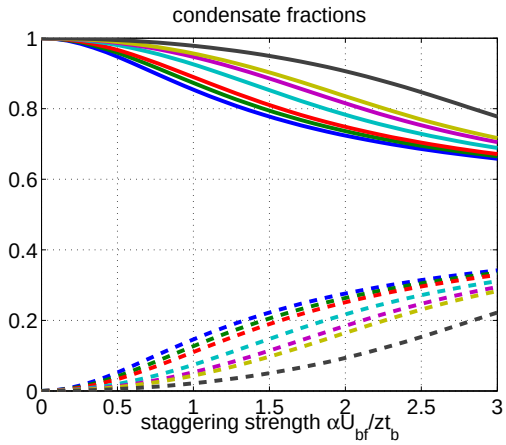

Figure 2.16: (color online): $\vec{k} = 0$ (solid) and $\vec{k} = \vec{\pi}$ (dashed) condensate fractions as a function of the interaction $\alpha U_{bf}/zt_b$ for fixed values of $U_{bb} = 0$ (blue), 1 (green), 5 (red), 8 (cyan), 10 (purple), 15 (yellow) and 20 (black line).

In this limit, we find

$$\mu \approx 2n_0U_{bb} + U_{bf} - \sqrt{(\alpha U_{bf})^2 + (n_0U_{bb} + zt_b)^2},$$
$$A(U_{bb}, \alpha U_{bf}) \approx \sqrt{\frac{1}{2}\left(1 + \frac{zt_b + n_0U_{bb}}{\sqrt{(\alpha U_{bf})^2 + (zt_b + n_0U_{bb})^2}}\right)}. \tag{2.46}$$

The leading order contribution to the $\vec{k} = 0$-condensate density reads

$$A^2(U_{bb}, \alpha U_{bf}) \overset{U_{bf}/zt_b \to 0}{\sim} 1 - \left(\frac{\alpha U_{bf}}{n_0U_{bb} + zt_b}\right)^2. \tag{2.47}$$

It follows that switching on the interactions, besides reducing the total condensate density n_0, we also find that populating the $\vec{k} = \vec{\pi}$-mode becomes harder with increasing αU_{bf}. The relevant scale for the process is set by $1 + n_0U_{bb}/zt_b$.

To understand the limit of large U_{bf}, it will be useful to look more carefully at the processes described by the 2^{nd} order terms, shown pictorially in Fig.2.17 as they enter the Bogoliubov Hamiltonian. The first thing to note is that the amplitude of the staggered potential h is modified by the interactions. In particular, it will be diminished when we turn on U_{bb} starting from zero.[16] Since this is a process that couples the two condensates resonantly, we see that

[16]The transformation $\alpha \to -\alpha$ leaves the physics invariant. Traced back to the description of the free staggered model, this transformation results in a sign flip $A^{\text{free}}/to - A^{\text{free}}$ in M^{free}, and hence $h \overset{\alpha \to -\alpha}{\to} h$ remains invariant.

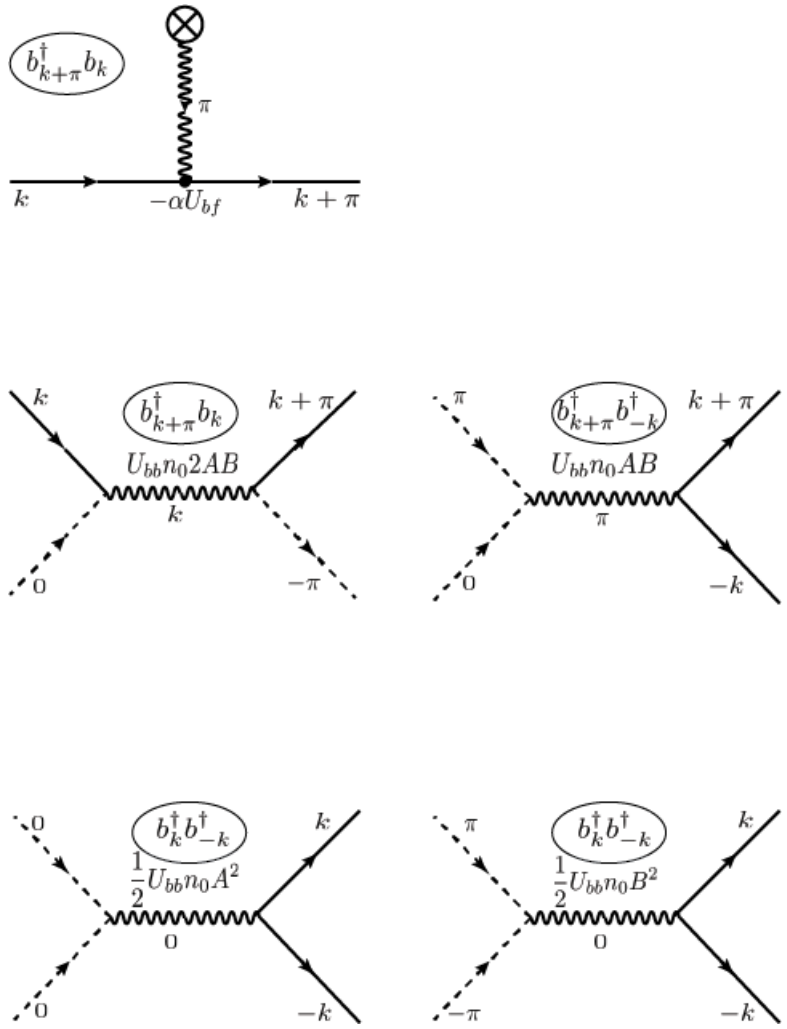

Figure 2.17: Pictorial representation of the relevant scattering processes within the generalized Bogoliubov approximation: second order processes of Eq. (2.44).

for small U_{bb} or large U_{bf}, the amplitudes of the $\vec{k} = 0$-condensate is modified according to

$$\begin{aligned} A(U_{bb}, \alpha U_{bf}) &\approx A^{\text{free}}(0, \alpha U_{bf} - 2A^{\text{free}} B^{\text{free}} U_{bb} n_0) \\ &= \sqrt{\frac{1}{2}\left(1 + \frac{zt_b}{\sqrt{(\alpha U_{bf} - \eta_0 U_{bb} n_0)^2 + (zt_b)^2}}\right)}, \end{aligned} \tag{2.48}$$

where we used $\eta_0 = 2A^{\text{free}} B^{\text{free}}$. Hence, this part of the interaction is responsible for renormalizing the staggering amplitude only. It might be tempting to conclude that we can induce a pure $\vec{k} = 0$ condensate in this way at a finite value of U_{bf}. This is not the case, as the approximation necessarily breaks down in the crossover regime $\alpha U_{bf} \approx \eta_0 U_{bb} n_0$. Nevertheless, we clearly see again that turning on weak interactions favours populating the $\vec{k} = 0$ condensate at the cost of a simultaneous depletion of the $\vec{k} = \vec{\pi}$ mode even for large staggering strengths.

The chemical potential in this limit reads

$$\mu \approx -zt_b + U_{bf} - \alpha U_{bf}\frac{B}{A} + n_0 U_{bb}(1+2B^2). \tag{2.49}$$

It is also interesting to give the asymptotic behaviour of the $\vec{k}=0$ fraction in the limit $U_{bf}/zt_b \gg 1$:

$$A^2(U_{bb}, \alpha U_{bf}) \overset{U_{bf}/zt_b\to\infty}{\sim} \frac{1}{2}\left(1 + \frac{zt_b}{\alpha U_{bf}} + \frac{zt_b n_0 U_{bb}}{(\alpha U_{bf})^2}\right) \tag{2.50}$$

We see that the interactions induce a sub-leading correction to the decay rate of the population of the $\vec{k}=0$ condensate for large U_{bf}.

In the following, we briefly have a look at the depletion terms which result from the decoupling of the quartic interaction in the Bogoliubov approximation. The depletion processes described by the $b_k^\dagger b_{-k}^\dagger$ terms couple equally strongly to particles in both condensates, with an interaction strength given by $U_{bb}/2$. Note that these processes tend to deplete them according to their populations. This follows from the presence of the factors $A^2 n_0$ and $B^2 n_0$ in the amplitude U, which arise from the Bogoliubov-type decoupling. Finally, events coming from $b_{k+\pi}^\dagger b_{-k}^\dagger$ describe scattering of atoms belonging to different condensates which leads to further depletion. It is important to note that these processes are strongly suppressed in the standard version of the approximation, as they are not resonant. On the contrary, they are needed here. It is through the staggered potential that they become resonant, and thus have to be taken into account. Furthermore, they are completely symmetric, and hence they also couple equally strong.

Were it not for the $b_{k+\pi}^\dagger b_{-k}^\dagger$ terms, the total average depleted fraction (and hence also the total condensate fraction) in the presence of the alternating potential would be the same as for $\alpha U_{bf}=0$ in the weakly interacting limit. This comes as no surprise, as the staggering potential merely shifts the density profile, inducing a CDW. Averaged over the unit cell, this effect cancels. However, due to this additional depletion, we now have

$$n_0(U_{bb}, U_{bf}) \neq n_0(U_{bb}, 0), \qquad n_{dep}(U_{bb}, U_{bf}) \neq n_{dep}(U_{bb}, 0) \tag{2.51}$$

in general, i.e. both the total average density fraction n_0, and the total average depleted fraction n_{dep} are dependent on the staggering strength U_{bf}, as are the corresponding on-site quantities $n_0(\vec{r}_i)$ and $n_{dep}(\vec{r}_i)$. The latter follows from a perturbative argument, starting from the staggered non-interacting case and the expression (2.31) for η_0.

The next step is to reduce the Brillouin zone. The above quadratic terms in 2^{nd}-order approximation transform according to

$$\begin{aligned}
\sum_{k\in \mathrm{BZ}} \varepsilon_k b_k^\dagger b_k &= \sum_{k\in \mathrm{BZ}'} \varepsilon_k \left(\alpha_k^\dagger \alpha_k - \beta_k^\dagger \beta_k\right) \\
\sum_{k\in \mathrm{BZ}} b_{k+\pi}^\dagger b_k &= \sum_{k\in \mathrm{BZ}'} \left(\alpha_k^\dagger \beta_k + h.c.\right) \\
\sum_{k\in \mathrm{BZ}} b_k^\dagger b_{-k}^\dagger &= \sum_{k\in \mathrm{BZ}'} \left(\alpha_k^\dagger \alpha_{-k}^\dagger + \beta_k^\dagger \beta_{-k}^\dagger\right) \\
\sum_{k\in \mathrm{BZ}} b_{k+\pi}^\dagger b_{-k}^\dagger &= 2\sum_{k\in \mathrm{BZ}'} \alpha_k^\dagger \beta_{-k}^\dagger
\end{aligned} \tag{2.52}$$

We shall keep the chemical potential in the equations, since we only give approximate expressions for it. At this point, it is advantageous to define $\vec{\alpha}_k = \left(\alpha_k, \beta_k \alpha_{-k}^\dagger, \beta_{-k}^\dagger\right)^t$, so we finally arrive at the expression for the quadratic Hamiltonian within the generalized Bogoliubov approximation

$$H = H_0 - \frac{1}{2}\sum_{k\in \mathrm{BZ}'} 2\tilde{\mu} + \\ + \frac{1}{2}\sum_{k\in \mathrm{BZ}'} \left(\alpha_k^\dagger, \beta_k^\dagger, \alpha_{-k}, \beta_{-k}\right) \begin{pmatrix} \varepsilon_k - \tilde{\mu} & h & U & V \\ h & -\varepsilon_k - \tilde{\mu} & V & U \\ U & V & \varepsilon_k - \tilde{\mu} & h \\ V & U & h & -\varepsilon_k - \tilde{\mu} \end{pmatrix} \begin{pmatrix} \alpha_k \\ \beta_k \\ \alpha_{-k}^\dagger \\ \beta_{-k}^\dagger \end{pmatrix} \tag{2.53}$$

with H_0 the 0^{th}-order contribution defined in Eq. (2.42), and $\tilde{\mu} = \mu - U_{bf} - 2U$.

Diagonalizing the Hamiltonian is possible with the methods from Appendix A. First, we define new operators via $\vec{\gamma}_k = M\vec{\alpha}_k$, where $\vec{\gamma} = \left(\gamma_{1,k}, \gamma_{2,k}, \gamma_{1,-k}^\dagger, \gamma_{2,-k}^\dagger\right)^t$. Denoting the new bands by $E_k^{(1/2)}$, we can write

$$\begin{aligned} H &= E_{gs} + \sum_{k\in \mathrm{BZ}'} E_k^{(1)} \gamma_{1,k}^\dagger \gamma_{1,k} + E_k^{(2)} \gamma_{2,k}^\dagger \gamma_{2,k}, \\ E_{gs} &= H_0 - \frac{1}{2} N_s \tilde{\mu} + \frac{1}{2}\sum_{k\in \mathrm{BZ}'} (E_k^{(1)} + E_k^{(2)}). \end{aligned} \tag{2.54}$$

The new bands are given by

$$E_k^{(1/2)} = \sqrt{h^2 - U^2 - V^2 + \varepsilon_k^2 + \tilde{\mu}^2 \pm 2\sqrt{\left(h\tilde{\mu} + UV\right)^2 + \left(\tilde{\mu}^2 - V^2\right)\varepsilon_k^2}}\ . \tag{2.55}$$

The requirement for the positivity of H translates to the following relation between μ and A:

$$\mu = U_{bf} + U_{bb} n_0 - \sqrt{\left(U_{bb} n_0 2AB - \alpha U_{bf}\right)^2 + (z t_b)^2}. \tag{2.56}$$

This equation can substitute for one of the equations in the system (2.45). The other one then determines the dependence of the amplitude A on the model parameters. It does not have a nice closed form and shall not be given here.

The two bands are plotted is Figs. 2.18 and 2.19. As expected, the two limiting cases $U_{bb} \to 0$ and $U_{bf} \to 0$ reproduce the already known band structure. The effect of the staggered potential is most pronounced at the edge of the reduced Brillouin zone where a gap opens. On the other hand, interactions make the Bose condensate a superfluid, which can be seen by the linear behaviour of the lower band about the origin.

We shall now continue to compute the average depleted fraction, and the amplitude of the bosonic charge density wave η. We follow the same methods, as in our previous discussion in

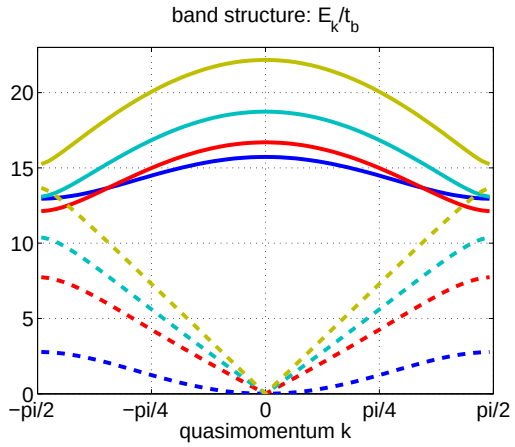

Figure 2.18: (color online): Band structure for $U_{bf}/t_b = 5$ and the values of $U_{bb} = 0$ (blue), 5 (red), 10 (cyan), and 20 (yellow).

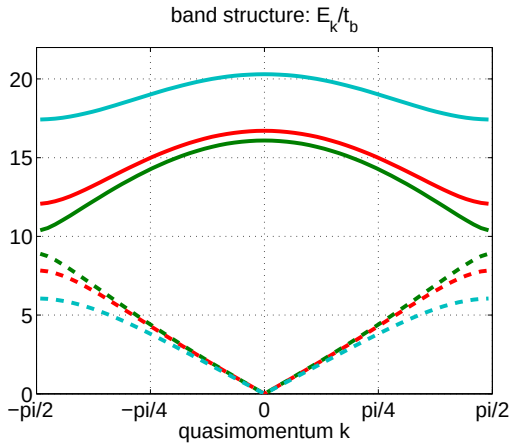

Figure 2.19: (color online): Band structure for $U_{bb}/t_b = 5$ for the values of $\alpha U_{bf} = 2$ (green), 5 (red) and 10 (cyan).

Chapter 2.1.3, and proceed to calculate the total density at $\vec{r}_i = 0$ first:

$$n(\vec{r}_i = 0) = \frac{1}{N_s} \sum_{k_1,k_2 \in \mathrm{BZ}} \langle GS | b^\dagger_{k_1} b_{k_2} | GS \rangle = \frac{1}{N_s} \sum_{k_1,k_2 \in \mathrm{BZ}'} \langle \alpha^\dagger_{k_1} \alpha_{k_2} + \beta^\dagger_{k_1} \beta_{k_2} + \alpha^\dagger_{k_1} \beta_{k_2} + h.c. \rangle$$

$$= \frac{1}{2N_s} \sum_{k_1,k_2 \in \mathrm{BZ}'} \left(\langle \vec{\alpha}^\dagger_{k_1} \underbrace{\begin{pmatrix} 1 & 1 & 0 & 0 \\ 1 & 1 & 0 & 0 \\ 0 & 0 & 1 & 1 \\ 0 & 0 & 1 & 1 \end{pmatrix}}_{=:P} \vec{\alpha}_{k_2} \rangle - 2\delta_{k_1,k_2} \right)$$

$$= \frac{1}{2N_s} \sum_{k_1,k_2 \in \mathrm{BZ}'} \left(\langle \vec{\alpha}^\dagger_{k_1} P \vec{\alpha}_{k_2} \rangle - 2\delta_{k_1,k_2} \right) \tag{2.57}$$

Next, we perform the Bogoliubov approximation according to Eq. (2.22):

$$n(\vec{r}_i = 0) \longrightarrow \frac{1}{2N_s} \left(N_0 \, (A, B, A, B) \, P \begin{pmatrix} A \\ B \\ A \\ B \end{pmatrix} + \sum_{k \in \mathrm{BZ}'} \left(\langle \vec{\gamma}^\dagger_k \underbrace{M^\dagger P M}_{=:\tilde{P}} \vec{\gamma}_k \rangle - 2\delta_{k_1,k_2} \right) \right)$$

$$= \frac{N_0}{N_s}(A + B)^2 + \frac{1}{2N_s} \sum_{k \in \mathrm{BZ}'} (\tilde{P}^{33}_k + \tilde{P}^{44}_k - 2). \tag{2.58}$$

At unit filling $N_s = N_0$, and noticing that $A^2 + B^2 = 1$, the expression simplifies to

$$n(\vec{r}_i = 0) = n_0(1 + 2AB) + \frac{1}{2N_s} \sum_{k \in \mathrm{BZ}'} (\tilde{P}^{33}_k + \tilde{P}^{44}_k - 2). \tag{2.59}$$

As before, we explicitly impose the filling condition. We can thus identify the first term in (2.59) as the condensate fraction on sublattice A, while the second term provides us with

the expression for the depleted density (again on sublattice A). Since we know there is also an induced CDW present, the above relation provides us with the modification of η_0 due to interactions:

$$\eta := n_0(1+2AB) + \frac{1}{2N_s}\sum_{k\in \mathrm{BZ}'}(\tilde{P}^{33}_k + \tilde{P}^{44}_k - 2) - 1. \tag{2.60}$$

A quick check for $U_{bb} = 0$ yields $n_0 = 1$, and $n_{dep} = 0$. Then we recover the familiar relation $\eta_0 = 2A^{\mathrm{free}}B^{\mathrm{free}}$. The exact numerical solution to Eq. (2.60) is shown in Figs. 2.20 and 2.21 for different values of U_{bf} and U_{bb}. We observe that the CDW amplitude is reduced with increasing interaction strength. While it rises monotonically all the way from 0 to 1 as a function of $\alpha U_{bf}/t_b$, the decrease rate a s function of the interaction U_{bb}/t_b is much weaker. Furthermore, the curvature of η as a function of U_{bb}/zt_b changes from positive to negative beyond a critical value of αU_{bf} (c.f. Fig. 2.20).

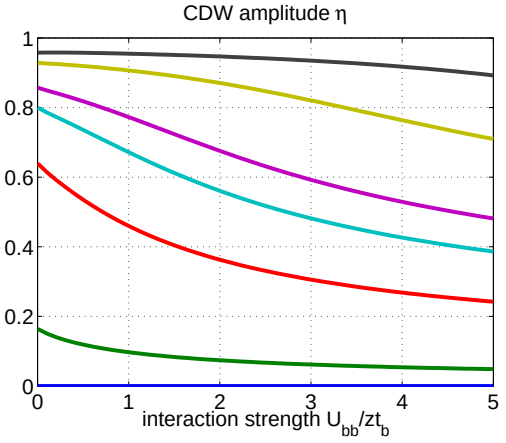

Figure 2.20: (color online): CDW amplitude in the weakly interacting limit as a function of the interaction U_{bb}/zt_b for fixed values of $\alpha U_{bf} = 0$ (blue), 1 (green), 2 (red), 5 (cyan), 8 (purple), 10 (yellow) and 20 (black line).

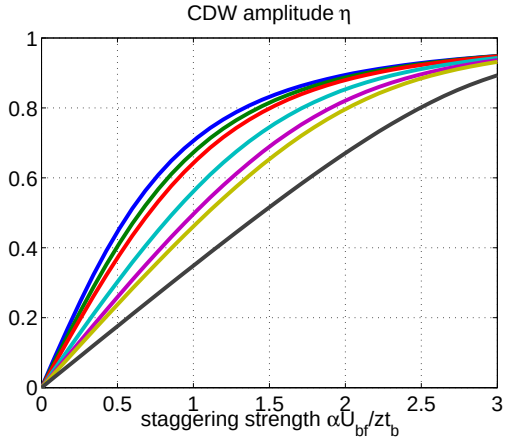

Figure 2.21: (color online): CDW amplitude in the weakly interacting limit as a function of the interaction $\alpha U_{bf}/zt_b$ for fixed values of $U_{bb} = 0$ (blue), 1 (green), 5 (red), 8 (cyan), 10 (purple), 15 (yellow) and 20 (black line).

We are not done yet, as we are missing the expression for the total average condensate density n_0. In order to obtain it, we need to calculate the local density profile at sublattice B. This is done straightforwardly as

$$\begin{aligned} n(\vec{r}_i = \vec{e}_x) &= \frac{1}{N_s}\sum_{k_1,k_2\in \mathrm{BZ}'} e^{i(k_1-k_2)}\langle \vec{\alpha}^\dagger_{k_1}\alpha_{k_2} + \beta^\dagger_{k_1}\beta_{k_2} - \alpha^\dagger_{k_1}\beta_{k_2} - h.c.\rangle \\ &\longrightarrow \frac{1}{2N_s}\left(N_0\,(A,B,A,B)\,R\begin{pmatrix} A \\ B \\ A \\ B \end{pmatrix} + \sum_{k\in \mathrm{BZ}'}\left(\langle \vec{\gamma}^\dagger_k \underbrace{M^\dagger R M}_{=:\tilde{R}}\vec{\gamma}_k\rangle - 2\delta_{k_1,k_2}\right)\right) \\ &= \frac{N_0}{N_s}(A-B)^2 + \frac{1}{2N_s}\sum_{k\in \mathrm{BZ}'}(\tilde{R}^{33}_k + \tilde{R}^{44}_k - 2), \end{aligned} \tag{2.61}$$

where the matrix R is given by

$$R = \begin{pmatrix} 1 & -1 & 0 & 0 \\ -1 & 1 & 0 & 0 \\ 0 & 0 & 1 & -1 \\ 0 & 0 & -1 & 1 \end{pmatrix}. \tag{2.62}$$

The total average density then reads

$$\begin{aligned} n &= n_0 + \frac{1}{4} \sum_{k \in \mathrm{BZ}'} (\tilde{R}_k^{33} + \tilde{R}_k^{44} + \tilde{P}_k^{33} + \tilde{P}_k^{44} - 4) \\ &= n_0 + \frac{1}{4} \sum_{k \in \mathrm{BZ}'} [(\tilde{R} + \tilde{P})_k^{33} + (\tilde{R} + \tilde{P})_k^{44} - 4] \\ &= n_0 + \frac{1}{2} \sum_{k \in \mathrm{BZ}'} [(M^\dagger M)_k^{33} + (M^\dagger M)_k^{44} - 2]. \end{aligned} \tag{2.63}$$

This is the generalized version of Eq. (2.18). Recalling that we are interested in a system at unit filling, we finally arrive at the number equation

$$1 = n_0 + \frac{1}{2} \sum_{k \in \mathrm{BZ}'} [(M^\dagger M)_k^{33} + (M^\dagger M)_k^{44} - 2]. \tag{2.64}$$

Notice first, that in the case $U_{bf} = 0$, we indeed recover (2.18) exactly. Moreover, since the matrix M depends on the modified amplitudes A and B, which are already known to the desired accuracy, the above relation provides again a self-consistency relation for the average total condensate number n_0 in the presence of the staggered potential. Solving this equation, we can substitute in Eq. (2.60) to find the modified CDW amplitude η. Figs. 2.22 and 2.23 show the behaviour of n_0 as a function of U_{bb} and U_{bf}.

These plots confirm our previous analysis that the role of interactions is to deplete the $\vec{k} = \vec{\pi}$ condensate. Observe that both the interactions and the staggering strength deplete the condensate fraction. Hence, these effects inevitably increase the ground state energy of the system.

As a final remark, let us mention that the self-consistent equation for the total condensate fraction n_0 can also be obtained from a minimization of the free energy Ω w.r.t. μ using the thermodynamic relation $n = -\frac{1}{N_s}\partial_\mu \Omega$. In the resulting equation, one should substitute the values for μ and A from Eq. (2.45) only after the minimization is complete. Alternatively, from the form of the Bose-Hubbard Hamiltonian in a staggered potential, one sees that the staggered strength αU_{bf} and the CDW amplitude η are also conjugate variables. Hence, it is possible to determine η from the thermodynamic relation $\eta = -\frac{1}{N_s}\partial_{(\alpha U_{bf})}\Omega$. In most practical cases, these relations are much easier to obtain, because of the computationally unhandy form of the transformation matrix M.

2.3 Conclusion

In this chapter, we revisited the physics of the Bose-Hubbard model, including Bose-Einstein condensation in lattice systems and superfluidity. We derived the MF phase boundary between the Mott insulator state within second-order perturbation theory, and reviewed the Bogoliubov approximation to describe the deep SF regime.

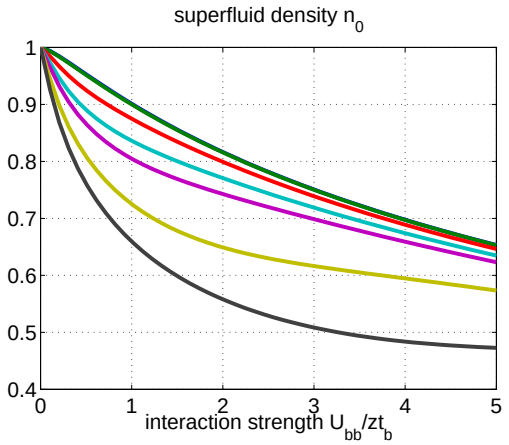

Figure 2.22: (color online): Total condensate fraction n_0 in the weakly interacting limit as a function of the interaction U_{bb}/zt_b for fixed values of $\alpha U_{bf} = 0$ (blue), 1 (green), 2 (red), 5 (cyan), 8 (purple), 10 (yellow) and 20 (black line).

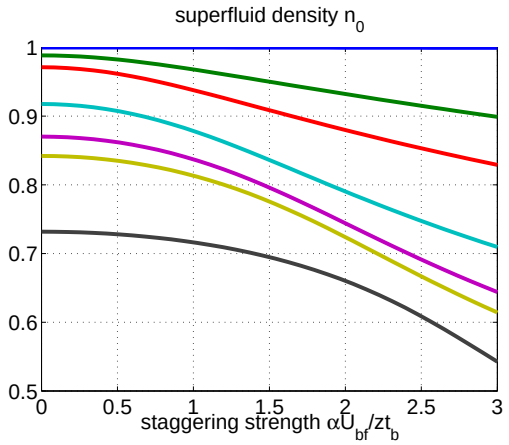

Figure 2.23: (color online): Total condensate fraction n_0 in the weakly interacting limit as a function of the interaction $\alpha U_{bf}/zt_b$ for fixed values of $U_{bb} = 0$ (blue), 1 (green), 5 (red), 8 (cyan), 10 (purple), 15 (yellow) and 20 (black line).

The BHM was then investigated in the presence of a staggered potential. Starting from free staggered bosons, we found that in terms of the initial operators of the model b and $b^\dagger$, a second mode at $\vec{k} = \vec{\pi}$ becomes macroscopically occupied, besides the expected $\vec{k} = 0$ condensation. This effect is solely due to the reduced translational symmetry of the lattice model. The condensate fractions in the two modes were then calculated exactly. We found that increasing the staggering strength shifts more bosons into the $\vec{k} = \vec{\pi}$ condensate, but equality of the two fractions is only achieved at infinite potential strengths. Furthermore, analytical expressions were obtained for the CDW amplitude as a function of the potential strength and the hopping amplitude. As expected, the former increases the CDW, while the latter leads to a reduction in the amplitude.

We proceeded with the correction to the MI-SF transition which was obtained with the help of the Cumulant Expansion Method. It allows to efficiently incorporate the remaining reduced translational symmetry of the problem, using a Green's functions approach equivalent to standard MF, but easily generalizable beyond it. The phase boundary is given by Eq. (2.2.2).

Finally, we generalized the Bogoliubov approximation to incorporate the effects of the staggered field in the deep SF regime. To this end, we proved a theorem of linear algebra (cf. Appendix A) which extends the concept of Bogoliubov transformations to higher matrix dimensions and allows to diagonalize any quadratic Hamiltonian consisting of more than one bosonic species. We found that interactions shift parts of the $\vec{k} = \vec{\pi}$ superfluid into the $\vec{k} = 0$ one via scattering of condensed bosons. Approximate expressions have been given for the chemical potential and the occupation of the two superfluid fractions, too. The staggering field was found to open up a gap at the edge of the reduce Brillouin zone, reminiscent of the free model discussed earlier. The interactions effectively linearize the dispersion relation in the centre of the Brillouin zone, thus rendering the Bose condensate a superfluid. Last, we remark that increasing either one of the potential or the interaction strength leads to a

further depletion of the total condensate fraction.

Chapter 3

The Fermi-Hubbard Model

The Fermi Hubbard Model (FHM) was initially proposed by Anderson to describe strongly correlated electrons in atomic lattices. Most of the attention of the condensed matter community is focused on two dimensions, where it is believed that the model is capable of explaining high-T_c superconductivity. Instead, here we provide a mean-field-based discussion of the ground state properties of the 3D Hubbard model with particular emphasis on the most symmetric case of half-filling.

The model describes fermions of spin $\sigma =\uparrow,\downarrow$ on a lattice. Each fermion can hop to the nearest-neighbour sites, gaining an energy t_f. When two fermions of different spin happen to be on the same lattice site, one needs to provide the energy U_{ff}. Since we are interested in low temperatures, fermions can only interact in the s-wave channel due to the Pauli Exclusion Principle. Last, the lattice filling is controlled by the chemical potential μ.

The Hamiltonian for this model is given by

$$H = -t_f \sum_{\langle ij\rangle,\sigma} \left(c^\dagger_{i\sigma} c_{j\sigma} + h.c. \right) - \mu \sum_i m_i + U_{ff} \sum_i m_{i\uparrow} m_{i\downarrow}, \tag{3.1}$$

where the c-operators satisfy fermionic commutation relations: $\{c_{i\sigma}, c^\dagger_{j\sigma'}\} = \delta_{\sigma,\sigma'}\delta_{ij}$. The number operator is given by $m_i = m_{i\uparrow} + m_{i\downarrow}$ with $m_{i\sigma} = c^\dagger_{i\sigma} c_{i\sigma}$. Half-filling is imposed by the condition $\langle m_i \rangle = 1$, which is equivalent to $\mu = E_F = 0$. We shall shortly show that the phase diagram of the model for a repulsive system $U_{ff} > 0$ can be derived using a symmetry transformation from that of attractive interactions $U_{ff} < 0$. Therefore, we shall focus on the attractive side throughout the entire thesis. It is noteworthy that despite its obvious simplicity, the model is not exactly solvable in 3D. This poses considerable challenge on understanding the physics behind it. To circumvent this formidable problem, different approximation schemes such as mean-field have been introduced.

An intuitive understanding of the physics can be gained by considering a lattice of two sites only, for which the model is exactly solvable. The interested reader is referred to [58].

We open the discussion by describing the phases of Superfluidity/Superconductivity (SF) and Charge Density Wave (CDW) in fermionic systems. Next, we examine the rich symmetries the FHM exhibits, and discuss their profound meaning for the phase diagram. Further, we review the most significant results of the BCS-BEC crossover. The main result of this chapter is the development of a self-consistent double mean-field description of the CDW and SF phases of the FHM, along the lines of a previous general MF discussion, [15, 43]. This allows to look for a supersolid state without overcounting the interaction energy. We shall conclude

the discussion by switching on an alternating potential, as was done previously in the case of bosons. Last, we briefly examine the FHM away from half-filling, including nearest-neighbour (nn) interactions, and discuss the consequences for the phase diagram.

3.1 BCS Theory of Superconductivity

The Bardeen-Schrieffer-Cooper (BCS) theory was introduced in 1957, [5], as the first microscopic theory of superconductivity. Ever since, it has been proved experimentally numerous times. Recently, superfluidity of fermions has also been observed using cold atoms in optical lattices, as mentioned in Chapter 1.

The underlying idea behind this theory is that fermions of opposite spin and momenta can form pairs (so-called Cooper pairs) in the vicinity of the Fermi surface in the case of attractive interactions, no matter how weak. These pairs can be effectively viewed as spinless bosons which condense and become superfluid (superconducting). Strange as it might seem, this new ground state consisting of Cooper pairs has a lower energy than the Fermi sea, and is hence preferred. A pictorial representation of the SF phase is given in Fig. 3.1. In the literature, this phenomenon is known as the (s-wave) pairing instability in fermionic systems. It must be mentioned that superconductivity is a pure many-body (or collective) phenomenon which does not occur in few-particle systems, where the notion of the Fermi sea is not well-defined.

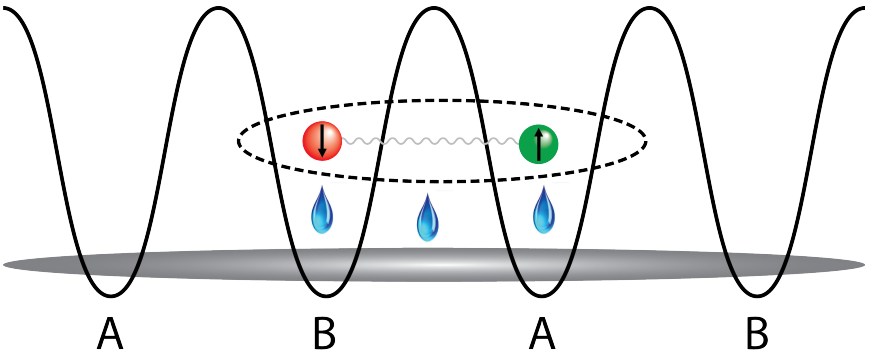

Figure 3.1: Pictorial representation of the SF state: a spin up (green) and a spin down (red) fermion pair together and delocalize (grey) over the entire lattice.

Since we want to describe pairing in momentum space, it is advantageous to cast the Hamiltonian (3.1) at half-filling in the form

$$H_{BCS} = \sum_{k\sigma} \varepsilon_k c^\dagger_{k\sigma} c_{k\sigma} + \frac{U_{ff}}{N_s} \sum_{k,k',q} c^\dagger_{k+q\uparrow} c^\dagger_{-k\downarrow} c_{-k'\downarrow} c_{k'+q\uparrow}. \tag{3.2}$$

The interaction term obeys momentum conservation. This particular way of assigning the momenta k, k' and q defines the so-called Cooper channel, depicted in Fig. 3.2.

To make progress, we need a way to cast the interaction part in the BCS-Hamiltonian (3.2) in a term quadratic in the operators c and $c^\dagger$, since quadratic theories are exactly solvable. This is done most easily in a MF description, whose essence was explained in Section 2.1.1. To this end, we define the gap function Δ_q by

$$\Delta_q = \frac{U_{ff}}{N_s} \sum_{k\in \mathrm{BZ}} \langle c^\dagger_{k+q\uparrow} c^\dagger_{-k\downarrow} \rangle. \tag{3.3}$$

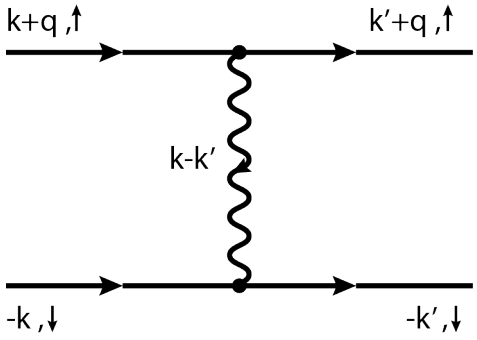

Figure 3.2: The Cooper channel for interacting fermions of opposite spin.

From the point of view of the theory of Phase Transitions and Critical Phenomena, this quantity defines the SF order parameter. Its physical meaning will become clear only in the very end of this section. It represents half the energy needed in order to break a pair of fermions. In general, the gap is a function of the quasi-momentum q. If expanded into the basis with respect to the point group of the underlying lattice, the different components correspond to s-, p-, d-wave pairing, etc. The isotropic s-wave pairing is then defined by the constant term Δ_0 in this generalized Fourier expansion. In many physical systems this is the dominating pairing process. However, the other types, also known as exotic (or unconventional) pairing, may also be taken into account.

In this chapter, we restrict our discussion to s-wave pairing only. Effects beyond this are reviewed later on in Chapter 5 in the context of the Bose-Fermi mixture. The mean-field decoupling takes the form

$$\frac{U_{ff}}{N_s}\sum_{k,k',q} c^\dagger_{k\uparrow}c^\dagger_{-k\downarrow}c_{-k\downarrow}c_{k\uparrow} \approx \Delta_0\sum_k c_{-k'\downarrow}c_{k'+q\uparrow} + \Delta_0^*\sum_k c^\dagger_{k+q\uparrow}c^\dagger_{-k\downarrow} - \frac{N_s}{U_{ff}}|\Delta_0|^2. \tag{3.4}$$

In general, Δ_0 takes values in the complex plane. We will do a further approximation, treating it as a real number. This is motivated by the fact that only the absolute value $|\Delta_0|$ enters the equations determining the phase boundary. The Hamiltonian takes the following quadratic form within the MF approximation

$$\begin{aligned} H &\approx -\frac{N_0}{U_{ff}}|\Delta_0|^2 + \sum_{k\in\mathrm{BZ}}\varepsilon_k c^\dagger_{k\sigma}c_{k\sigma} + \Delta_0\left(c_{-k\downarrow}c_{k\uparrow} + c^\dagger_{k\uparrow}c^\dagger_{-k\downarrow}\right) \\ &= -\frac{N_0}{U_{ff}}|\Delta_0|^2 + \sum_{k\in\mathrm{BZ}}\varepsilon_k + \sum_{k\in\mathrm{BZ}}\left(c^\dagger_{k\uparrow}, c_{-k,\downarrow}\right)\begin{pmatrix}\varepsilon_k & \Delta_0\\ \Delta_0 & -\varepsilon_k\end{pmatrix}\begin{pmatrix}c_{k\uparrow}\\ c^\dagger_{-k\downarrow}\end{pmatrix}. \end{aligned} \tag{3.5}$$

Due to the form of the tight-binding dispersion, we have $\sum_{k\in\mathrm{BZ}}\varepsilon_k = 0$, and hence the second term vanishes identically. The Hamiltonian can be diagonalized by a unitary transformation M given by

$$M = \begin{pmatrix} \sqrt{\frac{1}{2}\left(1+\frac{\varepsilon_k}{\sqrt{\varepsilon_k^2+|\Delta_0|^2}}\right)} & -\sqrt{\frac{1}{2}\left(1-\frac{\varepsilon_k}{\sqrt{\varepsilon_k^2+|\Delta_0|^2}}\right)} \\ \sqrt{\frac{1}{2}\left(1-\frac{\varepsilon_k}{\sqrt{\varepsilon_k^2+|\Delta_0|^2}}\right)} & \sqrt{\frac{1}{2}\left(1+\frac{\varepsilon_k}{\sqrt{\varepsilon_k^2+|\Delta_0|^2}}\right)} \end{pmatrix}. \tag{3.6}$$

Defining new operators $\vec{a}_k = M\vec{c}_k$ with $\vec{c}_k = (c_{k\uparrow}c^\dagger_{-k\downarrow})^t$, we arrive at

$$H = E_{gs} + \sum_{k\in \mathrm{BZ},\sigma} E_k a^\dagger_{k\sigma} a_{k\sigma},$$
$$E_{gs} = -\sum_{k\in \mathrm{BZ}} E_k - \frac{N_0}{U_{ff}}|\Delta_0|^2. \tag{3.7}$$

The new operators $\vec{a}_k$ are designed to describe the excitations of the system above the ground state with energy E_{gs}.[1] Their dispersion is given by $E_k = \sqrt{\varepsilon_k^2 + |\Delta_0|^2}$. It is gapped, and the gap Δ_0 gives half the energy necessary to break an s-wave pair. The dispersion is plotted in Fig. 3.3.

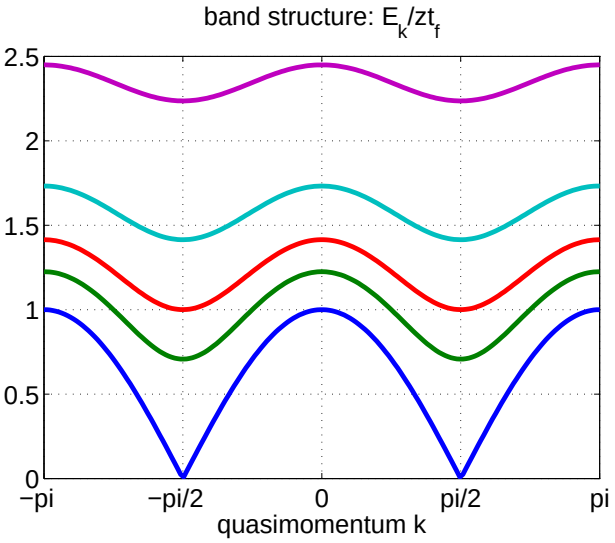

Figure 3.3: (color online): Dispersion relation of the Cooper pairs for the simple cubic lattice ($z = 6$), and values of the gap $\Delta_0/zt_f = 0$ (blue), 0.5 (green), 1.0 (red), 2.0 (cyan), 5 (purple).

Having diagonalized the MF Hamiltonian, we proceed to fix the value of the gap function. This can be done in two different but equivalent ways: one can either minimize E_{gs} w.r.t. Δ_0, or determine it self-consistently. Here, we follow the second route:

$$\Delta_0 = \frac{U_{ff}}{N_s}\sum_{k\in \mathrm{BZ}} \langle c^\dagger_{k\uparrow} c^\dagger_{-k\downarrow}\rangle = \frac{U_{ff}}{N_s}\sum_{k\in \mathrm{BZ}} \langle \vec{c}^\dagger_k \begin{pmatrix} 0 & 1 \\ 0 & 0 \end{pmatrix} \vec{c}_k\rangle$$
$$= \frac{U_{ff}}{N_s}\sum_{k\in \mathrm{BZ}} \langle \vec{a}^\dagger_k M^\dagger H M \vec{c}_k\rangle = \frac{U_{ff}}{N_s}\sum_{k\in \mathrm{BZ}} (M^\dagger H M)^{(22)}_k. \tag{3.8}$$

This way, we obtain the celebrated gap equation [5]

$$\Delta_0 = -\frac{U_{ff}}{2N_s}\sum_{k\in \mathrm{BZ}} \frac{\Delta_0}{\sqrt{\varepsilon_k^2 + |\Delta_0|^2}}. \tag{3.9}$$

[1] See the discussion in Appendix A for a better explanation of this fact.

The first thing to notice is that the above equation has a solution only for $U_{ff} < 0$. Therefore, any attractive interaction, no matter how small, changes the ground state of the system, inducing pairing between the electrons.

A quick inspection of (3.9) shows that $\Delta_0 = 0$ is always a solution. This corresponds to the normal phase of the system. In general, the solution to the above equation is not known. One can calculate it approximately for weak interactions with the methods of Section 5.5. It reads

$$\Delta_0 \approx \text{const} \times e^{-\frac{1}{\mathcal{N}(0)U_{ff}}}, \tag{3.10}$$

where $\mathcal{N}(0)$ is the density of states at the Fermi surface. We note that this behaviour is sensitive to the exact form of the density of states assumed which, in turn, depends strongly on the lattice dispersion relation. One immediately sees the non-analytic behaviour as a function of $\mathcal{N}(0)U_{ff}$. Clearly, such a result cannot be obtained within perturbation theory. This comes to no surprise, as MF is equivalent to a self-consistent Hartree-Fock approximation which sums up an infinite number of Feynman diagrams. The full solution is plotted in Fig. 3.4.

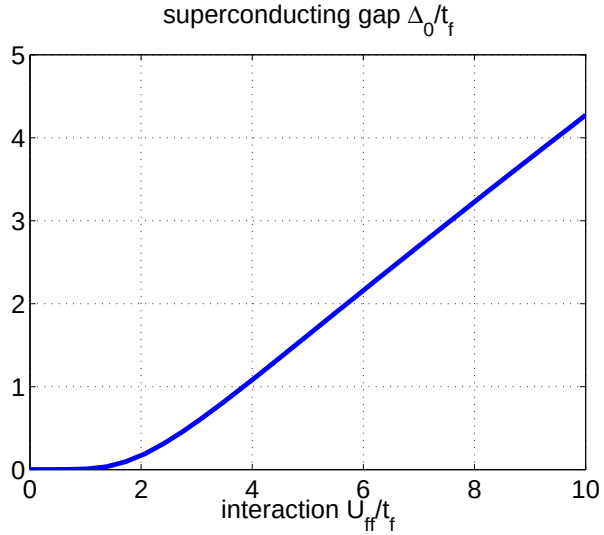

Figure 3.4: (color online): Energy gap Δ_0/t_f as a function of the fermion-fermion interaction U_{ff}/t_f for a simple cubic lattice ($z = 6$).

The linear behaviour for large values of U_{ff}/t_f can be obtained from a strong coupling expansion [30], and is given by $|\Delta_0|/t_f = \left(\frac{|U_{ff}|}{2t_f} + \frac{6t_f}{|U_{ff}|}\right)\sqrt{m(m-2)}$. The slope of $1/2$ agrees precisely with the numerical plot above. Last, we remark that BCS theory describes correctly the ground state of the FHM for interactions $|U_{ff}/t_f \lesssim 5$ (c.f. the discussion on the BCS-BEC crossover in Section 3.4)

3.2 Charge Density Waves

In this Section, we consider another instability of fermionic systems. At half-filling the Fermi surface exhibits perfect nesting, when translated by the vector $\vec{\pi} = (\pi, \pi, \pi)$ in momentum space. This makes it possible for a charge density wave (CDW) to form. This state is easily

pictured in the case of $t_f = 0$, where two fermions of opposite spin occupy every second site of the lattice establishing what we shall later refer to as *diagonal long-range order* (DLRO).[2] Such a ground state is depicted in Fig. 3.5. This phase is also gapped like the SF, since one needs a minimum energy to overcome the attractive interaction and put a fermion to a neighbouring site. In fact, both phases share a lot of common features, as will become clear from the following discussion.

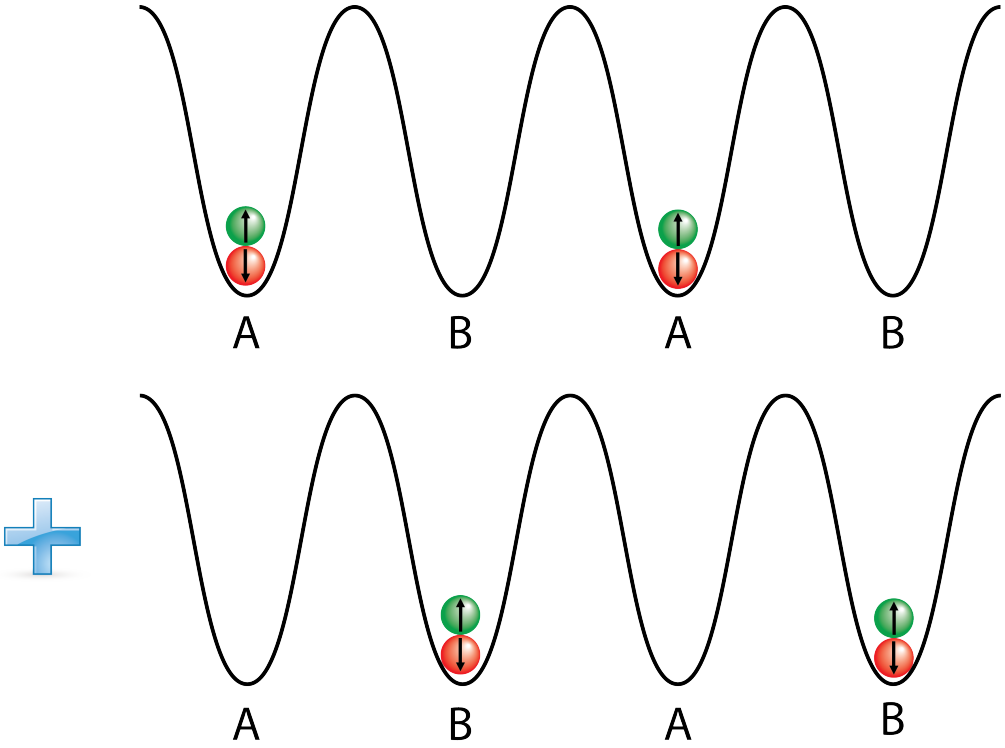

Figure 3.5: Pictorial representation of the CDW state for $t_f = 0$: a spin up (green) and a spin down (red) fermion stack up on top of each other leaving every other site empty. The ground state is doubly degenerate in 1d.

Since the spin degree of freedom is not essential to the calculations, we omit the spin index. Keep in mind, however, that it is the spin degree of freedom that enables two fermions to occupy the same lattice site at low energies, without violating the Pauli Principle. This time, the interaction is mediated through the Density channel, given in Fig. 3.6.

Again, we need the Hamiltonian in momentum space, to make use of the nesting condition:

$$H = \sum_k \varepsilon_k c_k^\dagger c_k + \frac{U_{ff}}{N_s} \sum_{k,k',q} c_{k+q}^\dagger c_k c_{k'-q}^\dagger c_{k'}. \tag{3.11}$$

Motivated by the perfect nesting property, we expect the mode $\vec{q} = \vec{\pi}$ to give the dominant contribution to the interaction. Therefore, we single it out and neglect the other terms in the q-summation. This allows for a mean-field decoupling in terms of a real order parameter Δ_c

[2] This name comes in contrast to a superfluid phase where there is *off-diagonal long-range order* (ODLRO).

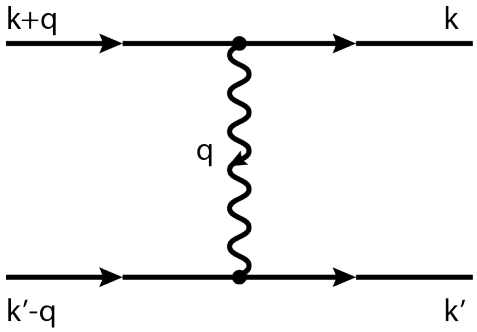

Figure 3.6: The Density channel for interacting spinless fermions.

defined by

$$\Delta_c = \frac{U_{ff}}{N_s} \sum_{k \in \mathrm{BZ}} \langle c^\dagger_{k+\pi} c_k \rangle = \frac{U_{ff}}{N_s} \sum_{k \in \mathrm{BZ}'} \langle c^\dagger_{k+\pi} c_k + c^\dagger_k c_{k+\pi} \rangle, \tag{3.12}$$

where BZ′ denotes the reduced Brillouin zone, shown in Fig. 2.4. As in the previous chapter, this parameter is proportional to the energy gap in the dispersion relation of the excitations. Following the same procedure, we obtain for the interaction term

$$\frac{U_{ff}}{N_s} \sum_{k,k',q} c^\dagger_{k+q} c_k c^\dagger_{k'+q} c_{k'} \approx -\frac{N_s}{U_{ff}} |\Delta_c|^2 + 2\Delta_c \sum_{k \in \mathrm{BZ}'} c^\dagger_{k+\pi} c_k + c^\dagger_k c_{k+\pi}. \tag{3.13}$$

Plugging this into the Hamiltonian (3.11) yields

$$\begin{aligned} H &\approx -\frac{N_s}{U_{ff}} |\Delta_c|^2 + \sum_{k \in \mathrm{BZ}'} \varepsilon_k \left(c^\dagger_k c_k - c^\dagger_{k+\pi} c_{k+\pi} \right) + 2\Delta_c \sum_{k \in \mathrm{BZ}'} c^\dagger_{k+\pi} c_k + c^\dagger_k c_{k+\pi} \\ &= -\frac{N_0}{U_{ff}} |\Delta_c|^2 + \sum_{k \in \mathrm{BZ}'} \left(c^\dagger_k, c^\dagger_{k+\pi} \right) \begin{pmatrix} \varepsilon_k & 2\Delta_c \\ 2\Delta_c & -\varepsilon_k \end{pmatrix} \begin{pmatrix} c_k \\ c_{k+\pi} \end{pmatrix}. \end{aligned} \tag{3.14}$$

The Hamiltonian is diagonalized by the same transformation M given in (3.6), with the replacement $\Delta_0 \longrightarrow 2\Delta_c$. Again, we define operators $\vec{a}_k = M_k \vec{c}_k$, and find

$$H = -\frac{N_0}{U_{ff}} |\Delta_c|^2 + \sum_{k \in \mathrm{BZ}'} E_k \left(a^\dagger_{1,k} a_{1,k} - a^\dagger_{2,k} a_{2,k} \right), \tag{3.15}$$

with $E_k = \sqrt{\varepsilon_k^2 + |2\Delta_0|^2}$ the dispersion relation. The crucial difference this time is made by the ground state, which is defined by filling in the entire negative band, i.e. the band corresponding to the operators $a_{2,k}$: $|GS\rangle = \prod_{k \leq |k_F|} a^\dagger_{2,k} |0\rangle$. The ground state energy is given by

$$E_{gs} = -\frac{N_0}{U_{ff}} |\Delta_c|^2 - \sum_{k \in \mathrm{BZ}'} E_k. \tag{3.16}$$

Minimizing w.r.t. Δ_c, we obtain the gap equation for the CDW order parameter Δ_c:

$$\Delta_c = -2 \frac{U_{ff}}{N_s} \sum_{k \in \mathrm{BZ}'} \frac{\Delta_c}{\sqrt{\varepsilon_k^2 + |2\Delta_c|^2}}. \tag{3.17}$$

We see that the properties of Δ_c are essentially the same as these of the superconducting gap Δ_c. In order to understand this coincidence at first sight, we need to carefully examine the symmetries of the FHM.

3.3 Symmetries of the Fermi Hubbard Model

The FHM allows various symmetry transformations. They are very important for constructing low-energy effective theories, as is the goal of this thesis, since the ground state of the system must transform in the representation of its symmetry group. Furthermore, the model has effectively two free parameters (the chemical potential and the interaction strength).[3] Relations between the different values they take can be established. For instance, the Lieb-Mattis transformation discussed below maps the repulsive FHM to the attractive one, while the Particle-Hole transformation changes the sign of the chemical potential $\mu \longrightarrow -\mu$. These symmetries are usually very helpful when performing any kind of numerical simulations, since they can tremendously reduce the cost of computations, but also often serve as consistency checks.

3.3.1 Lieb-Mattis and Particle-Hole Symmetries

In this subsection, we present the Particle-Hole and the Lieb-Mattis transformations. The aim is to understand how they can be used to obtain parts of the phase diagram from other by introducing a one-to-one mapping between them.

We begin with the *Particle-Hole symmetry*. Consider first the FHM on a bipartite lattice[4] at half-filling. The relevant physical question behind the transformation reads: What is the relation between the distribution of fermionic particles, created by the operator $c^\dagger$, and holes (antifermions) created by c in the eigenstates of the Hamiltonian[5]

$$H = -t_f \sum_{\langle ij\rangle,\sigma} \left(c^\dagger_{i\sigma} c_{j\sigma} + h.c. \right) - \mu \sum_i m_i + U_{ff} \sum_i \left(m_{i\uparrow} - \frac{1}{2} \right) \left(m_{i\downarrow} - \frac{1}{2} \right). \tag{3.18}$$

In other words, we seek a transformation of the model parameters which leaves H invariant and maps particles to holes. Simply interchanging the roles $c \longleftrightarrow c^\dagger$ of the two operators would not do the job, because of the fermionic commutation relations which would map the kinetic term to its negative (effectively replacing the hopping constant $t_f \longrightarrow -t_f$). However, we can do better, provided we can divide the lattice into two interlaced sublattices, which is equivalent to requiring that the lattice be bipartite. To get the correct sign of the hopping parameter, we introduce a checker-board-type staggered term $(-1)^i = (-1)^{i_x+i_y+i_z}$. This amounts to a local gauge transformation and it affects non-local terms only (such as the kinetic one). Since the interaction term is local, it is left invariant. Having said all this, we are ready to give the exact Particle-Hole transformation:

$$c^\dagger_{i\sigma} \longrightarrow (-1)^i c_{i\sigma}. \tag{3.19}$$

[3] When we normalize them by the hopping amplitude t_f.

[4] This is an essential condition, as can be seen from the definition of the transformation itself.

[5] Notice that we slightly changed the form of the interaction here, without changing the physics. We shall comment on this shortly.

As already mentioned, it leaves the kinetic term invariant. The particle density is mapped to the hole density $c^\dagger_{i\sigma}c_{i\sigma} \longrightarrow 1 - c^\dagger_{i\sigma}c_{i\sigma}$. We see that at half-filling ($\langle m_i\rangle = 1$ and $\mu = -U_{ff}$) the particle number operator is mapped to the corresponding one for holes. One can check that the interaction term is also invariant under this transformation.

Actually, this is the reason why it is advantageous to define the interaction term with the help of the factors 1/2. Had we not done this, the half-filled case would correspond to $\mu = 0$, such that μ intersects the energy bands exactly in the middle. Having made this point clear, from now on we use the interaction term $U_{ff}\sum_i m_{i,\uparrow}m_{i,\downarrow}$.

Hence, we have found a transformation which interchanges the roles of particles and holes. The real advantage comes when we go away from half-filling. Clearly, as the density operator is mapped to its negative, we see that the chemical potential term changes sign and the transformation no longer leaves the full Hamiltonian invariant. We now have $H(\mu/t_f, U_{ff}/t_f) \longrightarrow H(-\mu/t_f, U_{ff}/t_f)$. But this implies that every quantity which depends on μ (in particular, the expectation value of the number operator) will exhibit an axial symmetry w.r.t. the line $\mu = 0$. From this, we can deduce that the phase diagram away from half-filling will be symmetric w.r.t. the line $\langle m_i\rangle = 1$.

The second important symmetry we discuss here is given by the *Lieb-Mattis transformation*. It is also known as a partial particle-hole transformation, since it is performed only on one spin species. It is defined through

$$\begin{aligned} c^\dagger_{i\downarrow} &\longrightarrow (-1)^i c_{i\downarrow} \\ c^\dagger_{i\uparrow} &\longrightarrow c^\dagger_{i\uparrow}. \end{aligned} \tag{3.20}$$

Again, the kinetic term is left invariant, due to the local gauge $(-1)^i$. The interaction term, however, changes sign, since we only transform one spin species. We immediately see that the Lieb-Mattis transformation is a symmetry of the Hamiltonian if and only if we impose half-filling. We have established a mapping $H(0, U_{ff}/t_f) \longrightarrow H(0, -U_{ff}/t_f)$. According to the considerations above, this implies that the ground state phase diagram of the FHM at half-filling is symmetric w.r.t. the line given by the non-interacting point $U_{ff} = 0$. Therefore, one needs to consider solely attractive (or repulsive) interactions only. Here, we choose to work on the attractive side.

In order to translate the statements to the repulsive side, it is useful to keep in mind the following dictionary:

$$\begin{aligned} m_{i\uparrow} + m_{i\downarrow} = m_i &\longleftrightarrow M_{z,i} = m_{i\uparrow} - m_{i\downarrow} \\ c^\dagger_{i\uparrow}c^\dagger_{i\downarrow} = \Delta_{0,i} &\longleftrightarrow M^+_i = c^\dagger_{i\uparrow}c_{i\downarrow} \\ c_{i\uparrow}c_{i\downarrow} = \Delta^*_{0,i} &\longleftrightarrow M^-_i = c_{i\uparrow}c_{i\downarrow}, \end{aligned} \tag{3.21}$$

where m_i denotes the fermion particle number operator, while M_i denotes the onsite magnetization operator. It is very interesting to note that spin correlations along the z-direction are mapped onto the charge operator m_i, whereas spin correlations in the xy-plane (being linear combinations of M^+ and M^-) are mapped onto the s-wave (or on-site) pairing operator $\Delta_{0,i}$.

This comes as a surprise on the attractive side, where the two phases CDW and SF appear very different from the physical perspective. On the repulsive side, however, they appear as different manifestations of the same magnetic order. We have almost anticipated such relations from our previous discussion of the two phases, which resulted in the same gap equation for the order parameters Δ_0 and Δ_c.

These relations appear even more surprising, if one recalls that the components of the magnetization $M_{i,z}$ and $M_i^{\pm}$ are defined w.r.t. a coordinate system which we are free to choose. The latter suggests that, due to the Lieb-Mattis transformation, we can view the CDW state as a SF state, if we choose to label the magnetization axes differently. In order to get a better insight into this peculiarity from a theoretical point of view, we need to look at the full symmetry group of the Fermi-Hubbard model.

3.3.2 The Full SO(4) Symmetry Group

The Fermi-Hubbard model has a rich symmetry structure which is inevitably reflected by the dimension of its symmetry group. It is responsible for the variety of different phases proposed in the literature, and the present controversies concerning the ground state properties of the model. It is our goal in this subsection to gain a solid understanding of the similarities and differences between the charge order represented by the CDW ground state, and the superfluid order present in the SF state.

To this end, we start again with the FH Hamiltonian at half-filling. The experienced eye recognizes immediately that it is symmetric under the exchange of the two spin species $\uparrow$ and $\downarrow$. This is obviously true for the kinetic term, while the interaction term requires to notice that the number operators for the spin species are bosonic (consisting of two fermions), and hence $[m_{i\uparrow}, m_{i\downarrow}] = 0$. Therefore, the model exhibits an $SU(2)$ spin symmetry with generators given by the spin operators

$$\begin{aligned} \sigma^- &= \sum_i c_{i\uparrow}^\dagger c_{i\downarrow} \\ \sigma^+ &= \sum_i c_{i\downarrow}^\dagger c_{i\uparrow} \\ \sigma^z &= \frac{1}{2}\sum_i (m_{i\downarrow} - m_{i\uparrow}). \end{aligned} \tag{3.22}$$

From these, we define $\sigma^{x,y}$ in the standard way via $\sigma^{\pm} = \sigma^x \pm \sigma^y$. It is straightforward to show that the the spin operators satisfy the $SU(2)$ algebra given by

$$[\sigma^\alpha, \sigma^\beta] = i\epsilon_{\alpha\beta\gamma}\sigma^\gamma \tag{3.23}$$

for $\alpha = x, y, z$. However, this is not the only symmetry present in the model. In 1989 Yang and Zhang [60] showed that the FHM on a bipartite lattice at half-filling obeys a further symmetry, the so-called pseudo-spin symmetry. It is generated by the pseudo-spin operators

$$\begin{aligned} \eta^- &= \sum_i (-1)^i c_{i\uparrow} c_{i\downarrow} \\ \eta^+ &= \sum_i (-1)^i c_{i\downarrow}^\dagger c_{i\uparrow}^\dagger \\ \eta^z &= \frac{1}{2}\sum_i (m_{i\downarrow} + m_{i\uparrow} - 1). \end{aligned} \tag{3.24}$$

As before, we define $\eta^{x,y}$ by $\eta^{\pm} = \eta^x \pm \eta^y$ to arrive at the $SU(2)$ pseudo-spin algebra

$$[\eta^\alpha, \eta^\beta] = i\epsilon_{\alpha\beta\gamma}\eta^\gamma. \tag{3.25}$$

The model then enjoys an $SO(4) = SU_\eta(2) \times SU_\sigma(2)/Z_2$ symmetry [12], i.e. $[H, \eta^\alpha] = 0 = [H, \sigma^\alpha]$. On a lattice with even number of sites, one has to divide by the group Z_2 to avoid double counting of states [60].

We are now in a position to proceed with the group theoretical description of the SF and CDW phases, which both represent second-order (Landau) phase transitions. According to Landau's theory [31], such a transition has to break a continuous symmetry reducing the total symmetry group of the model. The discussion on superfluidity in Chapter 2.1.1 showed that in the bosonic case, the $U(1)$-symmetry of the Bose-Hubbard model is broken by the emergence of an order parameter related to the SF density. In the fermionic case, the $U(1)$ group is not explicitly present. Instead, one needs to break either one of the $SU(2)$ spin groups available. This fact can be inferred from numerical simulations, which put the Hubbard model at half-filling into the Heisenberg universality class, corresponding to an $SO(3)$ symmetry group [49].

To understand this better, we recall that $U(1)$ is the group of unitary transformations in one complex dimension which can be thought of as the group of rotations in the real plane $SO(2)$. On the other hand, the real rotations in the plane constitute a proper subgroup of the real rotations in three dimensions, i.e. $SO(2) \subset SO(3)$. The relation between orthogonal rotations in three dimensions and unitary transformations in two dimensions is given by the Lie algebra isomorphism $\mathfrak{so}(3) \simeq \mathfrak{su}(2)$. This makes it plausible that $U(1) \subset SU(2)$, and it is precisely the part of $SU(2)$ which gets broken by the real part of the order parameter Δ_0.

The previous paragraph raises the question, which one of the pseudo-spin and the spin $SU(2)$ takes part in the symmetry breaking. To answer this, it will be helpful to define the following set which consists of the three operators of interest:

$$\begin{aligned} \Delta^- &= \sum_i c_{i\uparrow} c_{i\downarrow} \\ \Delta^+ &= \sum_i c^\dagger_{i\downarrow} c^\dagger_{i\uparrow} \\ \Delta^z &= \frac{1}{2} \sum_{i\sigma} (-1)^i m_{i\sigma}. \end{aligned} \tag{3.26}$$

Taking the ground state expectation value of these operators, we recover the familiar order parameters Δ_0 and Δ_c.[6] Symmetrizing the SF order parameters via $\Delta^\pm = \Delta^x \pm \Delta^y$, a straightforward calculation yields

$$[\eta^\alpha, \Delta^\beta] = i\epsilon_{\alpha\beta\gamma} \Delta^\gamma. \tag{3.27}$$

Therefore the order parameters transform in the representation of the pseudo-spin group $SU_\eta(2)$. The commutator relation (3.27) says that the pseudo-spin operators can rotate one order parameter into the other, pretty much the same way we anticipated this towards the end of the previous subsection. This ultimately proves the degenerate nature of the ground state of the FHM at half-filling: superfluidity and the charge density wave are present simultaneously, the ground state being an arbitrary superposition of both.

The transformation (3.27) ultimately sheds light on the question we posed earlier: it says that the pseudo-spin symmetry generators and the order parameters[7] are conjugate variables [12]. Hence, it is the pseudo-spin $SU_\eta(2)$ which gets broken in the ground state.

[6] Up to a proportionality factor, given by the interaction strength U_{ff}.

[7] The triplet $(\Delta^x, \Delta^y, \Delta^z)$ transforms in the vector representation of the $SU_\eta(2)$ group.

3.4 Phase Diagram of the FHM and the BCS-BEC Crossover

In this section, we discuss the phase diagram of the Fermi-Hubbard model at half-filling, putting the emphasis on the BCS-BEC crossover. Although we are ultimately interested in zero-T, we give a comprehensive review of the results also at finite T.

From the previous Section, we already know that the phase diagram must be symmetric w.r.t. flipping the sign of the interaction U_{ff} due to the Lieb-Mattis transformation. Moreover, based on symmetry arguments, we found that the ground state for attractive interactions is an arbitrary superposition of a CDW and SF state. Furthermore, it can be shown [38] that all physical quantities determined by the one-particle correlation functions (such as the specific heat and the entropy) are independent of the sign of U_{ff}.[8] Since we can freely rotate one order into the other by means of the $SU_\eta(2)$, these have to be considered as the two sides of the same medal. Hence, from now on we do not formally distinguish between them at half-filling.

One can further characterize the ground state by considering the limits of weak and strong interactions. Here we review their basic properties - for a comprehensive description, the reader is referred to Table V of [38].

Weakly interacting fermions, $|U_{ff}| \ll zt_f$, pair in the s-wave channel. The resulting Cooper pairs describe two fermions of opposite spin and momenta close to the Fermi surface. Having a definite momentum, in real-space these objects stretch over distances larger than the lattice spacing and parts of them overlap. This can be explained by the weak interactions assumed between them. The energy needed to break a pair is given by twice the s-wave gap Δ_0 which is exponentially small. Finally, this limit shall be referred to as the *BCS* regime.

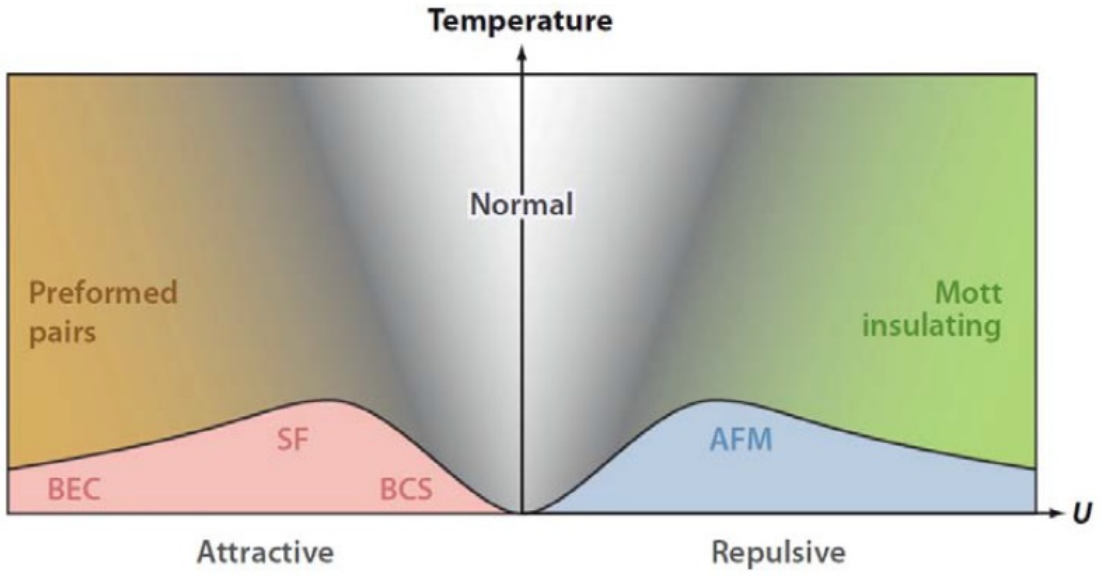

Figure 3.7: (color online): Temperature-interaction strength (T, U_{ff}) phase diagram of the Fermi-Hubbard model at half-filling [16].

[8] This is not true for the two-particle correlators and quantities derivable from them, such as their magnetic susceptibility which is suppressed by attractive interactions, [38].

In the opposite case of strongly interacting fermions, $|U_{ff}| \gg zt_f$, one expects the pairs (sometimes also called molecules in this limit) to be strongly localized in real-space, and completely delocalized in momentum-space. These molecules behave essentially as point-like bosons, and one obtains a very accurate description of the underlying physics by modelling the system as a condensate of bosonic molecules with half the particle number and twice the mass of a fermion constituent. The binding energy in this case is roughly set by the interaction strength $-|U_{ff}|$. The pairs hop along the lattice via the so-called *virtual ionization*. They can be described effectively by hardcore bosons with hopping amplitude $t_M = -2t_f^2/|U_{ff}|$ and nearest-neighbour repulsion given by $W = 2t_f^2/|U_{ff}|$, [38]. This limit is called the *BEC* regime.

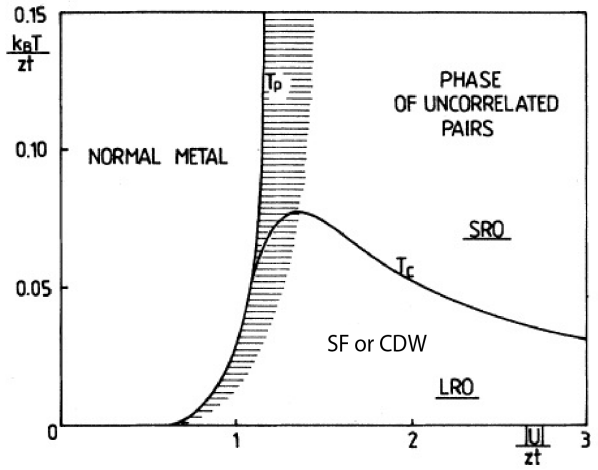

Figure 3.8: Temperature-interaction strength (T, U_{ff}) phase diagram of the Fermi-Hubbard model at half-filling. One distinguishes the lines of pair formation and condensation, given by T_p and T_c. The notations SRO and LRO signify short-range and long-range order, respectively. The superfluid phase (SF) and the charge-ordered phase (CDW) are degenerate at half-filling even at finite temperatures (figure adopted from [48]).

Despite the different physical mechanisms, it has been experimentally confirmed [16] that there is no phase transition between the two limits, meaning that the momentum distribution function m_k evolves smoothly from one regime to the other. As the interaction strength changes gradually, so do the molecular size and the statistics of the pairs. The BEC-BCS cross-over regime poses a considerable challenge from theoretical point of view and is not completely understood yet.

The phase diagram at finite temperature is shown in Figs. 3.7 and 3.8. One can clearly see the symmetry about the line $U_{ff} = 0$. Furthermore, the BCS and BEC regimes are found on the attractive side, the crossover lying in between. It is noteworthy, that the critical pairing temperature, denoted by T_p increases exponentially weakly, and sets the phase boundary in the BCS regime. In this weakly-interacting limit, the fermionic pairs appear and condense simultaneously. Conversely, in the limit of strong interactions the pairs form well above the condensation temperature T_c, but Bose-Einstein condensation does not occur until the T_c-line (see Fig. 3.8) is reached. Deep into the BEC regime, the condensation temperature decreases as $T_c \sim t_f^2/|U_{ff}|$.

3.5 Double MF-Description of the FHM at Half-Filling

The qualitative results based on symmetry arguments obtained in Section 3.3 make use of a general group-theoretical approach and are, therefore, exact. In this chapter, we are going to derive them qualitatively within a double mean-field approximation. The main result of this section is the coupled set of gap equations for the CDW and the SF gaps. We also show that, if carried out carefully, MF is capable of capturing the degeneracy in the ground state of the Fermi-Hubbard model.

Being familiar with the independent MF treatment of the CDW and the SF phases presented in Sections 3.1 and 3.2, the careful reader might have noticed one crucial difference in the two approaches: the decoupling of the interaction term in BCS theory is possible since we can precisely identify the interaction channel with the Cooper channel (Fig. 3.2). On the other hand, the CDW description requires us to decouple in the Density channel (Fig. 3.6). Since the two channels have a different physical meaning, which can be seen most easily from the Feynman graphs, we are not able to obtain a CDW-like decoupling from the Cooper channel or vice versa. This poses a fundamental problem on the basic MF ansatz.

Luckily, any self-consistent mean-field treatment is based on breaking the corresponding symmetry[9] and minimization of the ground state energy w.r.t. the introduced order parameters. Therefore, the way out is to assume a ground state in which the expectation value of the order parameters is non-zero. We make the following ansatz [15, 43] and apply Wick's theorem to the interaction term to obtain

$$\begin{aligned}
&\sum_{k_1,\dots,k_4,\sigma,\sigma'} \delta_{\sigma,\uparrow}\delta_{\sigma',\downarrow}\bar{\delta}\left(k_1-k_2+k_3-k_4\right)\langle c^\dagger_{k_1\sigma}c_{k_2\sigma}c^\dagger_{k_3\sigma'}c_{k_4\sigma'}\rangle \\
&= \sum_{k_1,\dots,k_4,\sigma,\sigma'} \delta_{\sigma,\uparrow}\delta_{\sigma',\downarrow}\bar{\delta}\left(k_1-k_2+k_3-k_4\right)\left[\langle c^\dagger_{k_1\sigma}c_{k_2\sigma}\rangle\langle c^\dagger_{k_3\sigma'}c_{k_4\sigma'}\rangle + \langle c^\dagger_{k_1\sigma}c^\dagger_{k_3\sigma'}\rangle\langle c_{k_4\sigma'}c_{k_2\sigma}\rangle\right],
\end{aligned} \tag{3.28}$$

where $\bar{\delta}$ denotes the delta function modulo the reciprocal lattice vector. This way, we allow for resonant process in both the Density and the Cooper channels. The dominating process from the Density channel is expected to occur when $k_1 = k_2 + \pi$ and $k_3 = k_4 + \pi$, whereas from the Cooper channel we retain the scattering processes at $k_3 = -k_1$ and $k_4 = -k_2$.

If we assume that $\Delta_\uparrow = \Delta_\downarrow$, and the two order parameters are given by

$$\begin{aligned}
\hat{\Delta}_c &= \frac{U_{ff}}{2N_s}\sum_{k\in\mathrm{BZ},\sigma} c^\dagger_{k+\pi,\sigma}c_{k,\sigma} = \frac{U_{ff}}{2N_s}\sum_{i,\sigma}(-1)^i c^\dagger_{i,\sigma}c_{i,\sigma} \\
\hat{\Delta}_0 &= \frac{U_{ff}}{N_s}\sum_{k\in\mathrm{BZ}} c^\dagger_{k,\uparrow}c^\dagger_{-k,\downarrow} = \frac{U_{ff}}{N_s}\sum_i c^\dagger_{i\uparrow}c^\dagger_{i\downarrow},
\end{aligned} \tag{3.29}$$

we can obtain the expectation value (3.28) in the following way: The effective quadratic interaction Hamiltonian, given by

$$H_{int} = \hat{\Delta}_c^2 + |\hat{\Delta}_0|^2, \tag{3.30}$$

together with the mean-field approximation $(\hat{\Delta}^\dagger_{c/0} - \Delta^*_{c/0})(\hat{\Delta}_{c/0} - \Delta_{c/0}) \approx 0$ yields

$$H^{(MF)}_{int} = \Delta_c\sum_{k,\sigma} c^\dagger_{k+\pi,\sigma}c_{k,\sigma} + \sum_k\left(\Delta_0 c_{-k,\downarrow}c_{k,\uparrow} + h.c.\right) - \frac{N_s}{U_{ff}}\left(\Delta_c^2 + |\Delta_0|^2\right). \tag{3.31}$$

[9] In the case of the FHM both orders are needed to break the symmetry group.

Here the hat denotes operators and the quantities without hats are their expectation values - the gap functions.

Before we continue, we make a short remark: in the bosonic case, the CDW induced by the external staggered potential also coupled the condensates at $\vec{k} = 0$ and $\vec{k} = \vec{\pi}$ via the term $b^\dagger_{k+\pi} b^\dagger_{-k}$. It would, therefore, seem natural to include another gap function, given by $\Delta_\pi = \frac{U_{ff}}{N_s} \sum_k \langle c^\dagger_{k+\pi\uparrow} c^\dagger_{-k\downarrow} \rangle = \frac{U_{ff}}{N_s} \sum_i (-1)^i \langle c^\dagger_{i\uparrow} c^\dagger_{i\downarrow} \rangle$, even without the presence of the staggered potential, as the CDW appears intrinsically in the ground state of the FHM. This quantity measures the difference of the superconducting order parameter Δ_0 on both sublattices A and B. Notice, however, that this Δ_π gap vanishes identically by symmetry arguments: it coincides precisely with the η^- generator of the pseudo-spin symmetry group $SU_\eta(2)$, given in Eq. (3.24). The group is broken to its $U(1)$ subgroup, generated by η^-. Hence, we find $\Delta_\pi = 0$ even in the case of a broken $SU_\eta(2)$ as a consequence of residual symmetry. Another way to see why $\Delta_\pi = 0$, as discussed in Chapter 3.6.1, is due to Particle-Hole symmetry at half-filling, [30].

The effective MF Hamiltonian at half-filling takes the form

$$\begin{aligned} H = & \underbrace{-\frac{N_s}{U_{ff}} \left(\Delta_c^2 + |\Delta_0|^2 \right)}_{=: H_0} \\ & + \sum_{k \in \mathrm{BZ}} \left[\left(\sum_\sigma \varepsilon_k c^\dagger_{k\sigma} c_{k\sigma} + \Delta_c c^\dagger_{k+\pi\sigma} c_{k\sigma} \right) + \Delta_0 \left(c^\dagger_{k\uparrow} c^\dagger_{-k\downarrow} + h.c. \right) \right]. \end{aligned} \tag{3.32}$$

Next, we reduce the Brillouin zone, defining operators $\alpha_{k\sigma}$ and $\beta_{k\sigma}$ via

$$c_{k\sigma} = \begin{cases} \alpha_{k,\sigma} & \text{for } \; k \in \mathrm{BZ}' \\ \beta_{k\pm\pi,\sigma} & \text{for } \; k \notin \mathrm{BZ}' \end{cases} \tag{3.33}$$

where the reduced Brillouin zone is given by $\mathrm{BZ}' := \{\vec{k} \in \mathrm{BZ} : \cos(k_x) + \cos(k_y) + \cos(k_z) \geq 0\}$. As in the case of bosons, the notation $k \pm \pi$ stands for the eight possible combinations of distributing the $\pm$-signs among the components of the vector $\vec{\pi} = (\pi, \pi, \pi)$. The crucial difference is that the operators α and β are fermionic and anti-commute with each other. The terms in the Hamiltonian in the new operators read

$$\begin{aligned} \sum_{k \in \mathrm{BZ}} \varepsilon_k c^\dagger_{k\sigma} c_{k\sigma} &= \sum_{k \in \mathrm{BZ}'} \varepsilon_k \left(\alpha^\dagger_{k\sigma} \alpha_{k\sigma} - \beta^\dagger_{k\sigma} \beta_{k\sigma} \right) \\ \sum_{k \in \mathrm{BZ}} c^\dagger_{k+\pi,\sigma} c_{k\sigma} &= \sum_{k \in \mathrm{BZ}'} \left(\alpha^\dagger_{k+\pi,\sigma} \beta_{k\sigma} + h.c. \right) \\ \sum_{k \in \mathrm{BZ}} c^\dagger_{k,\uparrow} c^\dagger_{-k\downarrow} &= \sum_{k \in \mathrm{BZ}'} \left(\alpha^\dagger_{k,\uparrow} \alpha^\dagger_{-k\downarrow} + \beta^\dagger_{k,\uparrow} \beta^\dagger_{-k\downarrow} \right). \end{aligned} \tag{3.34}$$

Hence, the Hamiltonian is given by

$$\begin{aligned} H = H_0 + & \sum_{k \in \mathrm{BZ}'} \varepsilon_k \left(\alpha^\dagger_{k\uparrow} \alpha_{k\uparrow} - \alpha_{k\downarrow} \alpha^\dagger_{k\downarrow} - \beta^\dagger_{k\uparrow} \beta_{k\uparrow} + \beta_{k\downarrow} \beta^\dagger_{k\downarrow} \right) \\ & + \Delta_c \left(\alpha^\dagger_{k\uparrow} \beta_{k\uparrow} + \beta^\dagger_{k\uparrow} \alpha_{k\uparrow} - \alpha^\dagger_{k\downarrow} \beta_{k\downarrow} - \alpha^\dagger_{k\uparrow} \beta_{k\uparrow} \right) \\ & + \Delta_0 \left(\alpha^\dagger_{k\uparrow} \alpha^\dagger_{-k\downarrow} + \beta^\dagger_{k\uparrow} \beta^\dagger_{-k\downarrow} + \alpha_{-k\downarrow} \alpha_{k\uparrow} + \beta_{-k\downarrow} \beta_{k\uparrow} \right). \end{aligned} \tag{3.35}$$

Defining the vector $\vec{\alpha}_k = (\alpha_{k\uparrow}, \beta_{k,\uparrow}, \alpha^\dagger_{-k\downarrow}, \beta^\dagger_{-k\downarrow})^t$, we make use of matrix notation to put it into the form

$$H = H_0 + \sum_{k\in \mathrm{BZ}'} \vec{\alpha}^\dagger_k H \vec{\alpha}_k, \tag{3.36}$$

where the matrix H is given by[10]

$$H = \begin{pmatrix} \varepsilon_k & \Delta_c & \Delta_0 & 0 \\ \Delta_c & -\varepsilon_k & 0 & \Delta_0 \\ \Delta_0 & 0 & -\varepsilon_k & -\Delta_c \\ 0 & \Delta_0 & -\Delta_c & \varepsilon_k \end{pmatrix}. \tag{3.37}$$

Introducing a unitary transformation M, which diagonalizes H, we define the new operators $\vec{\gamma}_k = M_k \vec{\alpha}_k$, such that $\vec{\gamma}_k = (\gamma_{1,k}, \gamma_{2,k}, \gamma^\dagger_{3,k}, \gamma^\dagger_{4,k})^t$, to arrive at

$$\begin{aligned} H &= H_0 + \sum_{k\in \mathrm{BZ}'} \vec{\alpha}^\dagger_k H \vec{\alpha}_k = H_0 + \sum_{k\in \mathrm{BZ}'} \vec{\gamma}^\dagger_k M^\dagger H M \vec{\gamma}_k \\ &= H_0 - \sum_{k\in \mathrm{BZ}'} E_k \left(\gamma_{k,3}\gamma^\dagger_{k,3} + \gamma_{k,4}\gamma^\dagger_{k,4} \right) + \sum_{k\in \mathrm{BZ}'} E_k \left(\gamma^\dagger_{k,1}\gamma_{k,1} + \gamma^\dagger_{k,2}\gamma_{k,2} \right) \\ &= \underbrace{H_0 - 2\sum_{k\in \mathrm{BZ}'} E_k}_{=:\, E_{gs}} + \sum_{k\in \mathrm{BZ}',\sigma} E_k \gamma^\dagger_{k,\sigma}\gamma_{k,\sigma}. \end{aligned} \tag{3.38}$$

The γ_σ operators describe the excitations above the ground state with energy E_{gs}. They populate the degenerate bands $E_k = \sqrt{\varepsilon_k^2 + \Delta_c^2 + |\Delta_0|^2}$. The index $\sigma = 1, \ldots, 4$ counts the different operators γ_σ. Clearly, all of them fill in the same excited band E_k, which is a manifestation of the residual spin symmetry.

In the remainder of this section, we fix the particle density using the fact that we are at half-filling, and derive self-consistently the gap equations. Minimizing E_{gs} w.r.t. the order parameters Δ_0 and Δ_c yields two equations, so that the ground state properties of the system are completely described within MF by a set of two coupled equations.

The procedure for fixing the filling is the same as in the bosonic case. This time, however, one has to be careful with the anti-commutator relations. Again, we choose to evaluate the

[10] We use the same notation for the Hamiltonian operator and the Hamiltonian matrix H.

density at the lattice site $\vec{r}_i = 0$ for simplicity:

$$\begin{aligned}
\langle \hat{m}_{\vec{r}_i=0} \rangle =& \frac{1}{N_s} \sum_{k_1,k_2 \in \mathrm{BZ},\sigma} \langle c^\dagger_{k_1\sigma} c_{k_2\sigma} \rangle \\
=& \frac{1}{N_s} \sum_{k_1,k_2 \in \mathrm{BZ}',\sigma} \langle \alpha^\dagger_{k_1\sigma}\alpha_{k_2\sigma} + \beta^\dagger_{k_1\sigma}\beta_{k_2\sigma} + \alpha^\dagger_{k_1\sigma}\beta_{k_2\sigma} + \beta^\dagger_{k_1\sigma}\alpha_{k_2\sigma} \rangle \\
=& \frac{1}{N_s} \sum_{k_1,k_2 \in \mathrm{BZ}'} \langle \alpha^\dagger_{k_1\uparrow}\alpha_{k_2\uparrow} + \alpha^\dagger_{k_1\downarrow}\alpha_{k_2\downarrow} + \beta^\dagger_{k_1\uparrow}\beta_{k_2\uparrow} + \beta^\dagger_{k_1\downarrow}\beta_{k_2\downarrow} \\
& + \alpha^\dagger_{k_1\uparrow}\beta_{k_2\uparrow} + \alpha^\dagger_{k_1\downarrow}\beta_{k_2\downarrow} + \beta^\dagger_{k_1\uparrow}\alpha_{k_2\uparrow} + \beta^\dagger_{k_1\downarrow}\alpha_{k_2\downarrow} \rangle \\
=& \frac{1}{N_s} \sum_{k_1,k_2 \in \mathrm{BZ}'} \langle \vec{\alpha}^\dagger_k \underbrace{\begin{pmatrix} 1 & 1 & 0 & 0 \\ 1 & 1 & 0 & 0 \\ 0 & 0 & -1 & -1 \\ 0 & 0 & -1 & -1 \end{pmatrix}}_{=:\, P} \vec{\alpha}_{k_2} \rangle + 2\delta_{k_1,k_2} \\
=& 1 + \frac{1}{N_s} \sum_{k \in \mathrm{BZ}'} \langle \vec{\gamma}^\dagger_k \underbrace{M^\dagger_k P M_k}_{=:\, \tilde{P}_k} \vec{\gamma}_k \rangle = 1 + \frac{1}{N_s} \sum_{k \in \mathrm{BZ}'} \left(\tilde{P}^{(33)}_k + \tilde{P}^{(44)}_k \right).
\end{aligned} \tag{3.39}$$

We assume an enhancement of the density on the sublattice containing $\vec{r} = 0$, which is equivalent to assuming that the CDW gap $\Delta_c \geq 0$ (c.f. Eq. (3.41)). Making the ansatz $\langle \hat{m}_{\vec{r}_i=0} \rangle \stackrel{!}{=} 1 + \alpha$, we arrive at the expression for the fermionic CDW amplitude

$$\alpha = \frac{1}{N_s} \sum_{k \in \mathrm{BZ}'} \left(\tilde{P}^{(33)}_k + \tilde{P}^{(44)}_k \right). \tag{3.40}$$

There exists a relation between the CDW gap and the CDW amplitude, given by

$$\Delta_c = \frac{U_{ff}}{2N_s} \sum_i (-1)^i \langle m_i \rangle = \frac{U_{ff}}{2N_s} \sum_i (-1)^i \left[1 - (-1)^i \alpha \right] = \frac{\alpha |U_{ff}|}{2} \geq 0. \tag{3.41}$$

Hence, Eq. (3.40) is equivalent to the gap equation for Δ_c, since the matrix $\tilde{P}$ depends on Δ_c through the transformation M.

The corresponding self-consistency equation for Δ_0 can be derived similarly. We omit the details here:

$$\Delta_0 = \frac{U_{ff}}{N_s} \sum_{k \in \mathrm{BZ}} \langle c^\dagger_{k\uparrow} c^\dagger_{-k\downarrow} \rangle = \cdots = \frac{U_{ff}}{N_s} \sum_{k \in \mathrm{BZ}'} \langle \vec{\gamma}^\dagger_k \underbrace{M^\dagger_k S_0 M_k}_{=:\, \tilde{S}_0} \vec{\gamma}_k \rangle, \tag{3.42}$$

where S_0 is given by

$$S_0 = \begin{pmatrix} 0_{2\times 2} & \mathbb{1}_{2\times 2} \\ 0_{2\times 2} & 0_{2\times 2} \end{pmatrix}. \tag{3.43}$$

The full set of equations determining the phase transition in the Fermi-Hubbard model

reads:

$$\begin{aligned}\Delta_c &= \frac{|U_{ff}|}{N_s}\sum_{k\in \mathrm{BZ}'}\frac{\Delta_c}{\sqrt{\varepsilon_k^2+\Delta_c^2+|\Delta_0|^2}}\\ |\Delta_0| &= \frac{|U_{ff}|}{N_s}\sum_{k\in \mathrm{BZ}'}\frac{|\Delta_0|}{\sqrt{\varepsilon_k^2+\Delta_c^2+|\Delta_0|^2}}\end{aligned} \tag{3.44}$$

Assuming we are in the ordered phase, we divide the first equation by Δ_c, the second by $|\Delta_0|$, and add them up. Comparing the resulting equation with either of the first two, we arrive at

$$1 = \frac{|U_{ff}|}{N_s}\sum_{k\in \mathrm{BZ}'}\frac{1}{\sqrt{\varepsilon_k^2+\Delta_c^2+|\Delta_0|^2}}. \tag{3.45}$$

Clearly, this equation is equivalent to any of the gap equations derived for the BCS and the CDW gaps separately, if we define $\Delta = \sqrt{|\Delta_0|^2+\Delta_c^2}$. Therefore, the general solution reads

$$|\Delta_0|^2 + \Delta_c^2 = const, \tag{3.46}$$

for some number depending on the model parameters t_f and U_{ff} (c.f. Eq. (3.10)). Hence, any pair (Δ_c, Δ_0) which satisfies the above relation is admissible. Moreover, the two order parameters enter in the ground state energy only through the combination $|\Delta_0|^2 + \Delta_c^2$, so that all these states indeed have the same energy.

This is the prove for the degeneracy of the ground state within the double MF description. It is an arbitrary superposition of the CDW and the SF state. The equation for $\Delta_c^2 + |\Delta_0|^2$ reduces to the usual MF one given by Eq. (3.9). Clearly, the above analysis agrees precisely with the conclusions drawn from symmetry considerations in Section 3.3.2.

3.6 FHM away from Half-Filling

With respect to our subsequent analysis of the Bose-Fermi mixture, it would be advantageous to devote parts of the discussion to fermionic systems away from half-filling. In particular, we are interested in studying the FHM in the presence of a staggered potential and nearest-neighbour (Coulomb) interactions. The first two effects will compete against each other to determine the MF phase diagram of the Bose-Fermi mixture, addressed in the next chapter, and are of special interest.

Clearly, any of these additional terms breaks the pseudo-spin symmetry of the model. Therefore, one may investigate the possibility for a mixed phase of a staggered superconductor away from half-filling. The relevant order parameter to describe it is given by

$$\Delta_\pi = \frac{U_{ff}}{N_s}\sum_{k\in \mathrm{BZ}}\langle c^\dagger_{k+\pi\uparrow}c^\dagger_{-k\downarrow}\rangle = \frac{U_{ff}}{N_s}\sum_{k\in \mathrm{BZ}}(-1)^i\langle c^\dagger_{i\uparrow}c^\dagger_{i\downarrow}\rangle. \tag{3.47}$$

The first thing to note is that this gap measures the difference of the superconducting gap Δ_0 on the two sublattices A and B induced by the staggered order. Since the pseudo-spin symmetry is no longer there, in principle one has to allow for a non-zero value of this

parameter. Second, it is clear from the form of the interaction term in the Cooper channel that this gap arises from this channel when one takes into account the momentum at $\vec{q} = \vec{\pi}$. This process is expected to be resonant just like in the bosonic case. Whether the gap Δ_π is present or not, will be determined from the extended set of the corresponding self-consistency equations.

To this end, we need to expand the analysis of the previous Section 3.5. We begin by making a convention: as before, we choose the CDW to diminish the average particle number on the even sublattice A which contains the origin, and to enhance it on the odd sublattice B, keeping $\Delta_c \geq 0$. The sign of the gap Δ_π is not easily determined. However, we can safely assume it to be real, since the phase difference between Δ_0 and Δ_π is easily found to be zero, [30], by minimization of the energy. Finally, we remark that we necessarily have $|\Delta_\pi| \leq |\Delta_0|$.

The mean-field Hamiltonian reads

$$H = \underbrace{-\frac{N_s}{U_{ff}}\left(\Delta_c^2 + |\Delta_0|^2 + |\Delta_\pi|^2\right)}_{=:\, H_0} + \sum_{k\in \mathrm{BZ}} \Bigg[\left(\sum_\sigma \left(\varepsilon_k - \mu\right) c^\dagger_{k\sigma} c_{k\sigma} + \Delta_c c^\dagger_{k+\pi\sigma} c_{k\sigma} \right) + \Delta_0 \left(c^\dagger_{k\uparrow} c^\dagger_{-k\downarrow} + h.c. \right) + \Delta_\pi \left(c^\dagger_{k+\pi\uparrow} c^\dagger_{-k\downarrow} + h.c. \right) \Bigg]. \tag{3.48}$$

Reducing the Brillouin zone, we supplement Eq. (3.34) by

$$\sum_{k\in \mathrm{BZ}} c^\dagger_{k+\pi\uparrow} c^\dagger_{-k\downarrow} = \sum_{k\in \mathrm{BZ}'} \left(\alpha^\dagger_{k,\uparrow} \beta^\dagger_{-k\downarrow} + \beta^\dagger_{k,\uparrow} \alpha^\dagger_{-k\downarrow} \right). \tag{3.49}$$

The rest of the procedure is similar to what we did earlier. The Hamiltonian matrix reads

$$H = \begin{pmatrix} \varepsilon_k - \mu & \Delta_c & \Delta_0 & \Delta_\pi \\ \Delta_c & -\varepsilon_k - \mu & \Delta_\pi & \Delta_0 \\ \Delta_0 & \Delta_\pi & -\varepsilon_k + \mu & -\Delta_c \\ \Delta_\pi & \Delta_0 & -\Delta_c & \varepsilon_k + \mu \end{pmatrix}, \tag{3.50}$$

and hence we need a different unitary transformation M to diagonalize it. This time the energy bands for the excitations are non-degenerate only for $\mu \neq 0$,[11] and are given by

$$E_k^{(1/2)} = \sqrt{\Delta_c^2 + |\Delta_0|^2 + \Delta_\pi^2 + \varepsilon_k^2 + \mu^2 \pm 2\sqrt{\left(|\Delta_0|\Delta_\pi + \mu\Delta_c\right)^2 + \varepsilon_k^2\left(\Delta_\pi^2 + \mu^2\right)}}. \tag{3.51}$$

They are reminiscent of the two excitation bands we derived for the Bose-Hubbard model within the Bogoliubov approximation in Chapter 2.2.3. The definition of the $\gamma_{k\sigma}$ operators is the same as in the previous Section. The Hamiltonian assumes the following diagonal form

$$H = H_0 - \sum_{k\in \mathrm{BZ}'} \left(E_k^{(1)} + E_k^{(2)} + 2\mu \right) + \sum_{k\in \mathrm{BZ}'} \left[E_k^{(1)} \left(\gamma^\dagger_{k,1}\gamma_{k,1} + \gamma^\dagger_{k,3}\gamma_{k,3} \right) + E_k^{(2)} \left(\gamma^\dagger_{k,2}\gamma_{k,2} + \gamma^\dagger_{k,4}\gamma_{k,4} \right) \right] \tag{3.52}$$

[11] At half-filling, due to Particle-Hole symmetry, we still have $\Delta_\pi = 0$.

The total ground state energy reads

$$E_{gs} = -\frac{N_s}{U_{ff}}\left(\Delta_c^2 + |\Delta_0|^2 + |\Delta_\pi|^2\right) - \sum_{k\in \mathrm{BZ}'}\left(E_k^{(1)} + E_k^{(2)} + 2\mu\right). \tag{3.53}$$

Minimizing w.r.t. the order parameters Δ_c, Δ_0, and Δ_π, and defining

$$X = \sqrt{\left(|\Delta_0|\Delta_\pi + \mu\Delta_c\right)^2 + \varepsilon_k^2\left(|\Delta_\pi|^2 + \mu^2\right)}, \tag{3.54}$$

we obtain the extended set of gap equations to be

$$\begin{aligned}
\Delta_c &= \frac{|U_{ff}|}{2N_s}\sum_{k\in \mathrm{BZ}'}\left(\frac{\Delta_c + \mu\frac{|\Delta_0|\Delta_\pi+\mu\Delta_c}{X}}{E_k^{(1)}} + \frac{\Delta_c - \mu\frac{|\Delta_0|\Delta_\pi+\mu\Delta_c}{X}}{E_k^{(2)}}\right)\\
|\Delta_0| &= \frac{|U_{ff}|}{2N_s}\sum_{k\in \mathrm{BZ}'}\left(\frac{|\Delta_0| + \Delta_\pi\frac{|\Delta_0||\Delta_\pi|+\mu\Delta_c}{X}}{E_k^{(1)}} + \frac{|\Delta_0| - \Delta_\pi\frac{|\Delta_0|\Delta_\pi+\mu\Delta_c}{X}}{E_k^{(2)}}\right)\\
\Delta_\pi &= \frac{|U_{ff}|}{2N_s}\sum_{k\in \mathrm{BZ}'}\left(\frac{\Delta_\pi + \frac{|\Delta_0|^2+\mu\Delta_c|\Delta_0|+\Delta_\pi\varepsilon_k^2}{X}}{E_k^{(1)}} + \frac{\Delta_\pi - \frac{|\Delta_0|^2+\mu\Delta_c|\Delta_0|+\Delta_\pi\varepsilon_k^2}{X}}{E_k^{(2)}}\right).
\end{aligned} \tag{3.55}$$

Before we continue, we wish to make a couple of remarks about the system of coupled equations above: first, in the limit of $\mu \to 0$ we have that $|\Delta_\pi| \to 0$, the above system reduces to Eq. (3.44). Second, we see that if $\Delta_c \to 0$, we immediately find $\Delta_\pi \to 0$ and thus the staggered superconductivity goes away. Due to the relation $|\Delta_\pi| \leq |\Delta_0|$, if $\Delta_0 \to 0$ so does Δ_π, which makes sense, since we cannot have a staggered superconductor with a vanishing superconducting gap Δ_0.

The last equation we need is the Number equation which fixes the chemical potential μ from the given filling m. We can readily obtain in from the expectation value of the fermion number operator $\hat{M}$:

$$m = \frac{1}{N_s}\langle\hat{M}\rangle = \frac{1}{N_s}\sum_{k\in \mathrm{BZ}'}\langle\vec{\gamma}_k^\dagger M^\dagger \begin{pmatrix} 1 & 0 & 0 & 0\\ 0 & 1 & 0 & 0\\ 0 & 0 & -1 & 0\\ 0 & 0 & 0 & -1 \end{pmatrix} M\vec{\gamma}_k\rangle + 2, \tag{3.56}$$

where the matrix M is the unitary transformation that diagonalizes the Hamiltonian (3.64). If we define four 2×2 matrices M_i via

$$M = \begin{pmatrix} M_1 & M_2\\ M_3 & M_4 \end{pmatrix}, \tag{3.57}$$

the unitarity of M implies $M_2^\dagger M_2 + M_4^\dagger M_4 = \mathbb{1}$. Using this, the number equation assumes the simple form

$$m = \frac{2}{N_s}\sum_{k\in \mathrm{BZ}'} 2\times \mathrm{tr}\left(M_2^\dagger M_2\right). \tag{3.58}$$

An equivalent way of finding the number equation is to consider a temperature-dependent system (c.f. Section 4.3) and put $T \to 0$ in the very end of the calculation. This gives the

number equation

$$m = \frac{2}{N_s} \sum_{k\in \mathrm{BZ}',s} \left[1 + \frac{\partial E_k^{(s)}}{\partial \mu} \tanh\left(\frac{\beta}{2} E_k^{(s)} \right) \right]. \tag{3.59}$$

Both approaches are, of course, equivalent. Finally, in terms of the model parameters, it takes the form

$$\begin{aligned} m = \; 1 + \frac{1}{2N_s} \sum_{k\in \mathrm{BZ}'} \Bigg[& \frac{\mu + \frac{|\Delta_0|\Delta_\pi \Delta_c + \mu\left(\Delta_c^2 + \varepsilon_k^2\right)}{X}}{E_k^{(1)}} \tanh\left(\frac{\beta}{2} E_k^{(1)} \right) \\ & + \frac{\mu - \frac{|\Delta_0|\Delta_\pi \Delta_c + \mu\left(\Delta_c^2 + \varepsilon_k^2\right)}{X}}{E_k^{(2)}} \tanh\left(\frac{\beta}{2} E_k^{(2)} \right) \Bigg]. \end{aligned} \tag{3.60}$$

Before we take a closer look at the special cases mentioned at the beginning of the section, we notice one final thing. As they stand, Eq's (3.55) might still need modification: the symmetry breaking via nearest-neighbour interactions or a staggered potential will change the expressions under the momentum summation for the different gaps via the dispersion relation. As we know from the analysis of the FHM in the previous section, the self-consistency equations are very sensitive towards this change.

3.6.1 FHM in a Staggered Potential

Let us now take a closer look at the consequences of applying a staggered potential. We add to the Fermi-Hubbard Hamiltonian an alternating term so that it takes the form

$$\begin{aligned} H = & - t_f \sum_{\langle ij\rangle,\sigma} \left(c_{i\sigma}^\dagger c_{j\sigma} + h.c. \right) \\ & - \mu \sum_i m_i + U_{bf} \sum_i \left[1 + (-1)^i \eta \right] m_i + U_{ff} \sum_i m_{i\uparrow} m_{i\downarrow}. \end{aligned} \tag{3.61}$$

The staggering strength is given by the parameter $\eta \in [0, 1]$. As in the bosonic case from Chapter 2, this form is motivated by a mean-field decoupling of the interspecies density-density interaction of the Bose-Fermi mixture. We see that a part of the staggered term induces a shift in the chemical potential. We choose the case $U_{bf} \geq 0$ which removes the internal degeneracy of the CDW state shown in Fig. 3.5, enhancing the fermionic density on the odd sublattice B.

Notice, however, that at half-filling Particle-Hole symmetry maps $m \to 1 - m$ and $U_{bf} \to -U_{bf}$, thus interchanging the role of the two sublattices. Therefore, in this special case, we also have $\Delta_\pi = 0$, even thought the pseudo-spin symmetry is explicitly broken by the staggered field [30].

Very recently, Iskin analyzed the effect of staggered potential on the superfluid phase of an interacting fermionic system, [30]. At half-filling, one finds a phase transition in the $(\eta U_{bf}, |U_{ff}|/t_f)$ plane given by the solution of the BCS gap equation (3.1). For high interaction strengths and low staggering strengths one finds an induced supersolid (staggered superfluid), while above the critical line the SF gap suddenly disappears and the ground state is a pure CDW. However, this analysis did not take into account the possibility for a degenerate SF-CDW ground state at half-filling when the staggered potential is switched off, as it

did not directly refer to the Fermi-Hubbard model. Therefore, below we provide an analytical investigation of this scenario.

The Hamiltonian for the system takes the form

$$\begin{aligned} H =& - t_f \sum_{\langle ij\rangle,\sigma} \left(c^\dagger_{i\sigma} c_{j\sigma} + h.c. \right) - (\mu - U_{bf}) \sum_i m_i \\ &+ \eta U_{bf} \sum_i (-1)^i m_i + U_{ff} \sum_i \left(m_{i\uparrow} - \frac{1}{2} \right) \left(m_{i\downarrow} - \frac{1}{2} \right). \end{aligned} \tag{3.62}$$

The staggered term enhances the CDW amplitude, which can be seen from its momentum-space representation:

$$\sum_i (-1)^i m_i = \sum_{k\in \mathrm{BZ},\sigma} c^\dagger_{k+\pi\sigma} c_{k\sigma} = \sum_{k\in \mathrm{BZ}'} \left(\alpha^\dagger_{k\sigma} \beta_{k\sigma} + h.c. \right). \tag{3.63}$$

The MF Hamiltonian assumes the following form, including the gap Δ_π:

$$\begin{aligned} H =& \underbrace{- \frac{N_s}{U_{ff}} \left(\Delta_c^2 + |\Delta_0|^2 + |\Delta_\pi|^2 \right)}_{=:\, H_0} + \sum_{k\in \mathrm{BZ}} \Bigg[\Bigg(\sum_\sigma (\varepsilon_k - \mu + U_{bf}) c^\dagger_{k\sigma} c_{k\sigma} \\ &+ \left[\Delta_c + \eta U_{bf} \right] c^\dagger_{k+\pi\sigma} c_{k\sigma} \Bigg) + \Delta_0 \left(c^\dagger_{k\uparrow} c^\dagger_{-k\downarrow} + h.c. \right) + \Delta_\pi \left(c^\dagger_{k+\pi\uparrow} c^\dagger_{-k\downarrow} + h.c. \right) \Bigg]. \end{aligned} \tag{3.64}$$

The ground state energy is given by

$$E_{gs} = \frac{N_s}{|U_{ff}|} \left(\Delta_c^2 + |\Delta_0|^2 + |\Delta_\pi|^2 \right) - \sum_{k\in \mathrm{BZ}'} \left(E^{(1)}_k + E^{(2)}_k - 2(\mu - U_{bf}) \right), \tag{3.65}$$

where the band structure is modified according to

$$\begin{aligned} E^{(1/2)}_k &= \sqrt{(\Delta_c + \eta U_{bf})^2 + |\Delta_0|^2 + |\Delta_\pi|^2 + \varepsilon_k^2 + (\mu - U_{bf})^2 \pm 2X'}, \\ X' &= \sqrt{\left(|\Delta_0| \Delta_\pi + (\mu - U_{bf})(\Delta_c + \eta U_{bf}) \right)^2 + \varepsilon_k^2 \left(|\Delta_\pi|^2 + (\mu - U_{bf})^2 \right)}. \end{aligned} \tag{3.66}$$

The self-consistency equations (3.55) and the Number equation (3.60) can be generalized easily, replacing on the right hand sides $\Delta_c \to \Delta_c + U_{bf}\eta$ and $\mu \to \mu - U_{bf}$.

This concludes the discussion on the FHM in the presence of a staggered field.

3.6.2 Nearest-Neighbour Interactions and the Extended FHM

The extended Fermi-Hubbard model takes into account nearest-neighbour (nn) interactions in addition to the already familiar on-site attraction (repulsion). The Hamiltonian reads

$$H = -t_f \sum_{\langle ij\rangle,\sigma} \left(c^\dagger_{i\sigma} c_{j\sigma} + h.c. \right) - \mu \sum_i m_i + U_{ff} \sum_i m_{i\uparrow} m_{i\downarrow} + \frac{W}{2} \sum_{\langle ij\rangle} n_i n_j. \tag{3.67}$$

Clearly, due to the presence of the nn interaction term we no longer have the pseudo-spin symmetry. Therefore, it can be shown that the degeneracy of the ground state is lifted, [38]. In the attractive FHM, a positive intersite interaction $W > 0$ will favour charge order and

the ground state prefers the DLRO of the CDW phase. This is intuitively clear, since the fermionic density distribution will tend to avoid configurations with neighbouring fermions, as they will cost more energy.

On the other hand, an attractive nn interaction, $W < 0$, enhances the ODLRO, and the system prefers the SF state. It would be energetically cheaper for the fermions to occupy every site at half-filling which clearly enhances and stabilizes the superconducting state.

In the strong-coupling limit, the Hamiltonian (3.67) can be mapped to a spin system using the mapping [48, 47].

TABLE II. Correspondence between electronic orderings and types of pseudospin orderings.

Long-range order (LRO) Diagonal (DLRO)	Long-range order (LRO) Off-diagonal (ODLRO)	Type of ordered state in extended Hubbard model with $U<0$	Ordering of pseudospins $\{\rho_i^\alpha\}$, $\alpha=+,-,z$
No	No	Nonordered phase (NO) Phase of uncorrelated local pairs, diamagnetic short-range order $n=\frac{1}{N}\sum_{i,\sigma}\langle n_{i\sigma}\rangle=\frac{1}{N}\sum_i\langle 2\rho_i^z+1\rangle.$	Ferromagnetic or paramagnetic ↑↑
Yes	No	Charge order (CO) $\Delta_Q=\frac{1}{N}\sum_{i,\sigma}\langle n_{i\sigma}\rangle e^{iQ\cdot R_i}=\langle\rho_A^z-\rho_B^z\rangle\neq 0$	Antiferromagnetic ↑↓ or more complicated orderings along z axis
No	Yes	Singlet (on-site) superconductivity (SS) $x_0=\frac{1}{N}\sum_i\langle c_{i\uparrow}^\dagger c_{i\downarrow}^\dagger\rangle=\frac{1}{N}\sum_i\langle\rho_i^x\rangle$ $=\langle\rho_A^x\rangle+\langle\rho_B^x\rangle\neq 0$	Spin flopped ↗ ↗
Yes	Yes	Mixed phase (M) of CO and SS $\Delta_Q\neq 0,\quad x_0\neq 0,$ $x_Q=\frac{1}{N}\sum_i\langle c_{i\uparrow}^\dagger c_{i\downarrow}^\dagger\rangle e^{iQ\cdot R_i}=\langle\rho_A^x\rangle-\langle\rho_B^x\rangle\neq 0$	Intermediate state ↗ ↘
Yes	No	Condensed phase of electron droplets (phase separation)	Droplets of ferromagnetic order $\cdots\uparrow\uparrow\uparrow\downarrow\downarrow\downarrow\cdots$

Figure 3.9: Different types of superconducting order parameters for the Fermi-Hubbard model with broken pseudo-spin symmetry (figure adopted from [38]).

$$\rho_i^+ = c_{i\uparrow}^\dagger c_{i\downarrow}^\dagger, \qquad \rho_i^- = c_{i\downarrow} c_{i\uparrow}$$
$$\rho_i^z = \frac{1}{2}\left(m_{i\uparrow} + m_{i\downarrow} - 1\right). \tag{3.68}$$

The resulting spin model Hamiltonian $\bar{H}$ is given by

$$\bar{H} = -J\sum_{\langle ij\rangle}\rho_i^+\rho_j^- + K\sum_{\langle ij\rangle}\rho_i^z\rho_j^z - \bar{\mu}\sum_i(2\rho_i^z+1) - \frac{zN_s}{4}(J+2W), \tag{3.69}$$

where $J = 2t_f/|U_{ff}|$ is the effective hopping strength, $K = J + 2W$ defines the effective strength of the intersite density-density interaction, and $\bar{\mu} = \mu + \frac{1}{2}U_{ff} - zW$ is the new chemical potential.

The main properties and definitions of the possible phases of this model are summarized in Fig. 3.9.

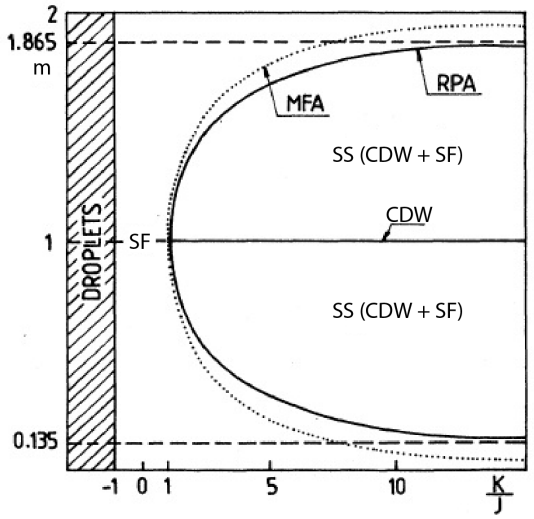

Figure 3.10: Phase diagram of the FHM at any filling $n \in [0, 2]$ for $K = J + 2W$. The phase boundaries were obtained simultaneously from a mean-field approximation (MFA) and a rotating phase approximation (RPA). (figure adopted from [38]).

The phase diagram of the model is given in Fig. 3.10. It is noteworthy that in the presence of repulsive nn interactions, and away from half-filling one finds a staggered superconducting phase, characterized by the non-vanishing order parameter Δ_π.

Before we finish this section, we finally mention that there exists a mapping from the FHM with attractive interactions at arbitrary filling to the extended Hubbard model with repulsive interactions at half-filling. It was first introduced in [48].

3.7 Conclusions

In retrospect, we have analyzed the properties of the Fermi-Hubbard model and its extension to nearest-neighbour interactions. At half-filling, the model enjoys a Particle-Hole symmetry, which postulates that the ground state phase diagram of the model is symmetric w.r.t. the line $\mu = 0$. The Lieb-Mattis transformation, on the other hand, allows to transfer all the results for the model from the attractive to the repulsive side of the interaction parameter U_{ff}. It provides a dictionary between the magnetic phases on the repulsive interaction side, and the CDW and SF (pairing) phases on the attractive side.

Moreover, at half-filling the full symmetry group of the FHM, $SO(4) = SU_\eta(2) \times SU_\sigma(2)/Z_2$, consists of a spin $SU_\sigma(2)$ subgroup and a pseudo-spin $SU_\eta(2)$ subgroup. In the ground state, there are two degenerate orders: the CDW and the SF (superconducting) one, and hence the true ground state is an arbitrary superposition of both. The emergence of the order parameters Δ_0 and Δ_c breaks the $SU_\eta(2)$ subgroup of the pseudo-spin part. Before, we break it, the pseudo-spin symmetry generators rotate one order parameter into the other, as described in Section 3.3.2. Within the CDW-SF state, the BCS-BEC crossover and its essential features were briefly discussed.

As a proof of this general statement based on symmetry arguments, an extended (double) mean-field decoupling scheme has been introduced. The results confirmed the group theoret-

ical predictions on a MF level, and we showed that both orders have the same energy, while any combination of a simultaneous CDW and SF state was observed to have higher energy, and should hence be rendered non-physical.

Through the remainder of the discussion, the FHM away from half-filling was considered, which inevitably breaks the pseudo-spin symmetry. Applying a staggered potential to the FHM, we calculated a set of four self-consistency equations: three from the CDW, SF and mixed gaps and one for the chemical potential. Further, we gave a brief survey over well-established results concerning the MF phase diagram of the extended Hubbard model. If the nearest-neighbour interaction strength is repulsive, it stabilizes the CDW order, while if it is attractive the SF phase will be preferred. Away from half-filling any negative nearest-neighbour interaction whatsoever stabilizes the SF, while a positive one drives the system into a mixed phase, characterized by the non-vanishing order parameter Δ_π which measures the difference between the values of the superconducting gap Δ_0 on the two sublattices A and B.

Chapter 4

Bose-Fermi Mixtures

Bose-Fermi mixtures describe interacting bosons and fermions in optical (or crystal) lattices. To motivate why it is useful to consider such a model, we briefly review several situations in which bosons modify the low-energy physics of fermions and vice-versa.

The modern theory of conventional superconductivity relies on the experimentally verified phonon-induced attractive interaction between fermions. On a fundamental level, this can be elegantly derived within a field-theoretical approach [1] from the Fröhlich Hamiltonian by integrating out the bosonic degrees of freedom. In order this to work, it is assumed that the phonons are interacting weakly enough, so that they can be treated within the Bogoliubov approximation. This leaves many questions open, among which: How does a strongly correlated bosonic system coupled to a strongly interacting fermionic one changes the physics of the model? What kind of phases of matter can occur in the ground state of such a model?

Other systems, whose physics can be described by Bose-Fermi mixtures, include ^{3}He-^{4}He mixtures, fermionic polarons and systems where electron-polaron interactions are dominating, and even quark-gluon plasmas (although we shall restrict to the non-relativistic limit of the model). Last but not least, the Bose-Fermi mixture is interesting on its own. Taking into account the recent progress made in cold-atom experiments, being able to simulate and investigate the rich physics of the model in a highly controllable way under laboratory conditions may be useful towards the future development of superconducting technology.

The goal of this chapter is to calculate the MF phase diagram of the model for bosons at unit filling and fermions at half-filling. We compare it to the result obtained via a single-site dynamical mean-field theory (DMFT) [2], which finds a double superfluid phase, mixed phases in which one of the species looses its superfluid properties but charge order is present, and a supersolid phase. We give intuitive physical explanations for the transition lines and, where appropriate and possible, mean-field arguments to supplement these. Further, a self-consistent mean-field theory of the BFM is proposed in the BCS limit which is capable of describing all the phases found of the DMFT phase diagram. However, it produces only two distinct phases, and is hence insufficient to capture the ground state properties entirely. Towards the end of this chapter, we include finite temperature effects. The discussion is closed with a critical analysis of the MF model compared to DMFT and real experimental conditions.

4.1 Properties of the Model

The Bose-Fermi mixture is described by the Bose-Hubbard model coupled to the Fermi-Hubbard model via a density-density-type instantaneous interaction. The Hamiltonian is given by

$$\begin{aligned} H &= H_b + H_f + H_{\text{int}} \\ H_b &= -t_b \sum_{\langle ij \rangle} (b_i^\dagger b_j + h.c.) - \mu_b \sum_i n_i + \frac{U_{bb}}{2} \sum_i n_i(n_i - 1) \\ H_f &= -t_f \sum_{\langle ij \rangle, \sigma} (c_{i\sigma}^\dagger c_{j\sigma} + h.c.) - \mu_f \sum_i m_i + U_{ff} \sum_i m_{i\uparrow} m_{i\downarrow} \\ H_{\text{int}} &= U_{bf} \sum_i n_i m_i. \end{aligned} \tag{4.1}$$

Here t_b and t_f define the bosonic and the fermionic hopping amplitudes to nearest-neighbouring sites, μ_b and μ_f are the chemical potentials, U_{bb} and U_{ff} are the bosonic and fermionic on-site interaction strengths. In this thesis, we assume a repulsive bosonic and an attractive fermionic interaction. The interspecies interaction is described by U_{bf}. We shall comment on its sign shortly. The Hilbert space for the model is given by the tensor product of a bosonic and a fermionic Fock space. We shall refer to the bosonic (fermionic) part of the ground state w.r.t. this factorization.

It is easily seen that the boson-fermion coupling breaks the Lieb-Mattis symmetry of the Fermi Hubbard model, since it maps the fermionic occupation number operator to the on-site magnetization operator (cf. Section 3.3.1). However the Particle-Hole symmetry of the fermions can be used to reduce the computational effort needed to determine the phase diagram. It follows that

$$H(t_f, t_b, U_{ff}, U_{bb}, \mu_f, \mu_b, U_{bf}) \xrightarrow{\text{p. h.}} H(t_f, t_b, U_{ff}, U_{bb}, -\mu_f, \mu_b, -U_{bf}) \tag{4.2}$$

Therefore, the sign of U_{bf} is irrelevant for the spinful BFM at half-filling. From now on, we shall work on the repulsive side assuming $U_{bf} \geq 0$.

Moreover, if we think for a moment of H_{int} as a term modifying the chemical potential of the fermions, it follows from the considerations in Section 3.3.2 that the charge sector of the symmetry group of the FHM $SU_\eta(2)$ is broken to its $U(1)$ subgroup, and hence we expect the degeneracy in the ground state in the fermionic sector to be lifted. The continuous part of the full symmetry group of the Bose-Fermi mixture reads

$$G = SU_\sigma(2) \times U_f(1) \times U_b(1), \tag{4.3}$$

where the subindices σ and b stand for the fermionic spin sector and bosons, respectively. We have omitted the discrete lattice point symmetry group which has to be added to obtain a complete group-theoretical description. The appearance of Charge Density Waves (CDW) in the phase diagram (Fig. 4.1) signals that this part also plays an important role for the low-energy physics.

In the following, we first discuss the DMFT ground state phase diagram of the model.

4.2 Analysis of the DMFT Phase Diagram at Half-Filling

As mentioned already several times, single-site dynamical mean-field theory (DMFT) has been employed to numerically simulate the Bose-Fermi mixture at unit filling for the bosons, and half-filling for the fermions [2]. The model was found to display a very rich ground-state phase diagram (c.f. Fig. 4.1). Four distinct phases have been found at temperatures $T/t_f = 0.2$ close to the absolute zero limit, containing charge density waves, superfluids and an exotic supersolid in the $(U_{bf}/t_f, t_b/t_f)$ plane. The fermionic hopping is used as an energy reference scale and can be thought to be put to unity. We also mention that the attractive interaction causes the fermions to pair in order to lower their energy. Whether these pairs remain localized (CDW) or delocalize over the entire lattice (SF) depends on the remaining parameters. In this section, we propose an intuitive explanation for the transition lines, some of which appear rather peculiar at first sight.

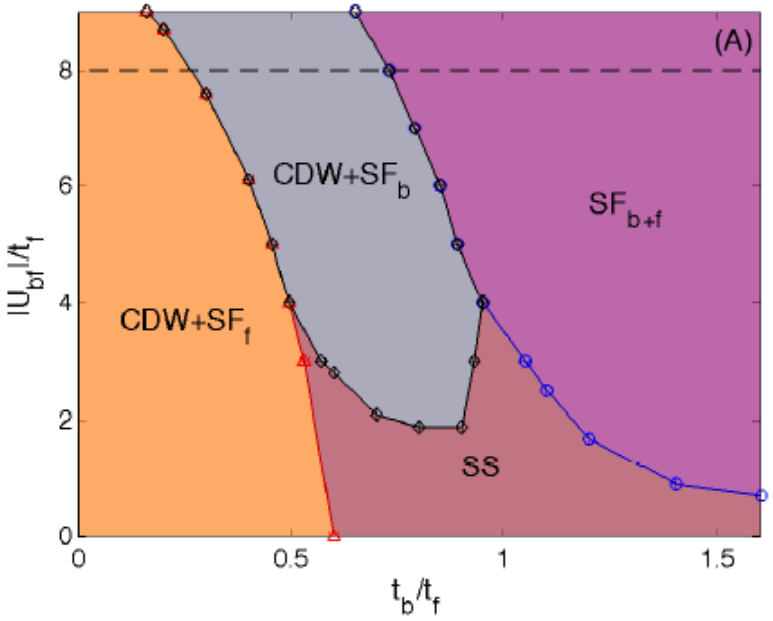

Figure 4.1: The DMFT phase diagram of the Bose Fermi mixture at unit filling for the bosons and half-filling for the fermions: the model parameters are $U_{bb}/t_f = 20$, $U_{ff}/t_f = -10$, and $T/t_f = 0.2$. The abbreviations of the phases stand for charge density wave (CDW), superfluid (SF) and supersolid (SS = CDW + SF$_{b+f}$). The subscripts b and f denote the bosonic and the fermionic sectors, respectively (image taken from [2]).

We begin by discussing the trivial cases of the lines $U_{bf} = 0$ and $t_b/t_f = 0$. The former describes the fully decoupled pure Hubbard models, discussed thoroughly in Chapters 2 and 3. Hence, starting from a critical value of the bosonic hopping $t_b/t_f \gtrsim 0.53$, the bosons become superfluid, in contrast to the Mott insulator which dominates in the regime $t_b/t_f \lesssim 0.53$. The ground state of the fermions, as explained in Section 3.3.2, is degenerate and constitutes an arbitrary superposition of a CDW and a superfluid.

Along the line $t_b/t_f = 0$, the bosons are completely frozen and their hopping between nearest-neighbouring sites is truly inhibited, while the fermions provide the background. This

line also contains a critical point, where the cost of putting two bosons on the same site is lower than the repulsive interaction between them. Hence, approximately at $U_{bf} \approx U_{bb}/2$ a bosonic CDW emerges, which in turn enhances the amplitude of the fermionic CDW.

The phase CDW+SF$_f$ is the only phase where the bosons are found insulating at a finite value of $U_{bf} > 0$. However, the insulator is perturbed by the CDW induced by the fermions. From Fig. 4.1 it can be inferred that a small but finite interspecies interaction removes the degeneracy in the fermionic ground state in favour of a simultaneous presence of both the SF and CDW orders. This results in a fermionic supersolid (or a staggered superfluid[1]). As the boson-fermion interaction is instantaneous, the bosonic density picks up the CDW immediately. This can be traced intuitively via the mechanism described in Section 2.2.2 which makes use of higher order correction to the ideal insulator state. It is natural to expect that increasing the bosonic hopping amplitude t_b/t_f, a similar transition to the MI-SF one in the Bose-Hubbard model will occur. This is intimately related to the observed shift of the MI-SF line reported in [6] for the spin-polarized mixture. Expressed in correct units, the MF description of the MI-SF transition in the presence of a staggered potential, derived in Section 2.2.2 produces an extremely similar result, shown in Fig. 4.2. Hence, we strongly believe that this entire line is governed by the bosonic insulator to superfluid transition.

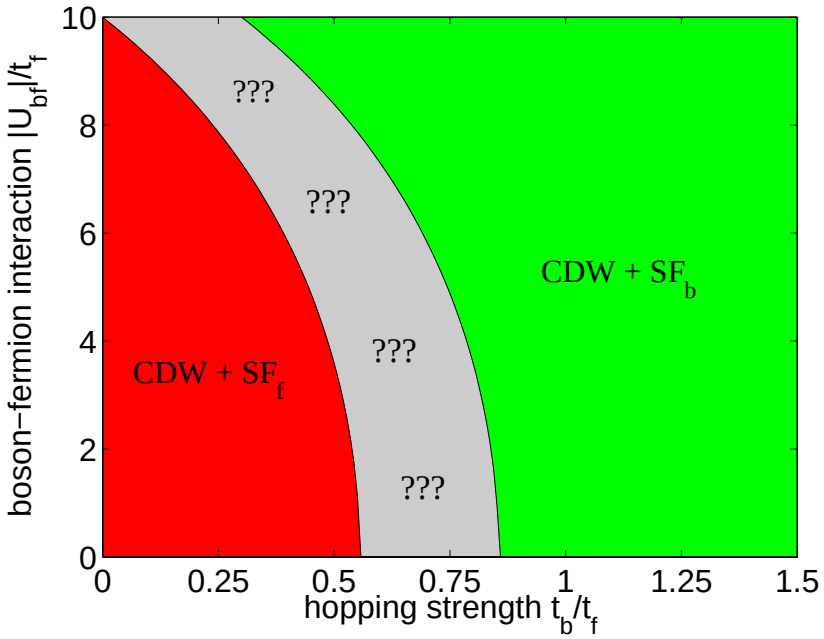

Figure 4.2: The MF phase diagram of the Bose Fermi mixture at unit filling for the bosons and half-filling for the fermions: the model parameters are $U_{bb}/t_f = 20$, $U_{ff}/t_f = -4$, and $T/t_f = 0$(abbreviations are the same as in Fig. 4.1). The MI-SF transition line for the bosons looks extremely similar to the one found by DMFT (for a detailed discussion, see Chapter 4.2). In the grey zone we could not make rigorous statements due to limitations of the Bogoliubov approximation used.

[1]This state is not to be confused with what is usually called a staggered superconductor. In the latter case the staggering refers to a non-vanishing Δ_π gap.

Depending on the value of U_{bf}, upon increasing the hopping t_b the system enters two different phases. For strong boson-fermion interactions, the fermions are found to loose their superfluidity and retain only the charge order. Moreover, this event coincides exactly with the bosonic MI-SF line which ultimately renders the transition first order. This peculiar abrupt change in the fermionic sector can be explained in the following intuitive way: at the moment when the bosons become superfluid, they delocalize completely. However, the fermionic background is staggered, which immediately enhances the CDW in the bosonic system. According to our previous analysis in Section 2.2.1, any further increase in the bosonic hopping t_b leads to a decrease in the bosonic CDW amplitude, c.f. Fig. 2.8. Hence, the bosonic CDW is strongest at the transition line, since it is certainly stronger there than in the insulating phase where the hopping of the bosons is disfavoured. Taking into account the strong boson-fermion repulsion, it is plausible that a strong bosonic CDW squeezes the fermionic wave function so much that the fermions eventually localize in the staggered superfluid bosonic background, and hence loose the superfluidity.[2]

Weak boson-fermion interactions, on the other hand, are insufficient to cause strong localization of the fermions. Therefore, the latter retain the superfluidity and the transition which is purely due to the bosons becomes second order. Although such U_{bf}'s do not cause a major change in the system, it is expected that due to the increase in the bosonic CDW, the fermionic CDW amplitude will also increase, in consistency with the back-action mechanism proposed in [37]. The mixture then enters a double supersolid phase where both species sustain both diagonal and off-diagonal long-range order. Starting from this SS phase, and increasing the value of U_{bf} naturally leads to the loss of the fermionic superfluidity. This is again due to the aforementioned squeezing induced by the bosons as a back-action, and the mixture enters the CDW+$\mathrm{SF_b}$ phase, undergoing a second-order phase transition.

The transition line to the double superfluid $\mathrm{SF_{b+f}}$ at large fixed values of U_{bf} can also be readily understood. Increasing the bosonic hopping amplitude beyond a critical value, the bosons would like to get rid of the staggered order. This can be seen from the fact that the square root of the density is proportional to the bosonic wave function, and any changes in the behaviour of the latter compared to the uniform case produces kinetic energy in excess. On the other hand, a similar statement applies to the fermions, except that the energy balance there is more subtle: the fermionic CDW is favoured to leading order for large values of U_{bf}, as the CDW is a direct consequence of the instantaneous density-density interaction. On the other hand, the boson-fermion interaction does not favour the fermionic superfluidity to first order.[3] Hence, a double superfluid state is possible, only if the gain in energy of the bosons is higher than the loss by the fermions. A compromise where the bosons exhibit a uniform SF while the fermions display a pure CDW is not possible due to the density-density type of coupling between the Hubbard models. This transition is again of second order.

A similar transition is found from the SS to the double $\mathrm{SF_{b+f}}$ state for lower values of U_{bf}. Since only the charge order is lost in this transition, it is of second order. We believe that the mechanism stabilizing the SS phase at any finite value of U_{bf} whatsoever is independent of the bosonic hopping strength t_b, and hence the SS phase extends to infinity, although it certainly shrinks down tremendously. Crossing this transition line to the $\mathrm{SF_{b+f}}$ state in

[2] A similar scenario is possible for attractive boson-fermion interactions, where the fermion wave functions are squeezed due to strong attraction on the sites with excess of delocalized bosons. This is consistent with the fact that the phase diagram at half-filling is symmetric w.r.t. $U_{bf} \to -U_{bf}$ due to Particle-Hole symmetry.

[3] The boson-induced attraction between the fermions is a second order process, and its strength scales as U_{bf}^2/U_{bb}.

Fig. 4.1 can be easily understood with the mechanism explained above, if we keep U_{bf} fixed and increase the bosonic hopping. Why the mixture prefers to get rid of the charge order at fixed hopping amplitude t_b with *increasing* boson-fermion interaction U_{bf} remains a mystery, since it is expected that the CDW is favoured in this case.

This concludes our brief summary of the phases and the explanation of the transition lines in the DMFT phase diagram. In the next chapter, we proceed to develop and examine the phases predicted by a self-consistent mean-field approach.

4.3 Mean-Field Theory of the Bose-Fermi Mixture

The physics of the Bose-Hubbard and the Fermi-Hubbard models has already been described on the level of MF in Chapters 2 and 3. Since we are interested in the modifications introduced by the interspecies density-density interaction, we propose the following natural mean-field decoupling scheme to incorporate the first-order corrections:

$$n_i m_i \approx n_i \langle m_i \rangle + \langle n_i \rangle m_i - \langle n_i \rangle \langle m_i \rangle. \tag{4.4}$$

To allow for diagonal long-range order which exist in the phases where a CDW is present, we assume to following form for the ground-state expectation values of the density operators

$$\begin{aligned} \langle n_i \rangle &= 1 + (-1)^i \eta, \\ \langle m_i \rangle &= 1 - (-1)^i \alpha, \end{aligned} \tag{4.5}$$

where $\eta,\ \alpha \in [0, 1]$ define the amplitudes of the bosonic and fermionic CDW's, respectively. The choice of sign for a particular sublattice is rather a convention, while the different signs of the alternating factor reflect the positivity of the boson-fermion interaction. This type of decoupling is equivalent to doubling the unit cell, or reducing the Brillouin zone. Hence, it also breaks the discrete translational symmetry group.

The parameters α and η shall be determined self-consistently. It will turn out that they are not independent of one another, and hence we implement the required back-action effect discussed in [37]. The Hamiltonian of the BF mixture assumes the form

$$\begin{aligned} H = &- t_b \sum_{\langle ij \rangle} (b_i^\dagger b_j + h.c.) - (\mu_b - U_{bf}) \sum_i n_i - \alpha U_{bf} \sum_i (-1)^i n_i + \frac{U_{bb}}{2} \sum_i n_i (n_i - 1) \\ &- t_f \sum_{\langle ij \rangle, \sigma} (c_{i\sigma}^\dagger c_{j\sigma} + h.c.) - (\mu_f - U_{bf}) \sum_i m_i + \eta U_{bf} \sum_i (-1)^i m_i + U_{ff} \sum_i m_{i\uparrow} m_{i\downarrow} \\ &- U_{bf} \underbrace{\sum_i \left(1 + (-1)^i \eta\right) \left(1 - (-1)^i \alpha\right)}_{= N_s (1 - \eta\alpha)}. \end{aligned} \tag{4.6}$$

The physical mechanism behind this approach is the following: First, we allow the fermions to obtain a CDW order in the ground state at a finite value of U_{bf}. Due to the instantaneity of the density-density interaction the fermions act to first order as a staggered external field imposed on the bosons. In accordance with the results of Section 2.2.3, the bosons will rearrange themselves and form a CDW. This, on the other hand, will act as a staggered field back on the fermions. Due to the repulsive nature of the interaction, this will increase the

fermionic CDW amplitude. This process will be iterated until a stable equilibrium is reached. Whether the charge order is preferred at all, will then ultimately be determined by comparing the ground state energies of the states with and without long-range order.

In a recent work [37], it has been shown that beyond the MF level, this process can induce long-range interactions between the species. Using a cumulant expansion scheme within the framework of many-body perturbation theory, one can find expressions for the induced long-range interaction strength. Naturally, the longer the range of the interaction, the weaker its strength becomes [37]. In the case of 1d spin-polarized mixtures, these higher order terms result in an ultraviolet divergence of the two-body interaction energy, if the back-action is not taken into account. However, in the case of a strong attractive interactions between the fermions in 3d, long-range corrections are expected to have an insignificant influence, since the induced n.n. interaction strength W will be small compared to U_{bf}.

If we look carefully at (4.6), we will recognize the decoupled Bose-Hubbard and Fermi-Hubbard models in the presence of a staggered potential, which we solved within a MF approximation in Chapters 2 and 3, respectively. It will be computationally advantageous to consider the bosonic CDW amplitude $\eta = \eta(\alpha)$ as a function of the fermionic one - α. We also remind the reader of Eq. (3.41) which states that $\alpha \sim \Delta_c$ with Δ_c the fermionic CDW order parameter. In the following discussion, we choose to use α instead of Δ_c.

Let us begin by specifying clearly the somewhat more complex MF scheme we want to implement. We restrict the analysis to the case where the bosons are superfluid, as the insulating case was discussed in the previous chapter. We also discuss the fermions in the BCS limit where the interaction strength is supposed to be $|U_{ff}| \leq 5$. This time, we consider the general MF theory of the BFM at any fermionic filling. We also include finite temperature effects through the parameter $\beta = 1/T$, denoting inverse temperature. The Bose and Fermi distribution functions are denoted by f_F and f_B, respectively: $f_{F/B}(\cdot) = (\exp(\beta(\cdot)) \pm 1)^{-1}$.

1. We pick a number $\alpha \in [0, 1]$, and consider the Bose-Hubbard model in the presence of a staggered field as in Section 2.2.3. Within the Bogoliubov approximation we choose a viewpoint considering the chemical potential $\mu_b(n_0)$ as a function of the total condensate fraction n_0. The chemical potential μ_b and the $\vec{k} = 0$ condensate fraction (and hence the $\vec{k} = \vec{\pi}$ condensate fraction) are determined as a solution of Eq. (2.45) which we repeat here

$$\begin{aligned}(-zt_b - \mu_b + U_{bf})A - \alpha U_{bf}B + n_0 U_{bb}A(1 + 2B^2) &\stackrel{!}{=} 0 \\ (zt_b - \mu_b + U_{bf})B - \alpha U_{bf}A + n_0 U_{bb}B(1 + 2A^2) &\stackrel{!}{=} 0.\end{aligned} \tag{4.7}$$

   We also recall the non-linear constraint $A^2 + B^2 = 1$ for completeness.

2. To fix the total condensate fraction, we calculate the bosonic density inside the (double) unit cell, using the condition for unit filling. It is given by the solution of the following self-consistency equation

$$1 = n_0 + \frac{1}{2N_s} \sum_{k \in \mathrm{BZ'},\mathrm{s}} \left[-1 + \frac{\partial E_k^{(b,s)}}{\partial \mu_b} \coth\left(\frac{\beta}{2} E_k^{(b,s)} \right) \right]. \tag{4.8}$$

   Recall that the energies $E_k^{(b,1/2)}$ both depend on α explicitly, and implicitly via the parameters A and μ_b, which we have already found.

3. The amplitude of the bosonic CDW, $\eta(\alpha)$, is determined from inside the unit cell by calculating the expectation value of the bosonic density at the sublattice A which contains the origin. This can be done with the help of the MF condition $\langle n_i \rangle = 1 + \eta$ which is equivalent to the minimization $\eta = -\frac{1}{N_s}\partial_{(\alpha U_{bf})}\Omega^b$, with Ω^b the bosonic free energy (c.f. Eq. (4.13)), and yields:

$$\eta = n_0 2AB - \frac{1}{2N_s}\sum_{k\in \mathrm{BZ}',\mathrm{s}} \frac{\partial E_k^{(b,s)}}{\partial(\alpha U_{bf})} \coth\left(\frac{\beta}{2}E_k^{(b,s)}\right). \tag{4.9}$$

Notice that the parameter dependence on μ_b, A and n_0 has been eliminated in the previous two steps, and hence $\eta(\alpha)$ is a function determined solely by the model parameters α, U_{bb}, t_b, and U_{bf}.

4. Next, we turn to the Fermi-Hubbard model in the presence of a staggered potential. The fermionic chemical potential is found again from the number equation for the full (double) unit cell, which results in

$$m = \frac{1}{2N_s}\sum_{k\in \mathrm{BZ}',s}\left[1 + \frac{\partial E^{(f,s)}}{\partial \mu_f}\tanh\left(\frac{\beta}{2}E_k^{(f,s)}\right)\right]. \tag{4.10}$$

The condition for half-filling is equivalent to $\mu_f = U_{bf}$, which corresponds to filling in the lower Hubbard bands completely. We recall that at half-filling, we furthermore have $\Delta_\pi = 0$ due to Particle-Hole symmetry. The band structure $E_k^{(f,1/2)}$ is given in Eq. (3.66).

5. Further, we need to find the gap equations for the s-wave gap Δ_0 and the π-momentum gap Δ_π. In this case, the minimization procedure is equivalent to the self-consistent calculation, leading to the equations:

$$\begin{aligned} |\Delta_0| &= \frac{|U_{ff}|}{2N_s}\sum_{k\in \mathrm{BZ}'}\frac{\partial E^{(f,s)}}{\partial|\Delta_0|}\tanh\left(\frac{\beta}{2}E_k^{(f,s)}\right) \\ \Delta_\pi &= \frac{|U_{ff}|}{2N_s}\sum_{k\in \mathrm{BZ}'}\frac{\partial E^{(f,s)}}{\partial\Delta_\pi}\tanh\left(\frac{\beta}{2}E_k^{(f,s)}\right). \end{aligned} \tag{4.11}$$

The precise form of these equations is not particularly illuminating. We remark that they are the same as in Eq. (3.55), with the replacements $\Delta_c \to \frac{|U_{ff}|\alpha}{2} + \eta(\alpha)U_{bf}$ and $\mu_f \to \mu_f - U_{bf}$.

6. Last, we fix the MF criterion $\langle m_i \rangle = 1 - \alpha$ for the fermionic density by calculating the total density at the origin (sublattice A). The resulting equation can be viewed as the

self-consistent equation for the fermionic CDW amplitude α. It reads

$$\begin{aligned}\alpha =&\frac{1}{N_s}\sum_{k\in \mathrm{BZ}'}\Bigg[\\ &\frac{\left(\frac{|U_{ff}|\alpha}{2}+\eta(\alpha)U_{bf}\right)+(\mu_f-U_{bf})\frac{|\Delta_0|\Delta_\pi+(\mu_f-U_{bf})\left(\frac{|U_{ff}|\alpha}{2}+\eta(\alpha)U_{bf}\right)}{X}}{E_k^{(f,1)}}\tanh\left(\frac{\beta}{2}E_k^{(f,1)}\right)\\ &+\frac{\left(\frac{|U_{ff}|\alpha}{2}+\eta(\alpha)U_{bf}\right)-(\mu_f-U_{bf})\frac{|\Delta_0|\Delta_\pi+(\mu_f-U_{bf})\left(\frac{|U_{ff}|\alpha}{2}+\eta(\alpha)U_{bf}\right)}{X}}{E_k^{(f,2)}}\tanh\left(\frac{\beta}{2}E_k^{(f,2)}\right)\Bigg].\end{aligned} \tag{4.12}$$

This determines the parameter α (Δ_c) self-consistently. Notice that this does *not!* correspond to minimization of the total ground state energy, since in general one would have to also take into account the functional dependence of $\eta(\alpha)$. The reason why this, and not the minimization one, is the correct equation is that we have to satisfy the MF constraint $\langle m_i\rangle = 1-\alpha$, which closes the cycle.

We can now iterate the above steps until a solution is found. It may well happen, that the system has multiple fixed points. In such a case, the correct solution will be determined by that one which minimizes the free energy Ω^{tot} of the Bose-Fermi mixture within the MF approximation, given by

$$\begin{aligned}\Omega^{\mathrm{tot}} &= \Omega^b+\Omega^f+\Omega^{\mathrm{int}}\\ \Omega^b &= N_0\left[-zt_b(A^2-B^2)-\mu_b+U_{bf}-\alpha U_{bf}2AB\right]+N_s\frac{U_{bb}}{2}n_0^2(A^4+6A^2B^2+B^4)\\ &\quad-\frac{1}{2}N_s(\mu_b-U_{bf}-2U)+\frac{1}{2}\sum_{k\in\mathrm{BZ}',\mathrm{s}}E_k^{(b,s)}-\frac{1}{\beta}\sum_{k\in\mathrm{BZ}',\mathrm{s}}\log\left[\frac{1+\coth\left(\frac{\beta}{2}E_k^{(b,s)}\right)}{2}\right]\\ \Omega^f &= \frac{N_s}{|U_{ff}|}\left(\left(\frac{|U_{ff}|}{2}\alpha\right)^2+|\Delta_0|^2+|\Delta_\pi|^2\right)\\ &\quad-\sum_{k\in\mathrm{BZ}',s}\left(E_k^{(f,s)}+(\mu_f-U_{bf})\right)+\frac{2}{\beta}\sum_{k\in\mathrm{BZ}',\mathrm{s}}\log\left[\frac{1+\tanh\left(\frac{\beta}{2}E_k^{(f,s)}\right)}{2}\right]\\ \Omega^{\mathrm{int}} &= -N_sU_{bf}\left(1-\eta(\alpha)\alpha\right),\end{aligned} \tag{4.13}$$

where the dispersion of the excitations $E_k^{(b,1)}$ and $E_k^{(f,1)}$ was calculated previously in Eqs. (2.55) and (3.55), respectively.

The results of the solution of these self-consistency equations will be discussed in the next section.

Before we close this section, we would like to give a generalization of the boson-induced fermion-fermion interaction of Eq. (1.3) to the case where the bosons display both the superfluid and the charge orders. A straightforward calculation yields

$$
\begin{aligned}
H_{ind} &= \frac{1}{N_s} \sum_{k_i, q \in \mathrm{BZ}', \sigma\sigma'} U_{ind}(q, \omega; k_i) c^\dagger_{k_1\sigma} c^\dagger_{k_2\sigma'} c_{k_3\sigma'} c_{k_4\sigma} \\
U_{ind}(q, \omega; k_i) &= \sum_s 2 n_0 U_{bf}^2 \Bigg(\frac{\bar{\epsilon}_k}{\omega^2 - \left(E_k^{(b,s)}\right)^2} \delta_{k_1,k} \delta_{k_2,k} \delta_{k_3,k+q} \delta_{k_4,k-q} \\
&\quad + 2AB \frac{\bar{\epsilon}_{k+\pi}}{\omega^2 - \left(E_{k+\pi}^{(b,s)}\right)^2} \delta_{k_1,k} \delta_{k_2,k} \delta_{k_3,k+q-\pi} \delta_{k_4,k-q} \Bigg),
\end{aligned} \tag{4.14}
$$

with $\bar{\epsilon}_k = \epsilon_k + \sqrt{(\alpha U_{bf})^2 + (z t_b)^2}$, and $\epsilon_k = -\sqrt{(\alpha U_{bf})^2 + \varepsilon_k^2}$ is the free dispersion in the presence of a staggered field. Clearly, the above formula reduces to Eq. (1.3) in the case of a missing charge order, i.e. $\alpha = 0$. This modification is important to study unconventional mechanisms of fermionic pairing within a supersolid phase. For instance exotic d-wave supersolids might be possible if a positive fermion-fermion interaction is used to effectively close the s-wave channel (c.f. the discussion in Chapter 5). Whether this makes the SS state collapse or not is a topic of future research.

4.4 Mean-Field Phase Diagram of the BFM

The $T = 0$ phase diagram at half-filling is governed by the following set of two self-consistency equations, derived as a special case from the procedure in the previous chapter:

$$
\begin{aligned}
\alpha &= \frac{2}{N_s} \sum_{k \in \mathrm{BZ}'} \frac{\frac{|U_{ff}|\alpha}{2} + \eta(\alpha) U_{bf}}{\sqrt{\varepsilon_k^2 + |\Delta_0|^2 + \left(\frac{|U_{ff}|\alpha}{2} + \eta(\alpha) U_{bf}\right)^2}} \\
|\Delta_0| &= \frac{|U_{ff}|}{N_s} \sum_{k \in \mathrm{BZ}'} \frac{|\Delta_0|}{\sqrt{\varepsilon_k^2 + |\Delta_0|^2 + \left(\frac{|U_{ff}|\alpha}{2} + \eta(\alpha) U_{bf}\right)^2}},
\end{aligned} \tag{4.15}
$$

where we have used that $\mu_f = U_{bf}$ and $\Delta_\pi = 0$ at half filling. The function $\eta(\alpha)$ is determined from Eq. (4.9). Notice that this set of equations is particle-hole symmetric: indeed, Particle-Hole symmetry is equivalent to sending $U_{bf} \to -U_{bf}$ and $\alpha \to -\alpha$. The statement then follows from the symmetry relation $\eta(-\alpha, -U_{bf}) = \eta(\alpha, U_{bf})$. To prove it, we use the defining equation (4.9) and notice that it is only through the combination αU_{bf} that the parameters enter the expressions for n_0 and $E_k^{(b)}$. A direct justification of this symmetry is possible in the limit of $U_{bb} = 0$, in which $\eta^{\mathrm{free}}(\alpha) = \alpha U_{bf} / \sqrt{(\alpha U_{bf})^2 + (z t_b)^2}$, and for small α, for which $\eta(\alpha) \overset{\alpha U_{bf} \to 0}{\sim} \alpha U_{bf}$.

The system (4.15) has only two non-trivial solutions.[4] This fact is a direct consequence of the broken pseudo-spin symmetry, which allowed a continuous family of solutions for the Fermi-Hubbard Model (c.f. Section 3.5). The two solutions can be found in the following way:

[4] There always exists the normal phase, characterized by $\alpha = 0$ and $\Delta_0 = 0$. This is a solution of (4.15), since for $\alpha = 0$ we necessarily have $\eta(0) = 0$

assume that we are in a phase where $\Delta_0 \neq 0$. We can use the second equation and plug it in the first one to obtain

$$\alpha = \frac{2}{|U_{ff}|}\left(\frac{|U_{ff}|}{2}\alpha + \eta(\alpha)U_{bf}\right). \tag{4.16}$$

Simplifying, we are left with $\eta(\alpha) \stackrel{!}{=} 0$, whose only solution is $\alpha = 0$, since $\eta(\alpha)$ is a monotonically increasing function. The other solution is found at $\Delta_0 = 0$. Hence, the resulting phase can either be a SF or a CDW, but not a superposition.

To understand which one of the two possibilities minimizes the total ground state energy, observe that a further consequence of (4.15) is $|U_{ff}|\alpha/2 \geq |\Delta_0|$. Hence, the charge order lowers the contribution to the GS energy of the fermionic sector by a certain amount which competes with the increase caused by the staggering in the density in the bosonic sector and the constant MF-decoupling term. The phase diagram is shown in Fig. 4.3.

The numerical comparison of the ground state energies of the two states clearly favours the charge order at relatively small U_{bf}. We believe that this can be traced back to the behaviour of the total GS energy as a function of the order parameters, observed in the numerical plots. The reason why the energy of the charge-ordered state is lower than that of the one of the double $\mathrm{SF_{b+f}}$ state is that the energy gain by the bosons is insufficient to overcome the sum of the energy loss of the fermions due to the enhanced CDW (c.f. the discussion of the CDW+$\mathrm{SF_b}$ to $\mathrm{SF_{b+f}}$ transition line in Section 4.2), and the MF decoupling energy (c.f. Ω_{int} in Eq. (4.13)). On the other hand, for large values of U_{bf}, we do find the double superfluid phase $\mathrm{SF_{b+f}}$, similarly to the DMFT phase diagram where the boson-fermion interaction is treated exactly.

The phase diagram in Fig. 4.3 has to be taken with care for the following reasons. Consider first the case of large t_b/t_f values. Since increasing the bosonic hopping diminishes the CDW amplitude of the bosons, beyond a certain value $t_b/t_f \sim 1.5$, the simple MF approach treats the bosons and the fermions as decoupled (since in this case $\eta \to 0$). Therefore, the MF phase diagram should not be trusted for $t_b/t_f \gtrsim 1.5$. This decoupling of the models is also the reason why the phase boundary approaches a constant value for $t_b/t_f \gg 1$.

The part of the phase diagram where $t_b/t_f \lesssim 1$ is also quite peculiar. If one considers a fixed and not so large U_{bf} (e.g. $U_{bf} = 6$) and gradually starts to increase the hopping, one would start in the $\mathrm{SF_{b+f}}$ phase and then inevitably enter the CDW+$\mathrm{SF_b}$. This is quite remarkable, since we know that the CDW amplitudes of both species should decrease along this trajectory which is naively expected to disfavour the charge order. Hence the positive slope in this part of the phase boundary, found by comparing the free energies of the two states, comes about due to the functional dependence of the total free energy on the parameters α and Δ_0. Therefore, we believe that, if taken into account, higher order corrections to our MF ansatz would change the slope of the transition line and produce a better agreement with the DMFT one (where the transition line has a negative slope through the entire phase diagram).

In the narrow parameter regime $1 \lesssim t_b/t_f \lesssim 1.5$, we find an qualitative agreement between MF theory and DMFT and the two curves look similar to one another. However, it should be properly stressed that, even in this case, our MF seems to be off by an order of magnitude.[5]

Finite temperature does not change the above analysis in any way. This has been confirmed by the numerical solution of the equations. Indeed, the values of the SF gap function

[5] We could not make an exact comparison, since the DMFT phase diagram is taken in the BEC regime of the fermion sector where our present treatment fails.

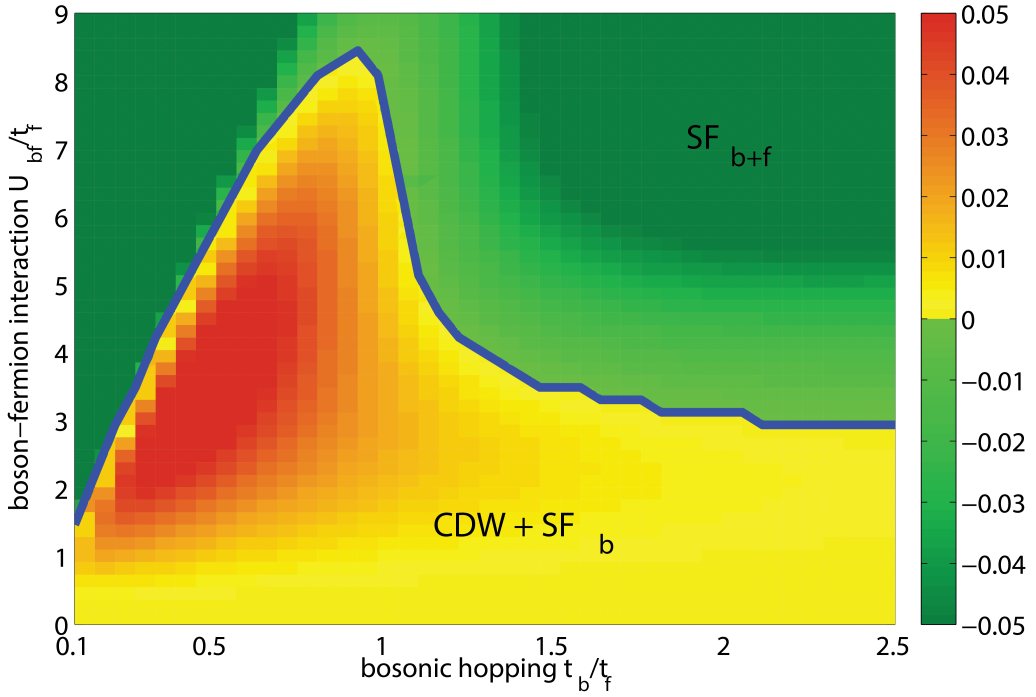

Figure 4.3: The MF phase diagram of the Bose Fermi mixture at unit filling for the bosons and half-filling for the fermions in the BCS regime of the fermionic sector and the deep SF limit for the bosons: the model parameters are $U_{bb}/t_f = 1$, $U_{ff}/t_f = -4$, and $T/t_f = 0$ (abbreviations are the same as in Fig. 4.1). The color bar shows the difference between the GS energy of the $\mathrm{SF_{b+f}}$ and the $\mathrm{CDW{+}SF_b}$ phases. The transition line (blue) is believed to reflect the true physics for $1 \lesssim t_b/t_f \lesssim 1.5$ within MF theory (c.f. text).

and the charge density wave amplitude decrease with increasing temperature and, eventually, beyond a certain value of T cease to exist, but finite temperature does not appear as a relevant factor in the MF model. It is this fact that enables us to compare the MF and the DMFT phase diagrams, although the former is computed at zero, while the latter at finite temperature. Due to the staggered field induced by the bosons, the CDW gap is larger than the SF one, and vanishes last with increasing temperature. This is intuitively clear, since temperature is competing with the two gaps at the finite-T transition boundary. Summarizing, the CDW state is preferred by the fermionic sector at finite temperature and half-filling for small U_{bf}, where the ground state of the BFM is a $\mathrm{CDW{+}SF_b}$, while for large enough U_{bf} we find the double superfluid phase $\mathrm{SF_{b+f}}$.

In summary, the MF description ultimately identifies a competition between the $\mathrm{CDW{+}SF_b}$ and the $\mathrm{SF_{b+f}}$ phases at half-filling in the region of the phase diagram where the bosons can be treated within the extended Bogoliubov approximation, and the fermions within BCS-theory, c.f. Fig. 4.3.

4.5 Outlook

In this chapter we proposed a self-consistent mean-field treatment of the Bose-Fermi Hubbard model. The fermionic sector enjoys a reduced symmetry even at half-filling, due to the density-density boson-fermion interaction which ultimately breaks the pseudo-spin $SU_\eta(2)$ symmetry of the pure FHM. As a consequence, the Lieb-Mattis transformation no longer applies. Nevertheless, a similar role for the model plays the Particle-Hole symmetry, which requires simultaneous flipping the sign of the fermionic density and the boson-fermion interaction strength. Therefore, the phase diagram of the model is axially symmetric w.r.t. the line $U_{bf} = 0$.

Treating the boson-fermion interaction along the lines of mean-field effectively decouples the bosons from the fermions. One then finds both the Bose and Fermi-Hubbard models in the presence of a staggered potential, whose strength is determined by the on-site density expectation value of the opposite species. This allows to look for exotic supersolid states, characterized by a simultaneous superfluid and crystalline long-range orders. We successfully calculated a very similar transition line to the one observed in DMFT for the CDW+$\mathrm{SF_f}$ to CDW+$\mathrm{SF_b}$ transition, as a consequence of the bosonic MI-SF transition in the presence of a staggered potential. Hence, this transition is strongly believed to be governed by the bosons.

As a solution to the self-consistency equations of the fermionic sector, we recover the familiar pure SF and CDW phases. A proof was given that a supersolid phase is not possible at half-filling within this description. As the main reason for this we identified the difference in the values of the CDW and SF gap induced by the staggered potential. The ultimate ground state of the entire mixture has been determined by comparing the total MF free energy of the solutions. We found that MF supports both the CDW+$\mathrm{SF_b}$ and the $\mathrm{SF_{b+f}}$ phases for small and large values of U_{bf}, respectively. The energy balance shows that the gain in energy in the bosonic sector due to the induced density modulations (compared to the uniform case) competes with the sum of the positive MF decoupling cost (due to Ω^{int}), and the loss in energy in the fermionic sector due to an increased CDW gap (by the back-action of the periodically modulated bosonic density).

This interplay of the energies enables both phases. However, we found that MF theory fails to produce the correct physics for large enough values of $t_b/t_f \gtrsim 1.5$, where the bosonic and the fermionic sectors decouple completely, due to a vanishing bosonic CDW amplitude η. In the opposite limit of $t_b/t_f \lesssim 1$, the MF transition line exhibits a peculiar negative slope (c.f. Fig. 4.3), which is attributed to the functional dependence of the GS energy on the order parameters α and Δ_0. We believe that the negative slope will be eliminated by considering higher order corrections in the MF approximation. In the form presented here, the latter is believed to produce the correct physics qualitatively in the window $1 \lesssim t_f/t_b \lesssim 1.5$. We also verified that finite temperature does not have any effect on the ground state phase properties but merely slightly shifts the transition line.

The MF description of the BFM clearly misses the SS phase found by DMFT while the transition line between the CDW+$\mathrm{SF_b}$ and the $\mathrm{SF_{b+f}}$ phases is off by an order of magnitude. Hence, it cannot be rendered a good enough description of the model. There are various reasons why it could potentially produce misleading results, for instance, the effect of quantum fluctuations, which are typically neglected within MF theory. Compared to DMFT, the main disadvantage of the MF approach is that it misses not only the higher-order corrections, but also any retardation effects. The latter certainly induce spontaneous density fluctuations which could stabilize one order or another, given the admittedly sensitive nature of our MF

theory. Furthermore, MF is not capable of capturing the BCS-BEC crossover regime at all.

Moreover, the above analysis treats the attractive FHM in the BCS regime. Therefore, its applicability is limited to values of $|U_{ff}|/t_f \lesssim 5$. It would be certainly possible to extend the analysis to the BEC side, where the fermions can be replaced by hardcore bosons with renormalized hopping and repulsive nearest-neighbour interaction strengths (c.f. the discussion is Section 3.4). Furthermore, the entire bosonic description applies in the deep superfluid regime only, due to the limited validity of the Bogoliubov approximation. Hence we are not able to make rigorous statements about the states of the fermionic sector which appear in the immediate vicinity of the boson-induced transition.

One advantage of the MF decoupling proposed in this chapter is that it implements in a natural way the back-action of the bosons on the fermions. This effect was argued to be of crucial importance if one wants to obtain a good description of the mixture [37, 58]. In the same work, Mehring and Fleischhauer considered a spin-polarized mixture which allowed them to effectively integrate out the fermions. This is not possible without further approximations in the spinful case, as it assumes that the ground state of the Fermi-Hubbard model is precisely known. Nevertheless, it should be theoretically possible to develop a MF description for the fermions and integrate out the effective quadratic Hamiltonian, but the analysis becomes computationally heavy. However, if carefully carried out, this procedure, in turn, would result in an effective bosonic Hamiltonian, with additionally induced long-range density-density interactions. They are definitely sub-leading terms, but could have a some influence on the ground-state energy, and may correct the slope of the phase boundary.

Last, but not least, even DMFT misses to implement significant effects found in experimental systems, such as the renormalization of the hopping parameters and the interaction strengths of the species due to the induced squeezing of the wave functions via the back-action mechanisms, as explained in [58]. Moreover, the effects of higher bands and the harmonic confinement potential are completely left out of consideration, but may still change parts of the ground-state physics. A comprehensive understanding of the Bose-Fermi mixture is expected to be able address these issues.

Chapter 5

Unconventional Superfluidity in Bose-Fermi Mixtures

5.1 Introduction

Due to advanced progress in recent experiments with ultra-cold atoms, theoretical work in the field of condensed matter has been thoroughly examined. Optical lattices provide excellent controllability over model parameters and allow for precise testing of theoretical results in modern laboratories. It is expected that in the nearest future these advancements will reach the technology and methodology to reveal the physics of one of the quite complex and exciting models - the Bose-Fermi mixture.

The Bose-Fermi mixture was initially proposed to model the mutual effect of interacting bosons on interacting fermions and vice-versa. Owing to recent success of BCS theory in describing conventional superconductivity, it has been proposed and proved [25] that in the limit of superfluid bosons, an effective attractive interaction between the fermions can be induced, leading to pairing between them.

In this chapter, we present a detailed mean-field analysis of different types of unconventional pairing mechanisms in a Bose-Fermi mixture.

Consider a system of spinless bosons and spinful fermions on a 3D cubic lattice with the fermionic (pseudo-) spin, as an internal degree of freedom, denoted by $s =\uparrow,\downarrow$. Both species are allowed to hop between nearest-neighbouring sites only, with hopping amplitudes t_b and t_f, respectively. Bosons can interact with each other and with fermions of either spin, via density-density coupling, whereas only fermions of opposite spin can interact with one another due to the Pauli Exclusion Principle. Such a system is called a Bose-Fermi mixture and its Hamiltonian is therefore given by

$$
\begin{aligned}
H &= H_b + H_f + H_{\text{int}}, \\
H_b &= -t_b \sum_{\langle ij \rangle} b_i^\dagger b_j - \mu_b \sum_i n_i^{\text{b}} + \frac{U_{\text{bb}}}{2} \sum_i n_i^{\text{b}}(n_i^{\text{b}} - 1), \\
H_f &= -t_f \sum_{\langle ij \rangle, s} c_{is}^\dagger c_{js} - \mu_f \sum_{i,s} n_{is}^{\text{f}} + U_{\text{ff}} \sum_i n_{i\uparrow}^{\text{f}} n_{i\downarrow}^{\text{f}}, \\
H_{\text{int}} &= U_{\text{bf}} \sum_{i,s} n_i^{\text{b}} n_{is}^{\text{f}},
\end{aligned}
\tag{5.1}
$$

with H_b and H_f the usual Bose and Fermi-Hubbard Hamiltonians. We are interested in the regime of unit filling for the bosons, i.e. $\langle n_i^{\text{b}} \rangle = 1$, and half-filling for the fermions, i.e. $\langle n_{is}^{\text{f}} \rangle = 1/2$. Furthermore, we assume a repulsive bosonic interaction, $U_{\text{bb}} > 0$, to avoid bosonic collapse and an attractive fermionic one, $U_{\text{ff}} < 0$, to enable unassisted fermionic pairing. At this particular commensurate filling, it can be verified using a Particle-Hole transformation that the physics for $U_{\text{bf}} < 0$ can be obtained from that of $U_{\text{bf}} > 0$. Therefore, we use $U_{\text{bf}} > 0$ throughout the rest of this note.

The purpose of this work is to investigate the different fermionic pairing scenarios that can be induced by superfluid bosons within mean-field theory. To assure for superfluidity, we consider low enough temperatures. Then the bosons can be treated within the Bogoliubov approximation and an effective fermion-phonon Hamiltonian is obtained [2, 55]:

$$
H_{\text{eff}} = \sum_{k,s} (\varepsilon_k^{\text{f}} - \mu_f) c_{ks}^\dagger c_{ks} + \frac{1}{2\Omega} \sum_{k,ss'} V_{k,ss'}^{\text{eff}} \rho_{k,s} \rho_{-k,s} \tag{5.2}
$$

with $\rho_{k,s} = \sum_{ps} c_{k+p,s}^\dagger c_{ps}$ the fermionic density operator of spin s and momentum k and the fermionic dispersion $\varepsilon_k^{\text{f}} = -2t_f[\cos(k_x) + \cos(k_y) + \cos(k_z)] =: -t_f \gamma_k$. The effective potential is given by

$$
V_{k,ss'}^{\text{eff}} = U_{\text{ff}} \delta_{s,-s'} + V_{\text{ind}}(k). \tag{5.3}
$$

The induced part of the potential $V_{\text{ind}}(k)$ is obtained within perturbation theory from the bosonic part of the Hamiltonian [2, 55]. In the fast-phonon limit, when the phonon velocity $s_{\text{ph}} = \sqrt{2 n_{\text{b}} U_{\text{bb}} t_{\text{b}}}$ is much larger than the Fermi velocity $v_{\text{F}} = \sqrt{2E_{\text{F}}/m^*}$, the frequency dependence of $V_{\text{ind}}(k)$, and thus any retardation effects, can be safely neglected to obtain

$$
V_{\text{ind}}(k) = -\frac{U_{\text{bf}}^2}{U_{\text{bb}}} \frac{1}{1 + \xi^2 (6 - \gamma_k)}, \tag{5.4}
$$

with $\xi = \sqrt{t_b / 2 n^{\text{b}} U_{\text{bb}}}$, the so-called bosonic correlation length. In this limit, the bosons induce a purely attractive potential for the fermions that can lead to pairing even when fermions have initially been free, i.e. for $U_{\text{ff}} = 0$. Moreover, fermions of the same spin s are now also interacting, allowing for the formation of exotic bound states, such as p-wave pairing.

Due to the momentum dependence of the potential, the gap function needed for the investigation of the unconventional pairing mechanisms will also exhibit a non-trivial dependence on the momentum k, a feature not present in BCS theory. Since for a general k-dependence no exact analytic results can be obtained, owing to the complexity of the gap equation (see

below), we choose to investigate the limit of small bosonic healing length, $\xi \ll 1$, and expand the potential as follows

$$V_{\mathrm{ind}}(k) \approx -\frac{U_{\mathrm{bf}}^2}{U_{\mathrm{bb}}}\left(\frac{1}{1+6\xi^2}+\frac{\xi^2}{(1+6\xi^2)^2}\gamma_k\right) = -U - W\gamma_k, \tag{5.5}$$

with the short-hand notation $U := U_{\mathrm{bf}}^2/U_{\mathrm{bb}}(1+6\xi^2)^{-1} > 0$, and $W := U_{\mathrm{bf}}^2/U_{\mathrm{bb}}\xi^2(1+6\xi^2)^{-2} > 0$. The approximation is valid for $\xi \lesssim 0.3$ within an error of at most 3%[1], as can be seen from Fig. 5.1. For example, if one has $U_{\mathrm{bb}}/t_f = 20$ and $t_b/t_f \approx 1$ one gets at unit filling $\xi = \sqrt{1/40} \approx 0.15$.

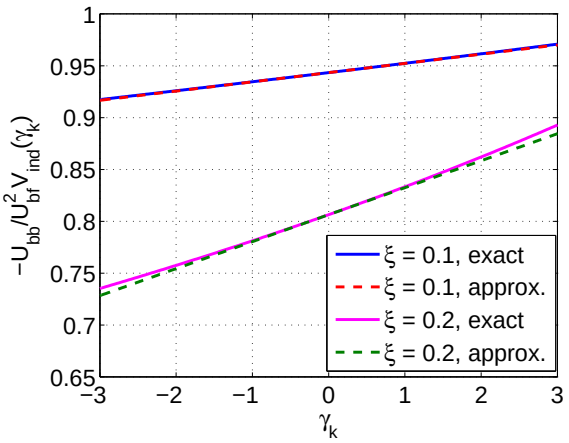

Figure 5.1: (color online): Linear approximation to $V_{\mathrm{ind}}(k)$ for different values of the bosonic healing length ξ within the 1st Brillouin zone

Although unconventional pairing is mostly pronounced in the limit of $\xi \approx 1$, [55], the above approximation allows for invaluable analytical results showing astonishing agreement with numerical simulations. We develop a method of low-T_c expansion to perform the complicated lattice integrals using an almost perfect approximation to the exact density of states. This leads to the derivation of transcendental equations for the critical temperature T_c of the different pairing bound states, which are eventually solved numerically to determine the functional dependence of T_c on the constants U and W.

5.2 Unconventional Pairing

Following the introduction in the previous chapter, we consider a system given by the Hamiltonian

$$H = \sum_{k,s} \varepsilon_k c_{ks}^\dagger c_{ks} + \frac{1}{2\Omega}\sum_{k,s,s'} V_{k,ss'}\rho_{k,s}\rho_{-k,s} \tag{5.6}$$

with the dispersion $\varepsilon_k = -t_f\gamma_k - \mu$ and $\gamma_k = 2[\cos(k_x)+\cos(k_y)+\cos(k_z)]$. The potential is given by $V_{k,ss'} = U_{\mathrm{ff}}\delta_{s,-s'} + V_{\mathrm{ind}}(k)$ with $V_{\mathrm{ind}}(k) = -U - W\gamma_k$.

[1] estimated as $max_{\gamma\in[-3,3]}\left|\frac{V_{\mathrm{exact}}(\gamma)-V_{\mathrm{approx}}(\gamma)}{V_{\mathrm{exact}}(\gamma)}\right| = 3\%$

We are interested in the different types of unconventional superconductivity within mean-field theory that the above model exhibits. The gap equation for a generic k-dependent gap function $\Delta_{k,ss'} = \Omega^{-1}\sum_p V_{s,s'}(k-p)\langle c^\dagger_{ps} c^\dagger_{-p,s'}\rangle$ is given by [55]

$$\Delta_{k,ss'} = -\frac{1}{2\Omega}\sum_p V_{s,s'}(k-p)\frac{\Delta_{s,s'}(p)}{E_p}\tanh\left(\frac{\beta E_p}{2}\right), \tag{5.7}$$

where $E_p = \sqrt{\varepsilon_p^2 + \Delta_p^2}$ and Ω is the volume of the system. We note that the $p-$summations in this chapter are always over the first Brillouin zone.
In the following, we shall distinguish between *singlet* (s- and d-wave) and *triplet* (p-wave) pairing mechanisms characterized by order parameters obeying the following symmetries [46, 3]:

$$\begin{aligned}
s\text{-wave:}\quad \Delta_k &= \frac{\Delta_s}{\sqrt{8\pi}},\quad \text{with } \Delta_s = const.\\
\text{extended } s\text{-wave:}\quad \Delta_k &= \Delta_{s^-}\frac{\gamma_k}{\sqrt{48\pi^3}}\\
d_{yz}\text{-wave:}\quad \Delta_k &= \frac{1}{\sqrt{2\pi^3}}\Delta_{yz}\sin k_y \sin k_z =: \Delta_{yz}\frac{\zeta^1_k}{\sqrt{2\pi^3}}\\
d_{xz}\text{-wave:}\quad \Delta_k &= \frac{1}{\sqrt{2\pi^3}}\Delta_{xz}\sin k_x \sin k_z =: \Delta_{xz}\frac{\zeta^2_k}{\sqrt{2\pi^3}}\\
d_{xy}\text{-wave:}\quad \Delta_k &= \frac{1}{\sqrt{2\pi^3}}\Delta_{xy}\sin k_x \sin k_y =: \Delta_{xy}\frac{\zeta^3_k}{\sqrt{2\pi^3}}\\
d_{z^2}\text{-wave:}\quad \Delta_k &= \Delta_{z^2}\frac{3\cos k_z - \frac{1}{2}\gamma_k}{\sqrt{24\pi^3}} =: \Delta_{z^2}\frac{\tau_k}{\sqrt{24\pi^3}}\\
d_{x^2-y^2}\text{-wave:}\quad \Delta_k &= \Delta_{x^2-y^2}\frac{1}{\sqrt{32\pi^3}}2(\cos k_x - \cos k_y) =: \Delta_{x^2-y^2}\frac{\eta_k}{\sqrt{32\pi^3}} \qquad (5.8)\\
p\text{-wave:}\quad \vec{d}_k &= \frac{\Delta^p}{\sqrt{4\pi^3}}(\sin k_x, \sin k_y, \sin k_z) \qquad (5.9)
\end{aligned}$$

The irrelevant normalization prefactors make sure that the functions on the RHS including γ_k, τ_k, η_k and the ζ^i_k's are orthonormal within the first Brillouin zone. The extended s-wave order parameter still preserves the full rotational symmetry of the gap function, but allows for several nodes on the Fermi surface compared to the conventional s-wave symmetry. The d_{z^2}- and the $d_{x^2-y^2}$-wave gap functions lead to degenerate transition temperatures, as mentioned in [46]. We shall also observe and verify this fact later on in our discussion.

Before we continue, we take a look at the RHS of the gap equation (5.7). We use a trigonometric identity to decompose $\gamma_{k-q} = \sum_i(\cos k_i \cos q_i + \sin k_i \sin q_i)$.

5.3 Singlet Pairing

Let us first consider singlet pairing only. The gap function is, consequently, an even function of p, and if we define $F(p) := \frac{\tanh(\beta E_p/2)}{E_p}$, $E_p = \sqrt{\varepsilon_p^2 + \Delta_p^2}$, which are also even, passing to the TD-limit $\left(\sum_p \longrightarrow \Omega\int_{BZ}\frac{d^3p}{(2\pi)^3}\right)$ the terms proportional to the odd functions $\sin p_i$ vanish

due to symmetry. Therefore, we have $\gamma_{k-q} \overset{\text{singlet}}{=} 2\sum_i \cos k_i \cos q_i$, and hence the potential factorizes. The next step is to further decompose γ_{k-q} into the ONB defined above. Once we have this decomposition, the gap equation for singlet pairing can be decomposed into several independent ones for the linearly independent, k-dependent coefficients. We make the ansatz (which turns out to be exact within the approximation of Eq. (5.5))

$$\gamma_{k-q} = c_1(k)\frac{1}{\sqrt{8\pi^3}} + c_\gamma(k)\frac{\gamma_q}{\sqrt{48\pi^3}} + c_\eta(k)\frac{\eta_q}{\sqrt{32\pi^3}} + c_\tau(k)\frac{\tau_q}{\sqrt{24\pi^3}} + \sum_i c_{\zeta^i}(k)\frac{\zeta^i(q)}{\sqrt{2\pi^3}} \tag{5.10}$$

Due to symmetries, the coefficients $c_1 = c_{\zeta^i} = 0$ all vanish. The remaining ones yield:

$$\gamma_{k-q} = a_\gamma \gamma_k \gamma_q + a_\eta \eta_k \eta_q + a_\tau \tau_k \tau_q, \tag{5.11}$$

with $a_\gamma = 1/6,\ a_\eta = 1/4$, and $a_\tau = 1/3$. Since singlet pairing requires $s = -s'$, the constant first term in the potential has to be added to the equation above. Defining $V := U_{\text{ff}} - U$, the part of the potential relevant for s- and d-wave pairing reads $V(k-q) = V - W(a_\gamma\gamma_k\gamma_q + q_\eta\eta_k\eta_q + a_\tau\tau_k\tau_q)$.

As mentioned before, for a general k-dependent potential the gap function is also k-dependent and can, therefore, be also expanded in the lattice ONB considered above. Neglecting higher order contributions, we have

$$\Delta^{(\text{singlet})}_{k,ss'} \approx \delta_{s,-s'}\left(\frac{\Delta_s}{\sqrt{8\pi^3}} + \frac{\Delta_{s^-}}{\sqrt{48\pi^3}}\gamma_k + \frac{\Delta_{x^2-y^2}}{\sqrt{32\pi^3}}\eta_k + \frac{\Delta_{z^2}}{\sqrt{24\pi^3}}\tau_k\right) \tag{5.12}$$

Plugging it into the gap equation and comparing the coefficients on both sides, and using $V = U_{\text{ff}} - U$, we obtain the following *self-consistency* equations:

$$\frac{\Delta_s}{\sqrt{8\pi^3}} = -\frac{V}{2\Omega}\sum_p \Delta_p F(p), \tag{5.13}$$

$$\frac{\Delta_{s^-}}{\sqrt{48\pi^3}} = \frac{W}{2\Omega}a_\gamma \sum_p \Delta_p \gamma_p F(p), \tag{5.14}$$

$$\frac{\Delta_{x^2-y^2}}{\sqrt{32\pi^3}} = \frac{W}{2\Omega}a_\eta \sum_p \Delta_p \eta_p F(p), \tag{5.15}$$

$$\frac{\Delta_{z^2}}{\sqrt{24\pi^3}} = \frac{W}{2\Omega}a_\tau \sum_p \Delta_p \tau_p F(p). \tag{5.16}$$

Recalling the purpose of this work, we proceed to investigate the transition temperatures for s-wave, extended s-wave, and d-wave pairing separately. Since the normal-to-superconductor transition is a continuous one, at the critical temperature the gap vanishes and we have $E_p = \varepsilon_p$.

For pure s-wave pairing (s- and extended s-wave simultaneously), putting $F_p(\beta) = F_p(\beta_c) = F_p$ and neglecting the d-wave contributions yields:

$$\Delta_s = -\frac{V}{2\Omega}\sum_p (\Delta_s + \frac{\Delta_{s^-}}{\sqrt{6}}\gamma_p)F_p, \tag{5.17}$$

$$\Delta_{s^-} = \frac{W}{2\Omega}a_\gamma \sum_p (\sqrt{6}\Delta_s + \Delta_{s^-}\gamma_p)\gamma_p F_p. \tag{5.18}$$

To keep the notation simple, we follow [39] and define the auxiliary functions

$$\varphi_1(\beta_c) := \frac{1}{2\Omega}\sum_p F_p(\beta_c) \tag{5.19}$$

$$\varphi_2(\beta_c) := \frac{1}{2\Omega}\sum_p \gamma_p F_p(\beta_c) \tag{5.20}$$

$$\varphi_\gamma(\beta_c) := \frac{1}{2\Omega}\sum_p \gamma_p^2 F_p(\beta_c). \tag{5.21}$$

Then the above system takes the form:

$$\begin{pmatrix} -(1+V\varphi_1) & -\frac{V}{\sqrt{6}}\varphi_2 \\ \sqrt{6}a_\gamma W\varphi_2 & a_\gamma W\varphi_\gamma - 1 \end{pmatrix} \begin{pmatrix} \Delta_s \\ \Delta_{s^-} \end{pmatrix} \stackrel{!}{=} 0, \tag{5.22}$$

which leads to the transcendental equation that determines the critical temperature:

$$a_\gamma V W \varphi_2^2(\beta_c) + (1+V\varphi_1(\beta_c))(1 - a_\gamma W\varphi_\gamma(\beta_c)) \stackrel{!}{=} 0. \tag{5.23}$$

The standard (conventional) s-wave pairing follows as a special case from (5.13) or (5.23) neglecting all the unconventional pairing contributions:

$$1 \stackrel{!}{=} -V\varphi_1(\beta_c). \tag{5.24}$$

The critical temperature for extended s-wave pairing only, on the other hand, reads

$$\frac{1}{a_\gamma W} \stackrel{!}{=} \varphi_\gamma(\beta_c). \tag{5.25}$$

The critical temperature for d-wave pairing is obtained in a similar fashion from equation (5.15), and is given by

$$\frac{1}{a_\eta W} \stackrel{!}{=} \varphi_\eta, \quad \text{with } \varphi_\eta(\beta_c) := \frac{1}{2\Omega}\sum_p \eta_p^2 F_p(\beta_c). \tag{5.26}$$

For completeness, we also give the corresponding equation for the d_{z^2} symmetry:

$$\frac{1}{a_\tau W} \stackrel{!}{=} \frac{1}{2\Omega}\sum_p \tau_p^2 F_p(\beta_c). \tag{5.27}$$

That the value for β_c obtained from (5.26) is the same as the one from (5.27) requires some algebra and will be shown shortly.

5.4 Triplet Pairing

Now, we turn back to p-wave pairing. The starting point is once again the trigonometric identity $\gamma_{k-q} = \sum_i (\cos k_i \cos q_i + \sin k_i \sin q_i)$. This time, however, the symmetry requires the gap function to be antisymmetric and the fermions couple with equal spin, i.e. $\Delta_i^{(t)}(k) := \delta_{s,s'} \Delta^p \frac{\sin k_i}{\sqrt{4\pi^3}}$. The gap equation takes the form

$$\Delta_i^{(t)}(k) = -\frac{1}{2\Omega} \sum_p \left[-U - W\gamma_{k-p}\right] \Delta_i^{(t)}(p) F_p(\beta). \tag{5.28}$$

Notice that the constant part of the potential $\propto U_{\text{ff}} \delta_{s,-s'}$ is not present here. Since the summation is over momenta in the first Brillouin zone only, for p-wave pairing the only remaining terms are $\gamma_{k-p} \overset{\text{triplet}}{=} 2\sum_i \sin k_i \sin p_i = 2\sum_i \lambda_{k_i} \lambda_{p_i}$, where $\lambda_{k_i} := \sin k_i$.

Plugging this into the gap equation (5.28), we observe that the part of the potential $\propto U$ sums up to zero too in the TD-limit: $\frac{U}{2\Omega} \Delta^p \sum_p \lambda_{p_i} F_p \longrightarrow \Delta^p \frac{U}{2} \int_{BZ} dp \lambda_{p_i} F_p \overset{\vec{p} \to -\vec{p}}{=} -\Delta^p \frac{U}{2} \int_{BZ} dp \lambda_{p_i} F_p$, since $\lambda_{p_i} F_p$ is odd for any $i \in \{x, y, z\}$.[2] Hence, we obtain the gap equation

$$1 \overset{!}{=} \frac{2W}{2\Omega} \sum_p \sin^2 p_i F_p(\beta). \tag{5.29}$$

Similar arguments as for singlet pairing show that the critical temperature for p-wave pairing in either direction i can be computed from

$$\frac{1}{2W} \overset{!}{=} \varphi_p(\beta_c), \quad \text{with} \quad \varphi_p(\beta_c) := \frac{1}{2\Omega} \sum_p \sin^2 p_x F_p(\beta_c). \tag{5.30}$$

5.5 Approximate Results for the Critical Temperature

Approximate results for the critical temperatures can be obtained using the density of states (DOS) on a 3D cubic lattice, denoted by $N_{3\text{D}}(\varepsilon)$. To this end, we need to compute (and invert, if possible) the functions $\varphi_j(\beta_c)$, $j \in \{1, 2, \gamma, \eta, p\}$. We proceed as follows:

1. We pass to the TD limit.
2. We make use of a logarithmic approximation to the 2D DOS to define the 3D DOS.
3. Due to the structure of $N_{3\text{D}}(\varepsilon)$, we use suitable approximations to $F_p(\beta_c)$ to divide the dimensionless half bandwidth interval (to be integrated over) in two pieces: $[0, 3] = [0, 1] \cup [1, 3]$.
4. We keep the full temperature dependence of $F_p(\beta_c)$ in the interval $[0, 1]$ where exact results for the 3D DOS can be obtained, while putting $\beta_c \gg 1$ in $[1, 3]$, thus replacing $\tanh(\beta_c \varepsilon/2) \approx 1$. Hence, we ignore the temperature contribution of the complicated part of $N_{3\text{D}}(\varepsilon)$ in the interval $[1, 3]$ evaluating the resulting integral to a non-universal constant.

[2] Here Δ^p is just the amplitude of the p-wave gap function and thus does not change its sign.

Let us recall the definitions

$$\begin{aligned}
\varphi_1 &= \frac{1}{2\Omega}\sum_p F_p, \qquad \varphi_2 = \frac{1}{2\Omega}\sum_p \gamma_p F_p \\
\varphi_\gamma &= \frac{1}{2\Omega}\sum_p \gamma_p^2 F_p, \qquad \varphi_\eta = \frac{1}{2\Omega}\sum_p \eta_p^2 F_p \\
\varphi_p &= \frac{1}{2\Omega}\sum_p \sin^2 p_x F_p
\end{aligned} \tag{5.31}$$

We begin by observing that $F_p = F(\gamma_p)$ and $N_{3\mathrm{D}}(\varepsilon) \sim N_{3\mathrm{D}}(\gamma_p)$. Therefore, φ_1, φ_2, and φ_γ are relatively easy to compute. The computation of φ_η turns out to be the hardest. Luckily, there exists a way to relate it to the others which we show here. First, define a measure $d\mu(p) := \frac{d^3p}{2(2\pi)^3}F_p$ to integrate over the first Brillouin zone. Now, observe that for any fixed i and any function $f = f(p_i)$ we have $\int d\mu(p) f(p_i) = \int d\mu(p) f(p_j)$ for any $i, j \in \{x, y, z\}$, since $F_p = F(\gamma_p)$, $\gamma_p = 2\sum_i \cos p_i$, and $p_i \in [-\pi, \pi]$. Then, we have

$$\begin{aligned}
3\varphi_\eta + \varphi_\gamma &= \int_{\mathrm{BZ}} d\mu(p) 3\eta_p^2 + \gamma_p^2 \\
&= \int_{\mathrm{BZ}} d\mu(p) 4\Big(4\left(\cos^2 p_x + \cos^2 p_y\right) + \cos^2 p_z \\
&\quad - \underline{4\cos p_x \cos p_y} + \underline{2\left(\cos p_x \cos p_z + \cos p_y \cos p_z\right)} \Big) \\
&\overset{p_i \leftrightarrow p_j}{=} \int_{\mathrm{BZ}} d\mu(p) 36\cos^2 p_x = 36(\varphi_1 - \varphi_p) =: 36\tilde{\varphi}_p,
\end{aligned} \tag{5.32}$$

where the underlined terms cancel each other out due to the aforementioned symmetry property. Finally, we obtain the relation

$$\varphi_\eta = 12\tilde{\varphi}_p - \frac{1}{3}\varphi_\gamma. \tag{5.33}$$

Using precisely the same symmetry argument, it follows that $a_\eta \varphi_\eta = a_\tau \varphi_\tau$, and hence Eqs. (5.26) and (5.27) for d_{z^2} and $d_{x^2-y^2}$ symmetry, respectively, yield the same critical temperature.

5.5.1 Calculation of φ_1 and $\tilde{\varphi}_p$

In order to calculate the integrals in the TD limit we need an approximation to the exact DOS on a simple cubic lattice. It can be calculated from the 2D one which is given by

$$N_{2\mathrm{D}}(\varepsilon) = \frac{1}{\pi^2}\int_0^\pi dp_x \int_0^\pi dp_y \delta(\varepsilon - 2t_f W(p_x, p_y)) = \frac{2}{D\pi^2} K\left(\sqrt{1 - \left(\frac{\varepsilon}{D}\right)^2}\right), \tag{5.34}$$

with $K(x)$ the complete elliptic integral of the first kind and $D = 4t_f$ the half bandwidth. The function $W(p_x, p_y) = -\cos p_x - \cos p_y$ is proportional to the 2D lattice dispersion. Since this is a special function we use a logarithmic approximation whose error turns out to be extremely small, as can be seen from Fig. 5.2:

$$N_{2\mathrm{D}}(\varepsilon) \approx \frac{2}{D\pi^2} \log \left| \frac{4\sqrt{2}D}{\varepsilon} \right|. \tag{5.35}$$

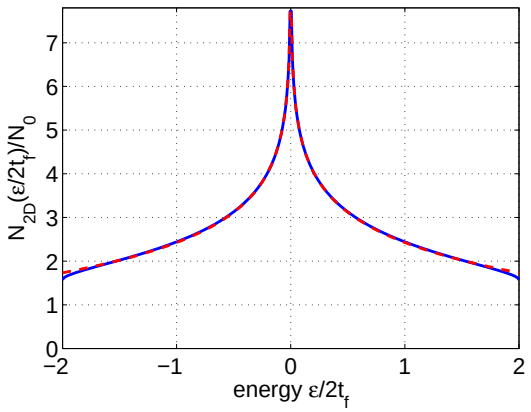

Figure 5.2: (color online): Density of states $N_{2\mathrm{D}}$ for a 2D square lattice: exact curve (solid blue line) vs. the logarithmic approximation (dashed red line).

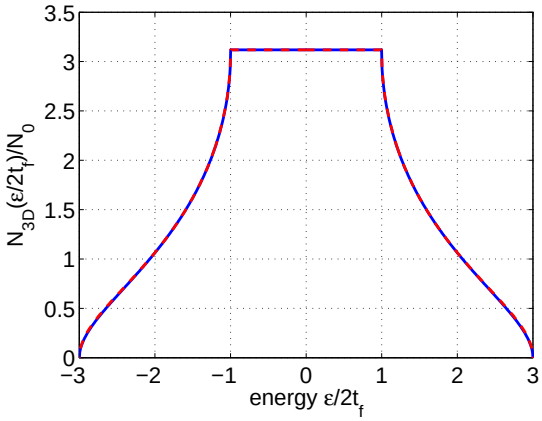

Figure 5.3: (color online): Density of states $N_{3\mathrm{D}}$ for a 3D cubic lattice: exact curve (solid blue line) vs. the logarithmic approximation (dashed red line).

The exact 3D DOS is obtained from the 2D one to be:

$$N_{3\mathrm{D}}(2t_f\gamma) = \frac{1}{\pi} \int_{\max\{-2,\gamma-1\}}^{\min\{2,\gamma+1\}} \frac{N_{2\mathrm{D}}(2t_f w)}{\sqrt{1-(\gamma-w)^2}}. \tag{5.36}$$

Within the logarithmic approximation, we have

$$N_{3\mathrm{D}}(2t_f\gamma) = \frac{N_0}{\pi} \left[\mathbb{1}\{\gamma \le -1\} \int_{-2}^{\gamma+1} dw + \mathbb{1}\{|\gamma| \le 1\} \int_{\gamma-1}^{\gamma+1} dw + \mathbb{1}\{\gamma \ge 1\} \int_{\gamma-1}^{2} dw \right] \frac{\log\left|\frac{8\sqrt{2}}{w}\right|}{\sqrt{1-(\gamma-w)^2}}, \tag{5.37}$$

where $N_0 = 1/(2t_f\pi^2)$, and we used $\varepsilon = 2t_f w$. Due to the even symmetry of the function we can restrict to positive arguments $\gamma > 0$ only:

$$N_{3\mathrm{D}}(2t_f\gamma) = \begin{cases} N_0 \frac{9}{2} \log 2 & ,0 \le \gamma \le 1 \\ \frac{N_0}{\pi} \int_{\gamma-1}^{2} dw \frac{\log\left|\frac{8\sqrt{2}}{w}\right|}{\sqrt{1-(\gamma-w)^2}} & ,1 \le \gamma \le 3 \end{cases}$$

The functional behaviour of $N_{3\mathrm{D}}$ over the whole bandwidth is shown in Fig. 5.3.

Now we are ready to proceed towards the calculation of φ_1. At the critical temperature

the gap closes and we have $E_p = \sqrt{\varepsilon_p^2 + \Delta_p^2} = \varepsilon_p$. Using this, we compute

$$\begin{aligned}
\varphi_1(\beta_c) &= \frac{1}{2\Omega}\sum_p F_p(\beta_c) \overset{\text{TD-limit}}{\longrightarrow} \frac{1}{2}\int_{\text{BZ}} \frac{d^3p}{(2\pi)^3} F_p(\beta_c) \\
&= \frac{1}{2}\int_{-6t_f}^{6t_f} d\varepsilon N_{3\text{D}}(\varepsilon) \frac{\tanh\left(\frac{\beta_c\varepsilon}{2}\right)}{\varepsilon} = \int_0^3 d\gamma N_{3\text{D}}(2t_f\gamma)\frac{\tanh(\beta_c t_f\gamma)}{\gamma} \\
&= N_0\left[\int_0^1 d\gamma \log(16\sqrt{2})\frac{\tanh(\beta_c t_f\gamma)}{\gamma} + \int_1^3 d\gamma \frac{N_{3\text{D}}(2t_f\gamma)}{N_0}\frac{\tanh(\beta_c t_f\gamma)}{\gamma}\right] \\
&= N_0\left[\frac{9}{2}\log 2\int_0^3 d\gamma \frac{\tanh(\beta_c t_f\gamma)}{\gamma} + \int_1^3 d\gamma\left(\frac{N_{3\text{D}}(2t_f\gamma)}{N_0} - \frac{9}{2}\log 2\right)\underbrace{\frac{\tanh(\beta_c t_f\gamma)}{\gamma}}_{\approx\frac{1}{\gamma}}\right] \\
&\overset{u:=t_f\beta_c\gamma}{=} N_0\left[\frac{9}{2}\log 2\int_0^{3\beta_c t_f} du\frac{\tanh u}{u} + \underbrace{\int_1^3 d\gamma\left(\frac{N_{3\text{D}}(2t_f\gamma)}{N_0} - \frac{9}{2}\log 2\right)\frac{1}{\gamma}}_{=:\kappa_1=-1.90}\right] \\
&\approx N_0\left[\frac{9}{2}\log 2\log\left(\frac{12e^C}{\pi}\beta_c t_f\right) + \kappa_1\right],
\end{aligned} \tag{5.38}$$

with $C \approx 0.577$ the Euler-Mascheroni constant.

The calculation of $\tilde{\varphi}_p$ is a little bit more involved, but it is it that enables us to obtain approximate analytic results for d-wave and p-wave pairing. This time, we shall need the 2D DOS, as will become clear shortly. We remind the reader of the previously defined function $W(p_x, p_y) = -\cos p_x - \cos p_y$, and we proceed:

$$\begin{aligned}
\tilde{\varphi}_p(\beta_c) &= \frac{1}{2\Omega}\sum_p \cos^2 p_x F_p(\beta_c) \overset{\text{TD-limit}}{\longrightarrow} \frac{1}{2}\int_{\text{BZ}}\frac{d^3p}{(2\pi)^3}\cos^2 p_x F_p(\beta_c) = \frac{1}{2}\int_{\text{BZ}}\frac{d^3p}{(2\pi)^3}\cos^2 p_z \frac{\tanh\left(\frac{\beta_c\varepsilon_p}{2}\right)}{\varepsilon_p} \\
&= \frac{1}{2}\int_{-6t_f}^{6t_f} d\varepsilon \frac{\tanh\left(\frac{\beta_c\varepsilon}{2}\right)}{|\varepsilon|}\int_{\text{BZ}}\frac{d^3p}{(2\pi)^3}\cos^2 p_z\,\delta(\varepsilon - 2t_f[W(p_x,p_y) - \cos p_z]) \\
&\overset{\varepsilon=2t_f\gamma}{=} \frac{1}{2}\frac{1}{2t_f}\int_{-3}^3 \frac{d\gamma}{\gamma}\tanh(\beta_c t_f\gamma)\int_{\text{BZ}}\frac{d^3p}{(2\pi)^3}\cos^2 p_z\,\delta(\gamma - [W(p_x,p_y) - \cos p_z]) \\
&= \frac{1}{2}\int_{-3}^3\frac{d\gamma}{\gamma}\tanh(\beta_c t_f\gamma)\frac{1}{2t_f\pi^3}\int_0^\pi dp_x\int_0^\pi dp_y \frac{(\gamma - W[p_x,p_y])^2}{\sqrt{1-(\gamma - W[p_x,p_y])^2}}\mathbb{1}\{|\gamma - W(p_x,p_y)| \le 1\} \\
&\overset{w:=W(p_x,p_y)}{=} \frac{1}{2}\int_{-3}^3\frac{d\gamma}{\gamma}\tanh(\beta_c t_f\gamma)\frac{1}{\pi}\int_{\max\{-2,\gamma-1\}}^{\min\{2,\gamma+1\}} dw N_{2\text{D}}(2t_f w)\frac{(\gamma-w)^2}{\sqrt{1-(\gamma-w)^2}},
\end{aligned} \tag{5.39}$$

where we made use of the definition of the 2D density of states (5.34) in the last equality. Next, we take a closer look at the inner integral and, making the substitution $w := \gamma + \sin\theta$ we define:

$$\mathcal{M}(\gamma) := \frac{1}{\pi}\int_{-\pi/2}^{\pi/2} d\theta \log\left|\frac{8\sqrt{2}}{\gamma + \sin\theta}\right|\sin^2\theta, \quad \text{for} \quad |\gamma| \le 1, \tag{5.40}$$

which is the part of $\mathcal{M}(\gamma)$ than can be evaluated analytically within the logarithmic approximation. Further, using the transformation $\gamma \to -\gamma$ and $\theta \to -\theta$ (or $w \to -w$, respectively) to shift the domain of γ to the positive reals, we end up with the compact expression

$$\tilde{\varphi}_p(\beta_c) = N_0 \int_0^3 \frac{d\gamma}{\gamma} \tanh(\beta_c t_f \gamma) \mathcal{M}(\gamma). \tag{5.41}$$

The complete function $\mathcal{M}(\gamma)$ is shown in Fig. 5.4, and has the following functional behaviour within the logarithmic approximation to the 2D DOS:

$$\mathcal{M}(\gamma) = \begin{cases} \frac{1}{2}\left(\gamma^2 - \frac{1}{2} + \frac{9}{2}\log 2\right) & ,0 \le \gamma \le 1 \\ \frac{N_0}{\pi} \int_{\gamma-1}^{2} dw \log\left|\frac{8\sqrt{2}}{w}\right| \frac{(\gamma - w)^2}{\sqrt{1-(\gamma-w)^2}} & ,1 \le \gamma \le 3 \end{cases}$$

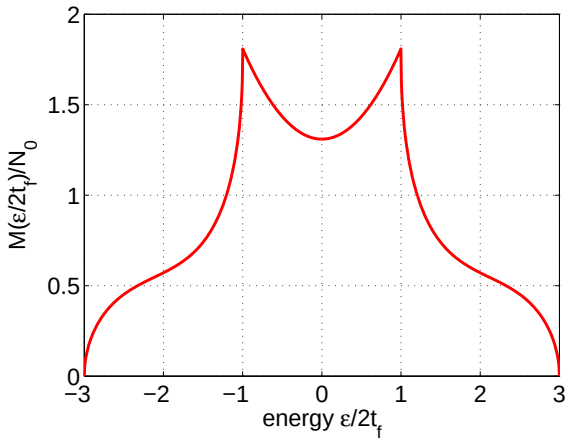

Figure 5.4: (color online): Auxiliary function $\mathcal{M}(\gamma)$

The rest of the calculation is similar to that for φ_1 and will not be given here. The final result reads

$$\tilde{\varphi}_p(\beta_c) \approx \frac{N_0}{4}\left(-\frac{\pi^2}{12}\frac{1}{(\beta_c t_f)^2} + (9\log 2 - 1)\log\left(\frac{12e^C}{\pi}\beta_c t_f\right) + \kappa_4\right) \tag{5.42}$$

with $\kappa_4 = -0.65$.

5.6 Approximate Results

The approximate functional behaviour of the other φ_j's in the limit $\beta_c t_f > 1$ is obtained in a similar fashion as in Section 5.5.1. Since the calculations are pretty lengthy, we only give the

final results:

$$\begin{aligned}
\varphi_1(\beta_c) &\approx N_0\left[\frac{9}{2}\log 2\log\left(\frac{12e^C}{\pi}\beta_c t_f\right)+\kappa_1\right]\\
\varphi_2(\beta_c) &\approx N_0\left[-\frac{9(\log 2)^2}{2}\frac{1}{\beta_c t_f}+\kappa_2\right]\\
\varphi_\gamma(\beta_c) &\approx N_0\left[-\frac{3\pi^2\log 2}{16}\frac{1}{(\beta_c t_f)^2}+\kappa_\gamma\right]\\
\varphi_\eta(\beta_c) &\approx N_0\left[\frac{\pi^2}{4}\left(\frac{\log 2}{4}-1\right)\frac{1}{(\beta_c t_f)^2}+3(9\log 2-1)\log\left(\frac{12e^C}{\pi}\beta_c t_f\right)+\kappa_\eta\right]\\
\tilde{\varphi}_p(\beta_c) &\approx \frac{N_0}{4}\left[-\frac{\pi^2}{12}\frac{1}{(\beta_c t_f)^2}+(9\log 2-1)\log\left(\frac{12e^C}{\pi}\beta_c t_f\right)+\kappa_4\right]\\
\varphi_p(\beta_c) &\approx \frac{N_0}{4}\left[\frac{\pi^2}{12}\frac{1}{(\beta_c t_f)^2}+(9\log 2+1)\log\left(\frac{12e^C}{\pi}\beta_c t_f\right)+\kappa_p\right]
\end{aligned}\tag{5.43}$$

with the non-universal, dimension-dependent constants κ_j given by

$$\begin{aligned}
&\kappa_1=-1.90, \quad \kappa_2=5.46, \quad \kappa_\gamma=5.47,\\
&\kappa_4=-0.65, \quad \kappa_p=-6.96, \quad \kappa_\eta=-3.78.
\end{aligned}\tag{5.44}$$

The accuracy of the approximation used so far has been tested via comparison to numerical calculations. The functions φ_j relevant for singlet pairing are shown in Fig. 5.5, while φ_p, relevant for triplet pairing, is shown in Fig. 5.6. The astonishing agreement observed serves as a justification of the low-T_c method used in the previous section.

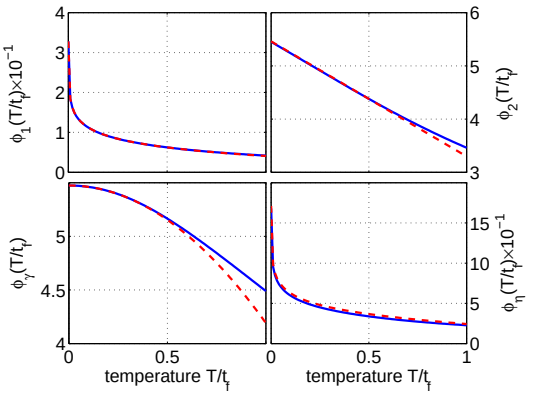

Figure 5.5: (color online): Comparison between exact curve (solid blue line) and approximate analytical result (dashed red line) for *singlet* pairing: $\phi_j=\varphi_j/N_0$

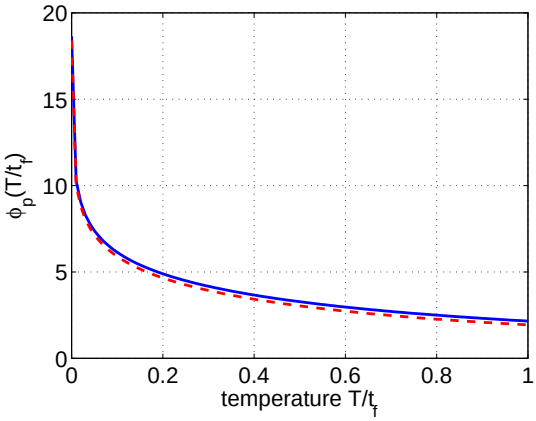

Figure 5.6: (color online): Comparison between exact curve (solid blue line) and approximate analytical result (dashed red line) for *triplet* pairing: $\phi_p=\varphi_p/N_0$

If we take a closer look at the above functions, we find that the critical temperature for the extended s-wave pairing only which is proportional to φ_γ (cf. Eq. (5.25)), therefore, has an algebraic decay. It can be solved for analytically, to give

$$\frac{T_c}{t_f} = \sqrt{\frac{16}{3\pi^2 \log 2}\left(\kappa_\gamma - \frac{1}{a_\gamma N_0 W}\right)}. \tag{5.45}$$

The above result is non-perturbative and compared to the numerical curve for the full φ_γ in Fig. 5.9, justifies once more the validity of the approximations used so far. Furthermore, it follows from Eq. (5.45) that there cannot be any extended s-wave pairing for $W < 1/(a_\gamma \kappa_\gamma N_0)$.

In contrast, the conventional s-wave pairing critical temperature exhibits exponential decay, cf. (5.24), which is a well-established result of BCS theory. Again, one needs a negative potential $V < 0$ in order to obtain a well-defined solution to the gap equation. The exact s-wave critical temperature can be solved for analytically to give

$$\frac{T_c}{t_f} = \frac{12e^C}{\pi} \exp\left[-\frac{2}{9\log 2}\left(-\kappa_1 + \frac{1}{N_0|V|}\right)\right]. \tag{5.46}$$

In Fig. 5.7 we give a numerical solution following Eq. (5.24).

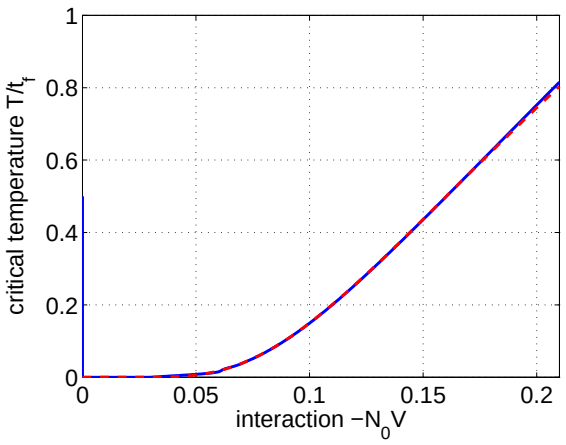

Figure 5.7: (color online): Critical temperature for s-wave pairing as a function of interaction strength V: exact curve (blue solid line) vs. approximate result (dashed red line). The result agrees with the one from BCS theory exhibiting an exponential decay.

However, the pure d-wave or p-wave pairing functions, φ_η and φ_p, contain both algebraic and logarithmic terms. Hence, inverting the corresponding equations (5.26) and (5.30) to obtain an analytical expression for the critical temperature is possible only numerically. For p-wave pairing, Efremov and Viverit, [14], predict an exponential decay of the critical temperature for a Bose-Fermi mixture *not* on a lattice using a similar expansion technique for the gap function. Therefore, the effect of the lattice structure for p-wave pairing can be traced back to the appearance of an algebraic term in $\varphi_p(\beta_c) \propto 1/(\beta_c t_f)^2$. Fig. 5.8 shows the behaviour of the critical temperature as a function of the interaction strength W. Similar results have been obtained in the 2D model by Micnas et al. [39]. The plot suggests that p-wave pairing is suppressed by d-wave pairing throughout the entire regime of validity, $\beta_c t_f \gtrsim 1$.

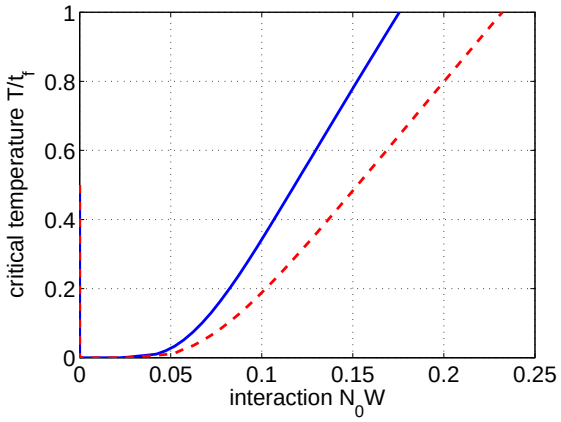

Figure 5.8: (color online): Critical temperature as a function of the interaction strength W for d-wave pairing (solid blue line) and p-wave pairing (dashed red line). The curves are obtained numerically.

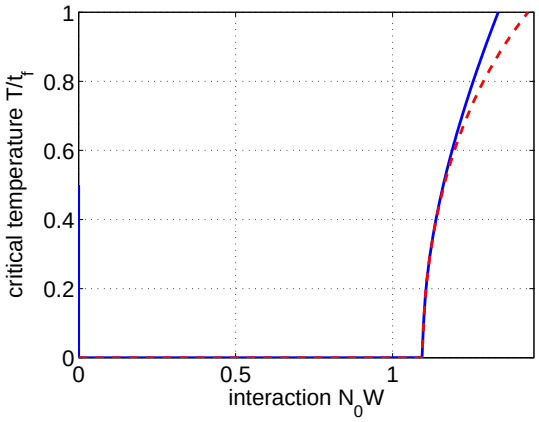

Figure 5.9: (color online): Critical temperature for extended s-wave pairing as a function of interaction strength W. The solid blue line represents the numerical curve and the red dashed line follows Eq.(5.45).

5.7 Analysis of the Results

In this section we address the issue of which one of the pairing instabilities is the dominant one. To this end, we exploit the full dependence of the model on the interaction strength parameters:

$$\begin{aligned} U &= \frac{U_{\mathrm{bf}}^2}{U_{\mathrm{bb}}} \frac{1}{1+6\xi^2} \\ W &= \frac{U_{\mathrm{bf}}^2}{U_{\mathrm{bb}}} \frac{\xi^2}{(1+6\xi^2)^2} \\ V &= U_{\mathrm{ff}} - U. \end{aligned} \tag{5.47}$$

A direct comparison between the pairing instabilities for extended s-, d- and p-wave pairing is possible, since their critical temperatures depend on the parameter W only. From Figs. 5.8 and 5.9 it becomes clear that d- and p-wave pairing is possible also for small W values where extended s-wave pairing is completely suppressed. We believe that for fixed W it is the d-wave that dominates among these pairing mechanisms.

The situation becomes more involved if we take the s-wave pairing into account, for its critical temperature is a function of $V < 0$ only. Hence, using the bare fermionic interaction U_{ff} it might be possible to tune the critical temperature for s-wave below that of d-wave (cf. Fig 5.7) or even switch it off completely in favour of the d-wave pairing, in which case a positive and large enough U_{ff} would be needed. We remark that dominant d-wave pairing has already been predicted in a 2D Bose-Fermi mixture on an isotropic square lattice by Mathey et al. using a Renormalization Group approach [36].

Another conceivable scenario becomes interesting when the bare fermionic interaction is completely switched off, i.e. $U_{\mathrm{ff}} = 0$. From Eq. (5.47) then one can establish a direct relation between U and W: $W = \xi^2(1+6\xi^2)^{-1}U$ which opens up a possibility for a direct comparison for any given fixed $\xi \ll 1$. However, within the validity of our approximation methods we

have $W \ll U$ and therefore the d-wave pairing is strongly suppressed. This result agrees very well with the observation in [55], according to which the unconventional pairing mechanisms are mostly pronounced for $\xi \sim 1$.

5.8 Conclusions

In this chapter, we investigated the Bose-Fermi mixture for unconventional pairing within mean-field theory. To this end, we consider small enough temperatures, making use of the Bogoliubov approximation for the bosons and neglecting retardation effects. To obtain analytical results, we further restrict our attention to the case of small bosonic healing length $\xi \ll 1$, after which only the leading linear k-dependence of the potential has been retained.

A low-temperature expansion method has been applied to obtain extremely accurate approximate results for $\beta_c t_f \gtrsim 1$. The key feature is using a very powerful logarithmic approximation to the 2D density of states, suitable for energies in the vicinity of the Fermi surface where pairing is expected to occur. Altogether this method allows for obtaining the equations determining the critical temperature T_c.

We also derive exact gap equations for unconventional s-, extended s-, pure s-, d- and p-wave pairing, obeying the required symmetries. The corresponding critical temperatures are obtained from them as a special case of vanishing gap parameter, which leads to transcendental equations, except for the cases of s- and extended s-wave pairing.

For s-wave, we recover the exponential decay, expected from BCS theory with appropriate prefactors within the mean field-approximation. For extended s-wave, we find a non-perturbative power-law dependence $T_c/t_f \sim \sqrt{(c_1 - c_2/(WN_0)}$. According to it, extended s-wave pairing is possible starting from a critical value $W_c = 1/(a_\gamma \kappa_\gamma N_0)$. Both results come in precise agreement with the numerical solutions for the gap equations.

The critical temperature for the remaining d- and p-wave pairing as a function of the dimensionless interaction strength WN_0 has been obtained numerically. We find the same scenario as [39]: both functions are convex and monotonically increasing within the validity of the considered approximation. The curve for d-wave pairing lies clearly above the one for p-wave, thereby rendering p-wave pairing suppressed.

Among the extended s-, d- and p-wave instabilities, the dominant one is the d-wave. Taking the s-wave stability into account there are two interesting scenarios: either one can use the bare fermionic interaction U_{ff} to effectively sweep the parameter V up to zero closing the s-wave channel, so that the s-wave instability succumbs to the d-wave one, or one can consider the $U_{\mathrm{ff}} = 0$, in which case we recover the observation of [55] that unconventional pairing is in general pronounced for $\xi \sim 1$ and hence the conventional s-wave pairing dominates.

Chapter 6

Supersymmetric Bose-Fermi Mixtures

6.1 Introduction

Supersymmetry has been attracting the attention of the physics community for a long time. Simplicity and beauty on a deep mathematical level predict that every elementary particle might have a heavy supersymmetric partner of the opposite type. If this is true, then the electron will come up in pair with a boson, dubbed selectron, while the photon's partner would be the spin-$\frac{1}{2}$ photino.

After it originated from high-energy physics, SUSY has rarely been applied to non-relativistic quantum systems. In 1984, Clark and Love [10] pioneered the development of a supersymmetric non-relativistic many-body quantum field theory. With the recent advancement of cold atom experiments, condensed matter theorists have looked for supersymmetry on several occasions, mainly in Bose-Fermi mixtures, where a sharp fermionic collective mode which can be identified with a Goldstino-like mode has recently been predicted [61]. Supersymmetric lattice gauge theories have also been considered in the context of cold atoms, [34].

In this chapter, we consider a theory of a spinful Bose-Fermi mixture in the non-degenerate regime above the SF-transition temperature. We show that the system exhibits a supersymmetric point in parameter space, upon exchanging a boson with a fermion. Starting from the SUSY Poincaré algebra, we employ the method of İnönü-Wigner contraction to find in the nonrelativistic limit the Galilean SUSY algebra, since a many-body theory is assumed to be non-relativistic in general. Using its representations, we define bosonic chiral superfields which incorporate manifestly the supersymmetric nature of the theory. Exploiting the consequences of this additional symmetry, we proceed to derive an effective single-field φ^4-theory in the real-space sector of a general supersymmetric field theory. The Grassmann sector is proved to be rigid to perturbation theory to any order, as a direct consequence of a manifest SUSY. We also address the issue of SUSY-breaking which provides a way to develop perturbation theory around the SUSY point.

6.2 The Spinful Bose-Fermi Mixture

The Hamiltonian of a general Bose-Fermi mixture of spinful fermions ψ_α ($\alpha = \uparrow, \downarrow$), and two types of bosons A, B is given by

$$\begin{aligned}
H &= H_0 + H^1_{\text{int}} + H^2_{\text{int}} \\
H_0 &= \int \mathrm{d}^3x A^\dagger(x)\left(-\frac{1}{2m_A}\nabla^2 + \mu_A\right)A(x) + B^\dagger(x)\left(-\frac{1}{2m_B}\nabla^2 + \mu_B\right)B(x) \\
&\quad + \sum_\alpha \psi^\dagger_\alpha(x)\left(-\frac{1}{2m_\alpha}\nabla^2 + \mu_\alpha\right)\psi_\alpha(x) \\
H^1_{\text{int}} &= \frac{1}{2}\int \mathrm{d}^3x g_{AA}A^\dagger(x)A^\dagger(x)A(x)A(x) + g_{BB}B^\dagger(x)B^\dagger(x)B(x)B(x) \\
&\quad + g_{FF}\psi^\dagger_\uparrow(x)\psi^\dagger_\downarrow(x)\psi_\downarrow(x)\psi_\uparrow(x) \\
H^2_{\text{int}} &= \frac{1}{2}\int \mathrm{d}^3x g_{AF}\sum_\alpha A^\dagger(x)A(x)\psi^\dagger_\alpha(x)\psi_\alpha + g_{BF}\sum_\alpha B^\dagger(x)B(x)\psi^\dagger_\alpha(x)\psi_\alpha \\
&\quad + g_{AB}A^\dagger(x)A(x)B^\dagger(x)B(x),
\end{aligned} \tag{6.1}$$

where the constants g_{ij} denote the interaction strength between species i and j. Due to the Pauli Exclusion Principle, the fermion-fermion interaction is possible only between fermions of different spin.

For a SUSY theory one needs the following general form of the fermion-fermion interaction:

$$H_\psi = \frac{g_{FF}}{2}\sum_{\alpha,\beta}\psi^\dagger_\alpha(x)\psi^\dagger_\beta(x)\psi_\beta(x)\psi_\alpha(x). \tag{6.2}$$

The factor $1/2$ comes from the fact that whenever $\alpha = \uparrow, \beta = \downarrow$, or vice-versa, we should recover the original interaction. However, if $\alpha = \beta$, using the commutator relations for fermions, we have $\psi^\dagger\psi\psi^\dagger\psi = \psi^\dagger\psi$ again due to the Pauli principle. These terms are then 'borrowed' from the chemical potential of the fermions. Hence, the H_0 and H^1_{int} terms can be cast into the form

$$\begin{aligned}
H_0 &= \int \mathrm{d}^3x A^\dagger(x)\left(-\frac{1}{2m_A}\nabla^2 + \mu_A\right)A(x) + B^\dagger(x)\left(-\frac{1}{2m_B}\nabla^2 + \mu_B\right)B(x) \\
&\quad + \sum_\alpha \psi^\dagger_\alpha(x)\left(-\frac{1}{2m_\alpha}\nabla^2 + \left(\mu_\alpha - \frac{g_{FF}}{4}\right)\right)\psi_\alpha(x) \\
H^1_{\text{int}} &= \frac{1}{2}\int \mathrm{d}^3x g_{AA}A^\dagger(x)A^\dagger(x)A(x)A(x) + g_{BB}B^\dagger(x)B^\dagger(x)B(x)B(x) \\
&\quad + \frac{g_{FF}}{2}\sum_{\alpha,\beta}\psi^\dagger_\alpha(x)\psi^\dagger_\beta(x)\psi_\beta(x)\psi_\alpha(x).
\end{aligned} \tag{6.3}$$

The requirement for the theory to exhibit SUSY then takes the form

$$\begin{aligned}
\mu_A = \mu_B = \mu_\alpha - \frac{g_{FF}}{4} &\stackrel{!}{=} \mu, \qquad \alpha = \uparrow, \downarrow \\
g_{AA} = g_{BB} = \frac{g_{FF}}{2} &\stackrel{!}{=} g, \\
g_{AF} = g_{BF} = g_{AB} &\stackrel{!}{=} 2g.
\end{aligned} \tag{6.4}$$

Under this conditions, and adopting the spinor notation $\sum_\alpha \psi_\alpha^\dagger \psi_\alpha = \psi\sigma^0\bar{\psi}$, where $\sigma_0 = -\mathbb{1}_{2\times 2}$, $\bar{\psi} = \psi^\dagger$, the total interaction term reads

$$H_{\text{int}} = \frac{g}{2}\int \mathrm{d}^3x A^\dagger \left(A^\dagger A + B^\dagger B + \psi\sigma^0\bar{\psi}\right) A + B^\dagger \left(A^\dagger A + B^\dagger B + \psi\sigma^0\bar{\psi}\right) B + \psi\sigma^0 \left(A^\dagger A + B^\dagger B + \psi\sigma^0\bar{\psi}\right) \bar{\psi}. \tag{6.5}$$

We shall later on observe that it can be cast in a manifestly supersymmetric way which will facilitate a further discussion on a diagrammatic level.

6.3 Supersymmetric extension of the Galilean Group

6.3.1 The İnönü-Wigner Contraction

The many-body description of bosons and fermions implicitly assumes a non-relativistic setting. Therefore, in this section, we derive the algebra of the SUSY extension of the Galilean group. To this end, we employ the method of İnönü-Wigner contraction [28] to contract the (relativistic) SUSY Poincaré algebra in the limit $c \to \infty$, where c denotes the speed of light. The resulting algebra is dubbed the *nonrelativistic SUSY algebra* and we shall later impose that the non-relativistic quantum fields describing the mixture of bosons and fermions shall transform according to its representations.

To clarify the method, we first take a look at the contraction of the Lorentz group to the Galilean group in the limit $c \to \infty$. Let J_i denote the generator of rotations (the angular momentum operator) and let K_i denote the generator of boosts in direction i, respectively. The Lorentz algebra is defined as

$$\begin{aligned}[J_i, J_j] &= i\varepsilon_{ijk}J_k,\\ [J_i, K_j] &= i\varepsilon_{ijk}K_k,\\ [K_i, K_j] &= -i\varepsilon_{ijk}J_k.\end{aligned} \tag{6.6}$$

We wish to derive from it the Galilean algebra, given by

$$\begin{aligned}[J_i, J_j] &= i\varepsilon_{ijk}J_k,\\ [J_i, K_j] &= i\varepsilon_{ijk}K_k,\\ [K_i, K_j] &= 0.\end{aligned} \tag{6.7}$$

To employ the limiting procedure $c \to \infty$, we seek a representation of the Lorentz algebra, in which the speed of light appears as a parameter. Such a representation is for example given by the well-known Lorentz transformation, which leaves two of the spatial dimensions invariant:

$$\Lambda(v) = \begin{pmatrix} \gamma & \gamma\frac{v}{c} \\ \gamma\frac{v}{c} & \gamma \end{pmatrix}. \tag{6.8}$$

Next, we introduce a singular transformation

$$U = \begin{pmatrix} c & 0 \\ 0 & 1 \end{pmatrix} \tag{6.9}$$

chosen such that

$$U\Lambda(v)U^{-1} \overset{c\to\infty}{\longrightarrow} \begin{pmatrix} 1 & v \\ 0 & 1 \end{pmatrix}. \tag{6.10}$$

The result of this procedure agrees precisely with the expected Galilei transformation.

To bring the discussion to a more general level, consider an algebra $\{X_i\}$, $i \in \{1, ..., n+m\}$, defined by

$$[X_i, X_j] = if_{ij}^k X_k, \tag{6.11}$$

with f_{ij}^k the structure constants. Further, consider a singular transformation U that defines new generators Y_i via

$$Y_i = U_i^j X_j. \tag{6.12}$$

Notice that due to the singular character of U, the elements Y_j define a different algebra, the so-called *contracted* algebra. It follows that the structure constants transform according to

$$f_{ij}^k = U_i^m U_j^n f_{mn}^l (U^{-1})_l^k. \tag{6.13}$$

We consider a U of the form

$$U = \begin{pmatrix} \mathbb{1}_{m\times m} & 0 \\ 0 & \epsilon\mathbb{1}_{n\times n} \end{pmatrix}, \tag{6.14}$$

where the two identities need not have the same dimension. In the limit $\epsilon \to 0$ the n generators are contracted, leaving a new algebra consisting of the properly chosen m ones. This should be done in such a way that $\{X_1, ..., X_m\}$ themselves form a subalgebra. These results can be summarized in the following two theorems by İnönü and Wigner [28], the proofs of which we omit.

Theorem 6.1. *Given a Lie group G, a contraction can be performed, if and only if there exists a nontrivial subgroup H. The algebra of H remains fixed under contraction, while the remaining contracted algebra generates an Abelian invariant subgroup of the contracted group G', called N. Furthermore, G' is the semidirect product of N and H, i.e. $H \simeq G'/N$.*

Theorem 6.2. *Conversely, the necessary condition for a subgroup G' to be derivable from another group by contraction is the existence on G' of an Abelian invariant subgroup N and a subgroup H, such that G' is the semidirect product of them.*

Going back to the contraction of the Lorentz group, we define new generators as follows:

$$\begin{aligned} J_i' &= J_i, \\ K_i' &= \epsilon K_i = \frac{1}{c} K_i. \end{aligned} \tag{6.15}$$

Hence, the Lorentz algebra for the primed variables becomes

$$
\begin{aligned}
[J'_i, J'_j] &= i\varepsilon_{ijk} J'_k, \\
[J'_i, K'_j] &= \frac{1}{c} i\varepsilon_{ijk} K_k = i\varepsilon_{ijk} K'_k, \\
[K'_i, K'_j] &= -\frac{1}{c^2} i\varepsilon_{ijk} J'_k \overset{c\to\infty}{\longrightarrow} 0,
\end{aligned} \tag{6.16}
$$

which is exactly the Galilean algebra. According to this prescription, one obtains rigorously the Galilean algebra from the Lorentz algebra by contracting the boosts.

6.3.2 The Non-relativistic SUSY Algebra

In this subsection, we employ the İnönü-Wigner contraction to derive the non-relativistic Galilean algebra, following the discussion in [10]. We start by defining the SUSY-extended Poincaré algebra

$$
\begin{aligned}
[P^\mu, P^\nu] &= 0, \\
\frac{1}{i}[J^{\mu\nu}, P^\lambda] &= \eta^{\mu\lambda} P^\nu - \eta^{\nu\lambda} P^\mu, && (6.17)\\
\frac{1}{i}[J^{\mu\nu}, J^{\lambda\rho}] &= \eta^{\mu\lambda} J^{\nu\rho} - \eta^{\mu\rho} J^{\nu\lambda} + \eta^{\nu\rho} J^{\mu\lambda} - \eta^{\nu\lambda} J^{\mu\rho}, && (6.18)\\
\{Q_\alpha, \bar{Q}_{\dot{\alpha}}\} &= 2\sigma^\mu_{\alpha\dot{\alpha}} P_\mu, && (6.19)\\
\frac{1}{i}[J^{\mu\nu}, Q_\alpha] &= -\sigma^{\mu\nu\beta}_\alpha Q_\beta, && (6.20)\\
\frac{1}{i}[J^{\mu\nu}, \bar{Q}^{\dot{\alpha}}] &= -\bar{\sigma}^{\mu\nu\dot{\alpha}}_{\dot{\beta}} \bar{Q}^{\dot{\beta}}, && (6.21)\\
[P^\mu, Q_\alpha] &= 0 = [P^\mu, \bar{Q}_{\dot{\alpha}}], && (6.22)\\
\{Q_\alpha, Q_\beta\} &= 0 = \{\bar{Q}_{\dot{\alpha}}, \bar{Q}_{\dot{\beta}}\}, && (6.23)
\end{aligned}
$$

where Q_α and $\bar{Q}_{\dot{\alpha}}$ are the fermionic generators of SUSY and we follow strictly [57] for our conventions. To perform the İnönü-Wigner contraction explicitly, we use the relativistic energy momentum relation and the boost contraction from the previous section, defining

$$
\begin{aligned}
P^0 &= \frac{1}{c}(Mc^2 + H), && (6.24)\\
J^{0i} &= cK'_i, && (6.25)\\
Q_\alpha &= \sqrt{c} Q'_\alpha, && (6.26)\\
\bar{Q}_{\dot{\alpha}} &= \sqrt{c} \bar{Q}'_{\dot{\alpha}}. && (6.27)
\end{aligned}
$$

The scaling of the SUSY generators $Q_{\dot{\alpha}},\ Q_\alpha$ follows from (6.24) and (6.19) and the condition to obtain a non-trivial anticommutator for the SUSY generators in the non-relativistic limit.

Taking now the limit $c \to \infty$, and dropping the primes for simplicity yields [10] the

expected Galilean algebra:

$$\begin{aligned}
[H, P_i] = 0, \quad [H, K_i] = iP_i, \quad [H, J_{ij}] = 0, \\
[H, M] = 0, \quad [P_i, P_j] = 0, \quad [P_i, K_j] = i\delta_{ij}M, \\
[P_i, M] = 0, \quad [J_{ij}, M] = 0, \quad [K_i, M] = 0, \\
[J_{ij}, P_k] = i(\delta_{ik}P_j - \delta_{jk}P_i), \\
[J_{ij}, K_k] = i(\delta_{ik}K_j - \delta_{jk}K_i), \\
[J_{ij}, J_{kl}] = i(\delta_{ik}J_{jl} - \delta_{il}J_{jk} + \delta_{jl}J_{ik} - \delta_{jk}J_{il}), \\
[K_i, K_j] = 0.
\end{aligned} \tag{6.28}$$

together with its SUSY extension:

$$\{Q_\alpha, \bar{Q}_{\dot{\alpha}}\} = -2\sigma^0_{\alpha\dot{\alpha}}M, \tag{6.29}$$

$$\begin{aligned}
\{Q_\alpha, Q_\beta\} = 0 = \{\bar{Q}_{\dot{\alpha}}, \bar{Q}_{\dot{\beta}}\}, \\
[Q_\alpha, H] = 0 = [\bar{Q}_{\dot{\alpha}}, H], \\
[Q_\alpha, M] = 0 = [\bar{Q}_{\dot{\alpha}}, M], \\
[Q_\alpha, P_i] = 0 = [\bar{Q}_{\dot{\alpha}}, P_i], \\
[Q_\alpha, K_i] = 0 = [\bar{Q}_{\dot{\alpha}}, K_i], \\
[J_{ij}, Q_\alpha] = -i(\sigma^{ij})^\beta_\alpha Q_\beta, \\
[J_{ij}, \bar{Q}^{\dot{\alpha}}] = -i(\bar{\sigma}^{ij})^{\dot{\alpha}}_{\dot{\beta}}\bar{Q}^{\dot{\beta}}.
\end{aligned} \tag{6.30}$$

As noted in [10], non-relativistic SUSY decouples from spacetime, in contrast to its relativistic counterpart, as can be directly seen from (6.29). Therefore, it behaves much more like an internal symmetry of the system. We shall discuss the consequences of this fact for SUSY breaking is a subsequent section.

Another interesting fact that follows from (6.29) is that the only Pauli matrix present is $\sigma^0 = -\mathbb{1}_{2\times 2}$. This will be reflected in the spacetime translations and will be the reason for the rigidity to perturbation theory of the Grassmann part of the propagator.

6.4 Superfield Description

In this section we derive the superfield formalism necessary to describe the supersymmetric Bose-Fermi mixture. From now on, we shall refer to non-relativistic SUSY simply as SUSY. Following [10] and the discussion in [57], we define the SUSY covariant derivatives as follows:

$$\begin{aligned}
D_\alpha &= \frac{\partial}{\partial\theta^\alpha} + m\sigma^0_{\alpha\dot{\alpha}}\bar{\theta}_{\dot{\alpha}}, \\
\bar{D}_{\dot{\alpha}} &= -\frac{\partial}{\partial\bar{\theta}^{\dot{\alpha}}} - m\theta^\alpha\sigma^0_{\alpha\dot{\alpha}}.
\end{aligned} \tag{6.31}$$

Here $\theta = (\theta_1, \theta_2)$ and $\bar{\theta} = (\bar{\theta}_1, \bar{\theta}_2)$ are tuples of independent Grassmann variables. They define what is sometimes referred to as a quantum dimension. As in the relativistic setup, these definitions yield the anticommutators

$$\begin{aligned}
\{D_\alpha, \bar{D}_{\dot{\alpha}}\} = -2m\sigma^0_{\alpha\dot{\alpha}}, \\
\{D_\alpha, D_\beta\} = 0 = \{\bar{D}_{\dot{\alpha}}, \bar{D}_{\dot{\beta}}\}.
\end{aligned} \tag{6.32}$$

An (anti-) chiral superfield ϕ is defined as a solution of the equation $\bar{D}_{\dot{\alpha}}\phi(\vec{x},t,\theta,\bar{\theta}) = 0$ (or $D_\alpha\bar{\phi}(\vec{x},t,\theta,\bar{\theta}) = 0$, respectively). The most general (anti-) chiral superfield is then constructed in the usual way by first solving the above equation in a reference frame, where ϕ is independent of $\bar{\theta}$, and then 'rotating' back:

$$\begin{aligned}\phi(\vec{x},t,\theta,\bar{\theta}) &= e^{m\theta\sigma^0\bar{\theta}}\left(\frac{1}{m}A(\vec{x},t) + \sqrt{\frac{2}{m}}\bar{\theta}^\alpha\psi_\alpha(\vec{x},t) + \theta^2 B(\vec{x},t)\right),\\ \bar{\phi}(\vec{x},t,\theta,\bar{\theta}) &= e^{m\theta\sigma^0\bar{\theta}}\left(\frac{1}{m}A^\dagger(\vec{x},t) + \sqrt{\frac{2}{m}}\bar{\theta}_{\dot{\alpha}}\bar{\psi}^{\dot{\alpha}}(\vec{x},t) + \bar{\theta}^2 B^\dagger(\vec{x},t)\right),\end{aligned} \tag{6.33}$$

where A, and B are bosonic fields and ψ_α is the fermion field of either spin up or down. The mass-dependent pre-factors are chosen such that the model corresponds to the standard conventions in many-body theory. Similar to many-body theory, the fields $A^\dagger$ and $B^\dagger$ create bosons of two different types (spins), while $\bar{\psi}_{\dot{\alpha}}$ creates a spin-1/2 fermion of spin $\dot{\alpha}$. As pointed out in [10], unlike non-relativistic SUSY, both bosonic fields A and B are dynamical, and so is the fermion field.

The canonical commutator relations of the superfields take the form

$$\begin{aligned}\delta(t_1-t_2)[\phi(1),\bar{\phi}(2)] &= \delta^{(4)}(x_1-x_2)\frac{1}{m^2}e^{2m\theta_1\sigma^0\bar{\theta}_2+m\theta_1\sigma^0\bar{\theta}_1+m\theta_2\sigma^0\bar{\theta}_2},\\ \delta(t_1-t_2)[\phi(1),\phi(2)] &= 0 = \delta(t_1-t_2)[\bar{\phi}(1),\bar{\phi}(2)],\end{aligned} \tag{6.34}$$

where we used the short-hand notation $1 = (\vec{x}_1, t_1, \theta_1, \bar{\theta}_1)$. The normalization of the above commutators is adopted to assure for the usual many-body conventions.

We are now in a position to write the BF mixture Hamiltonian in a manifestly supersymmetric form:

$$\begin{aligned}H &= H_0 + H_{\text{int}},\\ H_0 &= \int \mathrm{d}^3x\mathrm{d}^2\theta\mathrm{d}^2\bar{\theta}\frac{1}{2m}\nabla\bar{\phi}(\vec{x},\theta,\bar{\theta})\cdot\nabla\phi(\vec{x},\theta,\bar{\theta}) + \frac{\mu}{2m}\int \mathrm{d}^3x\mathrm{d}^2\theta\mathrm{d}^2\bar{\theta}\bar{\phi}(\vec{x},\theta,\bar{\theta})\phi(\vec{x},\theta,\bar{\theta}),\\ H_{\text{int}} &= \frac{1}{2}\int \mathrm{d}^3x\mathrm{d}^2\theta\mathrm{d}^2\bar{\theta}\mathrm{d}^3x'\mathrm{d}^2\theta'\mathrm{d}^2\bar{\theta}'\bar{\phi}(\vec{x},\theta,\bar{\theta})\bar{\phi}(\vec{x}',\theta',\bar{\theta}')V(\vec{x};\vec{x}')\phi(\vec{x}',\theta',\bar{\theta}')\phi(\vec{x},\theta,\bar{\theta}),\end{aligned} \tag{6.35}$$

with $V(\vec{x};\vec{x}') = g\delta^{(4)}(x-x')$ for some interaction strength g. Note that the potential is not a delta function of the Grassmann variables. Doing the integrals over the Grassmann variables results in the usual many-body Hamiltonian (6.3) for the four fields A, B, and ψ_α, as can be seen from Appendix C.1.

It is noteworthy that we use a different convention for the interaction term in the Hamiltonian (6.3) compared to [10], whose interaction part is not normal-ordered. However, we shall need the normal ordering to apply Wick's theorem in the next chapter, when we compute the corrections to the propagator within perturbation theory.

6.5 Propagator and Diagrammatics

In this section we shall explore the diagrammatics of the SUSY Hamiltonian and derive the Feynman rules for the SUSY Bose-Fermi mixture. It is through this that the superfield

description becomes useful, and provides not only a better book-keeping opportunity but also a better insight into the physics of the system.

We begin by writing the action of the theory S as a sum of a quadratic, and interaction terms:

$$\begin{aligned} S &= S_0 + S_{\text{int}}, \\ S_0 &= \int \mathrm{d}1 \bar{\phi}(1) \left(i\partial_t + \frac{1}{2m}\nabla^2 - \mu \right) \phi(1), \\ S_{\text{int}} &= \frac{1}{2} \int \mathrm{d}1\mathrm{d}2 \bar{\phi}(1)\bar{\phi}(2) V(1-2)\phi(2)\phi(1), \end{aligned} \tag{6.36}$$

with $V(1-2) = g\delta^{(4)}(x_1 - x_2)$. The position in which the fields appear in the interaction term is important, to correctly reproduce the well-known Hamiltonian (6.3). In the following, no additional sign changes are induces, since the superfield is bosonic, and hence no additional sign change will be induced upon pairing using Wick's theorem.

Following the derivation in [10], we recall that the free propagator can be derived using standard field-theoretical techniques. Due to translational invariance using a momentum-space representation is advantageous. It should be mentioned, however, that there is no analogue of this for the Grassmann variables, and hence they should be kept as they are. Therefore, we use the short-hand notation Ω_i which stands for $(\theta_i, \bar{\theta}_i)$. This fact will be confirmed by the form of the Green's function itself:

$$G^{(0)}(\vec{k}, \omega, \Omega_1, \Omega_2) = -\frac{1}{m^2} \frac{\exp\left(-2m\theta_2\sigma_0\bar{\theta}_1 + m\theta_1\sigma_0\bar{\theta}_2 + m\theta_2\sigma_0\bar{\theta}_2\right)}{\omega - \varepsilon_k - \mu}, \tag{6.37}$$

which does not depend on the differences $\theta_1 - \theta_2$ explicitly. It follows also from (6.37) that both species must obey the same dispersion relation ε_k, and the chemical potentials need to obey the specific relation (6.4), asserted in the end of the introductory Chapter 6.2.

The corrections to $G^{(0)}$ for small coupling constants g are derived using perturbation theory. Due to the structure of S_{int}, we can immediately adopt the standard diagrammatics scheme from many-body physics [17]. As mentioned above, the momentum-space representation is at first sight not good enough, due to the presence of the Grassmann variables. Therefore, in superspace the vertices in the Feynman diagrams will be labelled by integer numbers $1, 2, 3, ...$, such that $1 = (t_1, \vec{x}_1, \Omega_1)$.

Let us first take a look at the first order correction to the propagator, given by the Hartree and Fock diagrams:

$$\begin{aligned} G^{(1)}(1,2) = &\int \mathrm{d}1'\mathrm{d}2' G^{(0)}(1',1) G^{(0)}(2,1') G^{(0)}(2',2') V(1'-2') \\ &+ \int \mathrm{d}1'\mathrm{d}2' G^{(0)}(1',1) G^{(0)}(2',1') G^{(0)}(2,2') V(1'-2'). \end{aligned} \tag{6.38}$$

If we consider the tadpole only, notice that in $G(2',2')$ the exponent vanishes identically. Therefore, we have (c.f. Fig. 6.1):

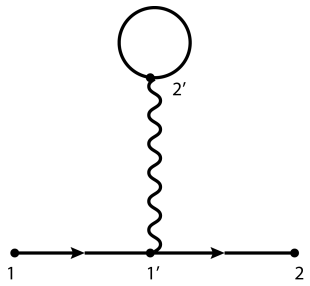

$$= \int d\Omega_2' G^{(0)}(k, \omega, \Omega_2', \Omega_2') \sim \int d\Omega_2' = 0$$

Figure 6.1: The Hartree first-order correction to the SUSY propagator vanishes due to quantum statistics.

This result is expected also without employing a SUSY description, since there would be four tadpole diagrams in the standard many-body perturbation theory to first order: two for the bosons, and two for the fermions. However, the latter two add up with a negative sign because of the sign change needed for a fermionic loop, and hence the cancellation. In this first occasion, we encounter the elegance of the SUSY approach.

The absence of tadpoles or fermionic loops in the theory is a general feature to every order in perturbation theory. This is a tremendous simplification, since, e.g. in second order only three out of the standard ten diagrams survive. They are given pictorially in Fig. 6.2.

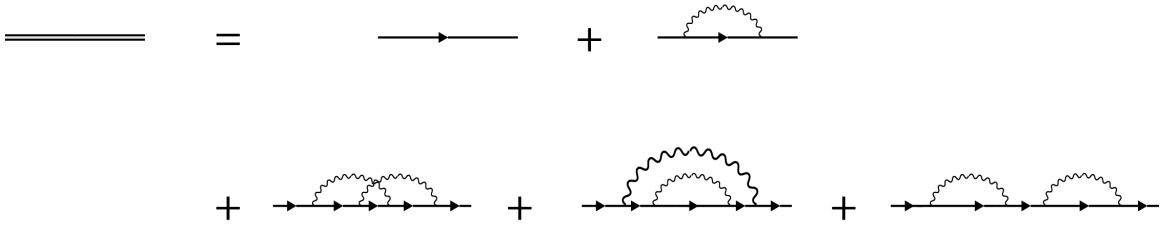

Figure 6.2

It is interesting to take a look at the only non-vanishing first-order diagram of Eq. (6.38). While the full calculation is given in Appendix C.2, here we discuss directly the result.

$$\begin{aligned} &\int \mathrm{d}1'\mathrm{d}2' G^{(0)}(1',1) G^{(0)}(2',1') G^{(0)}(2,2') V(1'-2') \\ &= F(\Omega_1, \Omega_2; m) g \int \frac{\mathrm{d}^3 k \mathrm{d}\omega}{(2\pi)^4} e^{ik(x_1 - x_2)} \left(\frac{1}{\omega - \varepsilon_k - \mu} \right)^2 \int \frac{\mathrm{d}^3 q \mathrm{d}\nu}{(2\pi)^4} \frac{1}{\nu - \varepsilon_q - \mu}. \end{aligned} \tag{6.39}$$

Mimicking the free propagator, the correction also factorizes in a purely Grassmann and a purely space-time part. The astonishing result is, however, that the factor $F(\Omega_1, \Omega_2; m)$ appears to be the same as for the free propagator, surviving the integration over the Grassmann variables:

$$F(\Omega_1, \Omega_2; m) = \exp\left(-2m\theta_2\sigma_0\bar{\theta}_1 + m\theta_1\sigma_0\bar{\theta}_2 + m\theta_2\sigma_0\bar{\theta}_2\right). \tag{6.40}$$

It obeys the remarkable *'robustness'* identity

$$\int \mathrm{d}\Omega_1' \Omega_2' F(\Omega_1, \Omega_1'; m) F(\Omega_1', \Omega_2'; m) F(\Omega_2', \Omega_2; m) = F(\Omega_1, \Omega_2; m), \tag{6.41}$$

which is derived also in Appendix C.2. Interestingly, it holds to any order in perturbation theory, which can be easily seen due to the fact the the propagator line is directed and always traverses the whole diagram, since the superfield cannot be created, nor annihilated in favour of an interaction line. A heuristic argument for this can be given as follows. In the second-order diagrams, Fig. 6.3, the last one reduces to two first-order ones, for which the above relation holds separately. In diagrams containing interaction lines of the type as in the middle one in Fig. 6.3, a systematic approach would be to begin with the innermost vertices and do the Grassmann integrals successively outwards. The situation is least obvious for the crossed diagrams on the left, which we explicitly show here using (6.41):

$$\begin{aligned}
&\int \mathrm{d}\Omega_1'\mathrm{d}\Omega_2'\mathrm{d}\Omega_3'\mathrm{d}\Omega_4' F(\Omega_1,\Omega_1';m)F(\Omega_1',\Omega_2';m)F(\Omega_2',\Omega_3';m)F(\Omega_3',\Omega_4';m)F(\Omega_4',\Omega_2;m)\\
&= \int \mathrm{d}\Omega_3'\mathrm{d}\Omega_4' F(\Omega_1,\Omega_3';m)F(\Omega_3',\Omega_4';m)F(\Omega_4',\Omega_2;m)\\
&= F(\Omega_1,\Omega_2;m). \qquad (6.42)
\end{aligned}$$

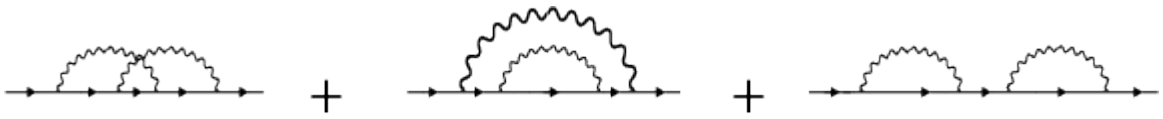

Figure 6.3

The physical meaning of (6.41) appears to be hidden in the philosophy of Supersymmetry itself. If we expand the free propagator in components according to the Grassmann variables $(1,\ \theta_1,\ \bar{\theta}_1,\ldots,\Omega_2^2)$ we will see that breaking SUSY, e.g. by varying the chemical potentials, the different non-vanishing components in the expansion give the propagators for the different fields [57]. In other words, the expansion in Grassmann variables incorporates the relation of the propagators of the different species to one another. Now, if a theory is supposed to be supersymmetric, then exchanging either two fields should not affect the physics. The 'robustness' identity shows that the relations between the propagators are conserved to all orders in perturbation theory, which is another manifestation of SUSY.

Towards the end of this section, we come to a very interesting consequence of equation (6.39). It appears to be the key to a reformulation of the theory. If we neglect for a moment the F pre-factor, we recover under the integrals the momentum-space propagator of a time-dependent bosonic φ^4-theory (cf. Fig. 6.4). This is not completely unexpected, since the interaction was chosen to be a contact one and of the same type between the fields. Taking into account our previous discussion, however, it follows that we can write down an exact φ^4-theory to describe the entire BF mixture, as the coupling between the propagators is given by multiplying the φ^4-propagator by the factor F. Apparently, SUSY is restrictive enough, so that even in the non-relativistic case, the degrees of freedom of the theory, consisting initially of four complex independent fields, can be reduced to an effective φ^4-theory theory for a single scalar field φ. It should be mentioned that this is possible exclusively due to the contact nature of the various interactions considered.

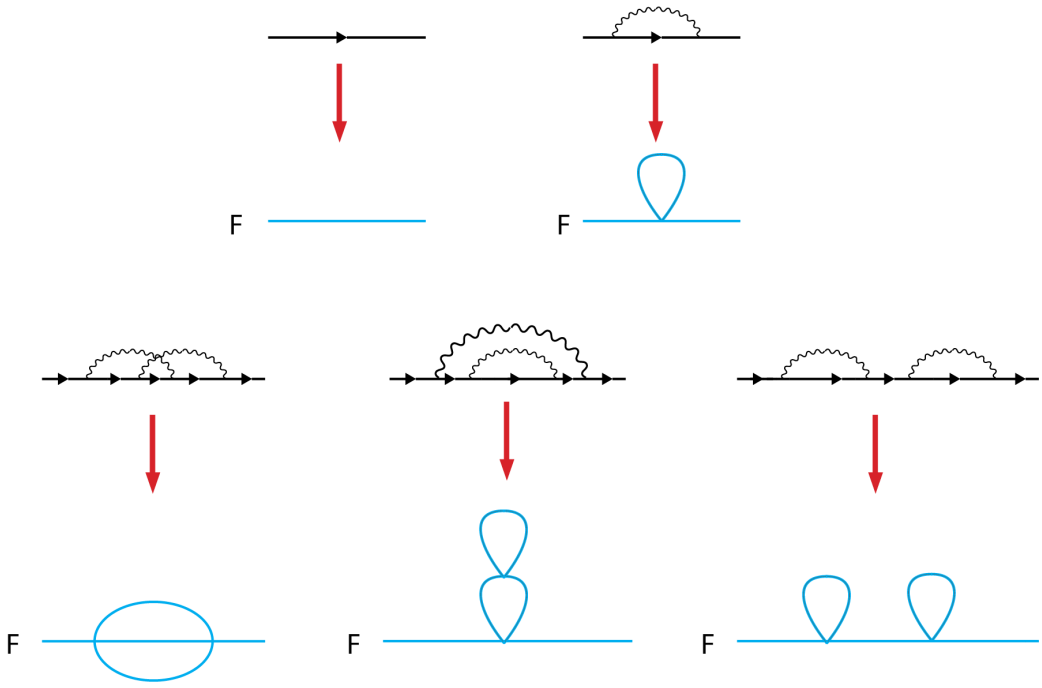

Figure 6.4: Pictorial derivation of the effective φ^4-theory.

6.6 SUSY Breaking

It was proven in [10] that due to the different nature of the particle statistics, the ground state of the supersymmetric many-body theory does not enjoy a SUSY. This can be understood intuitively, since any two fermions can never be in the same quantum state due to the Pauli principle (Spin Statistics Theorem)., while the bosons are expected to condense Hence, exchanging a fermion with a boson does not leave the lowest energy state invariant, and thus SUSY is broken in the ground state.

However, at high enough temperature, the quantum degeneracy of the particles is not present, and the ground state of the system may display SUSY. It is through the excitations modes that the remnants of a broken SUSY can be detected.

In this short section we discuss the hard-core SUSY breaking and derive perturbative expressions for the Green's function in the vicinity of the supersymmetric point. As was discussed previously near Eq. (6.37), in order the theory to be supersymmetric, bosons and fermions have to exhibit the same dispersion and chemical potential, and the interaction constants have to be in precise relation to one another.

Although in practice the φ^4-theory is not exactly solvable, its propagator can be calculated and renormalized by virtue of standard procedures to any arbitrary order in perturbation theory [31]. Therefore, in the following we shall assume that it is known exactly.

Here, we propose two ways of explicitly breaking SUSY in this model: this can be achieved by adding to the chemical potential for the bosonic field A a small perturbation $\tilde{\mu}$. The perturbation term reads

$$\tilde{\mu}A^\dagger A = \tilde{\mu}\int \mathrm{d}^2\theta \mathrm{d}^2\bar{\theta} m^2 \theta^2 \bar{\theta}^2 \bar{\phi}\phi. \tag{6.43}$$

The factor m^2 is necessary for the correct normalization, according to the definition of the

field ϕ. The above equation allows us to treat the perturbation in superspace. As we assumed that we can calculate the propagator for the SUSY theory to any order in perturbation theory exactly, Eq. (6.43) provides a way to obtain the corrections to the SUSY Green's function using standard perturbation theory and diagrammatic techniques (see, e.g. [17]). The corresponding Feynman rules would involve a factor of $m^2\theta^2\bar{\theta}^2$ for every vertex in superspace.

The second way of SUSY breaking is by adding a small constant λ to the interaction between, e.g. the A fields. This results in

$$\frac{\lambda}{2}\int \mathrm{d}^3x A^\dagger A^\dagger AA = \frac{1}{2}\int \mathrm{d}^3x_1\mathrm{d}^3x_2\mathrm{d}\Omega\mathrm{d}\bar{\Omega}m^2\theta_1^2\bar{\theta}_1^2\theta_2^2\bar{\theta}_2^2\bar{\phi}_1\bar{\phi}_2U(1-2)\phi_2\phi_1, \tag{6.44}$$

with $U(1-2) = \lambda\delta^{(3)}(\vec{x}_1 - \vec{x}_2)$. In this form, standard many-body perturbation theory also directly applies. This time, however, for every interaction vertex of the perturbation, one must account for a factor $m^2\theta_1^2\bar{\theta}_1^2\theta_2^2\bar{\theta}_2^2$, which will spoil the 'robustness' of the phase factor F discussed in the previous chapter, as is expected for a non-supersymmetric theory.

6.7 Conclusion

I summary, we have derived a supersymmetric ϕ^4-theory for the spinful Bose-Fermi mixture, under suitable conditions on the chemical potentials and the interaction constants. This allowed for a manifestly SUSY description using chiral superfields ϕ which, not only serves as a useful book-keeping tool for the zoo of Feynman diagrams present in the model, but also incorporates the symmetries due to quantum statistics.

We derived the Feynman rules in superspace, using standard many-body perturbation theory in the weak-coupling limit, proving the expected cancellation of all the tadpole diagrams. As a consequence, the number of diagrams to any order in the coupling constant in a SUSY field theory is reduced significantly.

Analyzing further the properties of the propagator in superspace, we found that its Grassmann part remains rigid to any order in perturbation theory, satisfying what we called the 'robustness' identity. Taken together with the contact nature of the interactions assumed throughout, this allows to write down an effective single-field bosonic φ^4-theory for the space-time part of the superfield propagator.

We also developed perturbation theory in the chemical potential and the contact interaction strength around the SUSY point, given by Eq. (6.4), in the superfield formalism, assuming the φ^4-propagator is known. This approach enables the description of systems not exhibiting an exact, but only an approximate supersymmetry.

Appendix A

Generalized Bogoliubov Transformations

In this Appendix, we generalize the concept of bosonic Bogoliubov transformations to Hamiltonians of matrix dimensions higher than two. Although this is in principle possible with the method of [4], the recipe we provide at the end of this Appendix allows to circumvent pages of unnecessary and lengthy algebra.

A very similar approach to the one discussed here was presented in Appendix B of [27]. However, it misses the precise conditions under which such a generalized Bogoliubov transformation exists, and a sloppy straightforward application of the procedure in [27] may often lead to inconsistent results. Nevertheless, it was the true inspiration for the work outlined below.

A.1 Motivation

Bogoliubov transformations are used widely in condensed matter theory to cast a quadratic Hamiltonian into the form $H = \sum_k \gamma_k^\dagger \gamma_k + const$, which is usually referred to as *diagonal*, since one can readily read out the corresponding dispersion or band structure. The crucial condition on transformation is to preserve quantum statistics (i.e. be canonical), so the new operators also obey bosonic (fermionic) commutation relations. The transformation itself is needed in subsequent computations of any physical quantities of interest, such as the total particle number, the ground state energy, the order parameter, etc.

To set up the stage, consider the following most general quadratic Hamiltonian in second quantized form.

$$\mathbf{H} = \sum_k \vec{a}_k^\dagger H_k \vec{a}_k = \sum_{\mu,\nu,k} a_{\mu,k}^\dagger H_k^{\mu\nu} a_{\nu,k}. \tag{A.1}$$

where the creation and destruction operators $\vec{a}_k = (a_{1,k}, \ldots, a_{n,k}, a_{n+1,k}^\dagger, \ldots, a_{m,k}^\dagger)^t$ and $\vec{a}_k^\dagger = (a_{1,k}^\dagger, \ldots, a_{n,k}^\dagger, a_{n+1,k}, \ldots, a_{m,k})$ obey either bosonic or fermionic commutation relations. The matrix $H_k = H_k^\dagger$ is necessarily Hermitian.[1] A quantum field theoretical description requires a collection of infinitely many independent modes a_k to model the excitations of a single field and, therefore, a summation is imposed over the mode index k. In contrast, independent

[1] Note that we use the bold-face letter $\mathbf{H}$ to denote the Hamiltonian while for the corresponding matrix we use H_k.

fields are represented by another index which, when used explicitly, shall be denoted by a Greek letter μ.

The goal of this section is to give a recipe to construct the generalized Bogoliubov transformation which puts **H** in a diagonal form, and renders the system solved giving its spectrum. Since this must be done for each mode index k independently, from now on, we are not interested in the summation over k. Therefore, we drop the index k and assume Einstein summation convention for the Greek indices, whenever they appear. It should be emphasized that the transformation itself and the resulting diagonal matrix *do* depend on k. In other words, we seek a matrix $M_{(k)}$, such that

$$\vec{a}^\dagger H \vec{a} = \vec{\gamma}^\dagger \underbrace{M^\dagger H M}_{=D} \vec{\gamma} = \vec{\gamma}^\dagger D \vec{\gamma} \tag{A.2}$$

with D some diagonal matrix, and $\vec{a} = M\vec{\gamma}$. The new operators $\vec{\gamma}$ are then given by $\vec{\gamma}_k = (\gamma_{1,k}, \ldots, \gamma_{n,k}, \gamma^\dagger_{n+1,k}, \ldots, \gamma^\dagger_{m,k})^t$. The canonical commutation relations for the initial set of operators can be cast into matrix form by considering

$$\begin{aligned}
(\vec{a}\vec{a}^\dagger)^t \pm (\vec{a}^\dagger)^t(\vec{a})^t &= \left[\begin{pmatrix} a_1 \\ \vdots \\ a_m^\dagger \end{pmatrix} (a_1^\dagger, \ldots, a_m)\right]^t \pm \left[\begin{pmatrix} a_1^\dagger \\ \vdots \\ a_m \end{pmatrix} (a_1, \ldots, a_m^\dagger)\right] \\
\begin{pmatrix} [a_1, a_1^\dagger]_\xi & \ldots & [a_m^\dagger, a_1^\dagger]_\xi \\ \vdots & \ddots & \vdots \\ a_1, a_m]_\xi & \ldots & [a_m^\dagger, a_m]_\xi \end{pmatrix} &= \begin{cases} \begin{pmatrix} \mathbb{1}_{n\times n} & 0 \\ 0 & \mathbb{1}_{m\times m} \end{pmatrix} = \mathbb{1}, & \text{fermions} \\ \begin{pmatrix} \mathbb{1}_{n\times n} & 0 \\ 0 & -\mathbb{1}_{m\times m} \end{pmatrix} =: \Sigma, & \text{bosons} \end{cases}
\end{aligned} \tag{A.3}$$

with $\xi = \pm$ for fermions/bosons, respectively. The off-diagonal elements all vanish, as the different types of oscillators are assumed independent. The above equation imposes a constraint on the transformation M to obey the canonical commutation relations in the following way:

$$MM^\dagger = \mathbb{1} \quad \text{for fermions,} \quad \text{and} \quad M\Sigma M^\dagger = \Sigma \quad \text{for bosons.} \tag{A.4}$$

These two relations define the unitary group $U(n+m)$ and the pseudo-unitary group $U(n|m)$, respectively. Moreover, in both cases it follows that M is an invertible transformation.

The standard textbook analysis is very often limited to diagonalizing quadratic Hamiltonians mixing only two independent harmonic oscillators described by a_1 and a_2. In this case, the Bogoliubov transformation is given by a 2×2 matrix which can be parametrized by a single angle θ.[2] For a symmetric H in the fermionic case, this matrix is the usual rotation matrix, while for bosons, one needs a hyperbolic rotation:

$$M^{\mathrm{f}} = \begin{pmatrix} \cos\theta & -\sin\theta \\ \sin\theta & \cos\theta \end{pmatrix}, \qquad M^{\mathrm{b}} = \begin{pmatrix} \cosh\theta & \sinh\theta \\ \sinh\theta & \cosh\theta \end{pmatrix} \tag{A.5}$$

Clearly, for fermions we have $M^{\mathrm{f}} \in U(2)$, while for bosons $M^{\mathrm{b}} \in U(1|1)$.

There are many reasons why generalizing such a transformation to matrix dimensions higher than two can be useful. One can consider, for instance, a mixture of different types of bosons (fermions) that are quadratically coupled to each other. The bosonic case includes

[2] θ will in general depend on the mode index k, too

the usual Bogoliubov approximation as the standard description of superfluidity in weakly interacting bosonic systems, or bosons in the presence of a staggered potential. Fermionic cases include various mean-field analyses such as CDW, SDW, BCS-theory, back scattering, fermions in a staggered potential, and many more. However, if one is interested in realizing a description in which more than one of these interaction types occur simultaneously, as in the case of a supersolid or any other more complex phases of matter, the dimension of the matrix H grows, and finding the proper transformation becomes much more involved, especially for bosons, where a straightforward parametrization in terms of angles becomes quite complicated.

A.2 Fermionic Bogoliubov Transformations

The fermionic case is straightforward and shall be revisited briefly in this section. We shall use the transformation to diagonalize two different types of Hamiltonians (in *matrix dimension* $D = 2$) and discuss the physical meaning of that procedure.

To begin with, let us define the problem precisely:

Given a Hermitian matrix $H = H^\dagger$ in $n + m$ dimensions, find a transformation M, such that $M^\dagger H M = D$ is diagonal, and $MM^\dagger = \mathbb{1}$.

The existence and uniqueness (up to a permutation of the eigenvalues in the non-degenerate case) of the transformation are guaranteed by the spectral theorem for self-adjoint matrices which asserts that every Hermitian matrix can be diagonalized by a unitary transformation. The columns of M then contain the properly normalized eigenvectors (w.r.t. the standard scalar product in $\mathbb{C}^{n+m}$):[3]

Theorem A.1 (Spectral Theorem)**.** *Given a Hermitian, $(n+m)\times(n+m)$ matrix H, there exists a (unique)[4] unitary transformation $M \in U(n+m)$, such that $M^\dagger H M = D$, with D diagonal and $MM^\dagger = \mathbb{1}$.*

To bring out the physical meaning of the transformation, let us take a look at two different ways of mixing the fermionic operators that can occur in $D = 2$. Consider first, for fermionic operators c_σ, a Hamiltonian given by

$$\mathbf{H} = \sum_k (c^\dagger_{k,\uparrow}, c_{-k,\downarrow}) \begin{pmatrix} \varepsilon_k & \Delta \\ \Delta & -\varepsilon_k \end{pmatrix} \begin{pmatrix} c_{k,\uparrow} \\ c^\dagger_{-k,\downarrow} \end{pmatrix} + \varepsilon_k, \tag{A.6}$$

with $\varepsilon_k = \varepsilon_{-k}$ the corresponding dispersion relation and Δ being the gap.[5] It appears naturally in the BCS theory of (s-wave) superconductivity. Using the transformation M^{f} from (A.5) one arrives at the following diagonal form:

$$\mathbf{H} = \sum_k E_k \left(\gamma^\dagger_{1,k}\gamma_{1,k} - \gamma_{2,k}\gamma^\dagger_{2,k}\right) + \varepsilon_k = \sum_k E_k \left(\gamma^\dagger_{1,k}\gamma_{1,k} + \gamma^\dagger_{2,k}\gamma_{2,k}\right) + \sum_k \varepsilon_k - E_k, \tag{A.7}$$

[3] This should be better viewed as a normalization w.r.t. the sesquilinear quadratic form $\mathbb{1}$ from the RHS of Eq. (A.3).

[4] up to reshuffling of the columns in the non-degenerate case

[5] We assume a real gap function $\Delta = \Delta^*$ here for simplicity.

with $E_k = \sqrt{\varepsilon_k^2 + \Delta^2}$. Notice the form of the new operator $\vec{\gamma} = (\gamma_1^\dagger, \gamma_2)^t$. That we chose to call the second entry γ_2 and not $\gamma_2^\dagger$ is, of course, a convention, since the commutation relations for fermions would be satisfied either way.[6] One reason why this is the correct choice is given by time-reversal symmetry: in BCS theory the latter requires flipping the sign of the (22)-component of H which is naturally achieved by the above choice.

Another advantage of this choice can be seen if one takes a look at the way the initial vacuum state transforms. Assuming a lattice model which results in a tight-binding dispersion $\varepsilon_k = -2t\sum_j \cos(k_j)$, the vacuum for the $c_{k,\sigma}$ operators is given by the unique vector in Fock space annihilated by both $c_{k,\uparrow}$ and $c_{-k,\downarrow}$ which we denote by $|0\rangle_c$. At half-filling, the ground state of the system is given by $|GS\rangle = \prod_{|k|\leq k_F} c_{k,\uparrow}^\dagger c_{-k,\downarrow}^\dagger |0\rangle_c$. Since $\gamma_{1,k} = u_k c_{k,\uparrow} - v_k c_{-k,\downarrow}^\dagger$ for some u_k and v_k with $u_k^2 + v_k^2 = 1$ and $\gamma_{2,k} = v a_k^\dagger + u c_{-k}$, we have that both $\gamma_{1,k}$ and $\gamma_{2,k}$ annihilate $|GS\rangle$ for $|k| \leq k_F$. This would have not been the case, had we chosen the other convention. Hence we have managed to map the problem to that of free fermions with $|GS\rangle$ being the Fermi sea.

The last thing left to notice is that we have two distinct $\gamma_{k,\sigma}$ operators. The reason for this is that we started mixing fermions of *different* spin species. If we had a coupling of the type $a_k a_{-k}$ (as is the case of Bogoliubov phonons), we would have to choose $\vec{\gamma}_k = (\gamma_k, \gamma_{-k}^\dagger)^t$ with the same γ_k in both components.

The second example we consider is described by the Hamiltonian

$$\mathbf{H} = \sum_k (a_k^\dagger, c_k^\dagger) \begin{pmatrix} \varepsilon_k & g \\ g & -\varepsilon_k \end{pmatrix} \begin{pmatrix} a_k \\ c_k \end{pmatrix}. \tag{A.8}$$

It is encountered when one studies a fermionic system on a lattice under the influence of a staggered potential of magnitude g that alternates along the lattice in a checkerboard manner, [20]. This time, however, it is useful to adopt the other convention for the γ-operators: $\vec{\gamma} = (\gamma_1, \gamma_2)$, since there is no time-reversal symmetry to obey. In this example, a and c describe the same fermionic species. Therefore, at half-filling the ground state is such that the lowest band is completely filled. To be able to write it down, we need to diagonalize the Hamiltonian first, for otherwise we cannot know the exact bands. It can be formally defined as $|GS\rangle = \prod_{k\in \mathrm{BZ}'} \gamma_{1,k}^\dagger |0\rangle_\gamma$, with BZ' being the reduced Brillouin zone. Notice further that in this case we have $|0\rangle_{a,c} = |0\rangle_\gamma$ since γ_σ mix only annihilation operators.

This second way of quadratic coupling in H is fundamentally different than the first one in terms of the underlying physics. Here, instead of considering pairs of fermions, one uses the transformation to take into account the staggered potential by reducing the Brillouin zone or, equivalently, doubling the unit cell.

Had we chosen the other convention, i.e. $\vec{\gamma} = (\gamma_1, \gamma_2^\dagger)$, after bringing the Hamiltonian into normal-ordered form, the constant we would pick up along the way due to the commutator relations corresponds precisely to the GS energy. Hence, in this case the operators would create and destroy excitations, as was the case in the previous example.

A detailed description of how to diagonalize Hamiltonians in second quantized form is given in [20].

[6] This will not be the case for bosons, though!

A.3 Bosonic Bogoliubov Transformations

Bosonic systems require more effort to put in a diagonal form than fermionic ones. To see this, let us again first formulate the problem in a clear way:

Given a Hermitian matrix $H = H^\dagger$ in $n+m$ dimensions, find a transformation M, such that $M^\dagger H M = D$ is diagonal, and $M\Sigma M^\dagger = \Sigma$.

The difference to the bosonic case is the condition on M, which results from the commutation relations for bosons, Eq.(A.3). It requires that M belongs to the pseudo-unitary group $U(n|m)$. From a mathematical point of view, such a transformation need not exist in the first place. However, the fact that the problem comes from physics suggests that this might be the case. This subsection gives a rigorous mathematical proof for this, under physical conditions on H to be determined. Moreover, the proof is constructive, and hence a 'recipe' for constructing the transformation M could be extracted.

To understand what might go wrong from a physical point of view, let us try go write down a simple Hamiltonian that describes pairing of bosons and conserves the momentum:

$$\mathbf{H} = \sum_k 2\varepsilon_k b_k^\dagger b_k + V(b_k^\dagger b_{-k}^\dagger + b_k b_{-k}) = \sum_k \left(b_k^\dagger, b_{-k}\right) \begin{pmatrix} \varepsilon_k & V \\ V & \varepsilon_k \end{pmatrix} \begin{pmatrix} b_k \\ b_{-k}^\dagger \end{pmatrix} - \varepsilon_k. \tag{A.9}$$

Since the dimension of the corresponding matrix H is clearly two ($D = 2$), we can use a hyperbolic rotation to bring it in the desired diagonal form. This time, there is no choice of convention, and we are required to use a vector of the form $\vec{\gamma} = (\gamma_k, \gamma_k^\dagger)$ to obey the proper commutation relations. Notice that in this case, unlike the fermionic one, it is the same operator γ_k in the components of the new basis. The fermionic case is physically different, since there are two spin degrees of freedom (corresponding to the two fermionic species). Here, there is only one species of bosons, and hence only one type of operator γ_k. As discussed previously in the case of fermions, the new operators γ describe excitations (this time bosonic) above the ground state. The diagonal Hamiltonian reads

$$\mathbf{H} = \sum_k E_k(\gamma_k^\dagger \gamma_k + \gamma_k^\dagger \gamma_k) + E_k - \varepsilon_k, \tag{A.10}$$

with $E_k = \sqrt{\varepsilon_k^2 - V^2}$. We observe that this dispersion can potentially become imaginary. For example, if we choose to work with a one dimensional tight-binding model, we have $\varepsilon_k^2 = 4t^2 \cos^2 k \geq 0$, and in particular there are some k's for which the value 0 is taken. Hence, for these k there exists no $V \neq 0$, such that E_k is real. This is a contradiction to the fact that $M^\dagger H M$ is Hermitian for all k, since H itself is, whence D must necessarily have real diagonal entries.

The problem obviously comes from the fact that we omitted the chemical potential μ from the model. In the fermionic case, this did not have any effect, since one usually considers systems at half-filling where $\mu = E_F = 0$. For bosons, however, this negative number that is usually added to the dispersion relation does matter. Fixing μ then, in particular, allows all values of V and E_k remains real. Clearly, this is not the case for all possible V. The reason for this is that the bosonic system can be unstable, pretty much the same way as a system of coupled classical harmonic oscillators can happen to have imaginary eigenfrequencies for certain real values of the spring constants.

To find the condition, under which the bosonic system is stable, we first map the bosonic problem to the one of coupled QM oscillators. Consider a general Hermitian matrix H given by

$$H = \begin{pmatrix} M_1 & M_2 \\ M_2^\dagger & M_4 \end{pmatrix}, \tag{A.11}$$

with $M_1^\dagger = M_1$ and $M_4^\dagger = M_4$. We are interested in analyzing the stability of the Hamiltonian. To map it back to a system of coupled oscillators, we define

$$\vec{a}^\dagger = (a_1^\dagger, \ldots, a_n^\dagger), \qquad \text{and} \qquad \vec{b} = (a_{n+1}, \ldots, a_m), \tag{A.12}$$

and recall the definitions $\vec{a}^\dagger = \frac{1}{\sqrt{2}}(\vec{q}_1 - i\vec{p}_1)$ and $\vec{b} = \frac{1}{\sqrt{2}}(\vec{q}_2 + i\vec{p}_2)$. Then, we have

$$\begin{aligned}(\vec{a}^\dagger, \vec{b}) H \begin{pmatrix} \vec{a} \\ \vec{b}^\dagger \end{pmatrix} &= \frac{1}{2}(\vec{q}_1 - i\vec{p}_1, \vec{q}_2 + i\vec{p}_2) \begin{pmatrix} M_1 & M_2 \\ M_2^\dagger & M_4 \end{pmatrix} \begin{pmatrix} \vec{q}_1 + i\vec{p}_1 \\ \vec{q}_2 - i\vec{p}_2 \end{pmatrix} \\ &= \frac{1}{2}(\vec{p}_1, \vec{p}_2, \vec{q}_1, \vec{q}_2) \begin{pmatrix} -i & 0 \\ 0 & i \\ 1 & 0 \\ 0 & 1 \end{pmatrix} \begin{pmatrix} M_1 & M_2 \\ M_2^\dagger & M_4 \end{pmatrix} \begin{pmatrix} i & 0 & 1 & 0 \\ 0 & -i & 0 & 1 \end{pmatrix} \begin{pmatrix} \vec{q}_1 \\ \vec{p}_1 \\ \vec{q}_2 \\ \vec{p}_2 \end{pmatrix}. \end{aligned} \tag{A.13}$$

Defining $\vec{P} = (\vec{p}_1, \vec{p}_2)^t$ and $\vec{Q} = (\vec{q}_1, \vec{q}_2)^t$, and skipping a tedious step in the algebra, we have

$$\begin{aligned} &= \frac{1}{2}(\vec{P}^t, \vec{Q}^t) \begin{pmatrix} \Sigma H \Sigma & -i\Sigma H \\ (-i\Sigma H)^\dagger & H \end{pmatrix} \begin{pmatrix} \vec{P} \\ \vec{Q} \end{pmatrix} \\ &= \frac{1}{4}(\vec{P}^t, \vec{Q}^t) \begin{pmatrix} \Sigma & -i\Sigma \\ i\mathbb{1} & \mathbb{1} \end{pmatrix} \begin{pmatrix} H & 0 \\ 0 & H \end{pmatrix} \underbrace{\begin{pmatrix} \Sigma & -i\mathbb{1} \\ i\Sigma & \mathbb{1} \end{pmatrix}}_{=:\, C} \begin{pmatrix} \vec{P} \\ \vec{Q} \end{pmatrix} \\ &= \frac{1}{4}(\vec{P}^t, \vec{Q}^t) C^\dagger \begin{pmatrix} H & 0 \\ 0 & H \end{pmatrix} C \begin{pmatrix} \vec{P} \\ \vec{Q} \end{pmatrix}. \end{aligned} \tag{A.14}$$

So far p_i and q_i were operators. Now, we pass to the classical picture leaving aside the quantum nature. Clearly, the above quadratic form is stable, if and only if the matrix H is positive definite, i.e. $H > 0$. Only then are the oscillations the system follows found around a stable equilibrium. This stability behaviour is inherited by the quantum system as well[7], and hence the positivity of H is a natural condition to put.

Going back to the example of the bosonic chain with a Bogoliubov-type interaction, we can compute the eigenvalues of H to be $\lambda_\pm = \varepsilon_k \pm V$. The stability of H then requires that $\lambda_\pm > 0$, and therefore $\lambda_1 \lambda_2 > 0$, which in turn is equivalent to $E_k \in \mathbb{R}$ for all k.[8]

To bring out further peculiarities of some bosonic systems, when compared to fermionic ones, we'll also have a look at the other way bosonic operators can be coupled. The interesting result in what will follow is that this type of coupling does not require a hyperbolic rotation,

[7] this can be justified using the concept of path integrals in which the classical action enters.

[8] E_k now contains the shift due to the chemical potential.

but rather the usual rotation. Our example is the one of bosons on a chain in the presence of a staggered potential, and assuming the Brillouin zone has already been reduced, we have

$$\mathbf{H} = \sum_k (a_k^\dagger, b_k^\dagger) \begin{pmatrix} \varepsilon_k & g \\ g & -\varepsilon_k \end{pmatrix} \begin{pmatrix} a_k \\ b_k \end{pmatrix}. \tag{A.15}$$

Indeed, defining $\gamma_1 := ua - vb$ and $\gamma_2 := va + ub$, with $|u|^2 + |v|^2 = 1$, it is readily checked that $[\gamma_1, \gamma_1^\dagger] = |u|^2 + |v|^2 = 1 = [\gamma_2, \gamma_2^\dagger]$, while $[\gamma_1, \gamma_2^\dagger] = uv - vu = 0 = [\gamma_2, \gamma_1^\dagger]$. Therefore, the band structure for this model is the same as in the fermionic case, and is given by $E_k = \sqrt{\varepsilon_k^2 + g^2}$. Due to the bosonic nature of the particles, the bands will be populated differently, though. This result is not completely unexpected: comparing with the structure of the matrix Σ, this example remains within a block of the same signature. It is only terms of the type $b^\dagger b^\dagger$ or $b^\dagger a^\dagger$ that couple the blocks of different signature, and for which a generalized hyperbolic rotation will be needed.

Now that we have had a look at the different models of coupled bosons, we are ready to prove the main result of this Appendix:

Theorem A.2 (Bosonic Spectral Theorem)**.** *Let $H \in \mathbb{C}^{n+m}$ be such that $H^\dagger = H > 0$. Let $\Sigma = \mathrm{diag}(\mathbb{1}_{n\times n}, -\mathbb{1}_{m\times m})$, and let ΣH be diagonalizable. Then there exists a (unique)*[9] *pseudo-unitary transformation $M \in U(n|m)$ (i.e. $M^\dagger \Sigma M = \Sigma$), such that $M^\dagger H M = D$, with D diagonal.*

Proof. We shall prove the theorem in two steps:

Step 1 Consider first the matrix ΣH. Since it is diagonalizable, let λ_k denote the eigenvalue corresponding to the eigenvector $|v_k\rangle$, or in other words $\Sigma H|v_k\rangle = \lambda_k|v_k\rangle$, for $k = 1, \ldots, n+m$. Define also the matrix $\tilde{D} = \mathrm{diag}(\lambda_1, \ldots, \lambda_{n+m})$ to consist of all the eigenvalues, listed with degeneracy (if necessary). Then we have

$$\lambda_k \langle v_k|\Sigma|v_k\rangle = \langle v_k|H|v_k\rangle > 0, \tag{A.16}$$

since H is positive definite by assumption. However, as Σ is Hermitian, we have that $\langle v_k|\Sigma|v_k\rangle \in \mathbb{R}$ is real. Therefore, necessarily $\lambda_k \neq 0$ must be real too. In particular, it also follows that $\langle v_k|\Sigma|v_k\rangle \neq 0$ for any eigenvector of ΣH, i.e. the eigenvectors can be normalized w.r.t. Σ.

Further, notice that for $k \neq l$

$$\lambda_l \langle v_k|\Sigma|v_l\rangle = \langle v_k|\Sigma\Sigma H|v_l\rangle = \langle v_k| \left(\Sigma H\right)^\dagger \Sigma^\dagger |v_l\rangle = \bar{\lambda}_k \langle v_k|\Sigma|v_l\rangle, \tag{A.17}$$

since ΣH is Hermitian. Rearranging, we obtain

$$(\lambda_l - \bar{\lambda}_k)\langle v_k|\Sigma|v_l\rangle = 0. \tag{A.18}$$

Therefore, we conclude that $\langle v_k|\Sigma|v_l\rangle = 0$, whenever the eigenvalues are non-degenerate, and so the eigenvectors of ΣH corresponding to different eigenvalues are orthogonal w.r.t. the metric Σ.

[9] up to reshuffling of the columns corresponding to eigenvalues of the same signature in the non-degenerate case

Step 2 We now proceed with the proof of the theorem. Keep in mind that in general the eigenvalues may happen to be degenerate. In Step 1, we proved that the eigenvectors of ΣH belonging to different eigenvalues still remain orthogonal, and the eigenvalues must necessarily be real, due to the positivity of H. Let us first define a matrix $\tilde{M}$ via

$$\tilde{M} := (|v_1\rangle, \ldots, |v_n\rangle, |v_{n+1}\rangle \ldots, |v_{n+m}\rangle)\,. \tag{A.19}$$

There is no need to consider the sign of the corresponding eigenvalues at this moment. It is advantageous to consider $\tilde{M}^\dagger \Sigma \tilde{M}$ first which is block-diagonal, due to the orthogonality of the eigenvectors (corresponding to different eigenvalues). Moreover, each block is Hermitian. Therefore, there exists a unitary block-diagonal transformation $U = \mathrm{diag}(U_1, \ldots, U_m)$ $(U_i U_i^\dagger = \mathbb{1}_i)$, such that

$$U\tilde{M}^\dagger \Sigma \tilde{M} U^\dagger = \begin{pmatrix} \lambda_1 & & 0 \\ & \ddots & \\ 0 & & \lambda_{n+m} \end{pmatrix}, \tag{A.20}$$

where the eigenvalues are listed with possible degeneracy. We can therefore normalize further using the matrix $A = \mathrm{diag}(1/\sqrt{|\lambda_1|}, \ldots, 1/\sqrt{|\lambda_m|})$ to arrive at a diagonal matrix containing ± 1 on the diagonal, and (if necessary) use a further permutation matrix P to finally obtain

$$PAU\tilde{M}^\dagger \Sigma \tilde{M} U^\dagger A^\dagger P^\dagger = \mathrm{diag}(1, \ldots, 1, -1, \ldots, -1) = \Sigma. \tag{A.21}$$

It should be mentioned that all the transformations used so far preserve the signature by Sylvester's theorem, and hence the final number of ± 1's matches precisely the signature of Σ due to the positivity of H.

We can now define the matrix $M := \tilde{M} U^\dagger A^\dagger P^\dagger$. It follows that

$$M\Sigma M^\dagger = \tilde{M} U^\dagger A^\dagger P^\dagger \Sigma P A U \tilde{M}^\dagger = \tilde{M} U^\dagger \mathrm{diag}\left(\frac{1}{\lambda_1}, \ldots, \frac{1}{\lambda_{n+m}}\right) U \tilde{M}^\dagger, \tag{A.22}$$

by definition of A and P. Inverting Eq. (A.20) it follows that

$$\mathrm{diag}\left(\frac{1}{\lambda_1}, \ldots, \frac{1}{\lambda_{n+m}}\right) = U\tilde{M}^{-1}\Sigma \left(M^\dagger\right)^{-1} U^\dagger, \tag{A.23}$$

and hence $M\Sigma M^\dagger = \Sigma$, as desired.

It remains to check that $M^{-1}\Sigma H M = \tilde{D}$, i.e. the additional matrices P, A, U leave the diagonal matrix $\tilde{D}$ invariant:

$$M^{-1}\Sigma H M = (P^\dagger)^{-1}(A^\dagger)^{-1} U \tilde{M}^{-1} \Sigma H \tilde{M} U^\dagger A^\dagger P^\dagger = PA^{-1} U \tilde{D} U^\dagger A P^{-1}, \tag{A.24}$$

where we used that any permutation matrix P is orthogonal, and A is diagonal. Now comes the crucial point: recall that $\tilde{D} = \mathrm{diag}\left(\tilde{D}_1, \ldots, \tilde{D}_k\right)$ is diagonal, such that $\tilde{D}_i = \lambda_i \mathbb{1}$, and U is block-diagonal, consisting of unitary matrices only. Therefore, $U\tilde{D}U^\dagger = \tilde{D}UU^\dagger = \tilde{D}$, which follows immediately from $U_i \tilde{D}_i U_i^\dagger = \lambda_i U_i U_i^\dagger = \tilde{D}_i$. Since $\tilde{D}$ and A are both diagonal, we readily have $A^{-1}\tilde{D}A = \tilde{D}$. Last, $P\tilde{D}P^{-1} = \tilde{D}$, as P is defined to permute diagonal elements only.

To finish the proof in this case, observe that since $M \in U(n|m)$ is pseudo-unitary, we have $\Sigma M^{-1} = M^\dagger \Sigma$. Multiplying (A.26) by Σ from the left yields $M^\dagger H M = \Sigma \tilde{D} =: D$, which gives the diagonal matrix D as well. This completes the proof of the theorem.

□

In particular, it follows from the above proof that since $H > 0$, the matrix ΣH has the signature of Σ, and so there are n positive and m negative eigenvalues. This is most easily seen from the fact that D must be positive, and hence the diagonal matrices Σ and $\tilde{D}$ necessarily have the same signature.

In the non-degenerate case, we can provide a recipe to construct M. Define the matrix M to contain the eigenvectors $|v_n\rangle$ as columns in such a way that the eigenvectors corresponding to the negative eigenvalues of ΣH are put in the last m columns, and we normalize them w.r.t. to Σ:

$$M := \left(\frac{|v_1\rangle}{\sqrt{\langle v_1|\Sigma|v_1\rangle}}, \ldots, \frac{|v_n\rangle}{\sqrt{\langle v_n|\Sigma|v_n\rangle}}, \frac{|v_{n+1}\rangle}{\sqrt{\langle v_{n+1}| - \Sigma|v_{n+1}\rangle}}, \ldots, \frac{|v_{n+m}\rangle}{\sqrt{\langle v_{n+m}| - \Sigma|v_{n+m}\rangle}} \right). \tag{A.25}$$

It follows directly from the orthogonality of the different eigenvectors and the above normalization that M is pseudo-unitary by construction: $M\Sigma M^\dagger = \Sigma$. Moreover, since M contains the eingenvectors of ΣH, it is also true that

$$M^{-1}\Sigma H M = \tilde{D}, \tag{A.26}$$

where $\tilde{D}$ is diagonal and contains the non-degenerate eigenvalues λ_n.

Appendix B

Effective Action for Mixtures of (hardcore) Bosons

In this Appendix we extend[1] the work of Bradlyn, dos Santos, and Pelster on the 'Effective Action Approach for Quantum Phase Transitions in Bosonic Lattices', [8, 13]. Recently, they developed a general theory for describing phase transitions in bosonic systems beyond mean field, using a cumulant expansion method. Among the numerous advantages of this scheme are the implementation of finite temperature effects, the possibility to go to higher order in the small parameter(s) of the theory, and including the effect of arbitrary external potentials (e.g. a staggered, or a harmonic potential) within the Local Density Approximation.

The extension we provide allows for applying the method to mixtures of bosons and hardcore bosons. Including fermionic compounds is possible in interaction-dominated (insulating) phases, since the theory is perturbative in the hopping matrix of the species. Further, we assume that the hopping integrals will be of similar magnitude. Here, we restrict our analysis to bosons (including hardcore bosons).

The Hamiltonian for the system is given by

$$\begin{aligned} H &= \sum_{\alpha} \left(H_{1,\alpha} + H_{0,\alpha}\right) + H_{0,\text{int}} \\ H_{1,\alpha} &= -\sum_{ij} t_{ij,\alpha} \left(a^{\dagger}_{i\alpha} a_{j\alpha} + h.c.\right) \\ H_{0,\alpha} &= \sum_{i} f_{i,\alpha}(\hat{n}_{i\alpha}) \\ H_{0,\text{int}} &= \sum_{i} g_{i}(\hat{n}_{i\alpha}). \end{aligned} \tag{B.1}$$

The operators $a_{i\alpha}$ obey the corresponding commutator relations for each species type α. The kinetic energy term $H_{1,\alpha}$ contains the hopping matrices $t_{ij,\alpha}$ which are assumed symmetric and small, compared to the interaction energy. $H_{0,\alpha}$ describes the interaction of the species α via an arbitrary *local* function $f_{i,\alpha}$ of the particle number operator $\hat{n}_{i,\alpha}$. The different species are allowed to be subject to different interaction terms, although it is the interaction strength that will usually be different. The *locality* condition is essential to the theory, and must be

[1] While the original work is designed for a single species of bosons, here we present a generalization applicable to arbitrary mixtures of bosons and hardcore bosons.

properly stressed. The function g_i models the density-density coupling of the species. As the notation suggests, both $f_{i,\alpha}$ and g_i can depend on the site index i, thus taking into account the effect of an external potential within the Local Density Approximation. Finally, we note that the functions f_α also contain the corresponding chemical potentials.

It will be useful to adopt the notation

$$\begin{aligned} H &= H_1 + H_0 \\ H_1 &= \sum_\alpha H_{1,\alpha} \\ H_0 &= \sum_\alpha H_{0,\alpha} + H_{0,\text{int}}. \end{aligned} \tag{B.2}$$

In the following we follow closely the analysis [8]. We begin by introducing currents $j_\alpha(\tau)$ to the action which break any global symmetries:

$$H_{1,\alpha} \longrightarrow H'_{1,\alpha} = -\sum_{ij} t_{ij,\alpha} \left(a^\dagger_{i\alpha} a_{j\alpha} + h.c. \right) + \sum_i \left(j_{i\alpha} a^\dagger_{i\alpha} + j^*_{i\alpha} a_{i\alpha} \right). \tag{B.3}$$

We shall use them as sources to generate a perturbative expansion in the standard field-theoretical manner. To this end, we pass to an imaginary-time interaction picture w.r.t. H_0. The evolution operator generates a one-parameter unitary group via Schrödinger's equation:

$$\begin{aligned} &\frac{\mathrm{d}}{\mathrm{d}\tau} U_I(\tau) = -H'_{1I}(\tau) U_I(\tau, \tau_0), \\ &U(\tau_0, \tau_0) = 1. \end{aligned} \tag{B.4}$$

Using this, for the total partition function we have

$$\mathcal{Z}[j_\alpha, j^*_\alpha] = \operatorname{tr}\left\{ T_\tau e^{-\int_0^\beta \mathrm{d}\tau H(\tau)} \right\} = \operatorname{tr}\left\{ e^{-\int_0^\beta \mathrm{d}\tau H_0(\tau)} U_I(\beta, 0) \right\}, \tag{B.5}$$

which is now a functional of the currents. Using the series expansion for the evolution operator we arrive at

$$\begin{aligned} \mathcal{Z} &= \mathcal{Z}^{(0)} + \sum_{n=1}^\infty \mathcal{Z}^{(n)}, \\ \mathcal{Z}^{(n)} &= \mathcal{Z}^{(0)} \frac{(-1)^n}{n!} \int_0^\beta \mathrm{d}\tau_1 \int_0^\beta \mathrm{d}\tau_2 \ldots \int_0^\beta \mathrm{d}\tau_n \left\langle T_\tau \left[H'_{1I}(\tau_1) H'_{1I}(\tau_2) \ldots H'_{1I}(\tau_n) \right] \right\rangle_0. \end{aligned} \tag{B.6}$$

where

$$\begin{aligned} \mathcal{Z}^{(0)} &= \prod_i \mathcal{Z}^{(0)}_i \\ \mathcal{Z}^{(0)}_i &= \sum_{n_\alpha} e^{-\beta \left[g_i(n_{i\alpha}) + \sum_\alpha f_{i\alpha}(n_{i\alpha}) \right]} \end{aligned} \tag{B.7}$$

The free energy of such a system is given by $\mathcal{F} = -\frac{1}{\beta} \log \mathcal{Z}$. It is noteworthy that due to the fact that H_0 is not quadratic, we cannon apply Wick's theorem. The situation is saved by the Linked-Cluster Theorem, [13], which asserts that $\mathcal{F}$ can be expanded diagrammatically in terms of cumulants which in general depend on all the lattice sites. However, since the

interaction terms are all local in nature, all cumulants can only depend on a single site index i. They can be calculated from

$$
{}_iC^{(0)}_{2n,\alpha_1,\ldots,\alpha_{2n}}(\tau'_1,\ldots,\tau'_n|\tau_1,\ldots,\tau_n) = \frac{\delta^{2n} C^{(0)}_0[j_\alpha, j^*_\alpha]}{\delta j_{i\alpha_1}(\tau'_1)\ldots\delta j_{i,\alpha_n}(\tau'_n)\delta j^*_{i\alpha_{n+1}}(\tau_1)\ldots\delta j^*_{i\alpha_{2n}}}(\tau_n),
$$

$$
C^{(0)}_0[j_\alpha, j^*_\alpha] = \log\frac{\mathcal{Z}}{\mathcal{Z}_0}\bigg|_{t_{ij,\alpha}=0} = \log\left\langle T_\tau \exp\left\{-\left(\sum_{i,\alpha}\int_0^\beta \mathrm{d}\tau\left[j_{i\alpha}(\tau)a^\dagger_{i\alpha} + j^*_{i\alpha}(\tau)a_{i\alpha}\right]\right)\right\}\right\rangle_0 \tag{B.8}
$$

The left-subscript denotes the site index, on which the cumulant is calculated. The superindex in parentheses gives the order in perturbation theory w.r.t. the hopping amplitude t. Further, the subindex $2n$ gives the number of the cumulant, and finally $\alpha_1\ldots\alpha_{2n}$ denote the corresponding species. We shall shortly see, that the index α can only assume n different values, as the rest will result in delta functions. Furthermore, it follows from the definition of the operators $a_{i\alpha}$ that all odd cumulants vanish identically, since the ground state of H_0 is a state of a definite particle number. Also, cumulants where the index α_i is present an odd number of times vanish identically, for creation and annihilation operators of different types commute with each other.

Since we are ultimately interested in deriving an effective low-energy Landau-Ginzburg theory, we only need cumulants up to 4^{th} order. For the 2^{nd} order cumulant, we have

$$
{}_iC^{(0)}_{2,\alpha\beta}(\tau_1|\tau_2) = \left\langle T\left[a^\dagger_{i\alpha}(\tau_1)a_{i\beta}(\tau_2)\right]\right\rangle_0 = \delta_{\alpha\beta}\left\langle T_\tau\left[a^\dagger_{i\alpha}(\tau_1)a_{i\alpha}(\tau_2)\right]\right\rangle_0 = \delta_{\alpha\beta}G^{(0)}_\alpha(i,\tau_1|i,\tau_2). \tag{B.9}
$$

Hence, we find that it is equal to the free Green's function. Moreover, it is diagonal in α-space which suggests to use the simpler notation ${}_iC^{(0)}_{2,\alpha}$. This is the reason why we only need n indices for α to distinguish the different cumulants. The 4^{th} order cumulant is given by

$$
\begin{aligned}
{}_iC^{(0)}_{4,\alpha\beta}(\tau_1,\tau_2|\tau_3,\tau_4) = &\left\langle T\left[a^\dagger_{i\alpha}(\tau_1)a^\dagger_{i\beta}(\tau_2)a_{i\alpha}(\tau_3)a_{i\beta}(\tau_4)\right]\right\rangle_0 \\
&-_i C^{(0)}_{2,\alpha}(\tau_1|\tau_3)\,{}_iC^{(0)}_{2,\beta}(\tau_2|\tau_4) -_i C^{(0)}_{2,\alpha}(\tau_1|\tau_4)\,{}_iC^{(0)}_{2,\beta}(\tau_2|\tau_3).
\end{aligned} \tag{B.10}
$$

Notice that this cumulant is symmetric w.r.t. the exchange of $\tau_1 \leftrightarrow \tau_2$, $\tau_3 \leftrightarrow \tau_4$, and $\alpha \leftrightarrow \beta$.

One could in principle set up a set of Feynman rules to picture the diagrammatic expansion. We remark that these rules are the same as in [8], except that there is a greater variety, since the number of species has also increased. Here, we directly give the correction to the free energy to first order in the hoppings and fourth order in the currents.

$$
\begin{aligned}
\mathcal{F}^{(1)} = &-\frac{1}{\beta}\sum_{i,\alpha}\left\{\int_{\tau_1,\tau_2}\left[a^{(0)}_{2,\alpha}(i,\tau_1|i,\tau_2)j_{i\alpha}(\tau_1)j^*_{i\alpha}(\tau_2) + \sum_j a^{(1)}_{2,\alpha}(i,\tau_1|j,\tau_2)t_{ij,\alpha}j_{i\alpha}(\tau_1)j^*_{i\alpha}(\tau_2)\right]\right\} \\
&-\frac{1}{\beta}\sum_{i,\alpha\beta}\left\{\frac{1}{4}\int_{\tau_1,\tau_2,\tau_3,\tau_4} a^{(0)}_{4,\alpha,\beta}(i,\tau_1;i,\tau_2|i,\tau_3;i,\tau_4)j_{i\alpha}(\tau_1)j_{i\beta}(\tau_2)j^*_{i\alpha}(\tau_3)j^*_{i\beta}(\tau_4)\right. \\
&+\frac{1}{2}\sum_j\int_{\tau_1,\tau_2,\tau_3,\tau_4}\left[t_{ij,\alpha}a^{(1)}_{4,\alpha\beta}(i,\tau_1;i,\tau_2|j,\tau_3;i,\tau_4)j_{i\alpha}(\tau_1)j_{i\beta}(\tau_2)j^*_{j\alpha}(\tau_3)j^*_{i\beta}(\tau_4)\right. \\
&\left.\left.+\, a^{(1)}_{4,\alpha\beta}(i,\tau_1;j,\tau_2|i,\tau_3;i,\tau_4)j_{i\alpha}(\tau_1)j_{j\beta}(\tau_2)j^*_{i\alpha}(\tau_3)j^*_{i\beta}(\tau_4)\right]\right\},
\end{aligned} \tag{B.11}
$$

with

$$\begin{aligned} a^{(0)}_{2,\alpha}(i,\tau_1|i,\tau_2) &= {}_iC^{(0)}_{2,\alpha}(\tau_1|\tau_2) \\ a^{(1)}_{2,\alpha}(i,\tau_1|j,\tau_2) &= \int_0^\beta \mathrm{d}\tau {}_iC^{(0)}_{2,\alpha}(\tau_1|\tau){}_iC^{(0)}_{2,\alpha}(\tau|\tau_2) \\ a^{(0)}_{4,\alpha\beta}(i,\tau_1;i,\tau_2|i,\tau_3;i,\tau_4) &= {}_iC^{(0)}_{4,\alpha\beta}(\tau_1,\tau_2|\tau_3,\tau_4) \\ a^{(1)}_{4,\alpha\beta}(i,\tau_1;i,\tau_2|j,\tau_3;i,\tau_4) &= \int_0^\beta \mathrm{d}\tau\ {}_iC^{(0)}_{4,\alpha\beta}(\tau_1,\tau_2|\tau,\tau_4){}_jC^{(0)}_{2,\alpha}(\tau|\tau_3). \end{aligned} \tag{B.12}$$

We seek an effective potential (Ginzburg free energy) for a set of order parameters ψ_α. To this end, one has to follow precisely the same steps as is [8], which we omit here. It should be mentioned that the derivation makes use of the translational invariance in the time domain, passing over to Matsubara space, where the above quantities are somewhat simpler to handle. It is this that enables us to incorporate finite-T effects in the theory. We define the complex order parameter field as the functional derivative of the free energy w.r.t. the current:

$$\psi_{i\alpha}(\omega_m) := \langle a_{i\alpha}(\omega_m)\rangle = \beta\frac{\delta\mathcal{F}}{\delta j^*_{i\alpha}(\omega_m)}, \tag{B.13}$$

where β is the inverse temperature. The effective potential (or Landau-Ginzburg free energy) can be calculated along the lines of [8] to be

$$\Gamma[\psi_\alpha,\psi^*_\alpha] = \mathcal{F}_0 + \frac{1}{\beta}\sum_{i,\alpha}\left\{\sum_{\omega_m}\left[\frac{|\psi_{i\alpha}(\omega_m)|^2}{a^{(0)}_{2,\alpha}(i,\omega_m)} - \sum_j t_{ij,\alpha}\psi_{i\alpha}(\omega_m)\psi^*_{j\alpha}(\omega_m)\right] - \right.$$

$$\left. -\sum_\beta\sum_{\omega_{m_1},\ldots,\omega_{m_4}}\frac{a^{(0)}_{4,\alpha\beta}(i,\omega_{m_1};i,\omega_{m_2}|i,\omega_{m_3};i,\omega_{m_4})}{4a^{(0)}_{2,\alpha}(i,\omega_{m_1})a^{(0)}_{2,\beta}(i,\omega_{m_2})a^{(0)}_{2,\alpha}(i,\omega_{m_3})a^{(0)}_{2,\beta}(i,\omega_{m_4})}\psi_{i\alpha}(\omega_{m_1})\psi_{i\beta}(\omega_{m_2})\psi^*_{i\alpha}(\omega_{m_3})\psi^*_{i\beta}(\omega_{m_4})\right\} \tag{B.14}$$

Having derived the general result, the above scheme provides a straightforward (though computationally involved) way to include higher order terms in the hopping matrix $t_{ij,\alpha}$. Instead, let us restrict the following analysis to a time-independent order parameter. We want to investigate the two cases of

1. A single component interacting bosons in the presence of a staggered potential.

   In the presence of an alternating potential, the order parameter will also assume a staggered modulation in general. Since there is a residual translational symmetry corresponding to a larger unit cell, we need only care about physical quantities inside this cell. If we denote the two sublattices by A and B, the effective potential at zero temperature takes the form

$$\begin{aligned} \Gamma[\psi] = \mathcal{F}_0 &+ \frac{N_s}{2}\left(\frac{|\psi_A|^2}{a^{(0)}_2(A,0)} + \frac{|\psi_B|^2}{a^{(0)}_2(B,0)}\right) - ztN_s\psi_A\psi_B \\ &- \frac{N_s}{2}\left(\frac{a^{(0)}_4(A,0)}{4\left[a^{(0)}_2(A,0)\right]^4}|\psi_A|^4 + \frac{a^{(0)}_4(B,0)}{4\left[a^{(0)}_2(B,0)\right]^4}|\psi_B|^4\right), \end{aligned} \tag{B.15}$$

   with N_s the number of sites.

2. A mixture of two species.

   In this case $\alpha = \{\psi, \phi\}$ can take only two values, and we denote the uniform order parameters by ψ and ϕ. All cumulants take the same value on each site due to translational symmetry, and we can safely neglect the index i. The effective action for this problem takes the form

$$\Gamma[\psi,\phi] = \mathcal{F}_0 + N_s\left(\frac{|\psi|^2}{a^{(0)}_{2,\psi}(i,0)} + \frac{|\phi|^2}{a^{(0)}_{2,\phi}(i,0)}\right) - N_s\left(zt_\psi|\psi|^2 + zt_\phi|\phi|^2\right)$$
$$- \frac{1}{4N_s}\left(\frac{a^{(0)}_{4,\psi\psi}(i,0)}{\left[a^{(0)}_{2,\psi}(i,0)\right]^4}|\psi|^4 + \frac{2a^{(0)}_{4,\psi\phi}(i,0)}{\left[a^{(0)}_{2,\psi}(i,0)\right]^2\left[a^{(0)}_{2,\phi}(i,0)\right]^2}|\psi|^2|\phi|^2 + \frac{a^{(0)}_{4,\phi\phi}(i,0)}{\left[a^{(0)}_{2,\phi}(i,0)\right]^4}|\phi|^4\right). \tag{B.16}$$

   The analysis of the rich phase diagram coming from such a Landau-Ginzuburg free energy with two coupled order parameters is given in the appendix of [33].

With this, we conclude our short discussion of the Cumulant Expansion Method.

Appendix C

SUSY Calculations

C.1 Derivation of the Hamiltonian

In this Appendix we review the straightforward but computationally involved derivation of the standard many-body Hamiltonian from the SUSY one. To begin with, note first that the three parts of (6.35), although they have different physical meaning, have the same structure w.r.t. the Grassmann integration: in the first one the Nabla operator refers to the spatial variables only, and in the last term the potential does not involve any of the Grassmann fields, and thus the integration over the primed and unprimed Grassmann variables can be performed independently, using the expansion of the superfield in components.

Therefore, we restrict our calculation to the part involving the chemical potential and drop the constant prefactor μ:

$$\begin{aligned}
\frac{1}{2m}\int \mathrm{d}^2\theta\mathrm{d}^2\bar{\theta}\bar{\phi}\phi = &\frac{1}{2m}\int \mathrm{d}^2\theta\mathrm{d}^2\bar{\theta}\left[e^{m\theta\sigma^0\theta}\left(\frac{1}{m}A(\vec{x},t)+\sqrt{\frac{2}{m}}\theta^\alpha\psi_\alpha(\vec{x},t)+\theta^2B(\vec{x},t)\right)\right]\\
&\times\left[e^{m\theta\sigma^0\theta}\left(\frac{1}{m}A^\dagger(\vec{x},t)+\sqrt{\frac{2}{m}}\bar{\theta}_{\dot{\alpha}}\bar{\psi}^{\dot{\alpha}}(\vec{x},t)+\bar{\theta}^2B^\dagger(\vec{x},t)\right)\right]\\
=&\frac{1}{2m}\int \mathrm{d}^2\theta\mathrm{d}^2\bar{\theta}\left[1+2m\theta\sigma^0\bar{\theta}+\frac{4m^2}{2}\underbrace{(\theta\sigma^0\bar{\theta})(\theta\sigma^0\bar{\theta})}_{=-\frac{1}{2}\theta^2\bar{\theta}^2\eta^{00}}\right]\\
&\times\left[\frac{1}{m}A(\vec{x},t)+\sqrt{\frac{2}{m}}\theta^\alpha\psi_\alpha(\vec{x},t)+\theta^2B(\vec{x},t)\right]\\
&\times\left[\frac{1}{m}A^\dagger(\vec{x},t)+\sqrt{\frac{2}{m}}\bar{\theta}_{\dot{\alpha}}\bar{\psi}^{\dot{\alpha}}(\vec{x},t)+\bar{\theta}^2B^\dagger(\vec{x},t)\right]\\
=&\frac{1}{2m}\int \mathrm{d}^2\theta\mathrm{d}^2\bar{\theta}\left[A^\dagger A\theta^2\bar{\theta}^2+B^\dagger B\theta^2\bar{\theta}^2+4(\theta\sigma^0\bar{\theta})(\bar{\theta}\bar{\psi})(\theta\psi)\right],
\end{aligned}\tag{C.1}$$

where in the last step we kept only the non-vanishing components under the Grassmann integration (to be carried out trivially in a subsequent step). The first two terms already have the desired form. To see that this is true for the fermionic term as well, we employ the

properties of the spinor algebra:

$$\begin{aligned}
4(\theta\sigma^0\bar{\theta})(\bar{\theta}\bar{\psi})(\theta\psi) &= 4\theta^\beta\sigma^0_{\beta\dot{\beta}}\bar{\theta}^{\dot{\beta}}\bar{\theta}_{\dot{\alpha}}\bar{\psi}^{\dot{\alpha}}\theta^\alpha\psi_\alpha \\
&= 4\theta^\beta\sigma^0_{\beta\dot{\beta}}\varepsilon^{\dot{\gamma}\dot{\beta}} \underbrace{\bar{\theta}_{\dot{\gamma}}\bar{\theta}_{\dot{\alpha}}}_{=-\frac{1}{2}\varepsilon_{\dot{\gamma}\dot{\alpha}}\bar{\theta}^2} \bar{\psi}^{\dot{\alpha}}\theta^\alpha\psi_\alpha \\
&= -2\sigma^0_{\beta\dot{\beta}}\underbrace{\varepsilon^{\dot{\gamma}\dot{\beta}}\varepsilon_{\dot{\gamma}\dot{\alpha}}}_{=\delta^{\dot{\beta}}_{\dot{\alpha}}}\bar{\theta}^2\theta^\beta\bar{\psi}^{\dot{\alpha}}\theta^\alpha\psi_\alpha \\
&= -2\bar{\theta}^2\sigma^0_{\beta\dot{\alpha}}(-\bar{\psi})^{\dot{\alpha}} \underbrace{\theta^\beta\theta^\alpha}_{=-\frac{1}{2}\varepsilon^{\beta\alpha}\theta^2} \psi_\alpha \\
&= -\bar{\theta}^2\theta^2\sigma^0_{\beta\dot{\alpha}}\bar{\psi}^{\dot{\alpha}}\psi^\beta = +\bar{\theta}^2\theta^2\psi\sigma^0\bar{\psi}. \qquad \text{(C.2)}
\end{aligned}$$

This term is normal ordered, since according to our convention [57], $\sigma^0 = -\mathbb{1}$ and the extra sign is cancelled by commuting the Grassmann fields.

Precisely the same calculation can be carried out for the kinetic term, keeping the gradients at each step, as they do not affect the Grassmann integration. In the interaction term, as mentioned before, the contact interaction only couples the spatial variables, and the above procedure together with the integral over $\delta^{(4)}(x-x')$ results in the standard two-body interaction for the different fields as given by Eq. (6.3).

C.2 Evaluation of the Hartree Diagram

In this Appendix, we show the computation of the Hartree diagram in superspace and derive the expression from Eq. (6.39).

Notice that, since the free propagator factorizes into a space-time term and a Grassmann term, it is sufficient to deal with both of them separately, to avoid lengthy expressions. Here we start with the space-time term, which reads

$$\begin{aligned}
&\int \mathrm{d}^4x_1'\mathrm{d}^4x_2' \int \frac{\mathrm{d}\omega\mathrm{d}^3k}{(2\pi)^4}\frac{\mathrm{d}\nu\mathrm{d}^3q}{(2\pi)^4}\frac{\mathrm{d}\tilde{\nu}\mathrm{d}^3\tilde{q}}{(2\pi)^4} e^{ik(x_1-x_1')}e^{iq(x_1'-x_2')}e^{i\tilde{q}(x_2'-x_2)} \\
&\times \frac{1}{\omega-\varepsilon_k-\mu}\frac{1}{\nu-\varepsilon_q-\mu}\frac{1}{\tilde{\nu}-\varepsilon_{\tilde{q}}-\mu} g\delta^{(4)}(x_1'-x_2') \\
&= g\int \frac{\mathrm{d}\omega\mathrm{d}^3k}{(2\pi)^4}\frac{\mathrm{d}\tilde{\nu}\mathrm{d}^3\tilde{q}}{(2\pi)^4}\mathrm{d}^4x_1' e^{(ix_1'(\tilde{q}-k))}e^{i(kx_1-\tilde{q}x_2)} \\
&\times \left(\int \frac{\mathrm{d}\nu\mathrm{d}^3q}{(2\pi)^4}\frac{1}{\nu-\varepsilon_q-\mu}\right)\frac{1}{\omega-\varepsilon_k-\mu}\frac{1}{\tilde{\nu}-\varepsilon_{\tilde{q}}-\mu} \\
&= g\int \frac{\mathrm{d}^3k\mathrm{d}\omega}{(2\pi)^4}e^{ik(x_1-x_2)}\left(\frac{1}{\omega-\varepsilon_k-\mu}\right)^2\int\frac{\mathrm{d}^3q\mathrm{d}\nu}{(2\pi)^4}\frac{1}{\nu-\varepsilon_q-\mu}. \qquad \text{(C.3)}
\end{aligned}$$

Next, we prove the 'robustness' identity, which amounts to calculating the Grassmann part of the Hartree diagram. Neglecting the mass prefactor $(-1/m^2)^3$, we have

$$\begin{aligned}
&e^{-2\theta_1'\sigma^0\bar{\theta}_1+\theta_1\sigma^0\bar{\theta}_1+\theta_1'\sigma^0\bar{\theta}_1'}e^{-2\theta_2'\sigma^0\bar{\theta}_1'+\theta_1'\sigma^0\bar{\theta}_1'+\theta_2'\sigma^0\bar{\theta}_2'}e^{-2\theta_2\sigma^0\bar{\theta}_2'+\theta_2\sigma^0\bar{\theta}_2'+\theta_2\sigma^0\bar{\theta}_2} \\
&= e^{2m[\theta_1'\sigma^0\bar{\theta}_1'+\theta_2'\sigma^0\bar{\theta}_2'-\theta_1'\sigma^0\bar{\theta}_1-\theta_2\sigma^0\bar{\theta}_2'-\theta_2'\sigma^0\bar{\theta}_1']}e^{m\theta_1\sigma^0\bar{\theta}_1+m\theta_2\sigma^0\bar{\theta}_2}. \qquad \text{(C.4)}
\end{aligned}$$

Since only the first factor contains the primed variables over which we integrate, we expand it term by term, and retain only the terms proportional to $\Omega_1'^2\Omega_2'^2$, as all other components will be set to zero by the Grassmann integration. It is most convenient to separate the five exponentials and expand them exactly to second order:

$$\begin{aligned}
&= \left(\underset{\sim}{1} + \underline{\underline{2m\theta_1'\sigma^0\bar{\theta}_1'}} + \underline{m^2(\theta_1')^2(\bar{\theta}_1')^2}\right)\left(\underset{\sim}{1} + \underline{\underline{2m\theta_2'\sigma^0\bar{\theta}_2'}} + \underline{m^2(\theta_2')^2(\bar{\theta}_2')^2}\right)\\
&\times \left(\underset{\sim}{1} - \underline{\underline{2m\theta_1'\sigma^0\bar{\theta}_1}} + \underset{\sim}{m^2(\theta_1')^2(\bar{\theta}_1)^2}\right)\left(\underset{\sim}{1} - \underline{\underline{2m\theta_2\sigma^0\bar{\theta}_2'}} + \underset{\sim}{m^2(\theta_2)^2(\bar{\theta}_2')^2}\right)\\
&\times \left(\underset{\sim}{1} - \underline{\underline{2m\theta_2'\sigma^0\bar{\theta}_1'}} + \underset{\sim}{m^2(\theta_2')^2(\bar{\theta}_1')^2}\right)\\
&= m^4\Omega_1'^2\Omega_2'^2 + m^6\Omega_1'^2\Omega_2'^2(\bar{\theta}_1)^2(\theta_2)^2 - 2^5m^5(\theta_1'\sigma^0\bar{\theta}_1')(\theta_2'\sigma^0\bar{\theta}_2')(\theta_1'\sigma^0\bar{\theta}_1)(\theta_2\sigma^0\bar{\theta}_2')(\theta_2'\sigma^0\bar{\theta}_1')\\
&= m^4\Omega_1'^2\Omega_2'^2 + m^6\Omega_1'^2\Omega_2'^2(\bar{\theta}_1)^2(\theta_2)^2 - 2m^5(\theta_2\sigma^0\bar{\theta}_1)\Omega_1'^2\Omega_2'^2\\
&= m^4e^{-2m\theta_2\sigma^0\bar{\theta}_1}\Omega_1'^2\Omega_2'^2
\end{aligned} \tag{C.5}$$

The penultimate equality will be shown below. Dividing by the mass pre-factor, executing the trivial integration over the Grassmann variables, and including the exponential from the second term in (C.4), one obtains for the full F

$$F(\Omega_1,\Omega_2;m) = -\frac{1}{m^2}\exp\left(-2m\theta_2\sigma_0\bar{\theta}_1 + m\theta_1\sigma_0\bar{\theta}_2 + m\theta_2\sigma_0\bar{\theta}_2\right). \tag{C.6}$$

The last step consists of showing the identity

$$2^5m^5(\theta_1'\sigma^0\bar{\theta}_1')(\theta_2'\sigma^0\bar{\theta}_2')(\theta_1'\sigma^0\bar{\theta}_1)(\theta_2\sigma^0\bar{\theta}_2')(\theta_2'\sigma^0\bar{\theta}_1') = 2m^5(\theta_2\sigma^0\bar{\theta}_1)\Omega_1'^2\Omega_2'^2. \tag{C.7}$$

To this end, we employ several times the identities $(\theta\phi)(\theta\psi) = -\frac{1}{2}(\phi\psi)\theta^2$ and $(\bar{\theta}\bar{\phi})(\bar{\theta}\bar{\psi}) = -\frac{1}{2}(\bar{\phi}\bar{\psi})\bar{\theta}^2$ proved in [57]:

$$\begin{aligned}
&2^5m^5(\underline{\theta_1'\sigma^0\bar{\theta}_1'})(\theta_2'\underline{\underline{\sigma^0\bar{\theta}_2'}})(\underline{\theta_1'\sigma^0}\bar{\theta}_1)(\theta_2\underline{\underline{\sigma^0\bar{\theta}_2'}})(\theta_2'\sigma^0\bar{\theta}_1')\\
&= 2^3(\theta_1'\sigma^0\theta_1'\sigma^0)(\bar{\theta}_1'\bar{\theta}_1)(\theta_2'\theta_2)(\sigma^0\bar{\theta}_2'\sigma^0\bar{\theta}_2')(\theta_2'\sigma^0\bar{\theta}_1')\\
&= 2^3(\theta_1'\theta_1')(\bar{\theta}_1'\bar{\theta}_1)(\theta_2'\underset{\sim}{\theta_2})(\bar{\theta}_2'\bar{\theta}_2')(\theta_2'\underset{\sim}{\sigma^0\bar{\theta}_1'})\\
&= -4(\theta_1')^2(\theta_2')^2(\bar{\theta}_2')^2(\underline{\underline{\theta_1}}\bar{\theta}_1')(\underline{\underline{\theta_2\sigma^0}}\bar{\theta}_1')\\
&= 2(\theta_1')^2(\theta_2')^2(\bar{\theta}_2')^2(\bar{\theta}_1')^2(\theta_2\sigma^0\bar{\theta}_1),
\end{aligned} \tag{C.8}$$

where we used the fact that $\sigma^0 = -\mathbb{1}$.

Bibliography

[1] A. Altland and B. Simons, *Condensed matter field theory*, Cambridge University Press, 2010.

[2] P. Anders, P. Werner, M. Troyer, M. Sigrist, and L. Pollet, *The Cooper problem and beyond in Bose-Fermi mixtures*, Phys. Rev. Lett. **109** (2012), 206401.

[3] J.F. Annett and J.P. Wallington, *s- and d-wave pairing in short coherence length superconductors*, ArXiv (1998).

[4] J. Avery, *Creation and annihilation operators*, McGrall-Hill, 1977.

[5] J. Bardeen, L.N. Cooper, and J.R. Schrieffer, *Theory of superconductivity*, Physical Review **108(5)** (1957), 1175.

[6] Th. Best, S. Will, U. Schneider, L. Hackermüller, D. van Oosten, I. Bloch, and D.-S. Lühmann, *Role of interactions in* ^{87}Rb-^{40}**K** *Bose-Fermi mixtures in a 3d optical lattice*, Phys. Rev. Lett. **102** (2009), 030408.

[7] M. J. Bijlsma, B. A. Heringa, and H. T. C. Stoof, *Phonon exchange in dilute Fermi-Bose mixtures: Tailoring the Fermi-Fermi interaction*, Phys. Rev. A **61** (2000), 053601.

[8] B. Bradlyn, F. Ednilson, A. dos Santos, and A. Pelster, *Effective action approach for quantum phase transitions in bosonic lattices*, Phys. Rev. A **79** (2009), 013615.

[9] H. P. Büchler and G. Blatter, *Supersolid versus phase separation in atomic Bose-Fermi mixtures*, Phys. Rev. Lett. **91** (2003), 130404.

[10] T. E. Clark and S. T. Love, *Non-relativistic supersymmetry*, Nuclear Physics **B 231** (1984), 91–108.

[11] M. Cramer, S. Ospelkaus, C. Ospelkaus, K. Bongs, K. Sengstock, and J. Eisert, *Do mixtures of bosonic and fermionic atoms adiabatically heat up in optical lattices?*, Phys. Rev. Lett. **100** (2008), 140409.

[12] E. Demler, W. Hanke, and S.C. Zhang, $SO(5)$ *theory of antiferromagnetism and superconductivity*, Rev. Mod. Phys. **76** (2004), 909–974.

[13] A. dos Santos and A. Pelster, *Quantum phase diagram of bosons in optical lattices*, Phys. Rev. A **79** (2009), 013614.

[14] D.V. Efremov and L. Viverit, *p-wave cooper pairing of fermions in mixtures of dilute Fermi and Bose gases*, Physical Review B **65** (2002), 134519.

[15] A.B. Eriksson, T. Einarsson, and S. Ostlund, *Symmetries and mean-field phases of the extended Hubbard model*, Phys. Rev. B **50** (1995), 3662.

[16] T. Esslinger, *Fermi-Hubbard physics with atoms in an optical lattice*, Annual Review of Condensed Matter Physics **1** (2010), 129–152.

[17] A. L. Fetter and J. D. Walecka, *Quantum theory of many-particle systems*, McGraw-Hill, 1971.

[18] R.P. Feynman, *Statistical mechanics: A set of lectures*, Perseus Books, Reading, Massachusetts, 1972.

[19] C.J. Foot, *Atomic physics*, Oxford University Press, 2005.

[20] T. Giamarchi, A. Iucci, and C. Berthod, *Introduction to many body physics*, Lecture Notes, University of Geneva (2008-2009).

[21] M. Greiner, *Ultracold quantum gases in three-dimensional optical lattice potentials*, PhD thesis, LMU München (2003).

[22] M. Greiner, O. Mandel, T. Esslinger, T. E. Hänsch, and I. Bloch, *Quantum phase transition from a superfluid to a Mott insulator in a gas of ultracold atoms*, Nature (London) 415 **39** (2002).

[23] Kenneth Günter, Thilo Stöferle, Henning Moritz, Michael Köhl, and Tilman Esslinger, *Bose-Fermi mixtures in a three-dimensional optical lattice*, Phys. Rev. Lett. **96** (2006), 180402.

[24] J. Heinze, S. Götze, J. S. Krauser, B. Hundt, N. Fläschner, D.-S. Lühmann, C. Becker, and K. Sengstock, *Multiband spectroscopy of ultracold fermions: Observation of reduced tunneling in attractive Bose-Fermi mixtures*, Phys. Rev. Lett. **107** (2011), 135303.

[25] H. Heiselberg, C. J. Pethick, H. Smith, and L. Viverit, *Influence of induced interactions on the superfluid transition in dilute Fermi gases*, Phys. Rev. Lett. **85** (2000), 2418–2421.

[26] I. Hen and M. Rigol, *Superfluid to Mott-insulator transition of hardcore bosons in a superlattice*, Phys. Rev. b **80** (2009), 134508.

[27] S. Huber, *Excitations and transport in strongly correlated bosonic matter*, PhD thesis, ETH Zürich (2008).

[28] E. İnönü and E. P. Wigner, *On the contraction of groups and their representations*, Proc. Nat. Acad. Sci. **39(6)** (1953), 550–24.

[29] M. Iskin, *Route to supersolidity for the extended Bose-Hubbard model*, Phys. Rev. A 83 **83** (2011), 051606(R).

[30] ———, *Quantum phase transition from a superfluid to a Mott insulator in a gas of ultracold atoms*, arXiv (2013), 1304.8111.

[31] M. Kardar, *Statistical physics of fields*, Cambridge University Press, 2007.

[32] W. Ketterle, *When atoms behave as waves: Bose-Einstein condensation and the atom laser*, Nobel Lecture (2001).

[33] K.-S. Liu and M. Fisher, *Quantum lattice gas and the existence of a supersolid*, Journal of Low Temperature Physics **10** (1973), Nos. 5/6.

[34] G.S. Lozanoa, O. P., F.A. S., and L. Sourrouille, *On 1 + 1 dimensional galilean supersymmetry in ultracold quantum gases*, Phys. Rev. A **75** (2006), 023608.

[35] Dirk-Sören Lühmann, Kai Bongs, Klaus Sengstock, and Daniela Pfannkuche, *Self-trapping of bosons and fermions in optical lattices*, Phys. Rev. Lett. **101** (2008), 050402.

[36] L. Mathey, S.-W. Tsai, and A. H. Castro Neto, *Competing orders in two-dimensional Bose-Fermi mixtures*, Physical Review Lett. **97** (2006), 030601.

[37] A. Mering and M. Fleischhauer, *One-dimensional Bose-Fermi-Hubbard model in the heavy-fermion limit*, Phys. Rev. A **77** (2008), 023601.

[38] R. Micnas, J. Ranninger, and S. Robaszkiewicz, *Superconductivity in narrow band systems with local nonretarded attractive interactions*, Rev. Mod. Phys. **62** (1990), 113–173.

[39] R. Micnas, J. Ranninger, S. Robaszkiewicz, and S. Tabor, *Superconductivity in a narrow-band system with intersite electron pairing in two dimensions: A mean-field study*, Physical Review B **37** (1988).

[40] W. J. Mullin, *Cell model of a Bose-condensed solid*, Phys. Rev. Lett. **26** (1971), 223.

[41] Quantum Optics Group of LMU, *http://www.quantum-munich.de/research/ultracold-fermions-in-optical-lattices/*.

[42] S. Ospelkaus, C. Ospelkaus, O. Wille, M. Succo, P. Ernst, K. Sengstock, and K. Bongs, *Localization of bosonic atoms by fermionic impurities in a three-dimensional optical lattice*, Phys. Rev. Lett. **96** (2006), 180403.

[43] S. Ostlund, *Symmetries and canonical transformations of the Hubbard model on bipartite lattices*, Phys. Rev. Lett. **69** (1992), 1695.

[44] W.D. Phillips, *Laser cooling and trapping of neutral atoms*, Nobel Lecture (1997).

[45] Lode Pollet, Corinna Kollath, Ulrich Schollwöck, and Matthias Troyer, *Mixture of bosonic and spin-polarized fermionic atoms in an optical lattice*, Phys. Rev. A **77** (2008), 023608.

[46] S. Raghu, S. A. Kivelson, and D. J. Scalapino, *Superconductivity in the repulsive Hubbard model: An asymptotically exact weak-coupling solution*, Physical Review B **81** (2010).

[47] S. Robaszkiewicz, R. Micnas, and K.A. Chao, *Chemical potential and order parameter of extended Hubbard model with strong intra-atomic attraction*, Phys. Rev. B **24** (1981), 1579.

[48] ———, *Thermodynamics properties of the extended Hubbard model with strong intra-atomic attraction and an arbitrary electron density*, Phys. Rev. B **23** (1981), 1447.

[49] R. Staudt, M. Dzierzawa, and A. Muramatsu, *Phase diagram of the three-dimensional Hubbard model at half-filling*, Eur. Phys. J. B **69** (1992), 11.

[50] H. T. Stoof, D. Dickerscheid, and K. Gubbels, *Ultracold quantum fields*, Springer, 2009.

[51] Sumanta Tewari, Roman M. Lutchyn, and S. Das Sarma, *Effects of fermions on the superfluid-insulator phase diagram of the Bose-Hubbard model*, Phys. Rev. B **80** (2009), 054511.

[52] L. Viverit, *Boson-induced s-wave pairing in dilute boson-fermion mixtures*, Phys. Rev. A **66** (2002), 023605.

[53] L. Viverit and S. Giorgini, *Ground-state properties of a dilute Bose-Fermi mixture*, Phys. Rev. A **66** (2002), 063604.

[54] L. Viverit, C. J. Pethick, and H. Smith, *Zero-temperature phase diagram of binary boson-fermion mixtures*, Phys. Rev. A **61** (2000), 053605.

[55] D.-W. Wang, M. D. Lukin, and E. Demler, *Engineering superfluidity in Bose-Fermi mixtures of ultracold atoms*, Physical Review A **72** (2005).

[56] Daw-Wei Wang, *Strong-coupling theory for the superfluidity of Bose-Fermi mixtures*, Phys. Rev. Lett. **96** (2006), 140404.

[57] J. Wess and J. Bagger, *Supersymmetry and supergravity*, Princeton University Press, 1983.

[58] S. Will, *Interacting bosons and fermions in three-dimensional optical lattice potentials: From atom optics to quantum simulation*, PhD thesis, LMU Mnchen (2011).

[59] S. Will, T. Best, S. Braun, U. Schneider, and I. Bloch, *Coherent interaction of a single fermion with a small bosonic field*, Phys. Rev. Lett. **106** (2011), 115305.

[60] C.N. Yang and S.C. Zhang, *SO_4 symmetry in a Hubbard model*, Modern Physics Letters B **4** (1990), 759–766.

[61] Y. Yu and K. Yang, *Supersymmetry and Goldstino-like mode in Bose-Fermi mixtures*, Phys. Rev. Lett. **100** (2008), 090404.

[62] M. W. Zwierlein, J. R. Abo-Shaeer, A. Schirotzek, C. H. Schunck, and W. Ketterle, *Vortices and superfluidity in a strongly interacting Fermi gas*, Nature **435** (2005), 03858.